

THE UNIVERSITY OF SOUTHAMPTON

Novel Chiral Cyclopentadienyl Metal Complexes

Peter Alan Wright MSci.

*A thesis submitted in partial fulfilment of the requirement for the degree of Doctor of
Philosophy*

The Department of Chemistry

June 2005

ABSTRACT

FACULTY OF ENGINEERING, SCIENCE & MATHEMATICS

CHEMISTRY

Doctor of Philosophy

Novel Chiral Cyclopentadienyl Metal Complexes

by Peter Alan Wright

The synthesis and applications of transition metal complexes containing cyclopentadienyl-phosphorus and amine bidentate ligands have been reviewed and the work of other research groups discussed.

The synthesis of the known three-carbon linked ligand *rac*-[3-cyclohexyl-3-(3*H*-inden-1-yl)propyl]-diphenyl-phosphine **201** has been optimised. This involves the novel 1,4-catalytic addition of indenyl lithium to an α,β -unsaturated ester. Complexation with $\text{RuCl}_2(\text{PPh}_3)_3$ to form its ruthenium(II) complex *rac*-**401**, has also been optimised, with the need for column chromatography under inert conditions no longer required. Complete control over the induction of chirality at the metal centre and high induction of planar chirality (66 % d.e.) remain. Its cationic version *rac*-**402** has been synthesised, however, the attempted synthesis of its tetrahydroindenyl analogue *rac*-**403** failed. Initial catalytic trials of *rac*-**401** and **402** have proved disappointing.

The novel three-carbon linked chiral ligand (*S*)-[3-cyclohexyl-3-(3*H*-inden-1-yl)-propyl]diphenyl-phosphine, (*S*)-**201** has been synthesised with an overall yield of 26 % after 7 steps in 98 % e.e. This involved initial asymmetric hydrogenation of **330** using a chiral bidentate phosphine-ruthenium complex and was achieved in 81 % yield and 99 % e.e. The displacement of the secondary mesylate **335** with indene, via an $\text{S}_{\text{N}}2$ mechanism, was the key step with enantiomeric purity being maintained. (*S*)-**201** has been complexed with $\text{RuCl}_2(\text{PPh}_3)_3$ to form its ruthenium(II) complex (*S*)-**401**, with 67 % d.e. induction of planar chirality and complete control over the induction of chirality at the metal centre. Its cationic version (*S*)-**402** has been synthesised, however, the attempted synthesis of its tetrahydroindenyl analogue (*S*)-**403** failed.

Displacement of PPh_3 on *rac*-**401** was attempted. This proved successful with a number of phosphines giving complexes *rac*-**417-419**. The thermodynamic product was formed in each case, suggesting a dissociative process.

A number of novel racemic three-tether carbon amine ligands were synthesised, **605**, **608-611**, and **614-618**. Complexation of ligand *rac*-*N*-[3-(3*H*-inden-1-yl)-propyl]-4-methyl-benzenesulfonamide, **618** with $[\text{RhCl}(\text{CO})_2]_2$ proved successful, however, X-ray quality crystals were not grown.

X-ray structures of five of the above organometallic complexes have been obtained, as well as six X-ray structures of intermediates formed during the syntheses of their ligands.

To Mum, Dad, Andy and Ali.

Table of Contents

Abstract	i
Acknowledgements	ii
Abbreviations	iii
Chapter 1: The Synthesis and Application of Transition Metal Complexes Containing Bidentate Cyclopentadienyl ligands.	1
1.1 General Introduction	1
1.1.1 Metallocenes	1
1.1.2 Chiral cyclopentadienyl complexes	1
1.1.3 C ₁ vs C ₂ symmetry	3
1.1.4 Second coordinating group	4
1.1.5 Project aims	5
1.2 Planar Chiral complexes	5
1.2.1 By resolution	5
1.2.2 By face selective metallation	6
1.2.3 Steric control from a fused ring	6
1.2.4 A directing chiral metal complex	7
1.2.5 Elaboration of the cyclopentadienyl ligand on the metal	8
1.3 Cyclopentadienyl - Phosphorus bidentate complexes of group 8 metals.	9
1.3.1 Linked non-chiral cyclopentadienyl complexes	9
1.3.2 Linked planar chiral complexes	10
1.3.3 Induction of metal-centred chirality on complexation	15
1.3.4 Induction of planar- and metal-centred chirality on complexation of di-substituted ligands	16
1.4 Cyclopentadienyl–Amine bidentate complexes of group 8 and 9 metals.	20
1.4.1 General properties of nitrogen as a ligating heteroatom	20
1.4.2 Non-chiral linked cyclopentadienyl-N complexes	21
1.4.2.1 Group 8 metals	21
1.4.2.2 Group 9 metals	23

1.4.3 Chiral linked cyclopentadienyl-N complexes of group 9 metals	31
1.5 Indenyl complexes	32
1.5.1 The “Indenyl Ligand Effect”	33
1.6 Conclusions	34
Chapter 2: The optimisation of the synthesis of a bidentate indenyl phosphine ligand containing a three-carbon bridge	36
2.1 Background and Aims	36
2.2 The Harrison synthesis of <i>rac</i>-201	37
2.3 Optimised synthesis of <i>rac</i>-201	38
2.3.1 A novel catalytic indenyl anion addition reaction	38
2.3.2 Use of alternative ester groups	39
2.3.3 Direct formation of borane stabilised diphenylphosphine ligand	40
2.3.4 Final optimised synthesis of the three-carbon bridged ligand, <i>rac</i> -201	42
2.4 Alternative substituents along the indene-phosphine bridge	43
2.5 Increasing the length of the Cp-phosphine tether chain	44
2.6 Conclusions	46
Chapter 3: The synthesis of a chiral bidentate indenyl ligand containing a three-carbon bridge and coordinating ‘anchor’ group	47
3.1 Background and aims	47
3.2 Attempted synthesis of an enantiopure form of 206 using a chiral auxiliary	48
3.2.1 Synthesis using (1 <i>R</i> ,2 <i>S</i> ,5 <i>R</i>)-(-)-Menthol, 301	48
3.2.2 Synthesis using (7 <i>R</i>)-10,10-dimethyl-5-thia-4-azatricyclo[5.2.1.0 ^{3,7}]decane-5,5-dioxide, 304	49
3.2.3 Synthesis using sulfonamide-isoborneol, 312	51
3.2.4 Synthesis using catalytic BuLi/sparteine	59
3.3 Synthesis by nucleophilic displacement of a chiral secondary alcohol	60

3.3.1 Asymmetric hydrogenation of a β keto ester	61
3.3.2 Synthesis of enantiopure alcohol, (<i>S</i>)-206	64
3.4 Synthesis of an enantiopure phosphine ligand, (<i>S</i>)-201	65
3.5 Conclusions	65
4. Chapter 4: The optimisation and synthesis of novel ruthenium complexes	67
4.1 Background and aims	67
4.2 The optimisation and synthesis of complexes	68
4.2.1 Optimised synthesis of <i>rac</i> -401	68
4.2.2 Synthesis of enantiopure (<i>S</i>)-402	69
4.3 Synthesis of cationic complexes	72
4.4 Attempted synthesis of ruthenium tetrahydroindenyl complexes	74
4.5 Ligand substitution reactions	76
4.5.1 Slip parameter of ruthenium complexes	80
4.6 Conclusions	81
5. Chapter 5: Catalytic studies of ruthenium complexes	82
5.1 Background and aims	82
5.1.1 Olefin cyclopropanation and ROMP	82
5.1.2 Ruthenium-catalysed allylic substitution	83
5.1.3 Hydrogenation	85
5.1.4 Transfer hydrogenation	85
5.2 Conclusion	86
6. Chapter 6: The synthesis of a chiral bidentate indenyl ligand containing a three-carbon bridge and co-ordinating amine ‘anchor’ group and subsequent complexation onto transition metals	87
6.1 Background and aims	87
6.2 Synthesis of amine ligands	88
6.2.1 Synthesis of racemic ligands with a substituent <i>alpha</i> to the indene ring.	88
6.2.2 Synthesis of chiral ligands with a substituent <i>alpha</i>	

to the indene ring	93
6.2.3 Synthesis of ligands without a substituent <i>alpha</i> to the indene ring	93
6.3 Complexation of amine ligands without a substituent <i>alpha</i> to the indene ring to rhodium	94
6.3.1 Complexation of the dimethylamine ligand, 616	94
6.3.2 Complexation of the primary amine ligand , 614	97
6.3.3 Complexation of the tosylamine ligand, 618	99
6.4 Conclusions	103
7. Chapter 7: Conclusions and further work	104
7.1 Conclusions	104
7.2 Further work	105
8. Chapter 8: Experimental	107
8.1 General Techniques	107
8.1.1 Air and moisture sensitive manipulations	107
8.1.2 Spectroscopic techniques	107
8.1.3 Reagent purification	108
8.1.4 Chromatography	109
8.1.5 Miscellaneous	110
8.2 Experimental for Chapter 2	111
8.2.1. Optimised synthesis of <i>rac</i> -[3-cyclohexyl-3-(3 <i>H</i> -inden-1-yl)- propyl]diphenyl-phosphane, 201	111
8.3 Experimental for Chapter 3	125
8.3.1 Synthesis of (<i>S</i>)-[3-cyclohexyl-3-(3 <i>H</i> -inden-1-yl)-propyl] diphenyl-phosphane, 201	125
8.4. Experimental for Chapter 4	150
8.4.1. Synthesis of ruthenium complexes	150
8.5 Experimental for chapter 5	161
8.5.1. Catalytic reaction details	161
8.6 Experimental for Chapter 6	163

8.6.1. Synthesis of amine ligands and complex	163
References	184
Appendices	192
Appendix 1 X-ray Structure of sultam 308	
Appendix 2 X-ray Structure of alcohol 312	
Appendix 3 X-ray Structure of ester 321	
Appendix 4 X-ray Structure of Michael addition-precursor 320	
Appendix 5 X-ray Structure of Ruthenium complex (<i>S</i>)-401a	
Appendix 6 X-ray Structure of Ruthenium complex (<i>S</i>)-401a	
Appendix 7 X-ray Structure of Ruthenium complex 402	
Appendix 8 X-ray Structure of Ruthenium complex 417	
Appendix 9 X-ray Structure of Ruthenium complex 418	
Appendix 10 X-ray Structure of tosamide <i>rac</i>-608	
Appendix 11 X-ray Structure of spiro cycle 629	

For appendices 1 and 2, X-ray structure solutions by R. Whitby.

For appendices 3-11, X-ray structure solutions by M.Light.

Thanks to Simon Coles and Mark Light for the collection of the X-ray crystal data.

Acknowledgements

First of all I would like to thank my supervisor Prof. Richard Whitby for his ideas, enthusiasm and at times, endless patience over the last three and a bit years. Richard, you are anything but “the great big ogre” I once believed you were. Thank you also to my advisor Dr. Richard Brown for his help, ideas and the odd game of football. Thanks must also go to my CASE supervisor Cliff Veighey for his help and advice and to Robin Fieldhouse at Avecia for helpful chats about chemistry.

My research was made much easier by the excellent NMR and mass spec services provided by Joan and Neil, and John and Julie respectively. Thanks Dr. Mark Light for providing the X-ray crystallography service.

My Ph.D. would not have been quite so memorable without the company of my lab-mates. Thank you Dr. Aunt Sal Dixon and Dr. Dave Dossett for your help when I first arrived. Dr. Dave “Naughty” Norton, a good mate, was always helpful and good for going to the pub. Dr. Rupert Hunter is a good mate. His help and various musical talents were much appreciated and made me laugh. Emma Thomas was great fun to work beside. Kishore showed everyone how much can be learnt in a year. Thank you Dave Pugh! Your help with the hydrogen cylinder and with the catalytic studies were great. Thanks to Sofia, Pam, Lionel, Linda and Thomas too. Big Rich, Tim, Geoff, Dicko, Alex, Ian and Pascoe made the dept a fun place to be! Thank you Dave Pugh, Dr Hunter, Dr Naughty, Dr Sal, Dave Pascoe, Ian, Claire, Nev and Ali for your proof reading. Gud joab! Thank you Stanley for the memorable Sunday afternoons. We will never see your like again!

Anna, Laurie and Paddy were great housemates and provided many laughs at No. 92. Cheers to the boys back home (Andy, Craig, Dave, Jamie, Chris, Brownie, Martin and Del) for not forgetting. Thanks Geoff and Kath for putting a roof over my head in the final few months.

Thank you Mum, Dad and Andy for all your love and support, both emotional and financial, even though I have been quite a distance from home

Finally, a HUGE thank you to Ali. You have no idea how much you helped me get through the last three and a bit years, with your unique love and support and for being my bestest friend. **THANK YOU!**

Abbreviations

Techniques

CI	Chemical Ionisation
COSY	Correlation Spectroscopy
DEPT	Distortionless Enhancement by Polarisation Transfer
ES	Electrospray
EI	Electron Ionisation
GC	Gas Chromatography
HPLC	High Pressure Liquid Chromatography
HRMS	High Resolution Mass Spectrometry
LRMS	Low Resolution Mass Spectrometry
IR	Infra-red spectroscopy
NMR	Nuclear Magnetic Resonance
TLC	Thin Layer Chromatography

Reagents

<i>n</i> -BuLi	<i>n</i> -butyllithium
<i>s</i> -BuLi	<i>sec</i> -butyllithium
DMF	Dimethylformamide
DCC	N,N'-dicyclohexyl-carbodiimide
TBAF	Tetrabutylammonium fluoride
HMPA	Hexamethylphosphoramide
TMEDA	<i>N,N,N',N'</i> -Tetramethylethylenediamine
THF	Tetrahydrofuran
dppm	bis(diphenylphosphine)methane
BINAP	2,2'-bis(diphenylphosphine)-1,1'-binaphthyl
MeO-BIPHEP	(6,6-dimethoxybiphenyl-2,2'-diyl)bis(diphenylphosphine)
coe	cyclooctene
cod	1,5-cyclooctadiene

Chemical groups

Me	Methyl
Et	Ethyl

<i>i</i> -Pr	<i>i</i> -Propyl
<i>t</i> -Bu	<i>t</i> -Butyl
<i>n</i> -Bu	<i>n</i> -Butyl
Cp	Cyclopentadienyl
Cy	Cyclohexyl
Bn	Benzyl
TBDMS	<i>tert</i> -Butyldimethylsilyl
Tf	Trifluoromethansulfonyl
Ms	Methanesulfonyl
Ind	Indenyl
Ts	Toluenesulfonyl
THT	Tetrahydrothiophene

Miscellaneous

h	Hour(s)
min	Minute(s)
RT	Room temperature
m.p.	Melting Point
e.e.	Enantiomeric excess
d.e.	Diastereomeric excess
cat.	catalytic
lit.	literature

Chapter 1: The Synthesis and Application of Transition Metal Complexes Containing Bidentate Cyclopentadienyl ligands.

1.1 General Introduction

1.1.1 Metallocenes

Following the discovery of the metallocene ferrocene **1** in 1951,¹ there has been great interest in organometallic chemistry. Metallocene complexes consist of two cyclopentadienyl ligands, which are η^5 -bonded to the metal centre to form a sandwich structure. Half sandwich complexes such as **2** consist of one cyclopentadienyl ligand which is η^5 -bonded to the metal centre are also of interest to the organometallic chemist (Figure 1.1).²

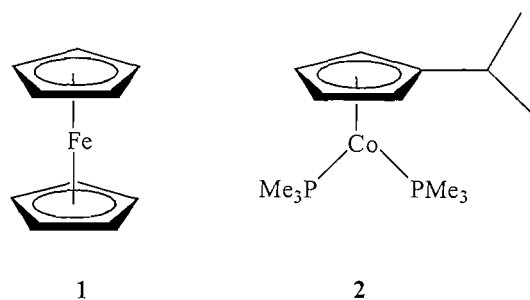


Figure 1.1

1.1.2 Chiral cyclopentadienyl complexes

Organometallic complexes containing chiral ligands are becoming increasingly important in synthetic chemistry as catalytic or stoichiometric mediators of organic transformations.² The application of cyclopentadienyl ligands as a support for introducing chirality is attractive due to their synthetic diversity and the strength of the metal-cyclopentadienyl bond. An organometallic complex may be chiral due to coordination of chiral or achiral ligands to a non stereogenic metal as shown by Kagan's chiral neomenthyl cyclopentadienyl complex **3** (Figure 1.2).³

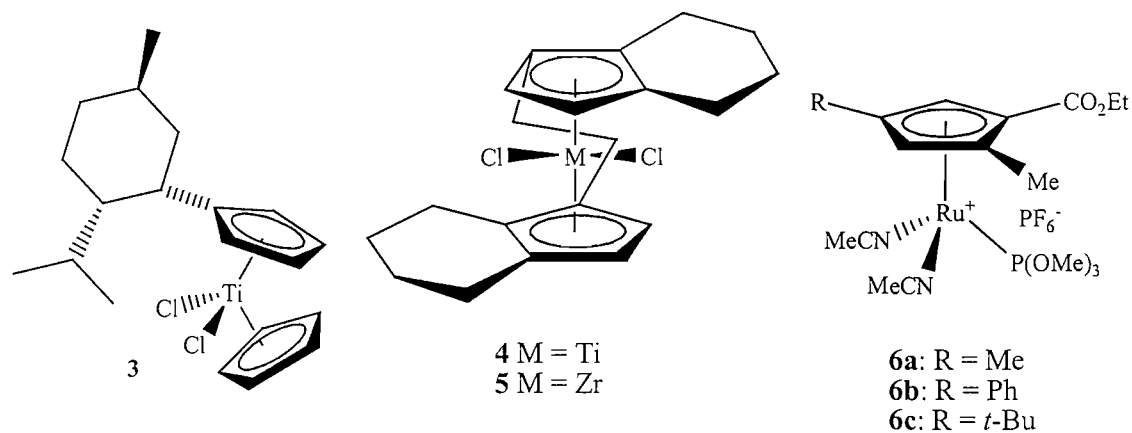


Figure 1.2

Another type of chiral cyclopentadienyl metal complex depends on how the two faces of the ligand are related to each other. Metallocenes **4** and **5** are chiral by virtue of planar chirality of a non-symmetrically substituted cyclopentadienyl ligand.^{4,5} Complex **5** is active in asymmetric carbomagnesiations giving products with high optical purity.⁶ However, C₂-symmetric complexes such as **4** and **5** do have disadvantages. The faces of the cyclopentadienyl rings of the ethylene-bridged indene ligand are enantiotopic; therefore on complexation to titanium and zirconium, mixtures of enantiomers and meso compounds are formed (Figure 1.3).^{4,5} To provide the homochiral catalyst, these enantiomers must be resolved by derivatisation, thus making the preparation of enantiomerically pure complexes **4** and **5** problematic and expensive. Recovery from catalytic reactions is difficult.⁷ The reduction in catalytic activity is a common feature of the bulky C₂-symmetric metallocenes, and can be attributed to crowding of the metal centre by the sterically demanding ligands. Takahashi's complex **6** is an example of a non-linked planar complex in which the faces of the cyclopentadienyl ligand are enantiotopic (Figure 1.2).⁸

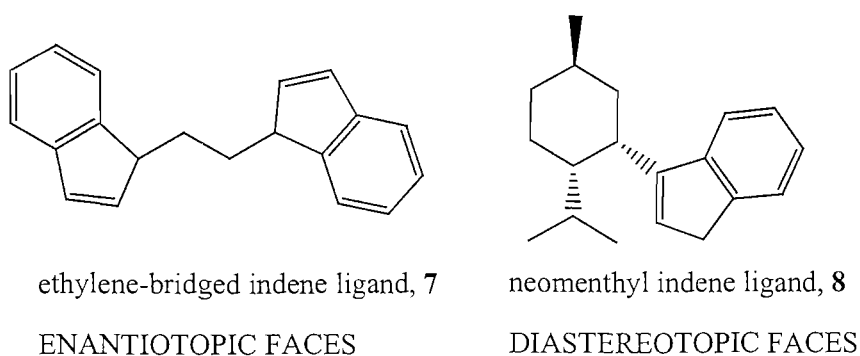


Figure 1.3

Using the chiral 1-neomenthyl ligand **8**, the non C_2 -symmetric chiral zirconocene **9** has been synthesised.^{9,10} Complex **9** has been found to be an efficient asymmetric ethylmagnesium catalyst, giving better results than Brintzingers catalyst **5** in some cases (Figure 1.4).

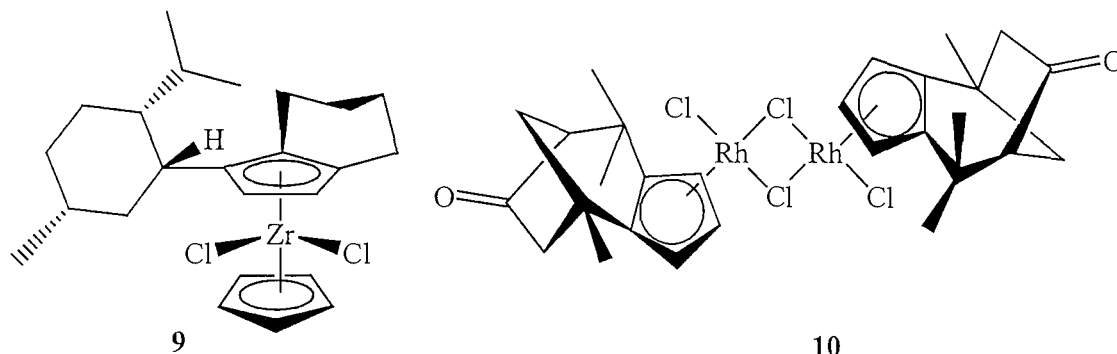


Figure 1.4

The presence of a chiral menthyl group in the neomenthylindene ligand **9**, makes the faces of the cyclopentadienyl ring diastereotopic. Thus on complexation to $CpZrCl_3$, a 20:1 mixture of diastereomers is formed and the major isomer **9** is isolated by recrystallisation.⁷ Direct metallation of annulated chiral cyclopentadienyl ligands is another method of preparing planar chiral complexes. An example of this is complex **10**.¹¹

1.1.3 C_1 vs C_2 symmetry

Both the C_1 and C_2 metallocenes may induce chirality in a reaction through interactions between the substrate and the ligand. For complex **5**, the alkene substrate would approach the metal centre of the C_2 -symmetric complex with the large substituent **R**, oriented away from the ligand. Approach from both sides of the complex would occur from the same enantioface of the substrate, thus allowing asymmetric catalysis to occur (Figure 1.5).

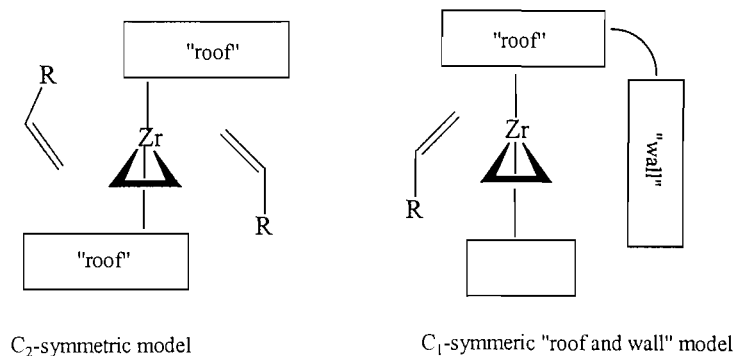


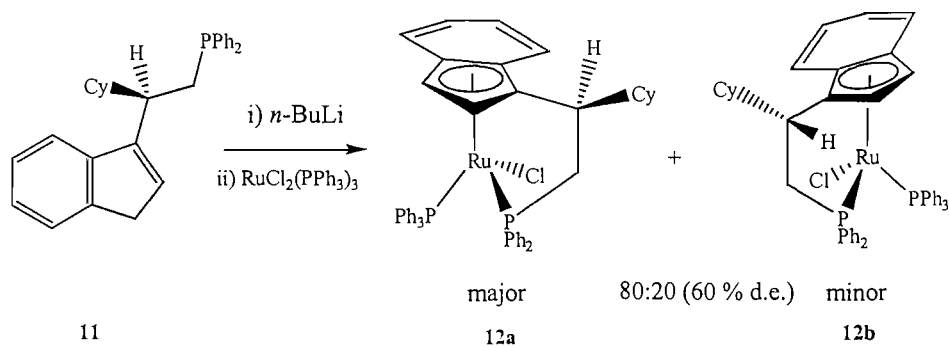
Figure 1.5

For the C₁-symmetric design developed by the Whitby group, the alkene substrate is forced to approach the metal centre from one side by a steric blocking “wall”, with the most bulky alkene substituent pointing away from the sterically hindered “roof”. This favours reaction at a particular enantioface. Whitby has demonstrated the effectiveness of the C₁-symmetric catalyst design.^{7,9,10}

1.1.4 Second coordinating group

The Whitby group is now focusing its efforts on extending the chiral cyclopentadienyl work to later transition metals.¹² The design of **9** is not suitable for these metals as the 12 electrons from the cyclopentadienyl ligand renders the complex coordinatively saturated and catalytically inactive. Therefore, we have chosen to concentrate on mono cyclopentadienyl complexes.

An important class of ligands are the bifunctional cyclopentadienyl ligands. They have a heteroatom attached to the cyclopentadiene *via* a covalent tether, typically an alkyl chain. Complexation of these ligands to a metal centre allows access to chelate complexes where the metal centre is bonded to both the cyclopentadienyl and heteroatom group, and is thus a powerful strategy for modifying the chemistry of cyclopentadienyl transition metal complexes.^{12,13} Comprehensive reviews on cyclopentadienyl ligands with pendant donors have appeared that have focused on nitrogen,^{14,15} oxygen,¹⁶ phosphorus,¹⁷ arsenic¹⁷ and sulfur¹⁷ donors. Harrison has recently synthesised indenyl systems **12a** and **12b** which induce planar chirality by the use of a chiral linking group with a diphenylphosphine group to direct metallation (Scheme 1.1).¹³



Scheme 1.1

Modification of the cyclopentadiene, the length of the alkyl spacer and the coordinating heteroatom should allow the design and synthesis of metal complexes with unique and “tailored” properties.

1.1.5 Project aims

The aim of this project is to synthesise novel complexes of chiral cyclopentadienyl ligands with a linked coordinating group. Then to use these complexes for production of synthetically useful chiral materials.

1.2 Planar Chiral Complexes

1.2.1 By Resolution

Resolution techniques have been developed for metallocenes **4** and **5**.^{4,5} One of these procedures involves the displacement of the chloride ligands with the chiral ligand (*S*)-binaphthol, **13**.⁴ However, only the (*S,S*) enantiomer is isolated with the (*R,R*) enantiomer being only partially purified. On the other hand, using *O*-acetyl-*R*-mandelic acid, **14** the separated diastereomers have been converted, *via* their dimethyl derivatives, into the corresponding titanocene and zirconocene enantiomers (Figure 1.6).⁵

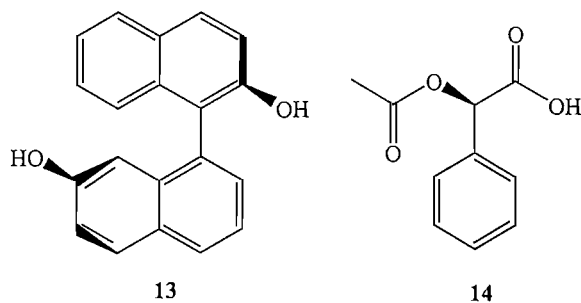
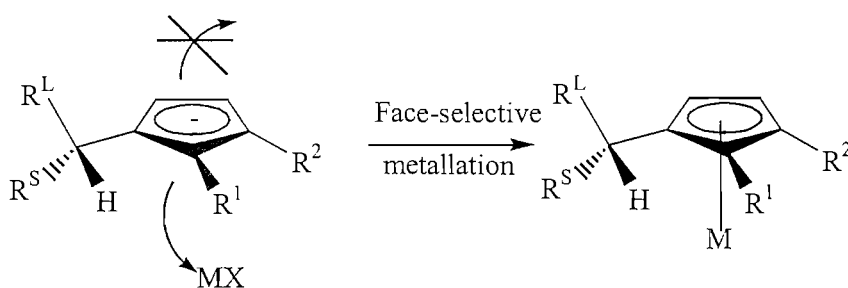


Figure 1.6

1.2.2 By Face Selective Metallation

By incorporating a chiral design into the ligand that enables preferential complexation of the metal to only one face of the cyclopentadiene, wasteful resolution and chromatographic techniques would be avoided. The presence of three different sized substituents (R^L , R^S , H) form a chiral centre next to the cyclopentadienyl-ring. The differing steric demands of these substituents result in one face of the cyclopentadiene being effectively blocked by the large R group in its lowest energy rotamer about the cyclopentadienyl-chiral centre bond. This leads to metallation occurring preferentially on the more accessible cyclopentadiene face with the outcome being the formation of a major diastereoisomer of the resulting planar-chiral complex (Scheme 1.2).



Scheme 1.2

1.2.3 Steric control from a fused ring

Another way of forming planar chiral complexes is by utilising chiral annulated bicyclic cyclopentadienyl ligands. Such ligands provide structural rigidity and face selective complexation depends on the relative steric hindrance on either side of the cyclopentadienyl. Starting from camphor, the chiral annulated cyclopentadiene **15** has

been synthesised,¹⁸⁻²⁰ and starting from verbenone the chiral annulated cyclopentadiene **16** has been synthesised (Figure 1.7).²¹

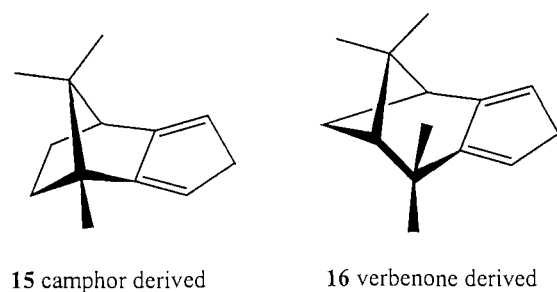
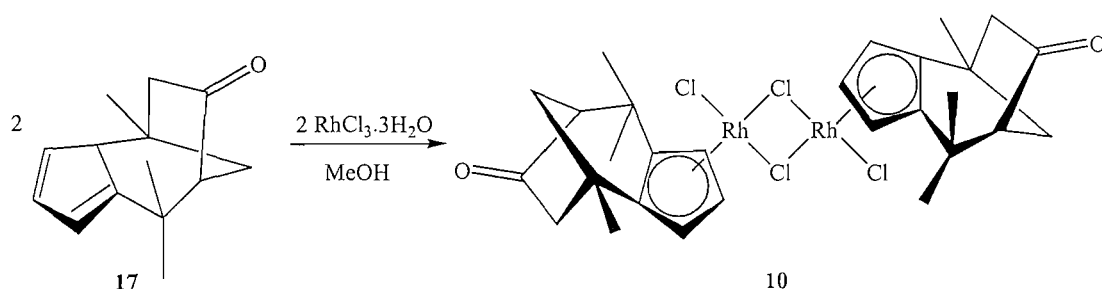


Figure 1.7

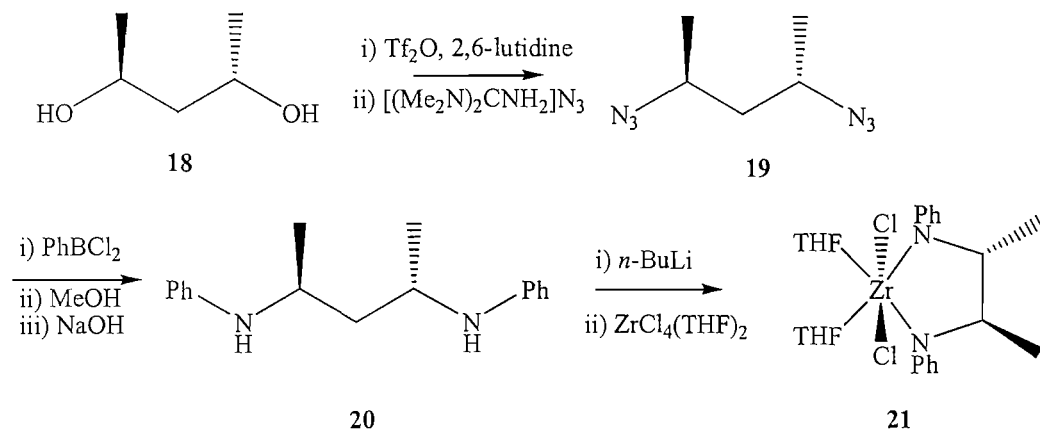
Green found refluxing chiral cyclopentadienyl **17** in methanol gave **10** as a single diastereomer (Scheme 1.3).¹¹ X-ray crystallography confirmed that complexation of the ligand occurred exclusively from the opposite face of the cyclopentadienyl ring to the ethano bridge.



Scheme 1.3

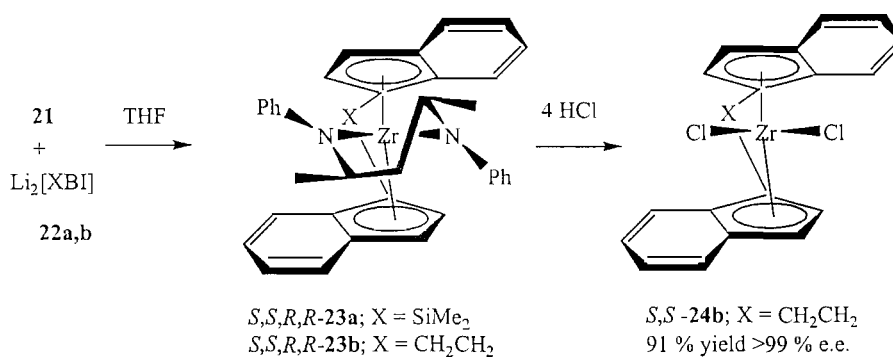
1.2.4 A directing chiral metal complex

Another way of forming planar chiral complexes is by directing the metal onto one face of an enantiotopic ligand using a chiral metal complex.²² Jordan has reported a diastereoselective “chelate-controlled” synthesis of racemic *ansa*-metallocenes, which is based on the reaction of $\text{Li}_2[\text{Cp}'\text{XCp}']$ salts with chelated bis-amide compounds.^{23,24} Starting from (2*S*,4*S*)-pentanediol, **18** the zirconium amine complex **21** was prepared as shown (Scheme 1.4).²²



Scheme 1.4

Subsequent reaction of **21** with Li[SBI](Et₂O) (**22a**) or Li[EBI](Et₂O) (**22b**) affords the corresponding metallocenes *S,S*-(SBI)Zr{(2*R*,4*R*)-PhNCHMeCH₂CHMeNPh} (*S,S,R,R*-**23a**) or *S,S*-(EBI)Zr{(2*R*,4*R*)-PhNCHMeCH₂CHMeNPh} (*S,S,R,R*-**23b**) in high yield.¹ A single set of resonances in the ¹H NMR spectra of **23a** and **23b**, suggested one diastereomer being formed in each case. Complex **23b** was converted to the corresponding enantiomerically pure dichloride *S,S*-**24b** by reaction with HCl, and chiral diamine **20** was recovered. The configurations of **23a** and **24b** were confirmed by X-ray crystallography (Scheme 1.5).²²



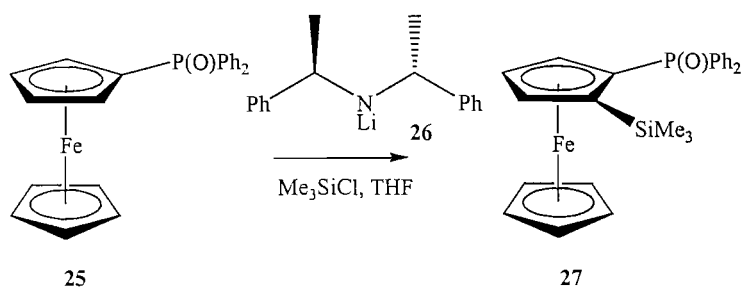
Scheme 1.5

1.2.5 Elaboration of the cyclopentadienyl ligand on the metal

Another way of forming planar chiral complexes is by using a chiral base such as **26**.²⁵ An example is the asymmetric metallation of **25** to give the silyl substituted product **27**, which was accomplished in 95 % yield and 54 % e.e using the chiral

¹ SBI, Me₂Si(indenyl)₂; EBI, 1,2-ethylene-bis(indenyl).

lithium amide base **26** (Scheme 1.6).²⁵ Attempts to extend this reaction to other ferrocenes were unsuccessful.



Scheme 1.6

1.3 Cyclopentadienyl – Phosphorus bidentate complexes of group 8 metals.

The amount of research into chemistry of the half-sandwich complexes of group 8 elements (Fe, Ru, Os) incorporating the intramolecular coordination of a pendant diphenylphosphine group is contrasting.¹⁷ A lot of the work has been done on the coordination of diphenylphosphine to ruthenium metal centres.¹⁷ However, there has been limited research into half-sandwich complexes featuring the coordination of a diphenylphosphine group to osmium and iron metal centres.^{26,27}

1.3.1 Linked non-chiral Cyclopentadienyl complexes

Bidentate ligands have proven important in a number of complexes, some of which are valuable in a number of catalytic processes. Ligands of this type can have identical (homobidentate) or different (heterobidentate) ligating groups. Cyclopentadienyl-phosphine ligands are heterobidentate ligands and have unique properties. Whereas a phosphine is a neutral donor and often subjected to ligand exchange processes, the cyclopentadienyl ligand is anionic and tightly bound to a metal. Complexes of cyclopentadienyl-phosphine bidentate ligands have been recently reviewed.¹⁷ Figure 1.8 shows some examples of ruthenium cyclopentadienyl-linked complexes.

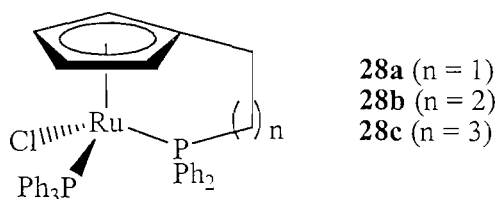
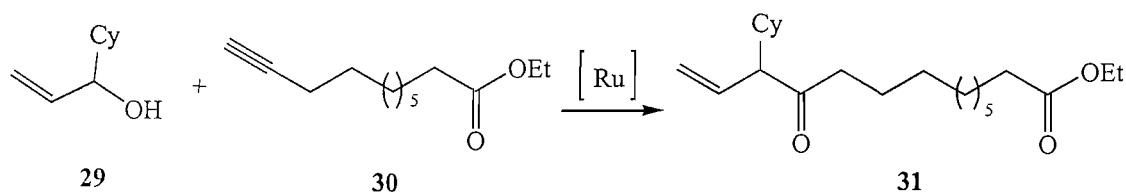


Figure 1.8

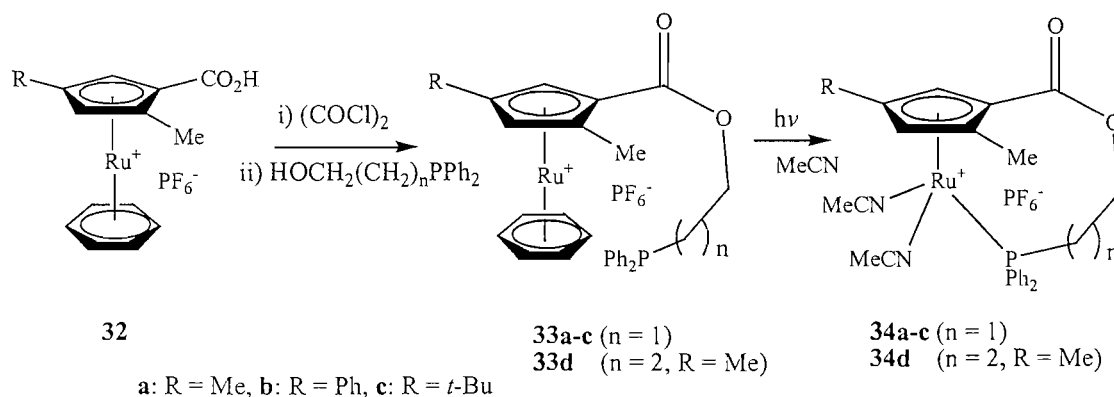
The first ruthenium cyclopentadienyl-phosphine alkyl-linked complexes **28a-c** were prepared by the reaction of the cyclopentadienyl-ligand with $\text{RuCl}_2(\text{PPh}_3)_3$, but they were incompletely characterised.^{28,29} However, **28a** was later fully characterised by an X-ray structure.³⁰ Complexes **28a-c** have found use as catalysts in the reconstitutive addition reaction between allylic alcohols and terminal alkynes (Scheme 1.7).²⁹



Scheme 1.7

1.3.2 Linked Planar Chiral complexes

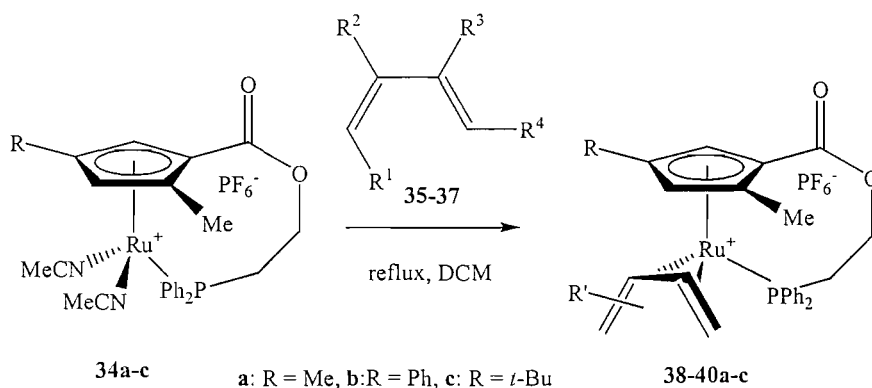
Takahashi has synthesised planar-chiral ruthenium complexes with bidentate cyclopentadienyl-pyridine and cyclopentadienyl-phosphorus ligands (Scheme.1.8).³¹



Scheme 1.8

With the presence of the strongly bonded η^6 -benzene ligand, in complexes **33a-d**, there is no coordination of the phosphine group to the ruthenium metal centre. After irradiation by UV light in acetonitrile, the difference in chemical shifts of the ³¹P NMR signals strongly suggested the coordination of the phosphine group to the metal centre.^{31,32} The phosphorus-ruthenium coordination was found to be independent of solvent, indicating the phosphorus was tightly bound to the ruthenium metal centre.³¹

Takahashi has investigated enantioface-selective complexation of pro-chiral dienes on planar-chiral cyclopentadienyl-ruthenium complexes.³³ However, the rotation of the cyclopentadienyl ring was inadequate for the construction of a rigid chiral environment around the active metal centre. This problem was solved with the synthesis of planar-chiral complexes **34a-d**, which possess an anchor phosphine ligand.^{31,34} Complexes **34a-c** were able to control the metal-centred chirality in some ligand exchange reactions and were used as a new catalyst for asymmetric allylic amination and alkylations with high enantioselectivity.³⁵ Takahashi has recently investigated the complexation of cyclopentadienyl-ruthenium complexes **34a-c** with prochiral dienes, **35-37**, giving complexes **38-40a-c** (Scheme 1.9).^{33,34}



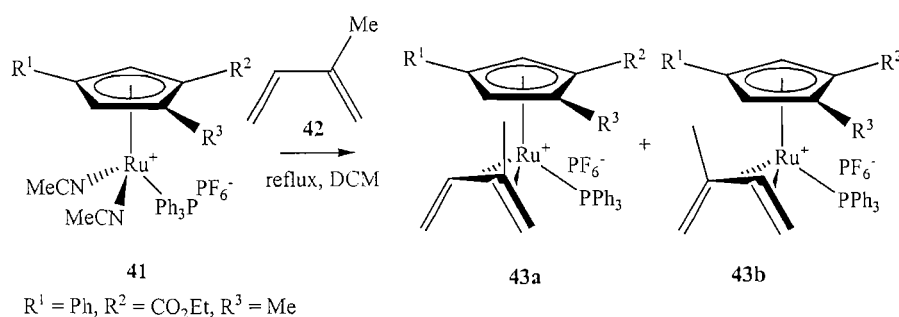
Scheme 1.9

The selectivity is controlled by the thermodynamic stability of the resulting diene complexes. Reaction of **34b** produces η^4 diene complexes with similar diastereoselectivities to **34a**. The steric effects of the methyl and phenyl group in complexes **34a** and **34b** are similar. Reaction of **34c** produces η^4 diene complexes with higher selectivities than those obtained with both **34a** and **34b**. The higher diastereoselectivity in the reactions of complex **34c** is derived from the larger steric repulsion between the *tert*-butyl group and the substituents on the diene. A selection of the results are shown in Table 1.1.

Complex	R ¹	R ²	R ³	R ⁴	Product	Yield (%)	d.e (%)
34a	H	H	H	Me	38a	93	34
34a	H	H	Me	H	39a	90	82
34a	H	H	Ph	H	40a	87	86
34b	H	H	H	Me	38b	86	36
34b	H	H	Me	H	39b	90	86
34b	H	H	Ph	H	40b	92	81
34c	H	H	H	Me	38c	74	66
34c	H	H	Me	H	39c	69	84
34c	H	H	Ph	H	40c	91	98

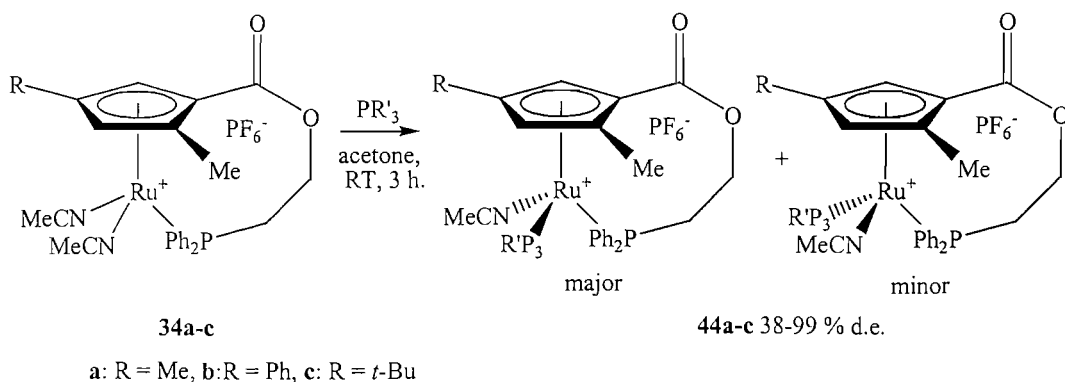
Table 1.1

Complex **41** has no anchored phosphine ligand and upon reaction with **42**, complex **43** was isolated in 83 % yield (Scheme 1.10).³⁴ The diastereoselectivity achieved (44 % d.e) was lower than that in a similar reaction with **34b**. This suggests that the anchor phosphine ligand prevents the rotation of the Cp ring and assists in the construction of an effective asymmetric environment by planar chirality.³⁴



Scheme 1.10

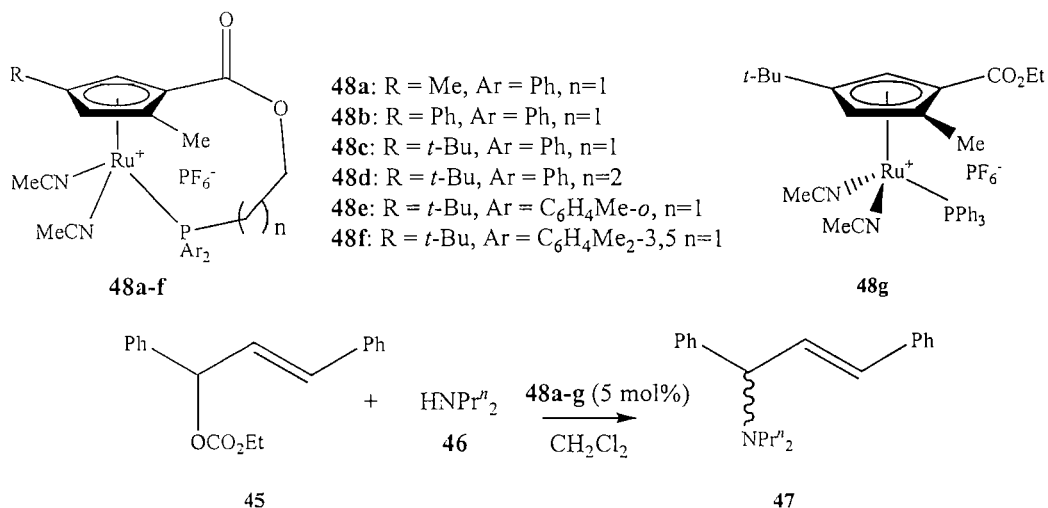
Takahashi has examined the induction of metal-centred chirality by the planar-chirality of ruthenium complexes **34a-c** containing cyclopentadienyl phosphine bidentate ligands, during an acetonitrile/phosphine ligand exchange reaction (Scheme 1.11).⁸



Scheme 1.11

The reaction was performed using a variety of phosphine ligands, and in almost all cases the reaction proceeded with quantitative yield.⁸ Clear trends were observed in the stereochemical outcome of the reaction. The highest diastereoselectivities were observed when the substituent on the cyclopentadienyl ligand was bulky (**34c**, R = *t*-Bu), or the incoming phosphine ligand contained bulky groups (e.g. PPh₃ or PBU₃). Selectivities were reduced when the substituent on the cyclopentadienyl ligand was small (**34a**, R = Me) or the phosphine ligand PMe₃ was used.⁸ The products of the reaction of triphenylphosphine with **34a** and **34b** were found to slowly isomerise at the metal centre in solution at RT.

Having found that ruthenium complexes **34a-c** can control metal centred-chirality with high selectivity, Takahashi decided to test them for catalytic activity. Initial experiments focused on allylic aminations involving reaction of allylic carbonate **45** with di-*n*-propylamine **46** (Scheme 1.12).³⁵



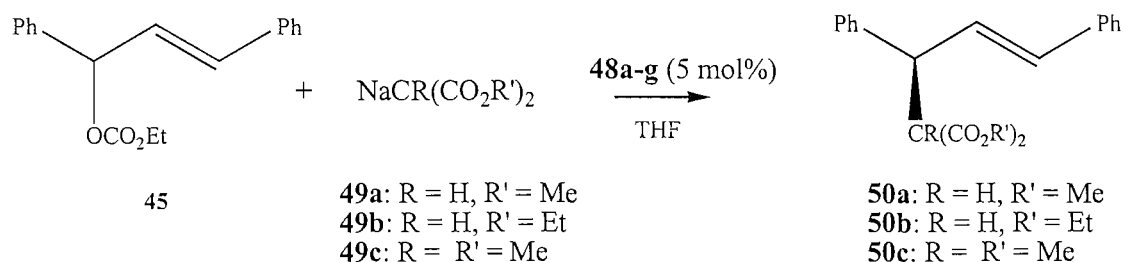
Scheme 1.12

It can be seen that complex **48a** gave similar results to **48b**, however the product had an opposite specific rotation. The reaction catalysed by **48g**, which has no tether between the cyclopentadienyl and phosphine ligands, gave comparable enantioselectivity to other complexes. Overall it appears that bulky substituents on the cyclopentadienyl ring and on the phosphine gave the best results (Table 1.2).³⁵

Catalyst	Conversion(%)	Yield(%)	e.e(%)
(<i>S</i>)- 48a	100	97	35(-)
(<i>S</i>)- 48b	98	90	20(+)
(<i>S</i>)- 48c	100	99	64(+)
(<i>S</i>)- 48d	100	94	56(+)
(<i>S</i>)- 48e	100	93	57(+)
(<i>S</i>)- 48f	100	98	74(+)
(<i>S</i>)- 48g	93	86	65(+)

Table 1.2

Ruthenium complexes **48a-g** also catalysed allylic alkylation with high enantioselectivity and yields. The reaction of allylic carbonate **45** with sodium malonates **49a-c** was investigated (Scheme 1.13).³⁵



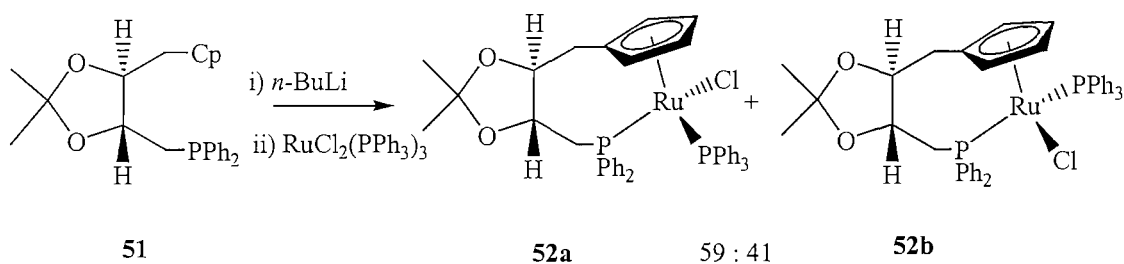
Scheme 1.13

It was found that the tether dramatically affected not only the enantioselectivity of the product but also the reactivity of the catalyst. In contrast to the amination reaction, the substituents on the aromatic rings on the anchor phosphine had little influence on the enantioselectivity in alkylation. In addition complex **48g** hardly catalysed the alkylation at all (3 % yield). In all cases the configurations of the products with **48a** were opposite to those obtained with other complexes. This suggests that the

substituents at the 4-position of the cyclopentadienyl ring play a vital role in controlling the stereochemistry in the reactions.

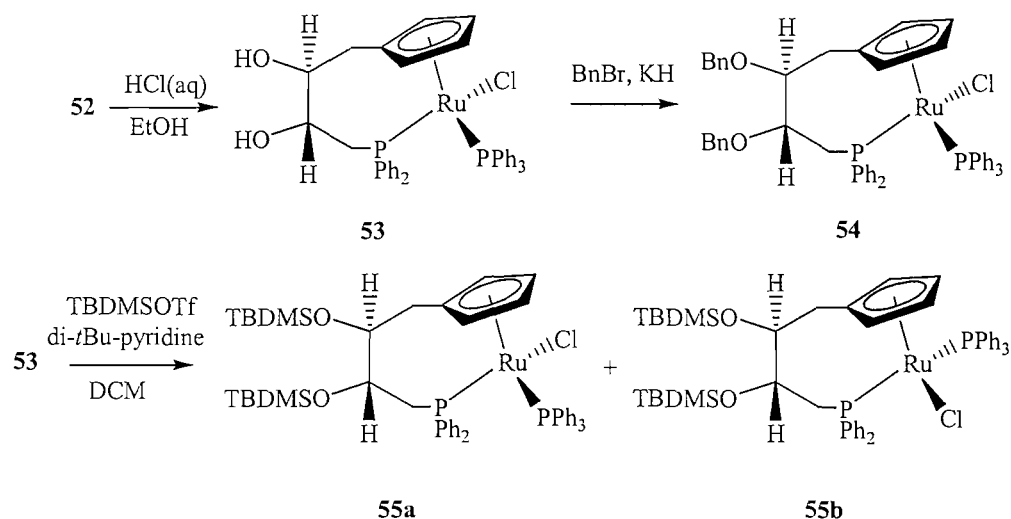
1.3.3 Induction of metal-centred chirality on complexation

The reaction of the lithium salt of the chiral cyclopentadienyl-phosphine bidentate ligand **51** with $\text{RuCl}_2(\text{PPh}_3)_3$ gave **52** in 49 % yield (Scheme 1.14).³⁶ The ^{31}P NMR spectrum revealed that **52** is formed as a mixture of two diastereoisomers **52a** and **52b**, in a 59:41 ratio, suggesting the generation of a new chiral centre at the metal. With a low 18 % d.e., this suggests the chiral information in the ligand is too far away from the metal centre to effectively induce metal-centred chirality.



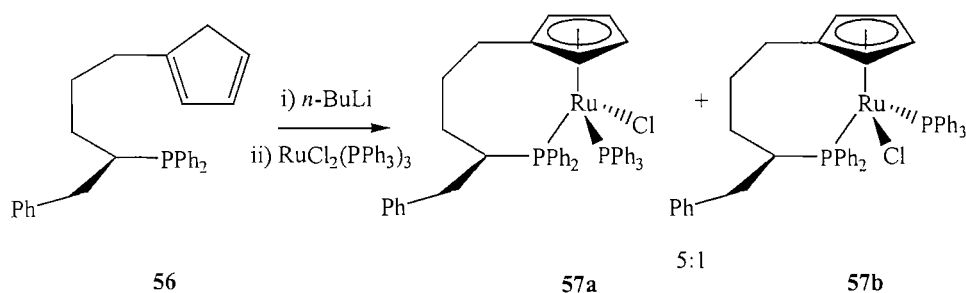
Scheme 1.14

Trost repeated the synthesis in Scheme 1.14, and found **52** forms as a 1.5:1.0 diastereomeric mixture at the ruthenium centre.²⁹ Attempts to increase this ratio involved modifying the diol protecting groups. This was done by initial cleavage of the acetonide using aqueous hydrochloric acid in ethanol, giving **53**. (Scheme 1.15) Subsequent Williamson ether synthesis yielded the dibenzyl ether complex **54**. However, the ratio of diastereomers remained at 1.5:1.0. Formation of the *tert*-butyldimethyl silyl derivative gave the diastereomeric complexes **55a** and **55b**, which were separated using preparative HPLC. Both isomers were stable at room temperature, but it was found that heating either isomer to 80 °C in toluene causes isomerisation to occur, restoring the 1.5:1.0 ratio, suggesting a thermodynamic ratio.



Scheme 1.15

Trost wanted to design a ligand that would generate a complex with a higher thermodynamic bias for one of the two isomers. One idea involved moving the chirality of the scaffold closer to the phosphorus and thus closer to the ruthenium atom (Scheme 1.16).²⁹



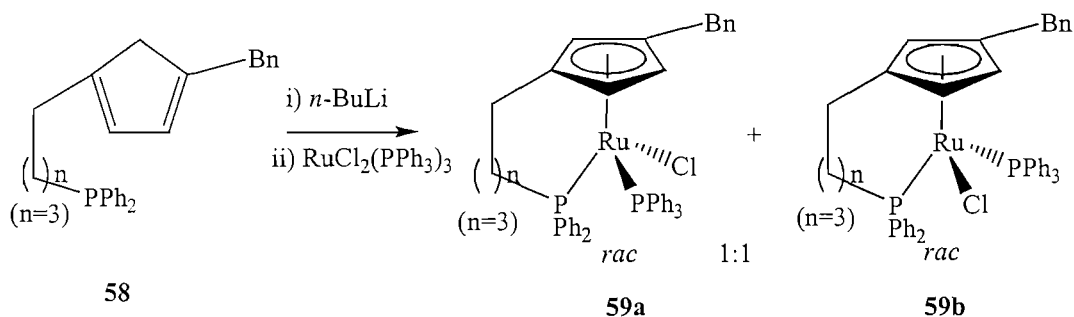
Scheme 1.16

Complexation of the lithium salt of **56** with $\text{RuCl}_2(\text{PPh}_3)_3$ gave the asymmetric complex **57**. Placement of the stereogenic centre closer to the phosphine-metal binding was advantageous, with the diastereomeric ratio of **57a** and **57b** increasing to 5:1 (Scheme 1.16).²⁹

1.3.4 Induction of planar- and metal-centred chirality on complexation of di-substituted ligands

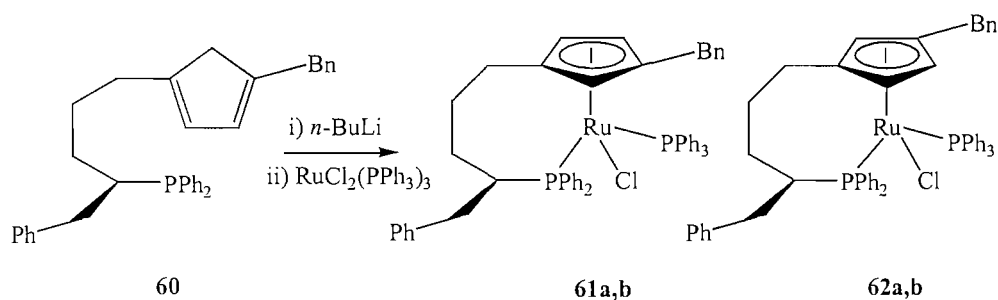
Trost reported that reaction of the lithium salt of the cyclopentadienyl ligand **58** with $\text{RuCl}_2(\text{PPh}_3)_3$ gave complex **59** as a 1:1 mixture of diastereomers (Scheme 1.17).²⁹ No

control was observed at the metal centre, but **59a** and **59b** could be separated by flash column chromatography. Complex **59** was found to be an active catalyst in the reconstitutive addition reaction.²⁹



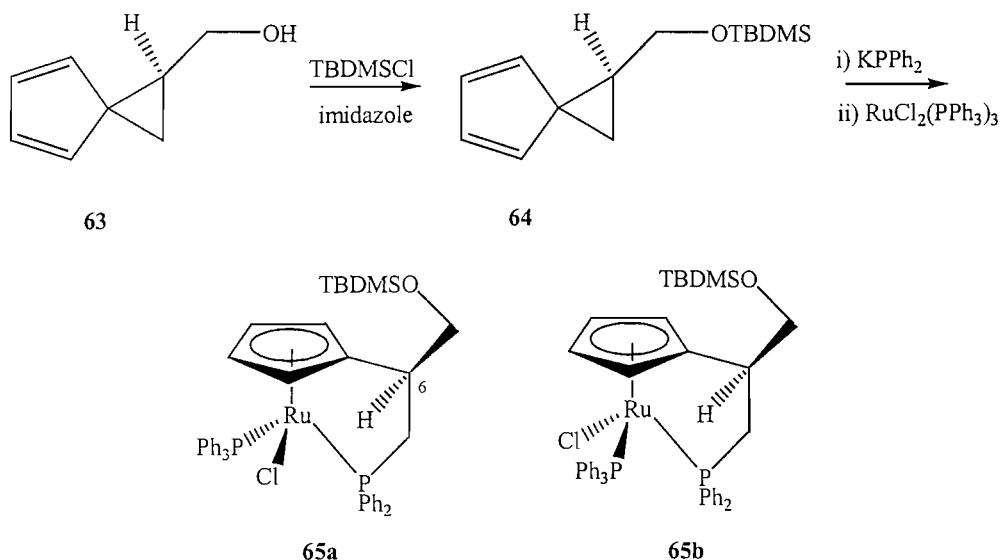
Scheme 1.17

Trost also reports reaction of the lithium salt of the benzylcyclopentadiene ligand **60** with RuCl₂(PPh₃)₃, giving a complex mixture of all four diastereomeric complexes. The complexity of the spectra made the determination of the exact ratio of **61a,b** and **62a,b** impossible (Scheme 1.18).²⁹



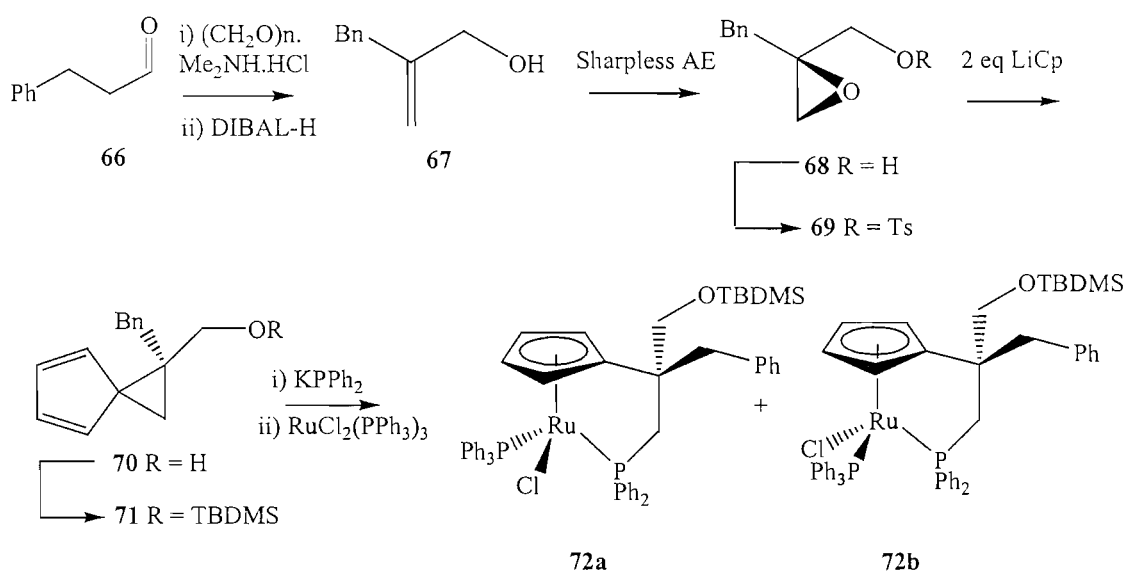
Scheme 1.18

Pagenkopf has reported the use of potassium diphenylphosphide as an efficient nucleophile for the ring opening of chiral spiro[2.4]hepta-4,6-dienes.³⁷ Whitby also used this method in the synthesis of planar chiral complexes, inducing metal centred chirality.³⁸ Addition of RuCl₂(PPh₃)₃ to a solution of the cyclopentadienyl anion generated from the cyclopropane ring opening reaction of **64** by KPh₂, afforded the ruthenium complex **65** as a 1:1 mixture of diastereomers (Scheme 1.19).³⁷ The diastereoisomers **65a** and **65b** were separated using flash chromatography on silica gel in 68 % yield. The structure of **65a** was confirmed by X-ray crystallography.



Scheme 1.19

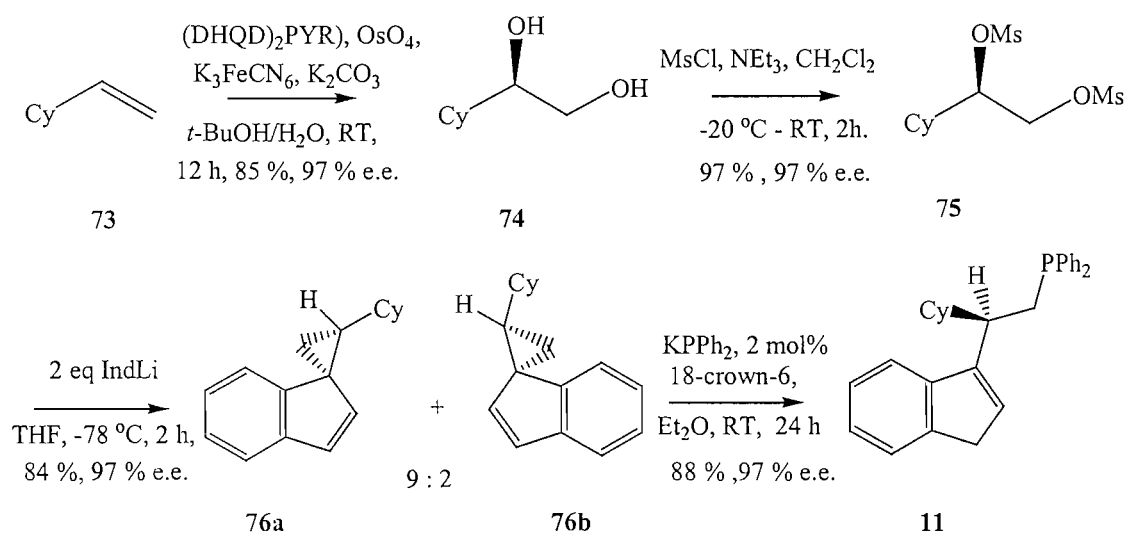
To explore the effects of tether substitution, Pagenkopf prepared a complex analogous to **65a** wherein the tether methine hydrogen at C6 was replaced with a benzyl group.³⁷ Allylic alcohol **67** was made in good yield from dihydrocinnamaldehyde using standard procedures.³⁹ After Sharpless asymmetric epoxidation, **68** was converted to tosylate **69**, and alkylation with 2 equivalents of lithium cyclopentadiene gave the substituted spiroheptadiene **70** in 82 % yield. Addition of KPPh_2 to **71** and trapping of the resultant Cp anion *in situ* with $\text{RuCl}_2(\text{PPh}_3)_3$ gave a planar chiral complex **72** with metal centred chirality in 54 % yield and as a 2:1 mixture of diastereoisomers (Scheme 1.20).³⁷ The structure of **72a** was confirmed by X-ray crystallography.



Scheme 1.20

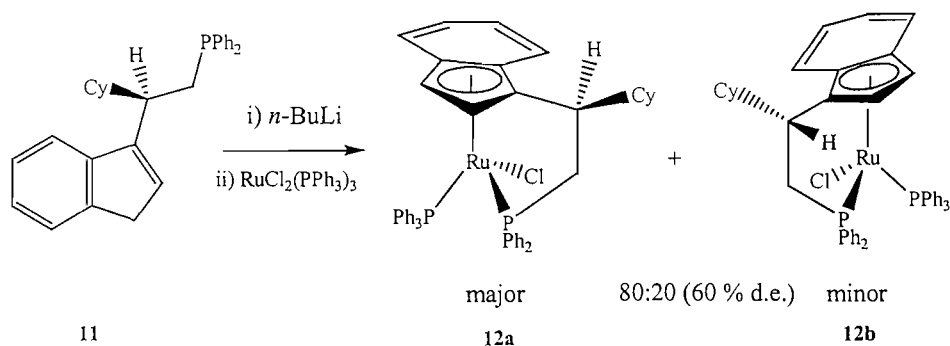
Substitution at C6 causes tether twisting, resulting in contraction of the P1-Ru-Cp bond angle.³⁷ The twisting occurs in order to minimize the quasi-1,3-allylic strain between the hydrogens on C2 and C3 of the cyclopentadiene and the α -substituents on the C6 of the tether.⁴⁰

Harrison has reported the synthesis of chiral ligand **11**.¹³ After initial Sharpless asymmetric dihydroxylation of vinylcyclohexane **73**, subsequent mesylation and reaction with two equivalents of indenyl lithium gave **76**. Treatment of spirocycle **76** with KPPH₂ in THF and catalytic 18-crown-6 provides the chiral air sensitive cyclopentadienyl ligand **11** in 4 steps, and 61 % overall yield and 97 % e.e (Scheme 1.21).¹³



Scheme 1.21

The reaction of the lithium salt of the chiral cyclopentadienyl-phosphine bidentate ligand **11** with RuCl₂(PPh₃)₃ gave **12** in 71 % yield (Scheme 1.22).¹³ A high induction of planar-chirality (60 % d.e.) and complete induction of metal centred chirality were observed.



Scheme 1.22

1.4 Cyclopentadienyl–Amine bidentate complexes of group 8 and 9 metals

Rhodium and iridium amine cyclopentadienyl complexes have found catalytic applications. Examples are the asymmetric transfer hydrogenation of imines and the asymmetric transfer hydrogenation of aromatic ketones.^{41,42} The application of bidentate cyclopentadienyl ligands to the group 9 metals is therefore an area of interest and the following review describes past work in the area of cyclopentadienyl ligands with nitrogen donors.

1.4.1 General properties of nitrogen as a ligating heteroatom.

Comprehensive reviews on cyclopentadienyl ligands with pendant donors have appeared that have focused on nitrogen.^{14,15} When nitrogen is the pendant donor atom, it acts as a 2-electron donor and can co-ordinate to metal centres, thus making them electron rich. A cyclopentadienyl ligand stabilises transition metals in high and low oxidation states. Amino groups favour co-ordination to metals in high oxidation states – hard to hard interaction according to Pearson’s concept. For metals in low oxidation states, only weak interactions are expected. Therefore the amino-functionalised cyclopentadienyl ligand should behave as a hemilabile ligand. This allows reversible co-ordination to a reactive metal centre and is of interest in catalytic studies (Figure 1.9). It seems possible to stabilise a highly reactive intermediate by weakly occupying the vacant co-ordination site, until the substrate coordinates, replacing the amino group.

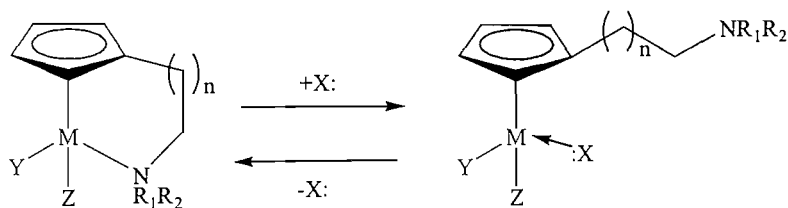


Figure 1.9

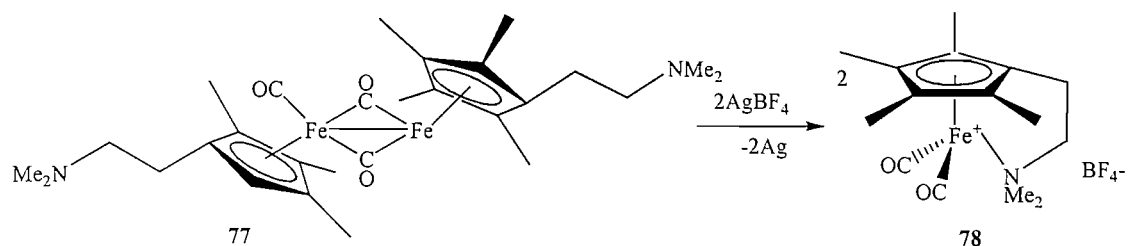
The nitrogen tether may also stabilise the binding of the ligand framework to the metal centre. During catalytic cycles where dissociation of the cyclopentadienyl ring from the metal centre could occur, the extra stabilisation gained by a strongly bound nitrogen atom tether would maintain the chiral integrity of the complex. This is an important feature for enantioselective catalysis.

The nitrogen atom can act as a Lewis base not only towards Lewis acid metal centres but also towards classic Lewis acids such a H^+ and R^+ . Protonation or alkylation of the N atom generates a cationic ammonium group. This would not only enhance its solubility in very polar solvents, but the ammonium-substituted tether will have different electronic and steric properties to the neutral amine tether. i.e. will not coordinate to the metal if there is a N-H group in the side chain. This would allow further functionalisation of the amino group by substitution reactions.

1.4.2 Non-chiral linked cyclopentadienyl-N complexes.

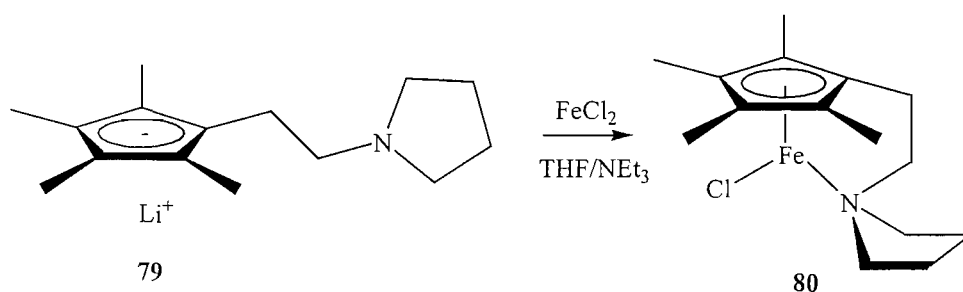
1.4.2.1 Group 8 metals

The chemistry of half sandwich complexes of the group 8 elements (Fe, Ru, Os) incorporating the intramolecular coordination of a pendant amine group is an area of organometallic chemistry that has been relatively untouched. However there are examples of such complexes. Jutzi has shown that the reaction of (1-[2-(N,N-dimethylamino)-ethyl]-2,3,4,5-tetramethyl cyclopentadienyl) with $Fe(CO)_5$ leads to the formation of the dimeric dicarbonyl(cyclopentadienyl)iron complex **77** (Scheme 1.23).⁴³ Subsequent reaction of **77** with $AgBF_4$ gives the cationic half sandwich complex **78** which is stabilized by intramolecular coordination of the amino group.



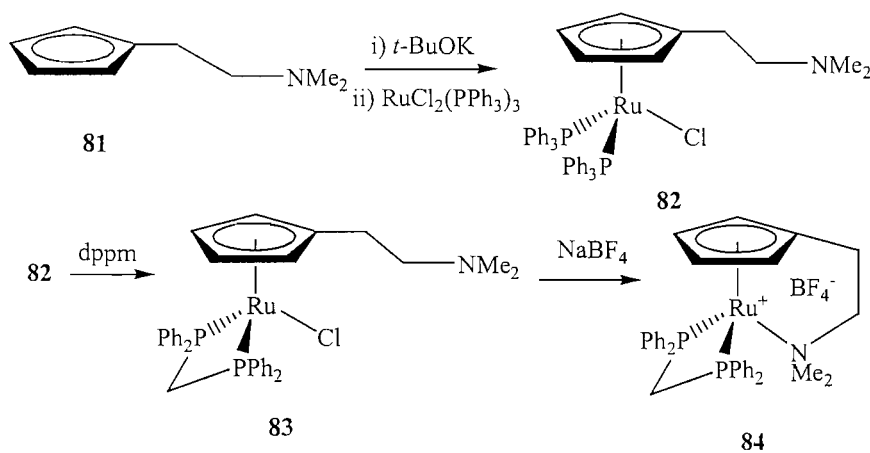
Scheme 1.23

Intramolecular coordination of a different amino group has been reported. Jonas has shown that reaction of FeCl_2 with lithiated **79** yields the corresponding neutral 16-electron complex, which is stabilized by intramolecular coordination of the amino group. This has been confirmed by X-ray crystallography (Scheme 1.24).^{44,45}



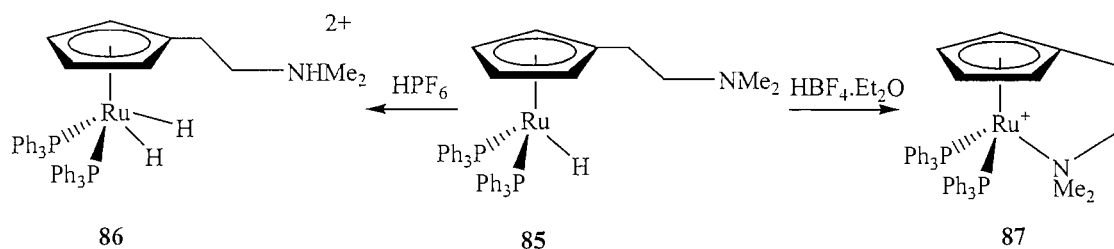
Scheme 1.24

Chu has reported intramolecular coordination of the amine moiety to a ruthenium half-sandwich complex. Reaction of the potassium salt of **81** with $\text{RuCl}_2(\text{PPh}_3)_3$ yields **82**. Subsequent reaction with *dppm* yields the hydride complex **83**, which upon reaction with NaBF_4 causes the elimination of H_2 and subsequent formation of the cationic complex **84** (Scheme 1.25).⁴⁶



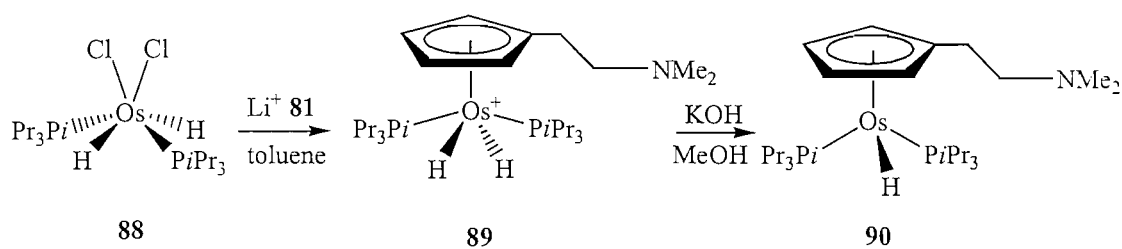
Scheme 1.25

Chaudret found that reacting the sodium salt of **81** with $\text{Ru}(\text{OCOMe})_2(\text{PPh}_3)_3$ yields the ruthenium hydride complex **85** (Scheme 1.26).⁴⁷ This has been confirmed by X-ray crystallography. Protonation of **85** with excess $\text{HPF}_6 \cdot \text{H}_2\text{O}$ yields the dicationic complex **86**, in which both the metal and the amine moiety have been protonated. Protonation of **85** with a stoichiometric amount of $\text{HBF}_4 \cdot \text{Et}_2\text{O}$ yielded **87**, which contains an intramolecular coordinating amine moiety after elimination of H_2 . This was confirmed by X-ray crystallography (Scheme 1.26).⁴⁷



Scheme 1.26

Royo has shown that treatment of the dihydride dichloro complex **88** with lithiated **81** yielded the cationic complex **89**. ^1H NMR suggested the nitrogen was not coordinated to the metal centre and this was confirmed by X-ray crystallography (Scheme 1.27).⁴⁸ Subsequent deprotonation of **89** results in the removal of one of the hydride protons and the formation of the neutral complex **90**. The amine moiety was not coordinated to the metal centre.⁴⁸

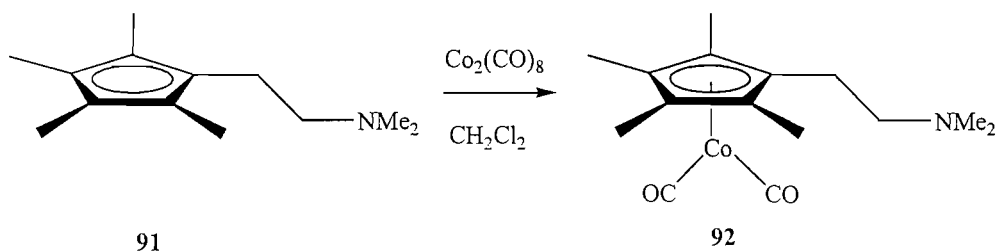


Scheme 1.27

1.4.2.2 Group 9 metals

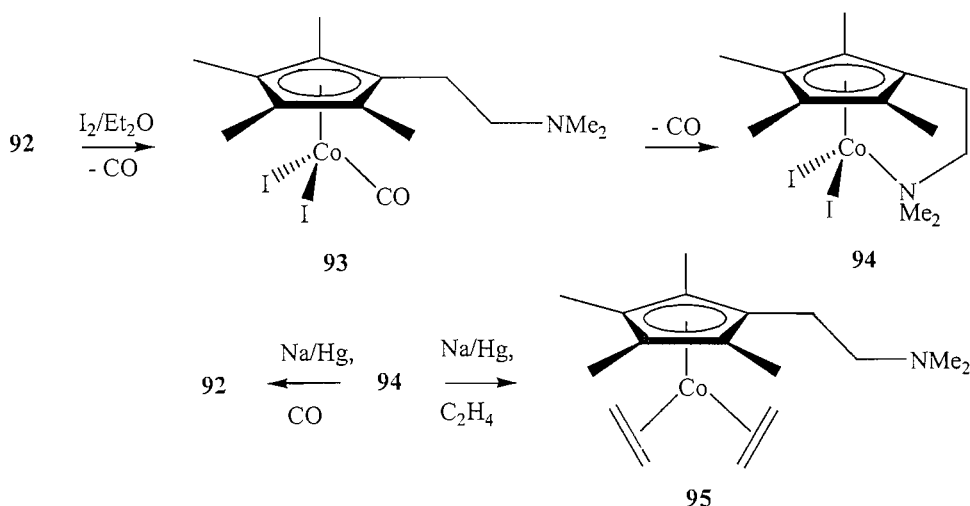
Jutzi found that refluxing a dichloromethane solution of $\text{Co}_2(\text{CO})_8$ and the protonated ligand **91**, gave the $\text{Co}(\text{I})$ complex **92** as a very air-sensitive red-brown oil in moderate

yield (Scheme 1.28).⁴⁹ ¹H NMR suggested no coordination of the nitrogen to the cobalt metal centre.



Scheme 1.28

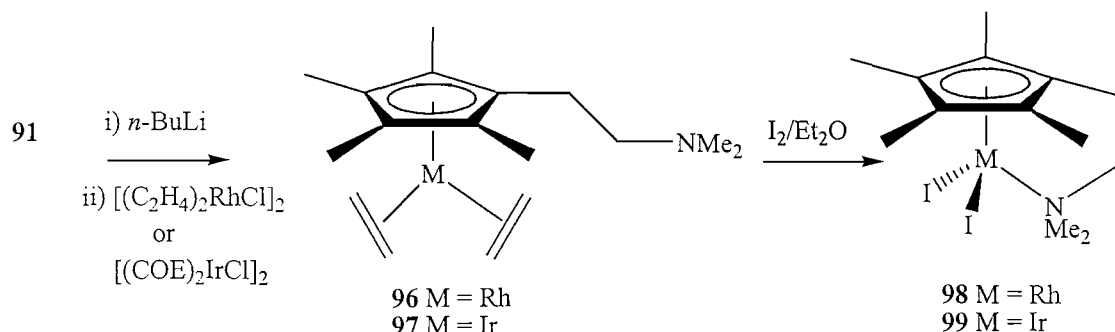
Photolysing a THF solution of **92** to eliminate the carbonyl groups from the metal centre did not lead to the corresponding intramolecularly coordinated complex **94**. Instead the formation of multinuclear cobalt complexes was observed. However, when iodine was added to an ether solution of **92**, the intramolecularly coordinated diiodo Co(III) complex **94** precipitated out as black microcrystals, leaving the diiodocarbonyl complex **93** in solution (Scheme 1.29).⁴⁹



Scheme 1.29

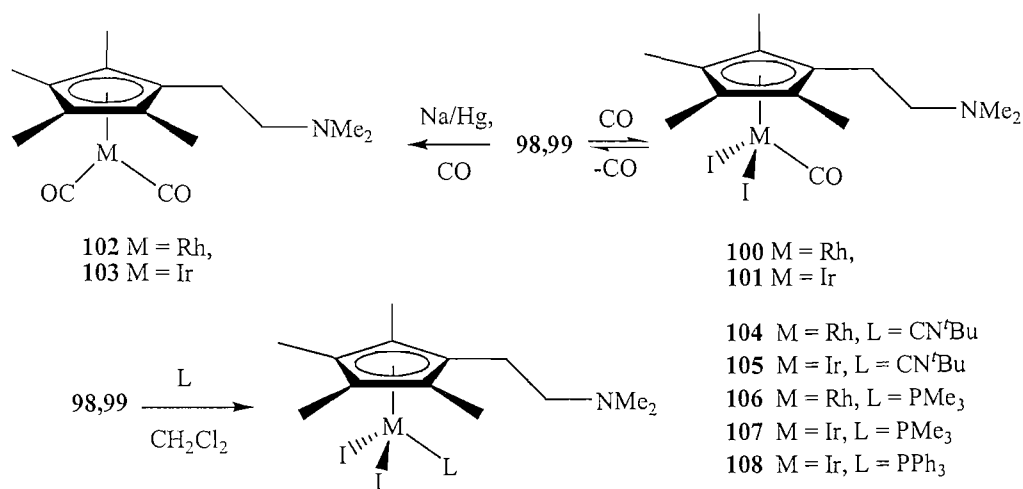
Reaction of **94** with sodium amalgam under a CO atmosphere yields **92**. Reaction of **94** with sodium amalgam under an ethylene atmosphere yields the Co(I) complex **95** (Scheme 1.29).⁴⁹ By treating solutions of [(C₂H₄)₂RhCl]₂ and [(coe)₂IrCl]₂ with lithiated **77**, Jutzi isolated the bis(ethene)rhodium and iridium complexes **96** and **97** as air-stable brown oils (Scheme 1.30).⁵⁰ Subsequent addition of iodine to ethereal solutions of **96** and **97** resulted in the formation of oxidative addition products **98** and

99. Coordination of the diethylamino group in **98** and **99** to the metal caused a deshielding of the relevant atoms and a downfield shift in the NMR data. This was confirmed by X-ray crystallography.⁵⁰



Scheme 1.30

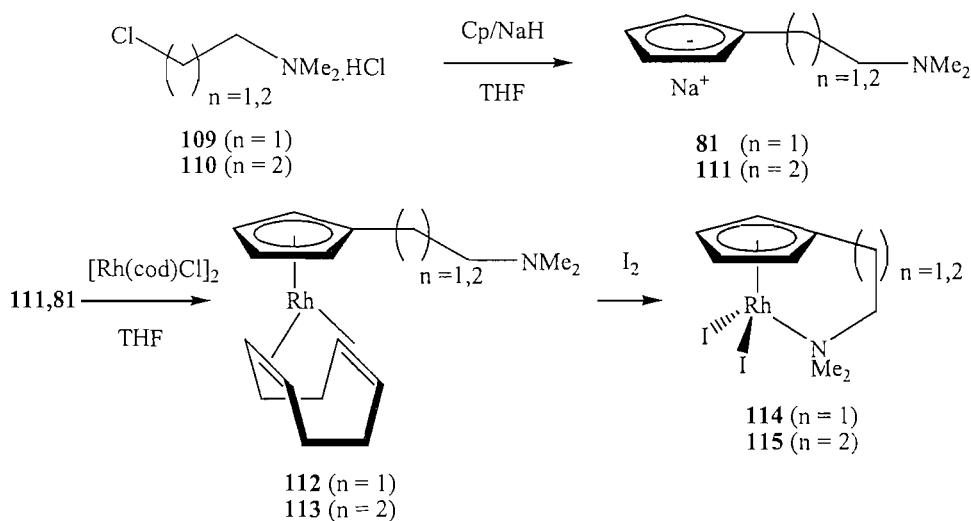
The reversible displacement of the intramolecularly coordinating dimethylamino group by carbon monoxide is successful for both **98** and **99**. Bubbling CO through a CDCl_3 solution of **98** leads to complete conversion to **100**. However **100** is only stable under an atmosphere of CO and thus CO is only weakly bound to the rhodium centre (Scheme 1.31).⁵⁰ In contrast to the very labile rhodium carbonyl complex **100**, the analogous iridium complex is stable. Complex **101** is prepared by stirring a dichloromethane solution of **99** under a CO atmosphere (Scheme 1.31).⁵⁰ The donating properties of CO are strong enough to compete with the dimethylamino group coordination at the metal centre, although intramolecular coordination is entropically favoured. Reaction of **98** and **99** with sodium amalgam under a CO atmosphere, yields the dicarbonyl complexes **102** and **103** as air-sensitive brown oils (Scheme 1.31).⁵⁰



Scheme 1.31

Treatment of rhodium complex **98** with *tert*-butyl isocyanide or trimethylphosphine in dichloromethane yielded complexes **104** and **106** respectively. Iridium complexes **105**, **107** and **108** were obtained by similar reaction of **99** with *tert*-butyl isocyanide, trimethylphosphine and triphenylphosphine respectively (Scheme 1.26). Complexes **104-108** could not be made analytically pure by Jutzi.⁵⁰ However, Hadjiliadis subsequently managed to synthesise and fully characterise **108**.⁵¹

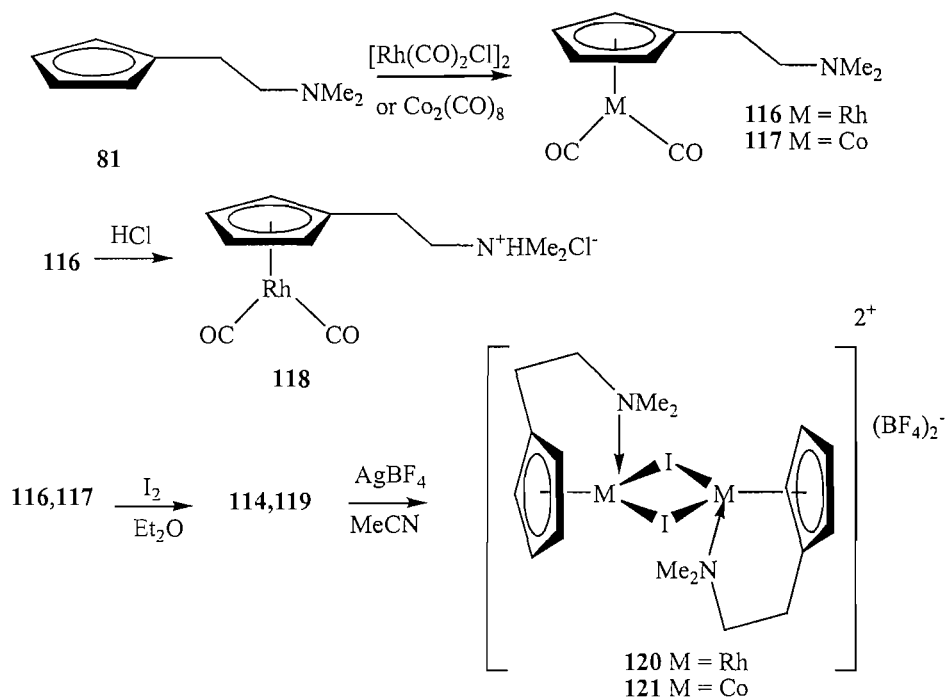
McGowan and co workers have found that reacting the hydrochloride salt of 2-chloro-1-(dimethylamino)ethane **109**, or 3-chloro-1-(dimethylamino)propane **110**, with excess sodium cyclopentadienyl in THF, gives the sodium salts **81** and **111** in good yield (Scheme 1.32).^{52,53} These air- and water- sensitive sodium salts are thermally stable and can be stored indefinitely under an inert atmosphere. Reaction of **111** with $[\text{Rh}(\text{cod})\text{Cl}]_2$ gave the Rh(I) complex **113**, and subsequent addition of iodine gave the intramolecularly coordinated diiodocobalt(III) complex **115** (Scheme 1.32).^{52,53}



Scheme 1.32

Hadjiliadis found that addition of lithiated **81** to a methanol solution of $[\text{Rh}(\text{CO})_2\text{Cl}]_2$ gave the Rh(I) dicarbonyl complex **116** as a very hygroscopic impure oil, which was fully characterised as its hydrochloride salt **118**.⁵⁰ The analogous Co(III) complex was formed by reaction of neutral **81** with $\text{Co}_2(\text{CO})_8$ (Scheme 1.33).⁵⁴ Subsequent oxidation of **116** and **117** with iodine gave the Rh(III) and Co(III) complexes **114** and **119** with the intramolecular coordination of the dimethylamino group being confirmed by X-ray crystallography.^{53,54} Reaction of **114** and **119** with silver

tetrafluoroborate in acetonitrile gave the bridging complexes **120** and **121** (Scheme 1.33).^{53,54}



Scheme 1.33

Enders has synthesised the functionalised cyclopentadienyl ligands **122** and **123** where the nitrogen donor atom is incorporated into a rigid framework (Figure 1.10).^{55,56} The donor properties of the nitrogen atoms in **122** and **123** are slightly different. Whereas **122** has an sp^3 -nitrogen atom without any acceptor properties, the sp^2 -nitrogen atom of the quinoline group in **123** is able to accept electron density as empty π^* -orbitals are available. Ligands **122** and **123** have been used to prepare cobalt (I), (II) and (III) half sandwich complexes.

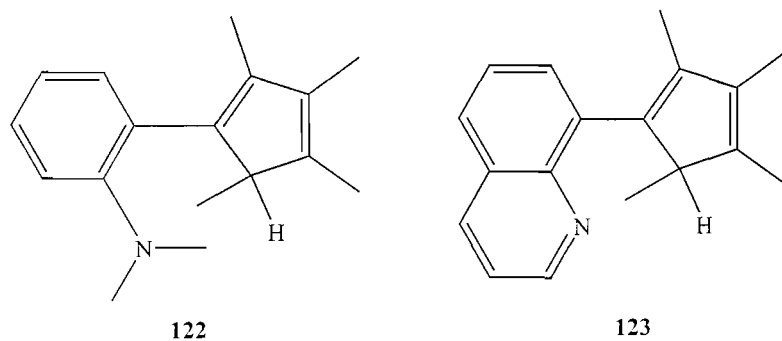
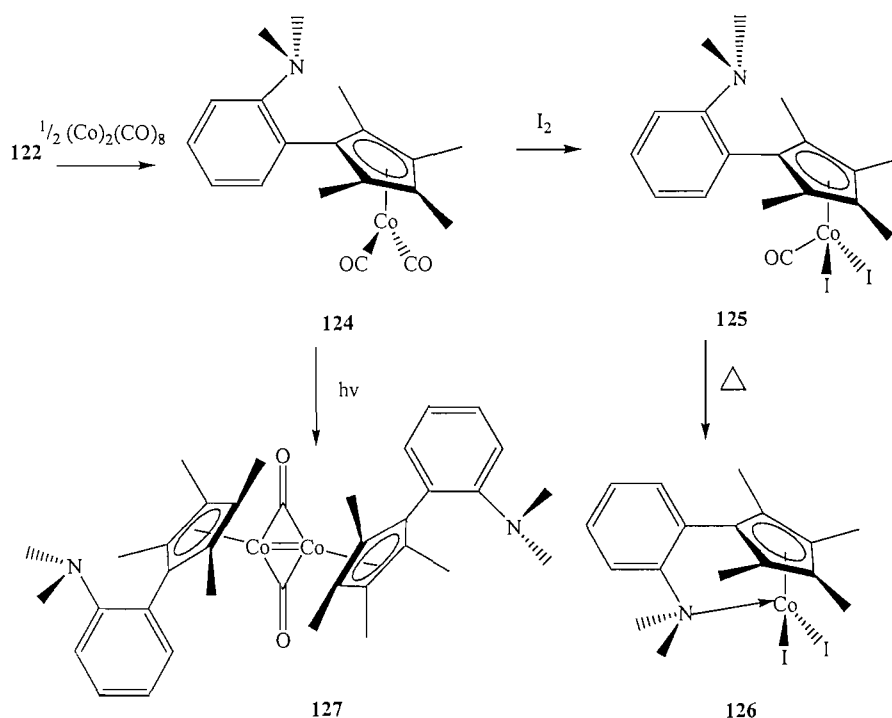


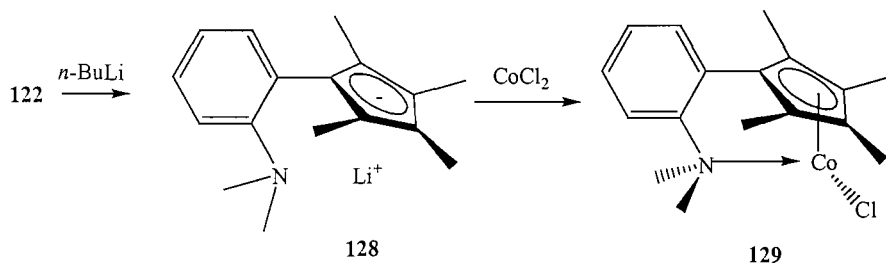
Figure 1.10

Treatment of **122** with $\text{Co}_2(\text{CO})_8$ gave dicarbonyl complex **124** as red-brown air-sensitive crystals. Nitrogen donors are weak ligands for low-valent late transition metals, so the aniline group could not displace a CO ligand. Complex **124** reacts with iodine to give **125** and subsequent heating replaced the CO ligand by intramolecular coordination of the dimethylamino group resulting in the Co(III) complex **126** (Scheme 1.34).⁵⁵ This was confirmed by X-ray crystallography. Complex **126** was active in the polymerisation of ethylene. Irradiation of **124** with a mercury high-pressure lamp gave **127** with a bridging carbonyl group. This was confirmed by X-ray crystallography.⁵⁵



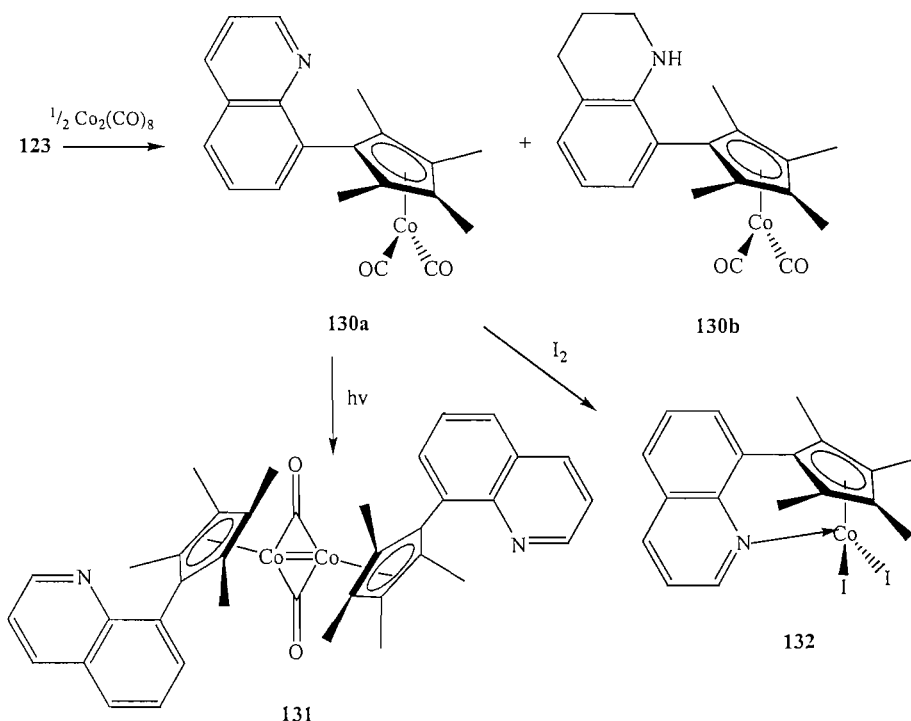
Scheme 1.34

Deprotonation of **122**, and subsequent treatment of the lithium salt **128** with CoCl_2 gave the Co(II) complex **129**. This was confirmed by X-ray crystallography. Complex **129** was active in the polymerisation of ethylene (Scheme 1.35).⁵⁵



Scheme 1.35

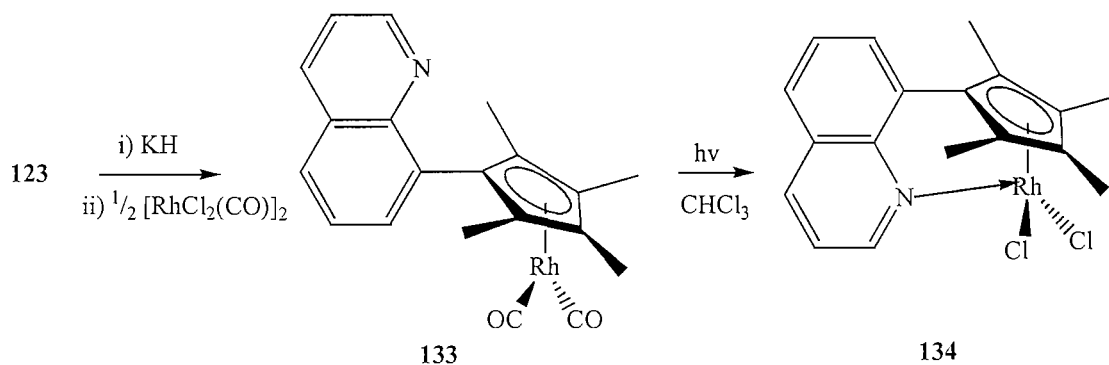
Ligand **123** was treated with $\text{Co}_2(\text{CO})_8$ to give the cobalt complex **130a**, and **130b** as a by-product (Scheme 1.36).⁵⁵ As with **124**, **130a** is transformed to bimetallic complex **131** with a bridging carbonyl group. However, **130a** shows different behaviour upon oxidation. Both CO ligands are eliminated on reaction with iodine, leading directly to **132** and this was confirmed by X-ray crystallography. This shows that the sp^2 -nitrogen atom of the quinolyl substituent is able to displace carbon monoxide easily in Co(III) complexes, whereas the dimethylaminoaniline ligand **122** binds less strongly to the metal (Scheme 1.36).⁵⁵



Scheme 1.36

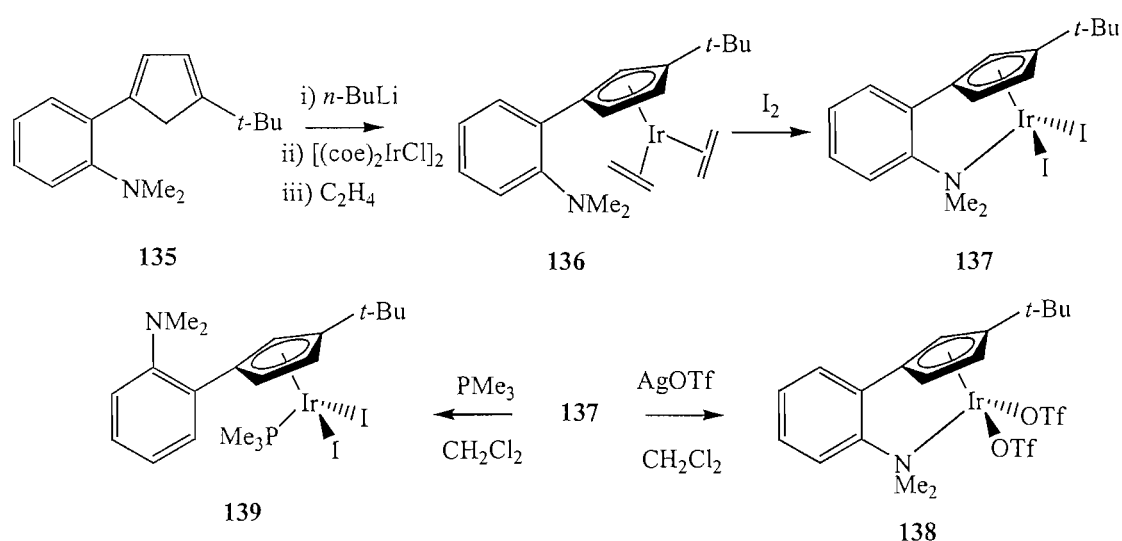
Reaction of the potassium salt of **123** with $[\text{Rh}(\text{CO})_2\text{Cl}]_2$ yields **133**. This was confirmed by X-ray crystallography (Scheme 1.37).⁵⁶ In order to allow for

coordination of the nitrogen to the rhodium centre, a chloroform solution of **133** was irradiated with UV light. It was found that the coordination of the nitrogen to the metal centre was achieved quantitatively giving **134** and this was confirmed by X-ray crystallography (Scheme 1.37).⁵⁶



Scheme 1.37

Bergman has investigated the formation of planar-chiral alkylphosphine and aniline substituted cyclopentadienyl metal complexes and their reactivity toward electrophiles.⁵⁷ Deprotonated dimethylaniline was added to 3-*tert*-butylcyclopent-2-ene-1-one and gave **135**. Complexation of lithiated **135** to $[(C_2H_4)_2IrCl]_2$ (generated *in situ* from $[(coe)_2IrCl]_2$ and 1 atm ethylene) gave **136**. This was confirmed by X-ray crystallography (Scheme 1.38).⁵⁷

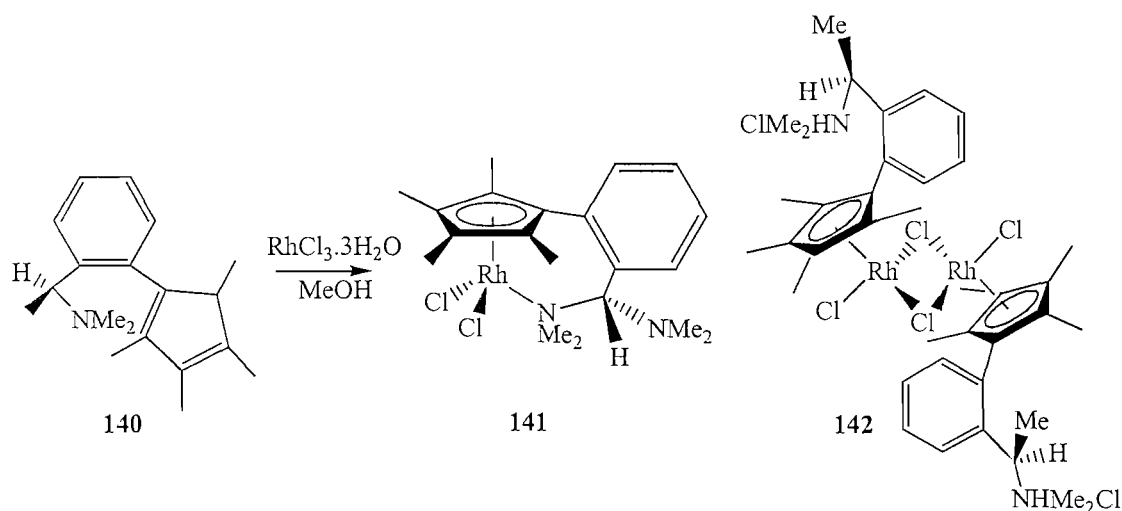


Scheme 1.38

Reaction of **136** with I_2 resulted in the formation of the Ir(III) complex **137**. 1H NMR showed one broad resonance for the two diastereotopic *N*-bound methyl groups on the nitrogen. Addition of AgOTf to **137** gave **138**, which showed two resonances in the 1H NMR for the two diastereotopic methyl groups of the aniline moiety. This suggested coordination of the dimethylamino group and was confirmed by X-ray crystallography.⁵⁷ The nitrogen atom of **137** was weakly and reversibly coordinated to the iridium centre, giving rise to the broad singlet. This was proved by the fact that the weakly bound amine in **137** was readily displaced by trimethylphosphine to form **139** (Scheme 1.38).⁵⁷

1.4.3 Chiral linked cyclopentadienyl-N complexes of group 9 metals

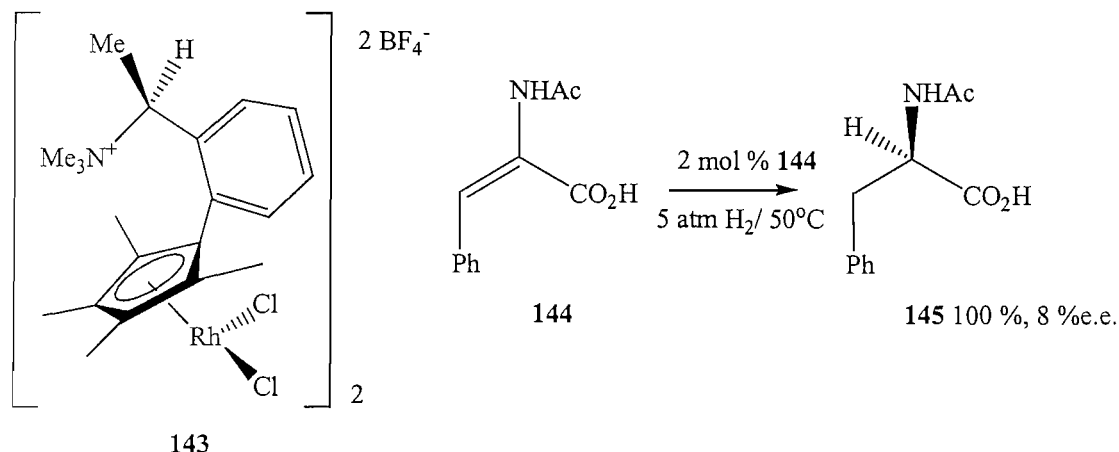
White has synthesised the enantiomerically pure cyclopentadienyl amine complex **141**. Treatment of the homochiral cyclopentadienyl amino ligand **140** with $RhCl_3 \cdot 3H_2O$ in refluxing methanol gave a mixture of the monomeric chelated rhodium complex **141** and the chloride dimer **142** (Scheme 1.39).⁵⁸ The intramolecular coordination of the amino group to the metal centre was confirmed by X-ray crystallography.⁵⁸



Scheme 1.39

The chelated rhodium complex **141** was found to be inactive towards the catalytic hydrogenation of alkenes. Quartermerisation of the amino group of **141** with $Me_3O^+ BF_4^-$ gave the rhodium dimer **143**, where the rhodium is no longer coordinated to the metal centre. Dimer **143** was found to be active in the hydrogenation of α -

acetamidocinnamic acid gave 100 % conversion to *N*-acetyl-(*S*)-phenylalanine with an 8 % e.e (Scheme 1.40).⁵⁸



Scheme 1.40

1.5 Indenyl complexes

Sections 1.3 and 1.4 have discussed bidentate cyclopentadienyl complexes of phosphorus and nitrogen complexes of group 8 and 9 metals respectively. A number of planar chiral rhodium and ruthenium complexes with indenyl phosphine bidentate ligands have been synthesised. Examples are **12a** and **146a-c** shown below (Figure 1.11).^{13,59}

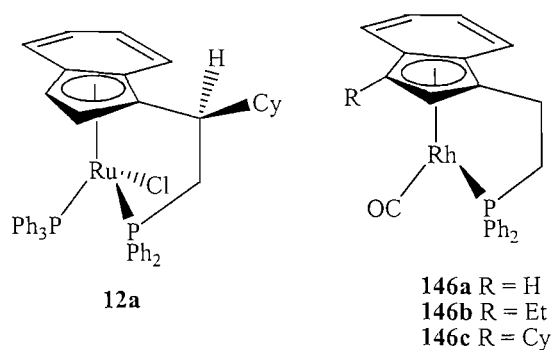


Figure 1.11

No group 9 metal indenyl complexes with a nitrogen donor atom have been reported in the literature. However, a number of indenyl complexes of early transition metals and lanthanide metals with a nitrogen atom have been reported (Figure 1.12).⁶⁰⁻⁶³

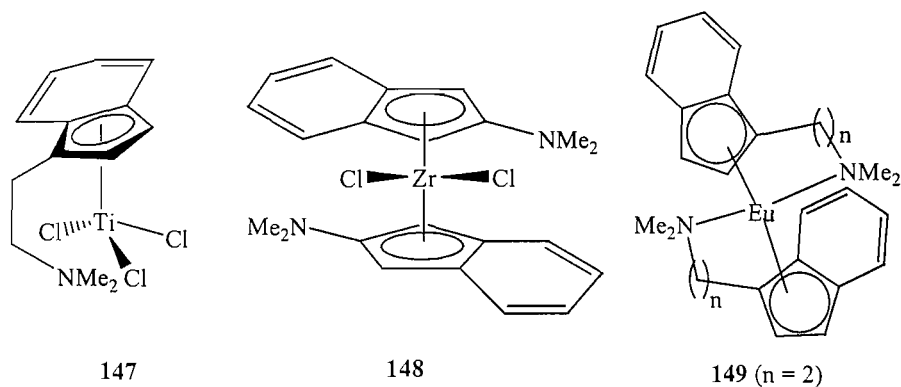
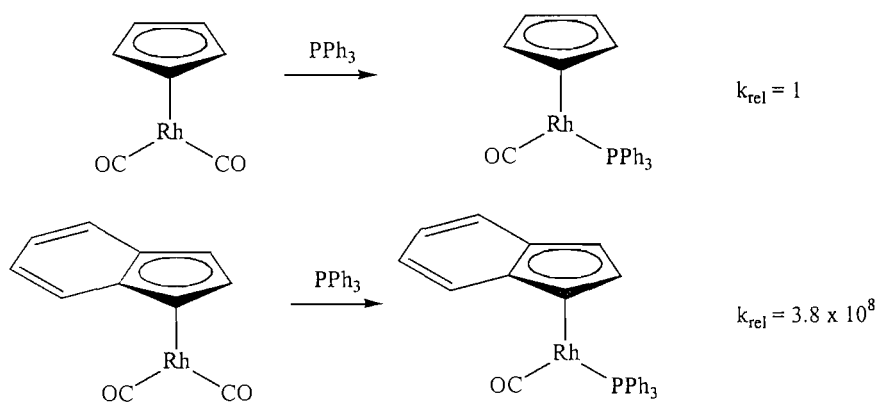


Figure 1.12

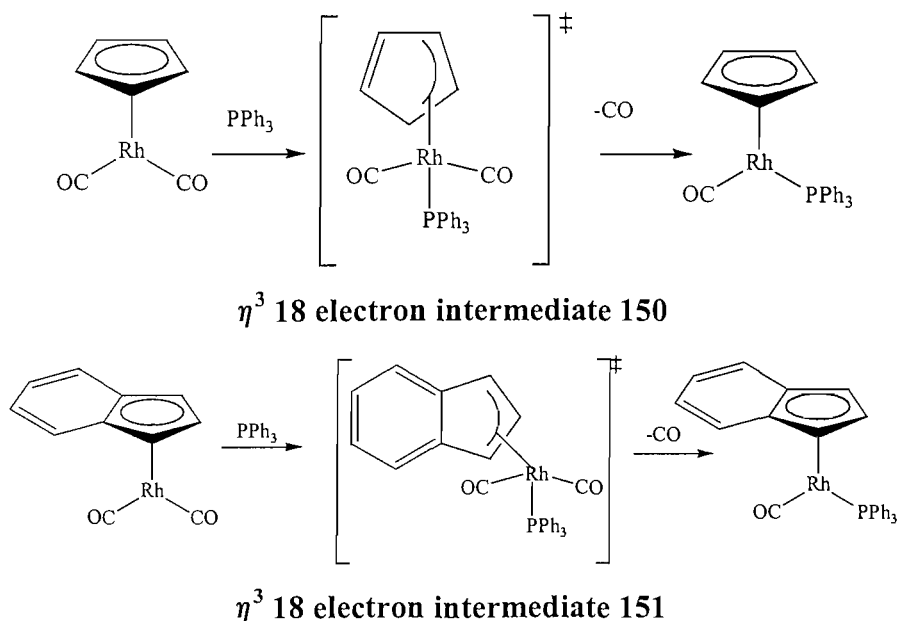
1.5.1 The “Indenyl Ligand Effect”

Basolo and co workers examined the reaction of $\text{Rh}(\eta^5\text{-C}_9\text{H}_7)(\text{CO})_2$ with PPh_3 .⁶⁴ It was found that the reaction proceeded *via* an $\text{S}_{\text{N}}2$ mechanism and that the reaction rate for the rhodium indenyl complex $\text{Rh}(\eta^5\text{-C}_9\text{H}_7)(\text{CO})_2$ was approximately 3×10^8 faster than the analogous reaction with the cyclopentadienyl complex $\text{Rh}(\eta^5\text{-C}_5\text{H}_5)(\text{CO})_2$ (Scheme 1.41).⁶⁴



Scheme 1.41

The cyclopentadienyl ligand allows an associative mechanism to occur by ring slippage from η^5 to η^3 coordination to avoid an unfavourable 20-electron intermediate complex (Scheme 1.412).^{65,66}



Scheme 1.42

The increase in reactivity between $\text{Rh}(\eta^5\text{-C}_9\text{H}_7)(\text{CO})_2$ and $\text{Rh}(\eta^5\text{-C}_5\text{H}_5)(\text{CO})_2$ can be explained by the indenyl ligand gaining extra stability from aromatisation of the benzene ring in the η^3 intermediate **151**. The addition of an electron-withdrawing group to the indenyl group makes the ring less electron-rich. Therefore it readily accepts an electron pair from the metal and accelerates substitution. Indenyl ligands enhance the reactivity of metal complexes in associative mechanisms which is of great benefit in catalysis.⁶⁶

1.6 Conclusions

The design of planar-chiral late-transition metal catalysts is a popular area of research as is shown in the preceding literature review. The design and synthesis of cyclopentadienyl-amine and cyclopentadienyl-phosphine bidentate complexes allows the stereochemical environment surrounding a metal centre to be controlled and thus applied to asymmetric catalysis. However, indenyl amine complexes of group 8 and 9 metals remain elusive.

Chapters 2, 3 and 6 describe the optimisation and synthesis of indenyl ligands with tethered phosphine and amine functionality. Chapters 4, 5 and 6 discuss the

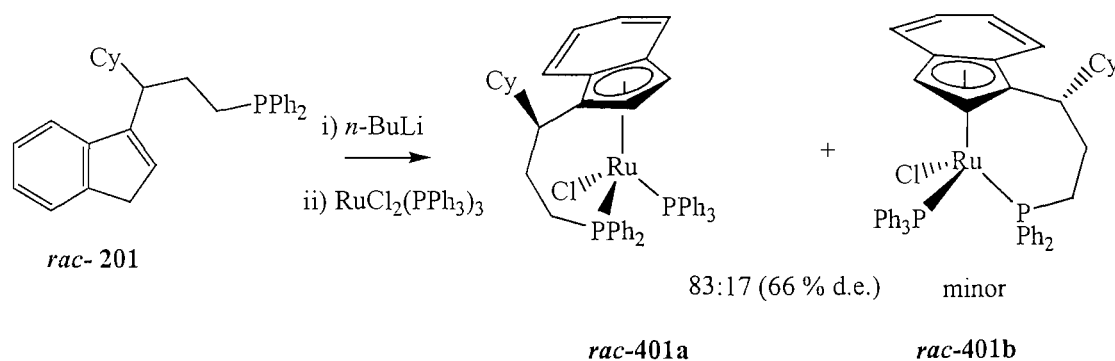
subsequent complexation to transition metals and their applications to asymmetric catalysis.

Chapter 2: The optimisation of the synthesis of a bidentate indenyl phosphine ligand containing a three-carbon bridge.

2.1 Background and Aims

Trost,²⁹ Tani,⁶⁷ and Takahashi,³⁵ have reported that the catalytic activities and asymmetric inductions of many ruthenium cyclopentadienyl-phosphine bidentate complexes. They also noted a considerable effect of tether chain length on catalytic activity.

Harrison synthesised the novel racemic three-carbon ligand bridged phosphine ligand **201** (Scheme 2.1).¹³ Complexation of *rac*-**201** with $\text{RuCl}_2(\text{PPh}_3)_3$ gives complex *rac*-**401**. Complete control at the metal centre is achieved and the high degree of induction of planar-chirality demonstrates the success of the ‘favoured rotamer’ complexation model (section 1.2.2) and the design of such alpha-substituted cyclopentadienyl-phosphine ligands.¹³

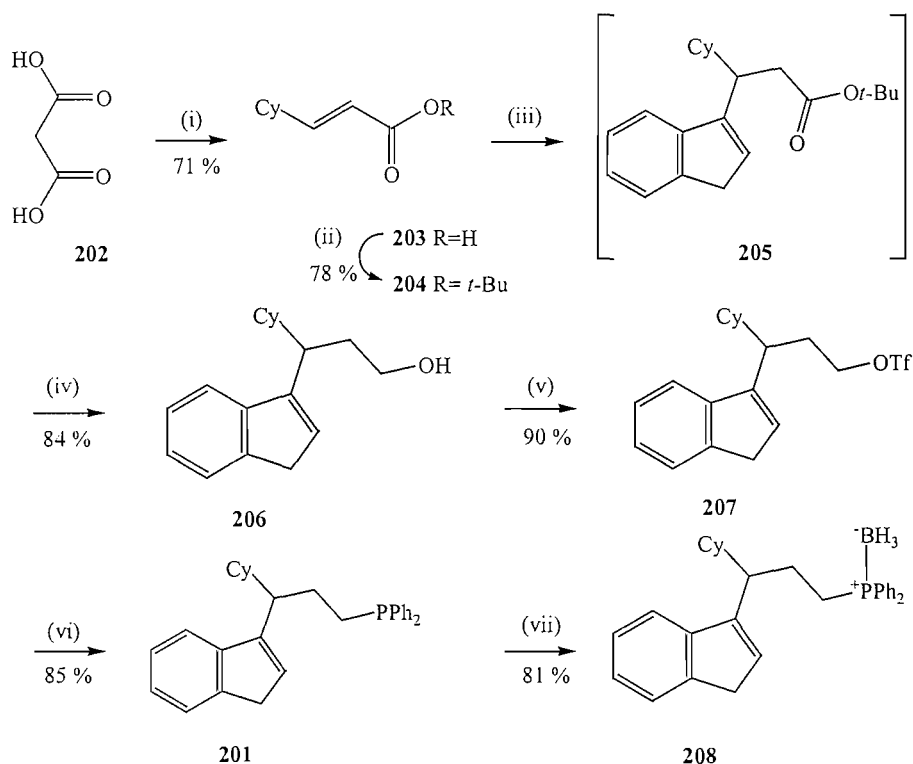


Scheme 2.1

The first aim was to optimise the synthetic route to ligand **201**, and to synthesise the homologue with a 4-carbon linking chain.

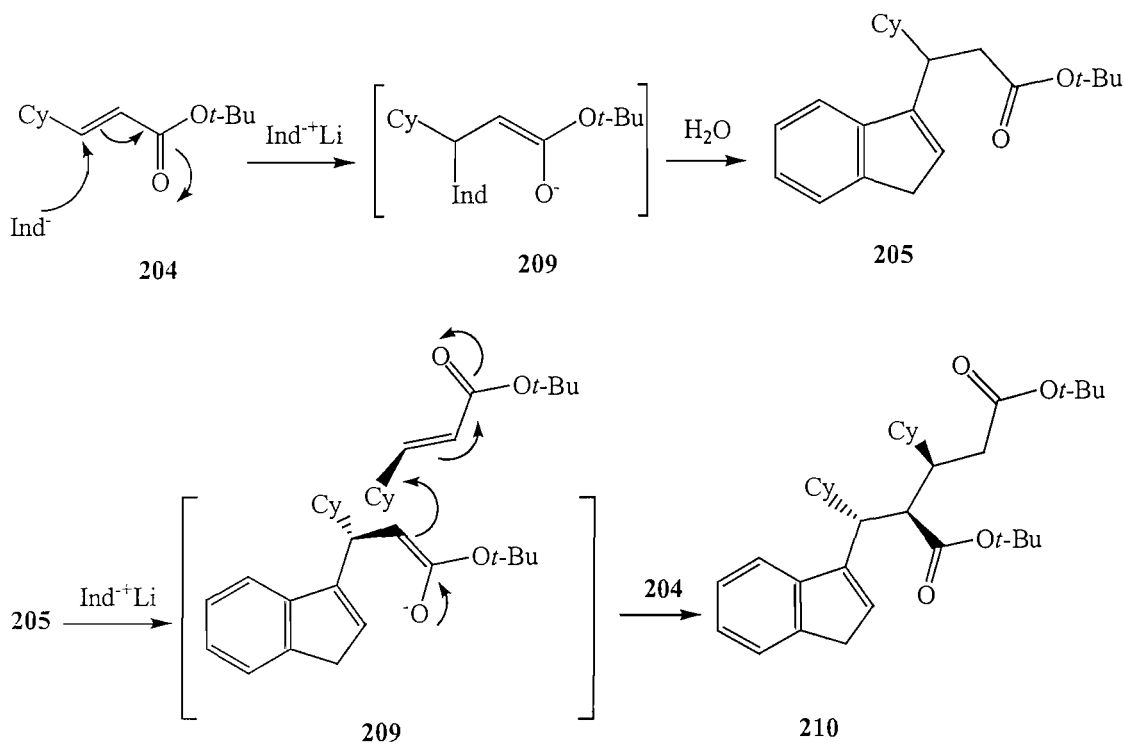
2.2 The Harrison synthesis of **201**.

Harrison's synthesis of **201** (Scheme 2.2) requires six steps with an overall yield of 36%, and has been performed on a 40 mmol scale.¹³ Purification by chromatography is only required on three occasions, to obtain ester **204**, alcohol **206**, and the final ligand **201**. There are a number of scale-limiting factors within the existing synthetic route. The first limiting step was the synthesis of *tert*-butyl ester **204**. This involved the condensation of 2-methylpropene gas in a measuring cylinder at $-15\text{ }^{\circ}\text{C}$ and subsequent transfer to a high pressure reaction vessel *via* cannula and reaction time of 48 h (Scheme 2.2).¹³ The reaction vessel was small and therefore limited the scale of the reaction. The 1,4-addition of indenyl anion was plagued by formation of the dimer **210**, (Scheme 2.3) minimisation of which required a large excess of indene and addition of *sec*-butyl lithium as the final component. Purification of the very air sensitive *rac*-**201** required column chromatography under argon, although in situ formation of the borane-protected ligand **208** as an air-stable white solid could be carried out.¹³



Scheme 2.2

Reagents and conditions: (i) Cyclohexanecarboxaldehyde, pyridine, cat. piperidine; (ii) isobutylene, CH_2Cl_2 , cat. H_2SO_4 ; (iii) indene, *s*-BuLi, 0.2M/THF; (iv) LiAlH_4 , Et_2O , $0\text{ }^{\circ}\text{C}$; (v) Tf_2O , pyridine, CH_2Cl_2 , $0\text{ }^{\circ}\text{C}$; (vi) LiPPh_2 , Et_2O , $0\text{ }^{\circ}\text{C}$; (vii) $\text{BH}_3\text{-SMe}_2$, THF, $0\text{ }^{\circ}\text{C}$.

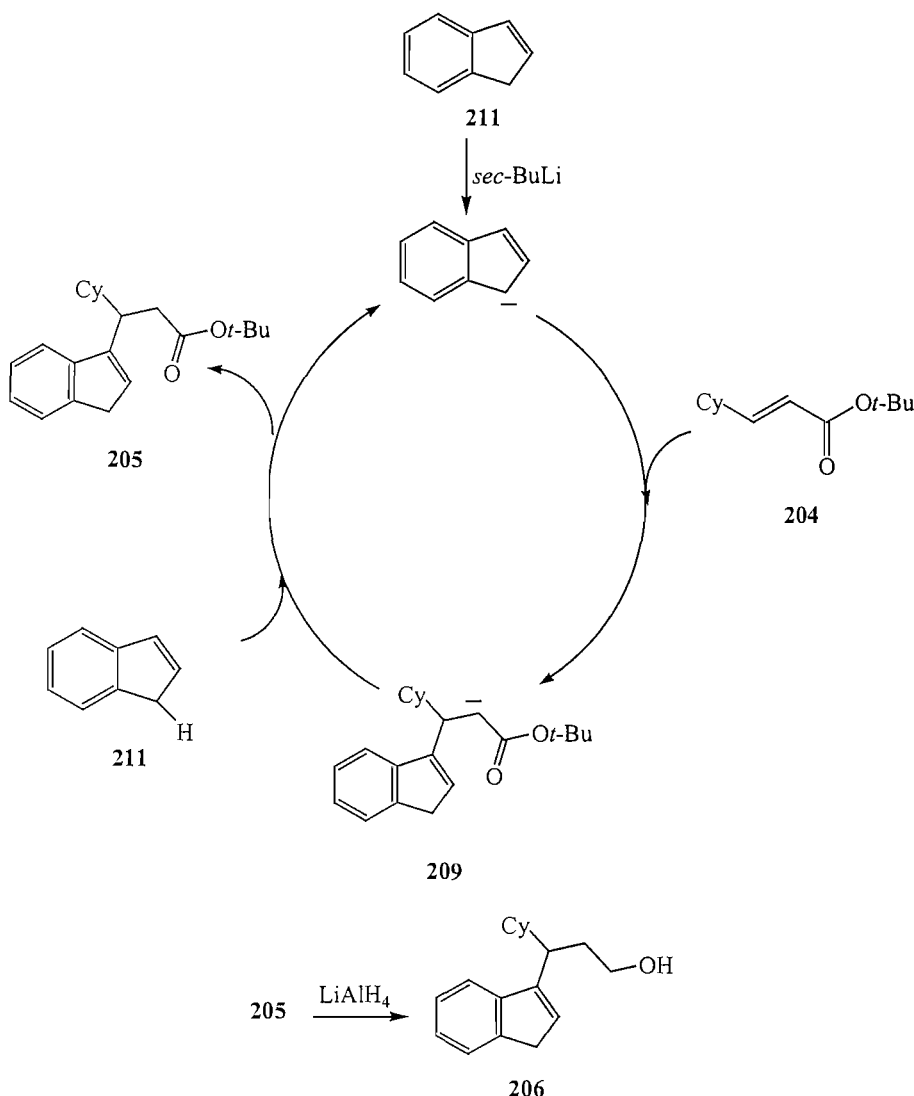


Scheme 2.3

2.3 Optimised synthesis of **201**

2.3.1 A novel catalytic indenyl anion addition reaction.

We noted that the optimum reaction conditions to favour the mono-addition product **205** and minimise the production of the double addition product **210**, involved addition of 1.2 equivalents of *sec*-butyl lithium to a 0.2 M THF solution of ester **204** and 3 equivalents of indene.¹³ The success of these conditions in suppressing double-addition product **210**, implied that the excess indene was re-protonating enolate **211**. Therefore in theory only a catalytic amount of base should be needed. We have demonstrated this to be the case with the use of 10 mol% *sec*-BuLi instead of 1.2 equivalents and only 1.5 equivalents of indene (Scheme 2.4). Subsequent lithium aluminium hydride reduction provides an easily separable mixture of unreacted indene and 3-cyclohexyl-3-(1*H*-3-indenyl)-1-propanol, **206** in 73 % yield.

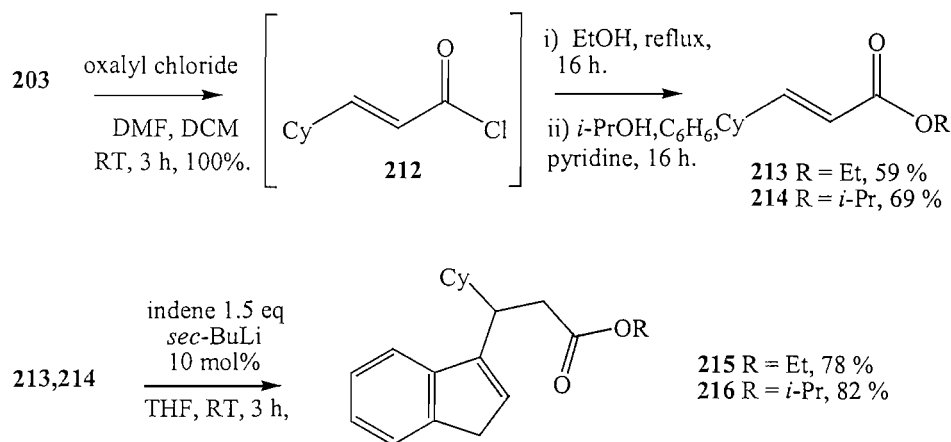


Scheme 2.4

2.3.2 Use of alternative ester groups.

A bottleneck in the synthesis of **206** was the preparation of *tert*-butyl ester **204**. It was believed that the bulky *tert*-butyl ester minimised possible 1,2-addition of the indenyl anion in the formation of **206**. With the success of the catalytic 1,4-addition of the indenyl anion, efforts then switched to using alternative α,β -unsaturated esters to investigate whether or not the sterics of the ester group were important in the 1,4-addition of the indenyl anion. The ethyl and *iso*-propyl esters **213** and **214** were synthesised from **203** either via the corresponding acid chlorides (59 % and 69 % respectively), or in the case of **213** also by acid catalysed reaction with ethanol (75 %).^{68,69} The synthesis of esters **213** and **214** are far more scalable than the preparation of the *tert*-butyl ester **204**. Purification by column chromatography is not required in

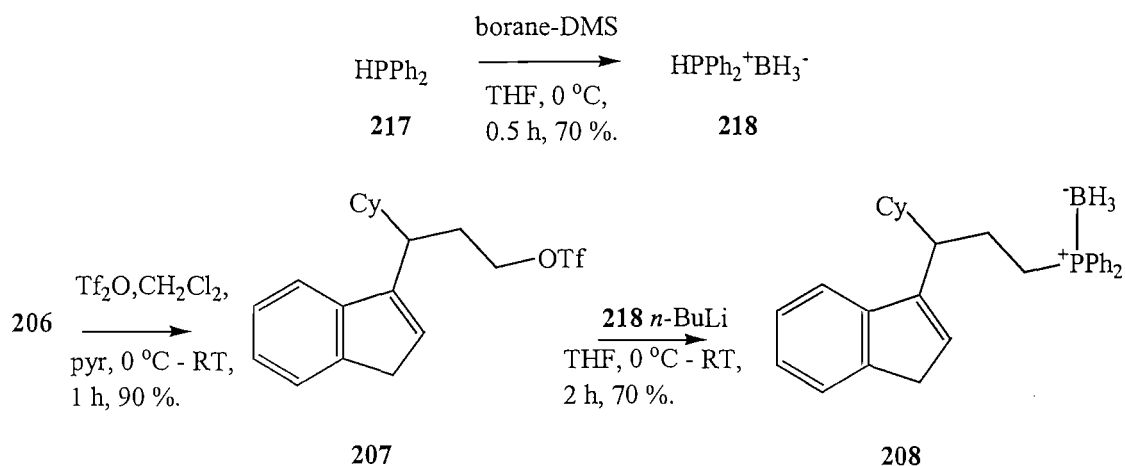
the synthesis of both **213** and **214**. Reaction of **213** and **214** under the catalytic indenyl anion conditions proved successful (78 and 82 % yields) with reaction times of 3 h (Scheme 2.5). Subsequent lithium aluminium hydride reduction of crude ester **215** provided an easily separable mixture of unreacted indene **211** and alcohol **206** in 73 % yield.



Scheme 2.5

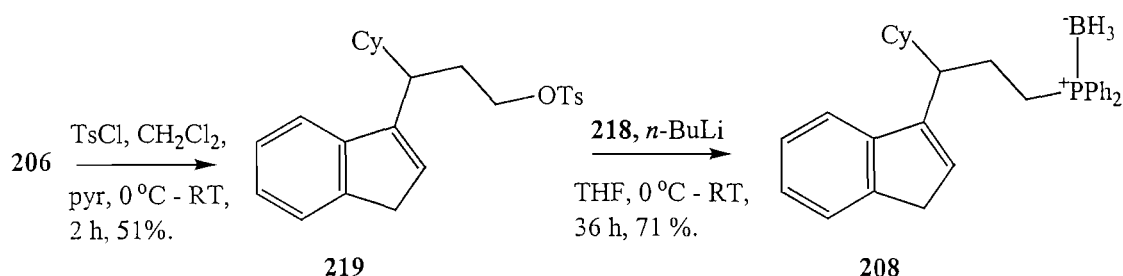
2.3.3 Direct formation of borane stabilised diphenylphosphine ligand

The existing synthesis of **201** (Section 2.2) suffered from the need for a technically challenging purification by chromatography under argon. It could be protected as the borane adduct **208**, but a more direct synthesis was needed. To that end borane protected diphenylphosphine, **218** was prepared in 75 % yield as an air-stable white solid. Deprotonation of **218** using an equimolar amount of *n*-BuLi, and subsequent reaction with an equimolar amount of triflate **207** was attempted.⁷⁰ After 2 h, aqueous work-up and column chromatography gave **208** in 70% yield as an air-stable white solid (Scheme 2.6). It was important to control the time and temperature of the reaction, as increased temperature and time may have led to the formation of by-products in the mixture. Hydroboration of the indene double bond could occur, as could formation of a spirocycle.



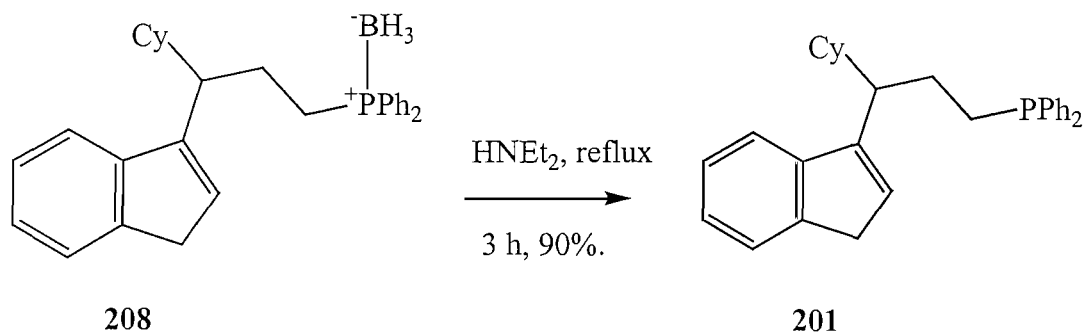
Scheme 2.6

This was a very encouraging result. There is no longer the need for any purification under an argon atmosphere and the reaction can be performed on a large scale. As an alternative, tosylate **219** was synthesised from alcohol **206** in moderate 51% yield. Reaction with lithiated **218** (36 h, RT), aqueous work-up and column chromatography gave **208** in 71% yield (Scheme 2.7).



Scheme 2.7

The yield of **208** from the reaction of triflate **207** with lithiated **218** is higher and the reaction time is considerably shorter when compared to similar reaction with tosylate **219**. Deprotection of borane protected phosphines can be achieved cleanly by reaction with an amine base.⁷¹⁻⁷³ The most attractive deprotection method for protected ligand **208** proved to be refluxing the borane adducts in neat diethylamine, under an inert atmosphere for 3 h.⁷² Quantitative yield of the decomplexed phosphine ligand **201** was obtained simply by removal of the diethylamine-borane complex along with remaining diethylamine under high vacuum (Scheme 2.8).

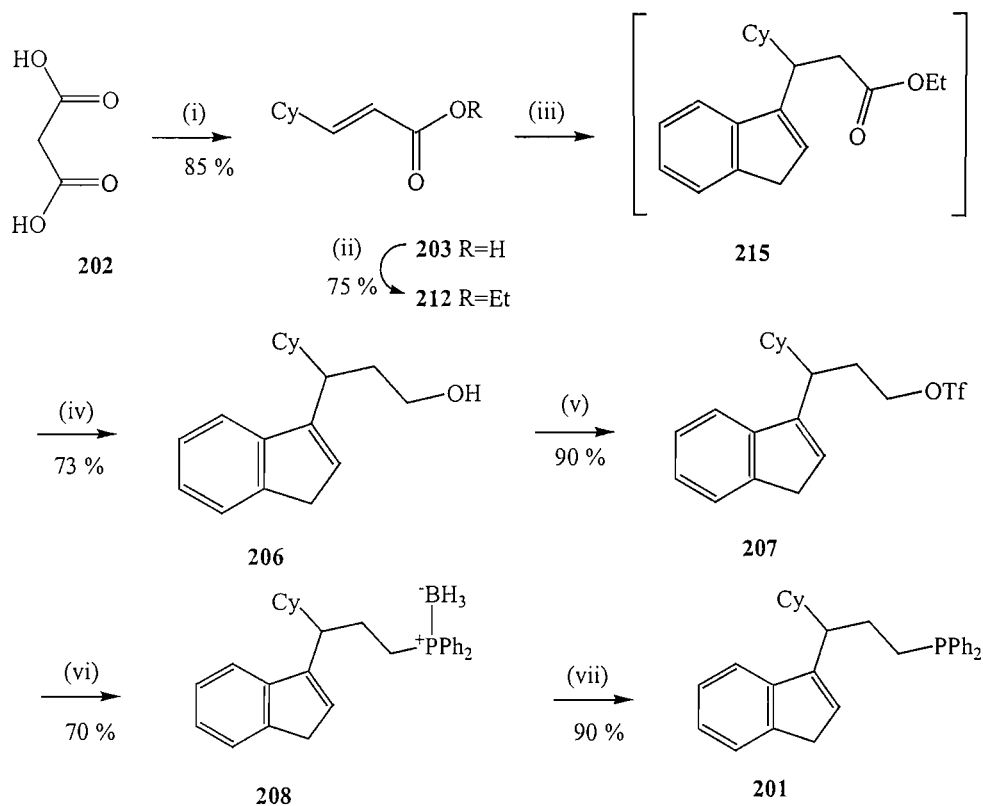


Scheme 2.8

Deprotection of the borane-protected phosphines was only carried out when complexation of the ligand to transition metals was attempted.

2.3.4 Final Optimised synthesis of the three-carbon bridged ligand, 201.

Following the optimisations described above, the synthesis of ligand **201** has now been carried out on a 60 mmol scale, with an overall yield of 26 % after seven steps (Scheme 2.9). Although the yield is lower than the route developed by Harrison, it may be carried out on a larger scale. Column chromatography is only needed on two occasions, to obtain alcohol **206** and borane-adduct **208**, and there is no longer the need for column chromatography under inert conditions. The synthesis of ester **204** is avoided. A major optimisation is the novel catalytic 1,4-addition of the indenyl anion to **213** yielding ester **215**. The reaction of **207** with an equimolar amount of lithiated **218**, leads directly to borane adduct **208**. This is a reaction that can be done a large scale and avoids the handling of air sensitive **201**. The phosphine ligand **201** is only synthesised when complexation is attempted onto transition metals. This will be discussed in Chapter 4.



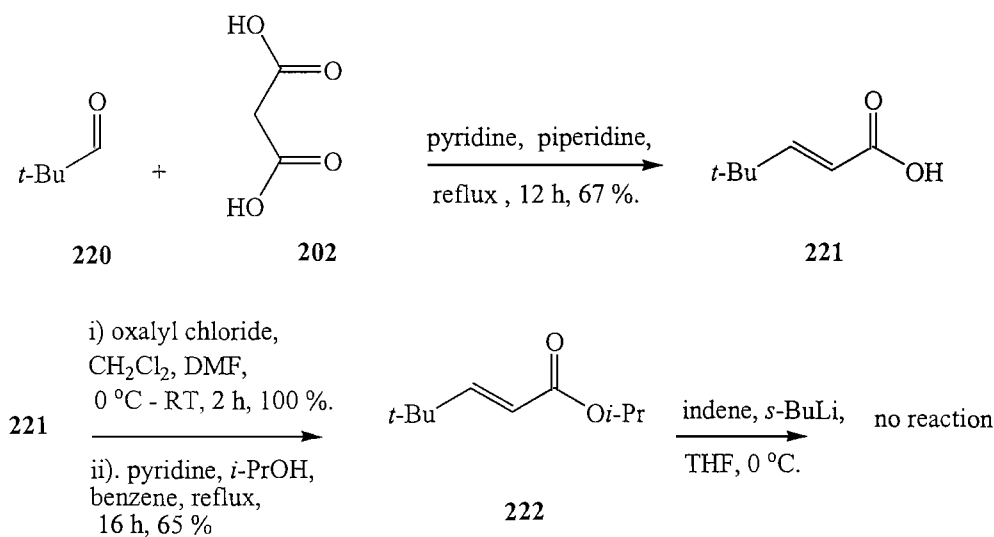
Scheme 2.9

Reagents and conditions: (i) Cyclohexanecarboxaldehyde, pyridine, cat. piperidine; (ii) EtOH, SOCl_2 , 0°C ; (iii) indene, 10 mol% *s*-BuLi, 0.2M/THF; (iv) LiAlH_4 , Et_2O , 0°C ; (v) Tf_2O , pyridine, CH_2Cl_2 , 0°C ; (vi) *n*-BuLi, $\text{BH}_3\text{-SMe}_2$, THF, 0°C ; (vii) HNEt_2 .

2.4 Alternative substituents along the indene-phosphine bridge.

The cyclohexyl ring substituent *alpha* to the indene ring fulfils the ‘favoured rotamer’ design requirements by imposing reasonable face-selectivity upon complexation to transition metals. However, an improvement on the typical 6 : 1 diastereocontrol obtained would be beneficial so we tried to synthesis the analogue carrying the bulkier *tert*-butyl group. Knoevenagel condensation between pivaldehyde **220** and malonic acid **202**, afforded (*E*)-3-*tert* butyl propenoic acid **221**, in 67 % yield. Acid **221** was converted to the corresponding *iso*-propyl ester **222**, in 65 % yield (Scheme 2.10).⁶⁸ The reaction of **222** with indenyl lithium under the catalytic reaction conditions proved unsuccessful and starting material was recovered. This was disappointing. It can be postulated that the steric bulk of the *tert*-butyl group caused this reaction to

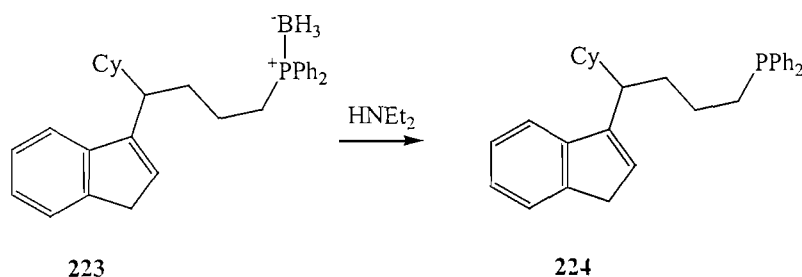
fail. Indenyl lithium addition under stoichiometric reaction conditions was not investigated (Scheme 2.10).



Scheme 2.10

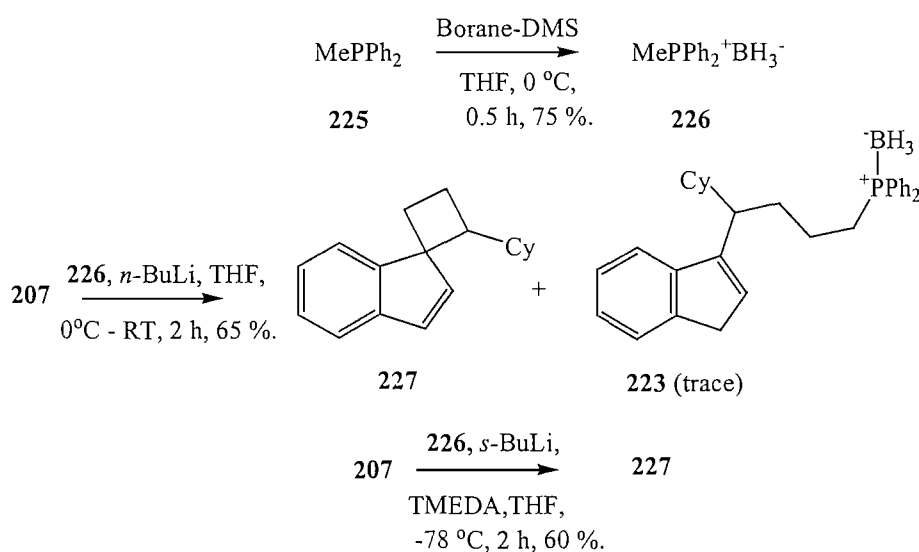
2.5 Increasing the length of the Cp-phosphine tether chain.

The catalytic activity and asymmetric induction of many ruthenium cyclopentadienyl-phosphine bidentate complexes can vary considerably depending on the length of the cyclopentadienyl-phosphine tether chain (Section 2.1). This effect of tether chain length on catalytic activity means that having efficient synthetic routes to cyclopentadienyl-phosphine tether chains of differing lengths is essential. Having already achieved good optimised synthetic routes to the two⁷⁴ and three carbon bridged cyclopentadienyl-phosphine ligands, it was decided to attempt the synthesis of the racemic four-carbon bridged phosphine ligand **224** (Scheme 2.11). Deprotection of borane adduct **223** would give free cyclopentadienyl-phosphine ligand **224**.



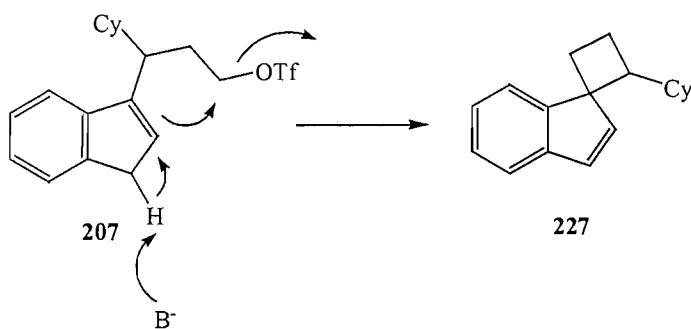
Scheme 2.11

With the successful displacement of triflate **207** with lithiated **218**, it was decided to attempt the synthesis of the racemic four-carbon bridged phosphine ligand **224**.⁷⁰ Borane protected methyl diphenyl phosphine, **226** was prepared in 75 % yield as an air-stable white solid. The first attempt involved deprotonation of **226** using an equimolar amount of *n*-BuLi, and subsequent reaction with an equimolar amount of triflate **207**.⁷⁰ After 16 h, ¹H NMR suggested no starting material remained. After aqueous work-up and column chromatography, spirocyclobutane **227** was mainly collected.¹³ A trace amount of the desired four-carbon bridged borane ligand **224** was isolated as well as unreacted **226** (Scheme 2.12). A second attempt was made with deprotonation of **226** using an equimolar amount of *s*-BuLi and TMEDA, and subsequent reaction with an equimolar amount of triflate **207**.⁷⁰ After 16 h, ¹H NMR suggested no starting material remained. However, spirocyclobutane **227** and unreacted **226** were isolated after aqueous work-up and column chromatography (Scheme 2.12).



Scheme 2.12

This was unfortunate. These reactions were probably unsuccessful due to *n*-BuLi deprotonating the indenyl moiety leading to intramolecular displacement of the triflate, forming spirocycle **227** rather than deprotonating the methyl diphenyl phosphine borane **226** (Scheme 2.13). Due to time constraints, this work was abandoned.



Scheme 2.13

2.6 Conclusions

- The optimised synthesis of ligand **201** has now been carried out on a 60 mmol scale, with an overall yield of 26 % after seven steps.
- The addition of the indenyl lithium anion goes exclusively in the 1,4-position in the formation of **205**, **215** and **216**. The use of 10 mol % *sec*-BuLi, means the 1,4-addition of indenyl lithium is catalytic, and the excess indene reprotonates enolate **209**. It has been proved that the size of the ester has no effect on possible 1,2-addition addition of indenyl lithium.
- The reaction of **222** with indenyl lithium under the catalytic reaction conditions proved unsuccessful. This was probably due to the steric influence *tert*-butyl group.
- The displacement of triflate group on **207** with Li⁺PPh₂BH₃, results in the synthesis of borane-adduct **208** not having to go *via* the free phosphine ligand **201**. There is no need for purification by column chromatography under argon.
- Increasing the length of the cyclopentadienyl -phosphine tether chain to four carbon atoms was attempted but proved unsuccessful. Deprotonation of the methyldiphenylphosphine borane-adduct, **226** and reaction with triflate, **207** resulted in the known spirocyclobutane **227** compound being isolated.

Chapter 3: The synthesis of a chiral bidentate indenyl ligand containing a three-carbon bridge and coordinating ‘anchor’ group.

3.1 Background and aims

The literature review in Chapter 1 includes descriptions of the few preparations of enantiomerically and diastereomerically pure planar-chiral Cp-ruthenium transition metal complexes that have been reported to date.

Trost,²⁹ Tani,⁶⁷ and Takahashi,³⁵ have reported that the catalytic activity and asymmetric induction of many ruthenium cyclopentadienyl-phosphine bidentate complexes can vary considerably depending on the length of the tether chain. Harrison has reported the efficient synthesis of the enantiopure two carbon tethered ligand **11** (Figure 3.1).^{13,75} With the synthetic route to *rac*-**201** having been optimised (Section 2.3), the development of an enantiopure synthesis of the three carbon ligand was now an important goal.

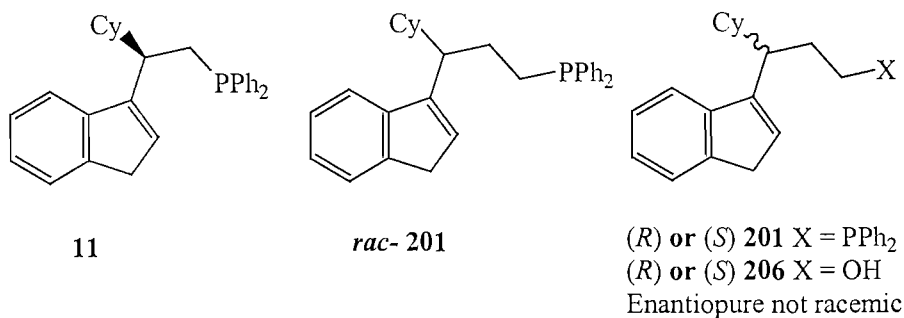


Figure 3.1

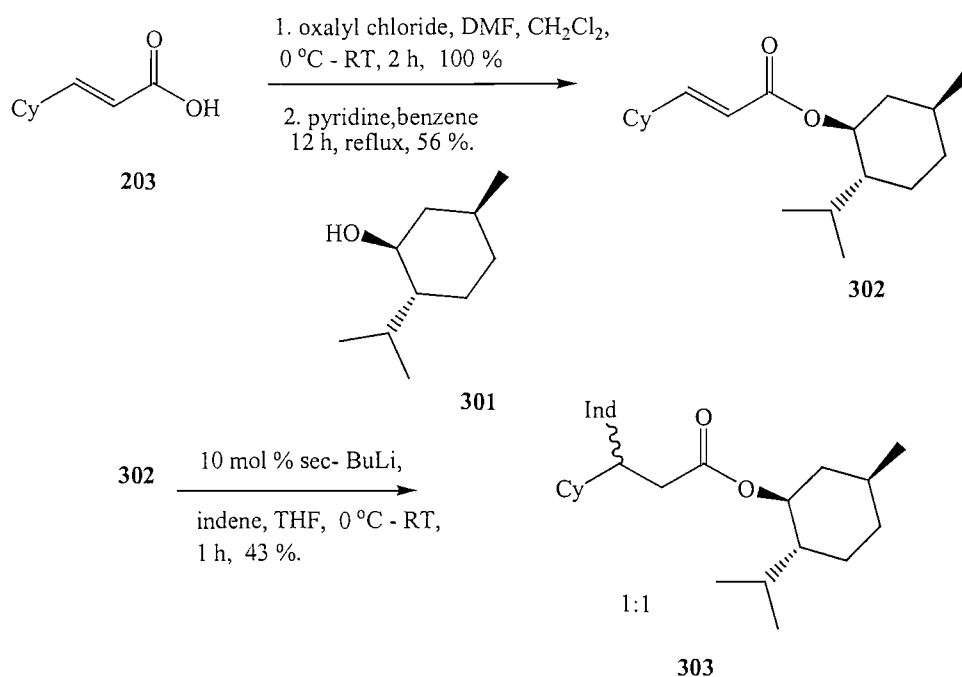
The use of a chiral auxiliary during the catalytic 1,4-addition of the indenyl anion to a 3-cyclohexylacrylate was a potential method of synthesising enantiopure **206**. Another approach was asymmetric hydrogenation of a β -keto ester and subsequent displacement of a leaving group by indene, or using a chiral bidentate phosphine-ruthenium complex of (*R*) or (*S*)-BINAP. Once enantiopure **206** has been formed, the

route previously developed for the racemic ligand would furnish the enantiopure three carbon-tethered ligand (*R*) or (*S*)-**201**.

3.2 Attempted synthesis of an enantiopure form of **206** using a chiral auxiliary.

3.2.1 Synthesis using (1*S*,2*S*,5*S*)-(-)-Menthol, **301**.

With the success of the catalytic indene addition to α,β -unsaturated esters, (Section 2.3.1) it was postulated that use of a chiral ester could result in enantioenriched **206**. The first attempt was made using (1*S*,2*S*,5*S*)-(-)-menthol **301** as a chiral auxiliary. Reaction of the acid chloride derivative of **203** with (1*S*,2*S*,5*S*)-(-)-menthol **301**, gave the desired ester **302** in 56 % yield (Scheme 3.1).⁶⁸



Scheme 3.1

Reaction of **302** with indenyl anion under both catalytic and stoichiometric conditions proved successful, giving **303** in moderate yield. Unfortunately a 1:1 mixture of diastereoisomers was obtained according to NMR, and these were inseparable by chromatography. The poor diastereoselectivity is probably due to the chiral auxiliary in **302** being remote from the reaction centre.

3.2.2 Synthesis using (7*R*)-10,10-dimethyl-5-thia-4-azatricyclo[5.2.1^{0,3,7}]decane-5,5-dioxide, 304.

Another attempt at synthesising enantiopure **206** was made using Oppolzer's crystalline sultam **304** as a chiral auxiliary (Figure 3.2).⁷⁶⁻⁷⁸ Sultam **304** has been used in Lewis acid catalysed Diels-Alder and asymmetric 1,4-addition reactions,^{76,77} and in conjugate additions to enoylsultams.⁷⁸

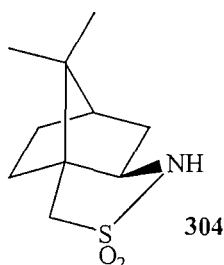
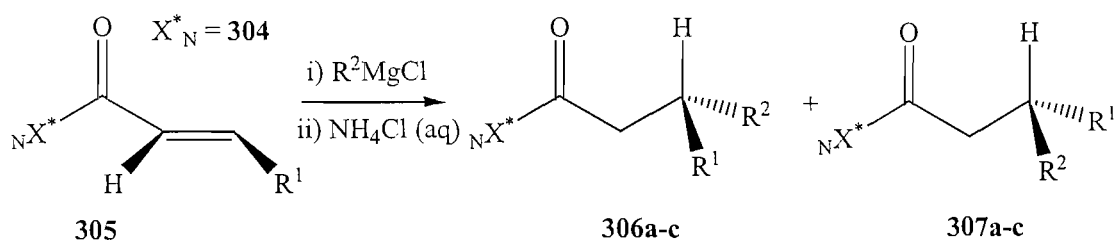


Figure 3.2

Simple alkylmagnesium chlorides add smoothly in a 1,4-fashion to β -substituted (*E*)-enoylsultams to give, on subsequent treatment with aq. NH_4Cl , amides **306a-c** and **307a-c** in good yields.⁷⁸ In all cases, **306** dominated significantly over its epimer **307** and no 1,2-additions were observed, except with methyl Grignards (Scheme 3.2) (Table 3.1).⁷⁸

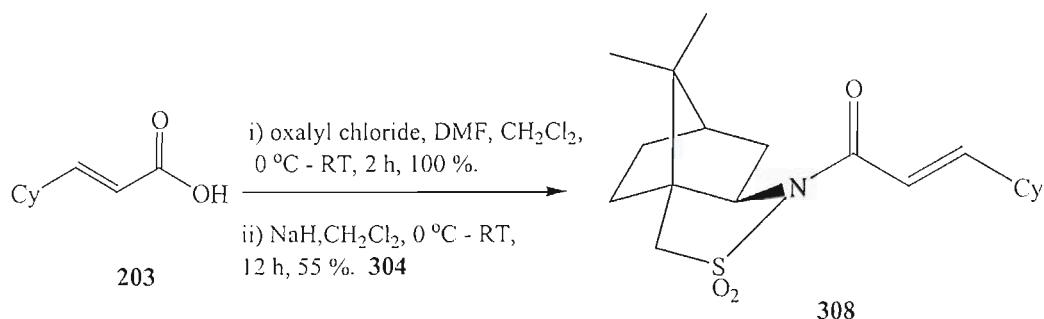


Scheme 3.2

Entry	R^1	R^2	Yield (%) of 306 +	
			307	Ratio of 306: 307
a	Me	Et	80	94.5:5.5
b	Me	Pr	90	92.6:7.4
c	Me	Bu	78	93.2:6.8

Table 3.1

It was hoped **304** would direct the indene anion preferentially onto one face of the olefin yielding enantiopure **206** following subsequent removal of the auxiliary. Reaction of the acid chloride derivative of **203** with the sodium salt of sulphonamide **304**, gave the desired sulphonamide **308** in 55 % yield (Scheme 3.3).⁶⁸



Scheme 3.3

Purification of **308** was achieved by recrystallisation and X-ray crystal analysis confirmed the structure was as shown (Figure 3.3).

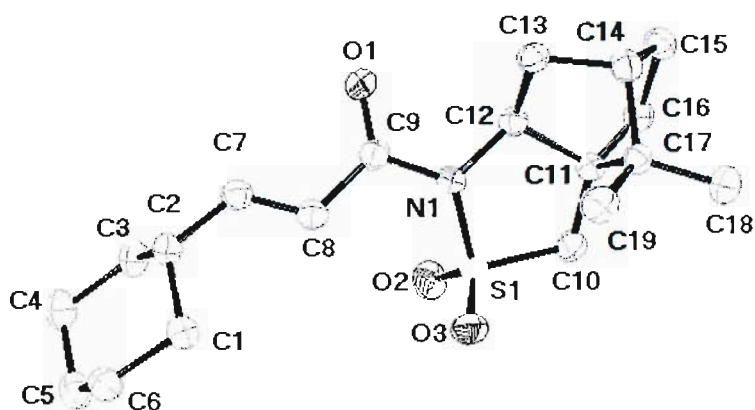


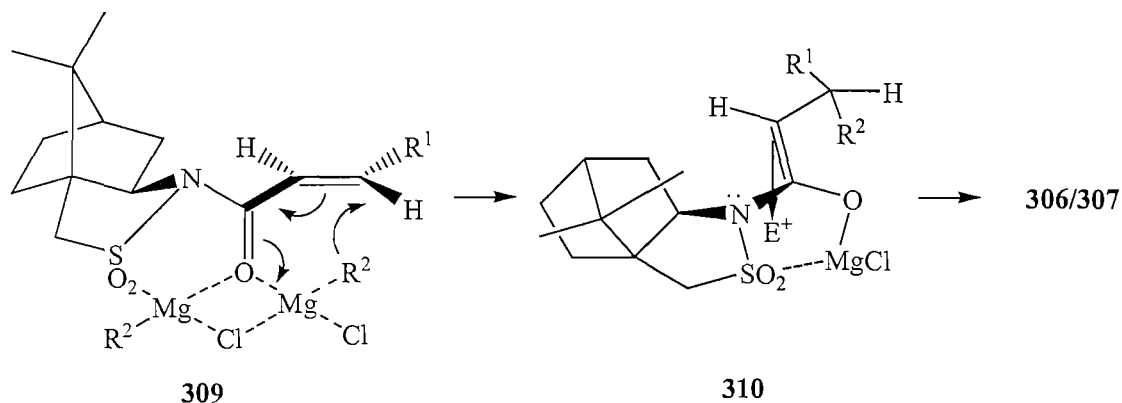
Figure 3.3

ORTEP view of **308**, thermal ellipsoids drawn at 30 % probability.

See appendix 1 for full details.

Reaction of **308** with the indenyl anion under the catalytic and stoichiometric reaction conditions proved unsuccessful with indene and sulphonamide **304** being recovered. This suggests nucleophilic attack on the carbonyl group and elimination of **304** occurred. The use of an alkyllmagnesium Grignard reagent may have had a positive effect on the stereoselectivity of the reaction.⁷⁸ The delivery of R² occurs from the bottom side of the olefin, opposite to the lone pair on the nitrogen, via a 6-membered transition state, **309**. The (*E*)-conformation changes into the 'enolate' (*Z*)-conformation, **310** and subsequent electrophilic attack from the bottom face yields

306 (Scheme 3.4).⁷⁸ The attack of the indenyl anion will be discussed later (Section 3.2.3)



Scheme 3.4

3.2.3 Synthesis using sulfonamide-isoborneol, **312**.

With the failure of the sultam **304** in directing the indene anion preferentially onto one face of the olefin (Section 3.2.2), we searched for a more powerful π -face shielding ester auxiliary. Oppolzer has used **311** as a practical acrylate stereoface-directing moiety in the Diels-Alder addition to cyclopentadiene.⁷⁹ An even more powerful π -face shielding sulfonamide moiety is **312** which was found to be a practical acrylate stereoface-directing moiety in the Diels-Alder additions (Figure 3.4).^{80,81}

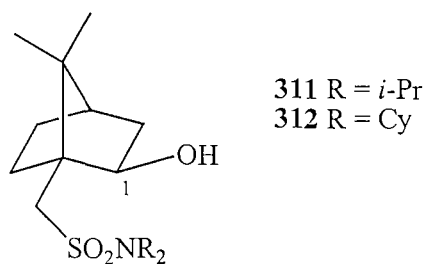
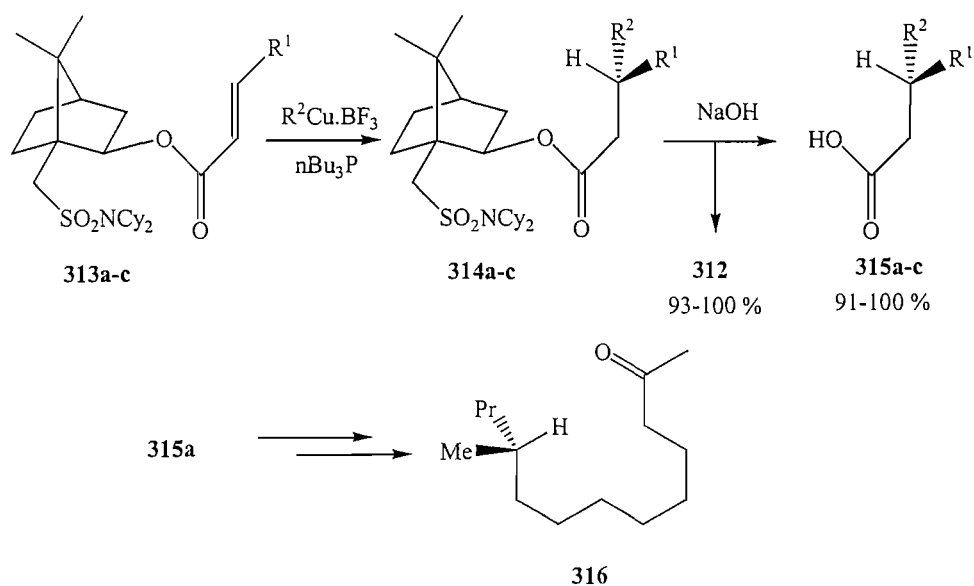


Figure 3.4

Oppolzer has shown that **312** is a regenerable chiral auxiliary in highly face selective C-C bond forming reactions using organocuprate reagents.⁸¹⁻⁸³ An example is the conjugate addition of organocuprates to enoates **313a-c** giving **314a-c**. After saponification, **312** is regenerated and β -substituted carboxylic acids **315a-c** are isolated in high yield and e.e as shown (Scheme 3.5) (Table 3.2).⁸¹

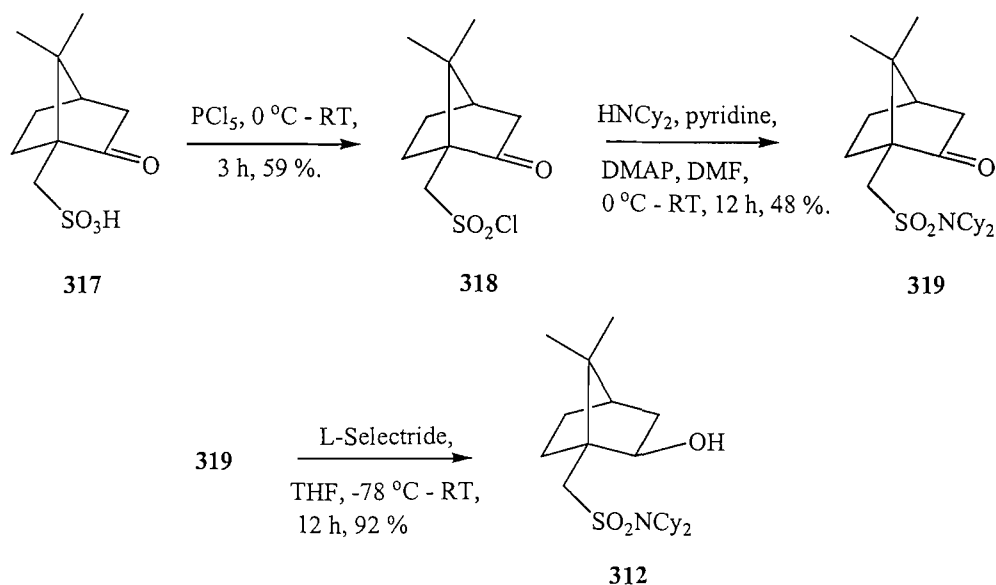


Scheme 3.5

Entry	R ¹	R ²	Yield (%) of 314	e.e. (%) of 315
a	Me	Pr	98	97
b	Me	Bu	89	97
c	Me	Vinyl	80	98

Table 3.2

Acid **315a** served as a key intermediate for the synthesis of the southern corn rootworm pheromone **316** (Scheme 3.5).⁸¹ It was believed that **312** would be successful in the 1,4 addition of the indenyl anion by π -face shielding to a greater extent than previously seen. The chiral auxiliary **307** was readily prepared starting from (-)-camphor-10-sulfonic acid, **317**. Treatment of **317** with PCl_5 gave the sulfonyl chloride **318**, in 59 % yield. Subsequent amidation with dicyclohexylamine gave **319** in 48 % yield and reduction gave **312** in 92 % yield (Scheme 3.6).⁸⁰



Scheme 3.6

Purification of **312** was achieved by recrystallisation and X-ray crystal analysis confirmed the structure was as shown. (Figure 3.5)

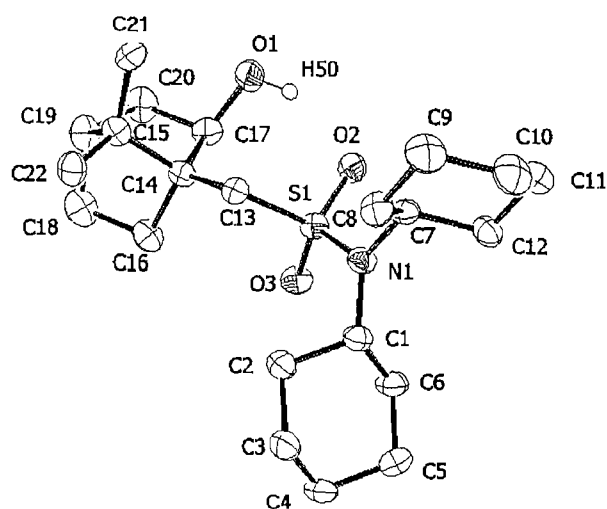
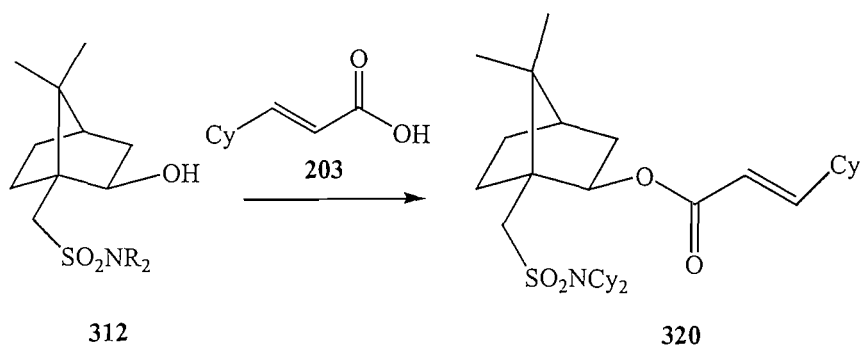


Figure 3.5

ORTEP view of **312**, thermal ellipsoids shown at 50% probability.

See Appendix 2 for full details

The next step was to form the Michael addition precursor, **320**. This involves reaction of alcohol **312** with acid **203** (Scheme 3.7). Esterification using α -chloro-N-methylpyridinium iodide was attempted initially.⁸⁰ After 24 h reflux, ¹H NMR suggested no reaction occurring with starting material remaining. This was surprising, as esterification had been achieved with acrylic acid under identical conditions.⁸⁰

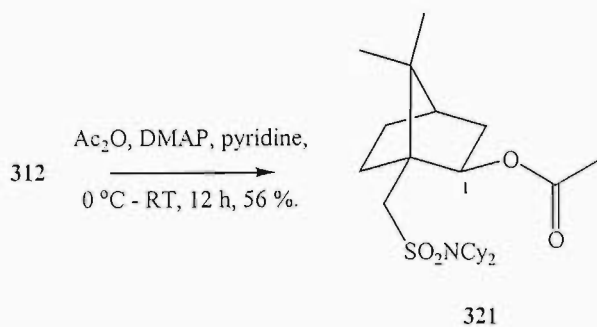


Scheme 3.7

Analysis of the X-ray structure of **312** suggests reasons for unreactivity of the alcohol (Figure 3.5). There is strong hydrogen bonding between the hydroxy proton **H50** and both oxygen atoms on the SO₂ group. The bond lengths are very short, 2.0 Å to O2 and 3.6 Å to O3 respectively, and the hydroxyl proton is pointing directly towards O2. The steric bulk of the cyclohexyl group of **203** may also have contributed to the failure of the reaction.

The method of Arad Yellin was also attempted.⁶⁸ This involves reaction of the acid chloride derivative of acid **203** with **312**. After 24 h reflux, ¹H NMR suggested no reaction occurring with starting material remaining. This was unfortunate as the reaction is being exposed to harsh conditions and has been successful in synthesising esters previously (Section 3.2.1). Coupling of **312** with acid **203** to give the sulfonamide **320** was also attempted using DCC following the method of Stoermer.⁸⁴ After 24 h at RT, and a further 16 h at reflux, ¹H NMR suggested only starting material remained. This was surprising as DCC is a reliable coupling agent in ester formation. After 24 h at RT, and a further 12 h refluxing in dichloroethane, ¹H NMR again suggested no reaction occurring.

An indication of where the key signal at C1 would appear in the ¹H NMR spectrum of sulfonamide **320** was needed. To achieve this **312** was reacted with acetic anhydride as shown (Scheme 3.8). After 12 h at RT, ¹H NMR suggested reaction had occurred with no starting material remaining, and a new signal at δ = 4.96 ppm. Purification by column chromatography isolated ester **321** in 56 % yield.



Scheme 3.8

Purification was achieved by recrystallisation and X-ray crystal analysis confirmed the structure of **321** was as shown (Figure 3.6).

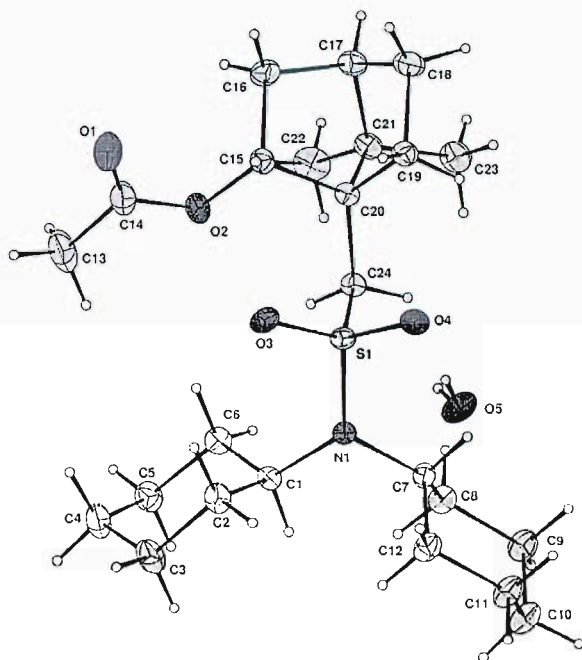
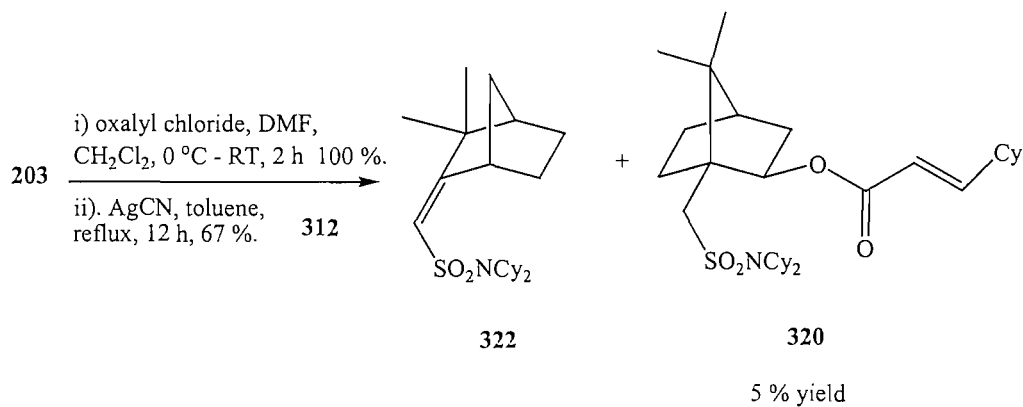


Figure 3.6

ORTEP view of **321**, thermal ellipsoids shown at 50 % probability.

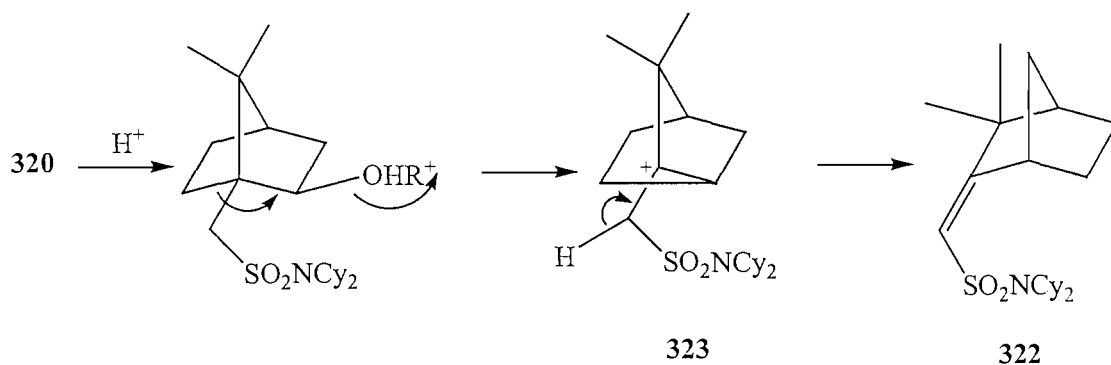
See Appendix 3 for full details

Literature suggested that acylation of auxiliary alcohol **312** with acid chlorides could be achieved in the presence of AgCN in good yield.⁸⁵⁻⁸⁷ The first attempt involved reaction of **312** with the acid chloride derivative of acid, **203** in the presence of AgCN in refluxing toluene (Scheme 3.9).⁸⁵ After 12 h reflux, ¹H NMR suggested the complete loss of alcohol **312**. Column chromatography isolated the major product as **322** in 67 % yield with the minor product being the required sulfonamide **320**. (Scheme 3.9).



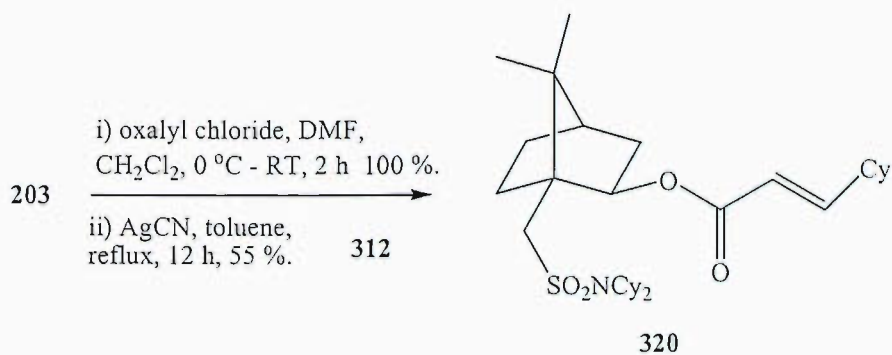
Scheme 3.9

It was found that a known acid catalysed rearrangement was occurring to give **322**. (Scheme 3.10).⁸⁸ Two ‘NMR-tube’ scale experiments proved that the rearrangement was not a thermal rearrangement of either alcohol **312** or ester **320**. The rearrangement is catalysed by HCN generated during the reaction, which gives the tertiary carbocation intermediate **323**. Subsequent proton extraction gives **322** (Scheme 3.10).



Scheme 3.10

If the length of time of reaction was reduced to 2 h, and the amount of AgCN increased to 2.2 equivalents, very little rearrangement occurs and ester **320** was isolated in reasonable 55 % yield (Scheme 3.11).⁸⁵ The AgCN either acts as a Lewis acid, or the acyl cyanide is formed and is subsequently more reactive than the acyl chloride. Unreacted alcohol **312** can be recovered and reused.



Scheme 3.11

Purification of **320** was achieved by recrystallisation and X-ray crystal analysis confirmed the structure was as shown. (Figure 3.7)

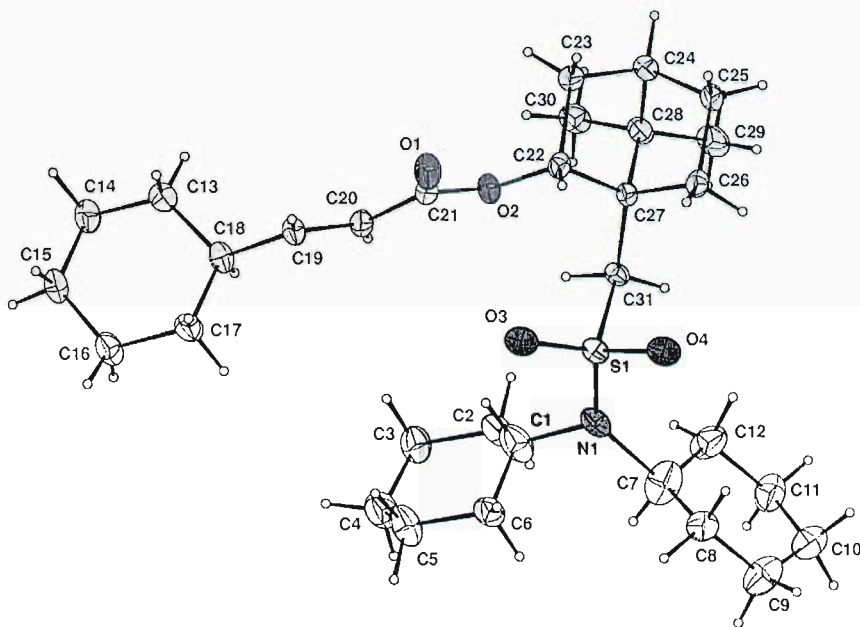
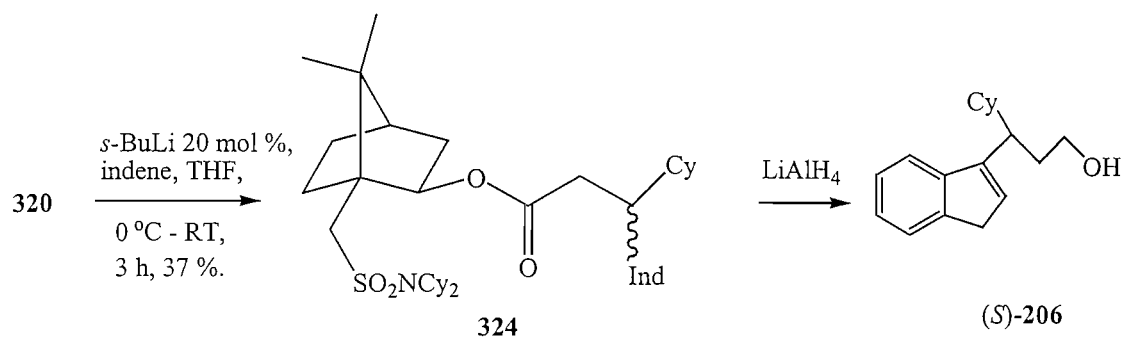


Figure 3.7

ORTEP view of **320**, thermal ellipsoids drawn at the 35 % probability level, only one position of the disordered SO_2 group is shown. All hydrogen atoms were placed in idealised positions and refined using a riding model. The SO_2 group occupies 2 positions with occupancies of 70 and 30 %. See Appendix 4 for full details.

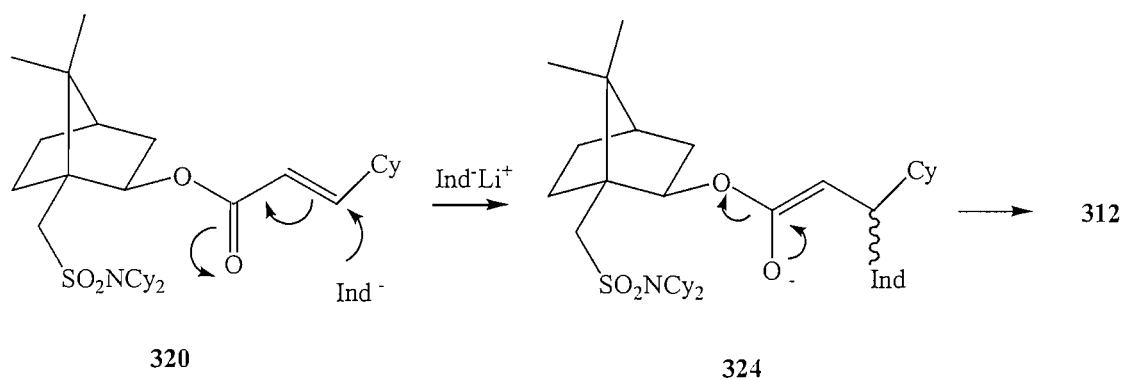
The reaction of **320** with indenyl anion under the catalytic reaction conditions proved successful giving **324** in moderate 37 % yield (Scheme 3.12). Subsequent reduction of **324** using LiAlH_4 gave alcohol **312** and **206**. Analysis by chiral HPLC showed that (*S*)-**206** had been synthesised with 6 % e.e. HPLC analysis, Chiracel OD-H column 10

% IPA / hexanes, 1 mL / min with retention times 27.7 and 31.9 (major enantiomer) minutes.



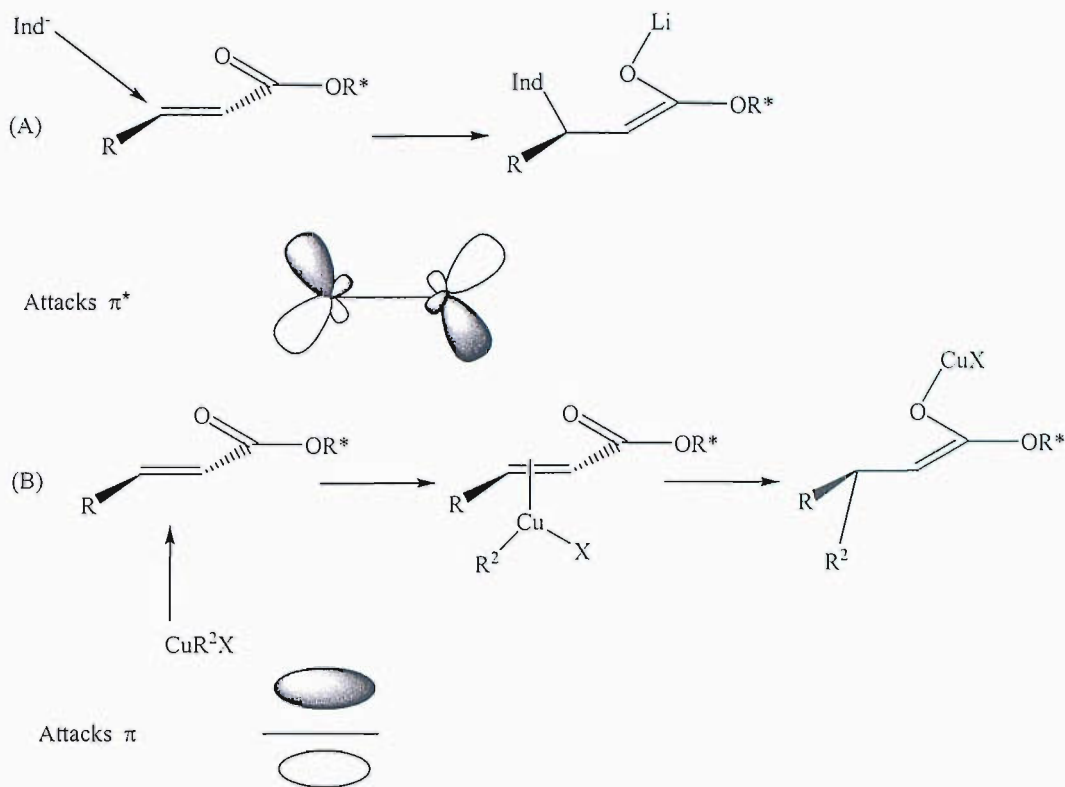
Scheme 3.12

Reaction of **320** with stoichiometric indenyl anion yielded alcohol **312** (Scheme 3.13). This suggests that elimination competes with indenyl lithium addition but this was never proved.



Scheme 3.13

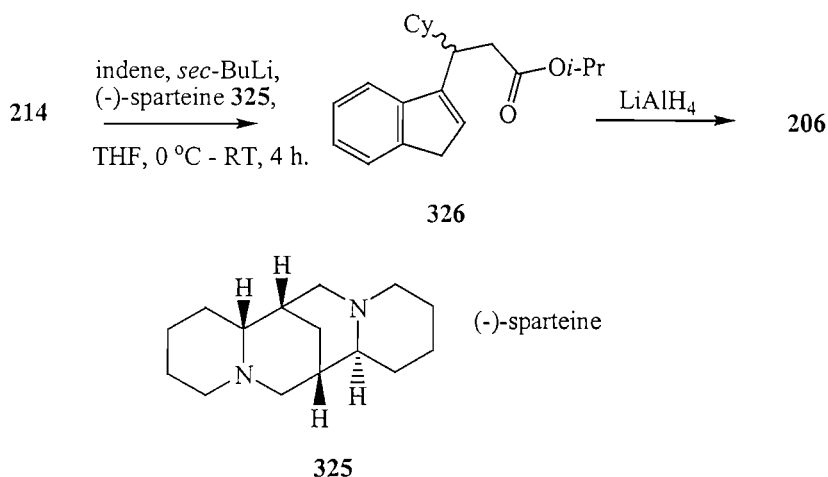
This was a disappointing result. Chiral auxiliary **312** was obviously not a good π -face shielding sulfonamide moiety. The addition of the indenyl anion can occur with high diastereoselectivity. The use of an organocuprate reagent may have had a positive effect on the e.e., as the conjugate additions of such reagents occur with high diastereoselectivity.^{89,90} Organocopper reagents probably initially form a π -complex with one face of the alkene so they are much closer to the auxiliary, thus giving high diastereoselectivity (Scheme 3.14).^{89,90} The indenyl anion is undergoing direct nucleophilic attack via a Burgi-Dunitz trajectory on the π^* antibonding orbital of the alkene which is oriented away from the auxiliary (Scheme 3.14). A new synthetic route is required to synthesise **206** as a single enantiomer.



Scheme 3.14

3.2.4 Synthesis using catalytic BuLi/sparteine.

The next attempt synthesise of **206** as a single enantiomer was to use (-)-sparteine **325** in the catalytic indene anion reaction (Scheme 3.15).⁹¹ Laqua has reported the synthesis of enantioenriched indene-derived bicyclic alcohols *via* (-)-sparteine-mediated lithiation of a racemic precursor.⁹¹ The next attempt to synthesise **206** as a single enantiomer was to make the nucleophile chiral itself, thus inducing enantioinduction. Equimolar amounts of *sec*-BuLi and (-)-sparteine, **325** were used and after 4 h at RT, GC indicated formation of product (Scheme 3.15).

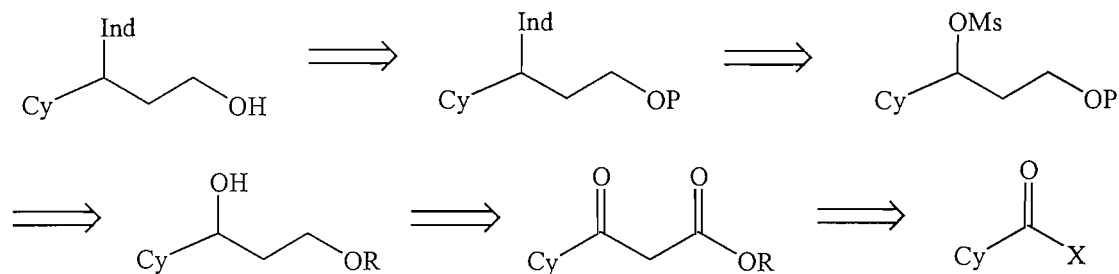


Scheme 3.15

Unfortunately a 1:1 mixture of enantiomers was obtained according to ^1H NMR. Subsequent reduction using LiAlH_4 and analysis by chiral HPLC confirmed the 1:1 mixture of enantiomers. HPLC analysis, Chiracel OD-H column 10 % IPA / hexanes, 1 mL / min with retention times 27.7 and 31.9 minutes. This was not ideal.

3.3 Synthesis by nucleophilic displacement of a chiral secondary alcohol.

With the failure of synthesising **206** as a single enantiomer using a chiral auxiliary as a stereoface-directing moiety, it was decided to turn our efforts to an alternative synthetic approach. Scheme 3.16 shows a homochiral retrosynthetic analysis of the desired alcohol **206**. The displacement of a secondary mesylate with indene is the key step with inversion of configuration via an $\text{S}_{\text{N}}2$ mechanism being envisaged. Continuing the retrosynthetic analysis, the selective protection of a primary alcohol preceded by an asymmetric hydrogenation using a chiral bidentate phosphine-ruthenium complex of a β -keto ester, were also envisaged.



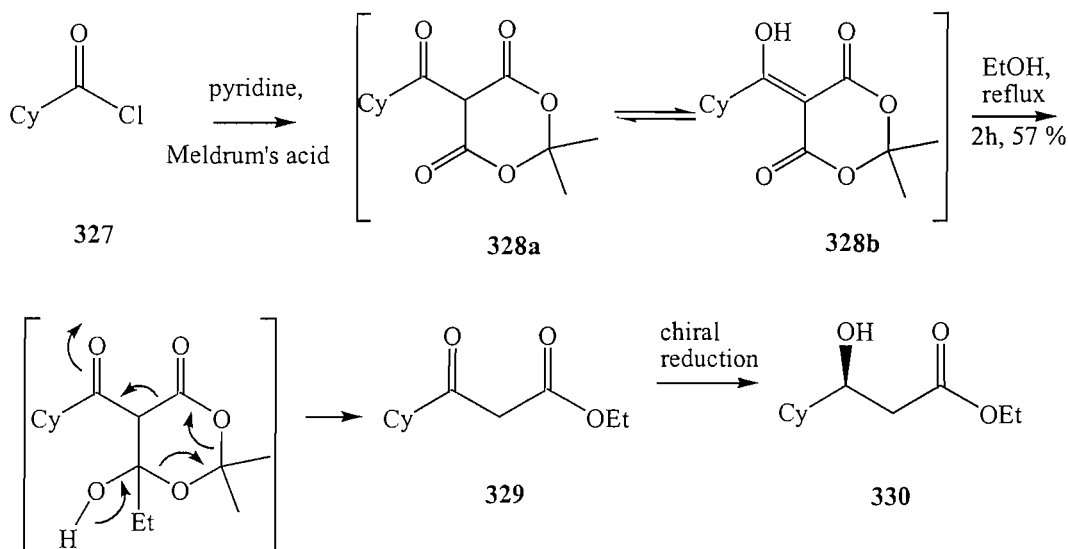
Scheme 3.16

The results of the forward synthesis of **206** as a single enantiomer via this route are discussed below.

3.3.1 Asymmetric hydrogenation of a β -keto ester.

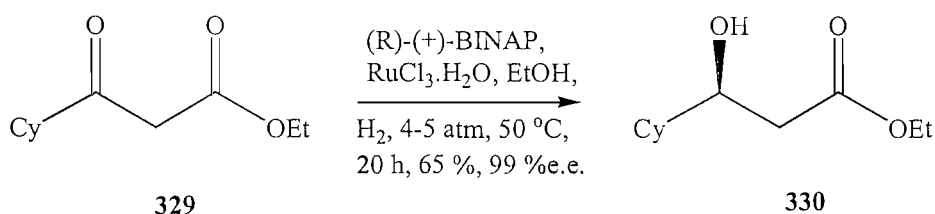
Burk has reported the hydrogenation of a cyclohexyl substituted β -ketoester in 99.1 % e.e using a ruthenium-1,2-bis(trans-2,5-diisopropylphospholano)ethane catalyst.⁹² Our preferred method, on base of cost and experimental ease, was reported for the substrate with an isopropyl group instead of the cyclohexyl group, using (*S*)-MeO-BIPHEP / RuCl₃.⁹³ It was believed that cheaper BINAP would also work well under these conditions.^{94,95}

Large scale reaction of **327**, with 2,2-dimethyl-1,3-dioxane-4,6-dione gave an intermediate that underwent decarboxylation when refluxed in EtOH to give β -keto ester **329** in 57 % yield. (Scheme 3.17).^{96,97}



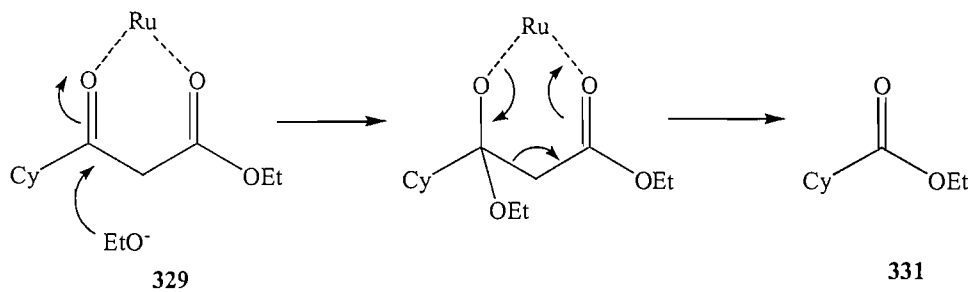
Scheme 3.17

The first attempt at an asymmetric hydrogenation using a chiral bidentate phosphine-ruthenium complex involved in the *situ*-generation of a chiral ruthenium-diphosphine catalyst from RuCl_3 and (R)-(+)-BINAP (Scheme 3.18).⁹³ Using a 1 mol % catalyst loading, after 16 h at 50 °C, and 4-5 atm H_2 , GC suggested loss of ester **329**. After purification, it was found that reaction had occurred and analysis by chiral HPLC showed that hydroxy ester **330** had been synthesised in 99 % e.e. and 65 % yield. HPLC analysis, Chiracel OD-H column 5 % IPA / hexanes, 1 mL / min with retention times 7.3 (major enantiomer) and 11.2 (minor enantiomer) minutes.



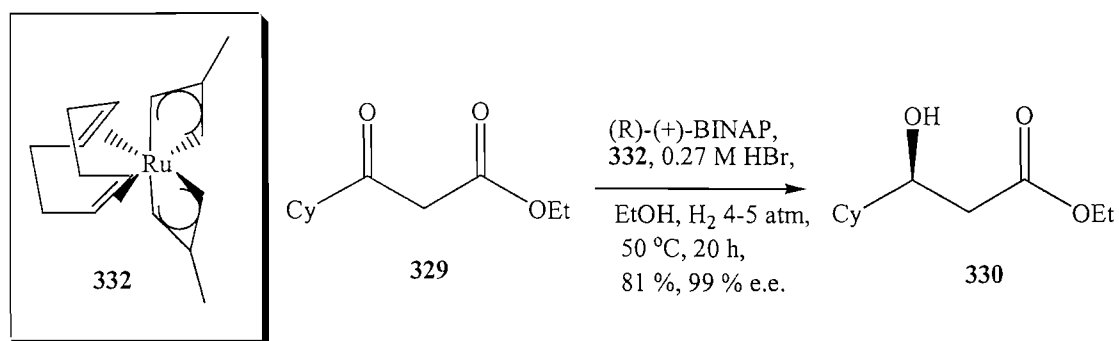
Scheme 3.18

This was an encouraging result. However, both a 65 % yield and a 1 mol % catalyst loading were not ideal. On a large scale this would be an expensive process, but the use of hydrous RuCl_3 made ease of handling reagents good. It was found that the low yield was due to a competing ruthenium catalysed retro aldol condensation also occurring with ester **331** being formed (Scheme 3.19).⁹⁸



Scheme 3.19

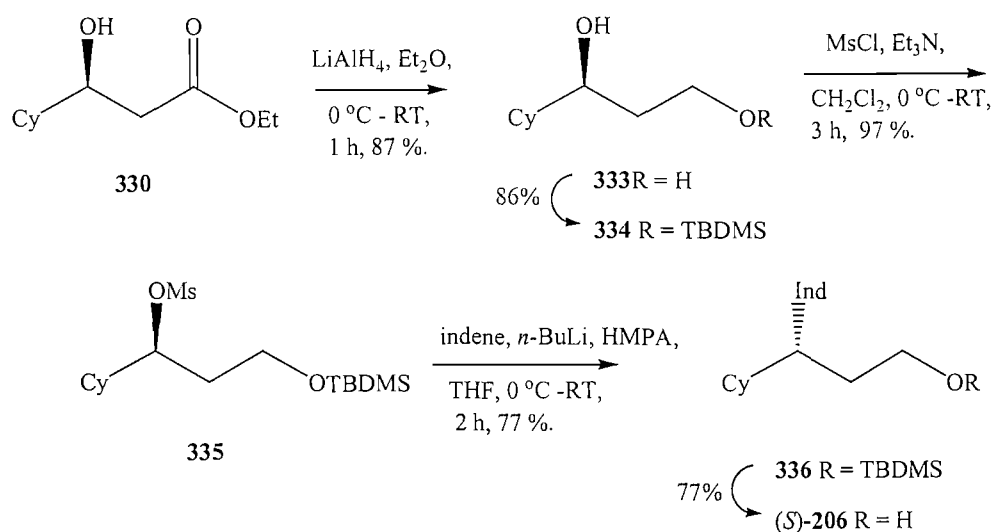
The second attempt at an asymmetric hydrogenation involved the in situ generation of a chiral bidentate phosphine ruthenium complex from (R)-(+)-BINAP, an excess of HBr (0.27 M soln in MeOH) and η^4 -1,5-cyclooctadiene)bis(η^3 -2-methylallyl)ruthenium(II), **332**.⁹⁹⁻¹⁰² Using a 0.1 mol % catalyst loading, after 16 h at 50 °C, and 4-5 atm H₂, GC suggested loss of ester **329** (Scheme 3.20). After purification, it was found that reaction had occurred and analysis by chiral HPLC showed that hydroxy ester **330** had been synthesised in 55 % yield and 99 % e.e. This was more encouraging as a reasonable yield and a high e.e. were being achieved with a lower catalyst loading. Optimisation resulted in performing the reaction on a 30 mmol scale with 0.4 mol % catalyst loading and this gave the enantiomerically pure hydroxy ester **330** in 81 % yield and 99 % e.e (Scheme 3.20). HPLC analysis, Chiracel OD-H column 5 % IPA / hexanes, 1 mL / min with retention times 7.3 (major enantiomer) and 11.2 (minor enantiomer) minutes.



Scheme 3.20

3.3.2 Synthesis of enantiopure alcohol, (*S*)-206.

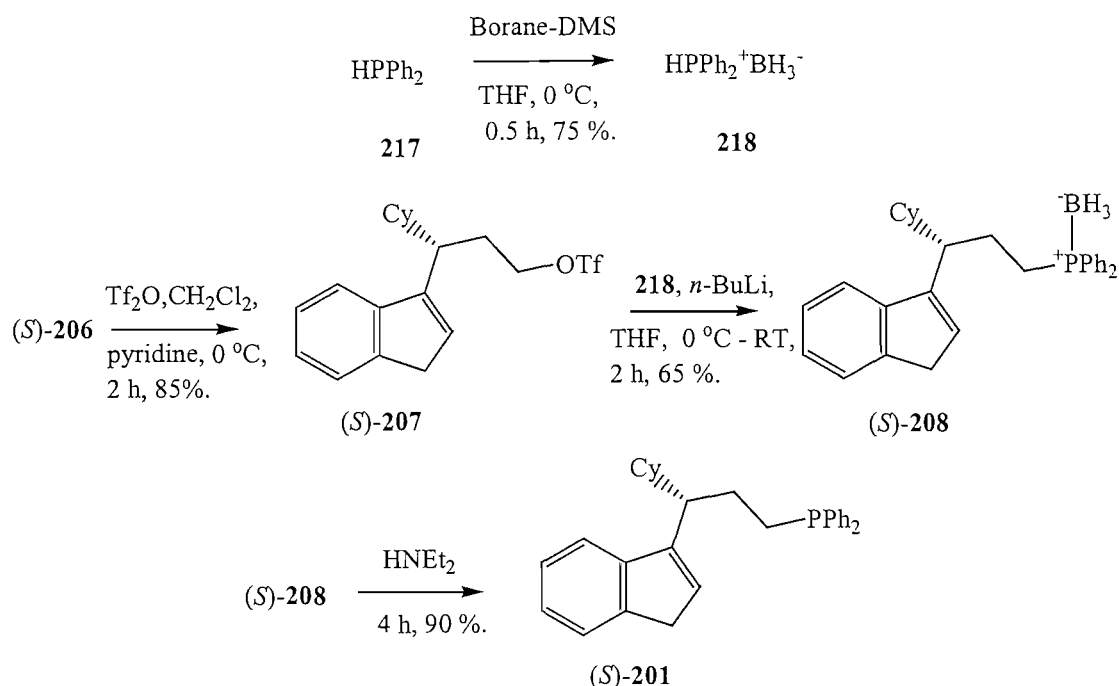
With the enantiomerically pure hydroxy ester **330** now formed, the next task was to synthesise **206** as a single enantiomer (Scheme 3.21). Reduction of **330** with LiAlH_4 gave diol **333**. Protection of the primary alcohol was attempted using TBDMSCl but this proved unsuccessful with none of the desired product being observed.¹⁰³ However, reaction with TBDMSTf was successful giving **334** in high yield. Reaction of **334** with methanesulfonyl chloride gave **335**. Displacement of the secondary mesylate **335** with indene was the key step with inversion of configuration via an $\text{S}_{\text{N}}2$ mechanism being envisaged. Formation of **336** was achieved in very reasonable yield. However, the addition of HMPA was essential to give the desired kinetic product, as without HMPA, a mixture of double bond isomers was isolated according to ^1H NMR. Isomerisation of the mixture to the desired product using *n*-BuLi was attempted but this proved unsuccessful. Subsequent removal of the protecting group to gave the enantiomerically pure alcohol (*S*)-**206** in 77 % yield and 98 % e.e (Scheme 3.21).¹⁰⁴ HPLC analysis, Chiracel OD-H column 2 % IPA / hexanes, 1 mL / min with retention times 31.1 (minor enantiomer) and 35.6 (major enantiomer) minutes.



Scheme 3.21

3.4 Synthesis of an enantiopure phosphine ligand, (*S*)-201

The formation of the enantiopure phosphine ligand (*S*)-201 was achieved as discussed earlier (Section 2.2.3). Enantiopure borane (*S*)-208 was isolated in 65 % yield.⁷⁰ Subsequent removal of the borane protecting group gave enantiopure (*S*)-201 in high yield (Scheme 3.22).⁷²



Scheme 3.22

As (*S*)-201 is very air- and moisture-sensitive, deprotection of the borane-protected phosphines was only carried out when complexation of the ligand to ruthenium was attempted.

3.5 Conclusions

- The use of chiral auxiliary **307** as a powerful π -face shielding sulfonamide moiety, proved unsuccessful with (*S*)-206 being isolated in 6 % e.e.
- The asymmetric hydrogenation of **330** using a chiral bidentate phosphine-ruthenium complex was achieved in 81 % yield and 99 % e.e.
- The synthesis of alcohol (*S*)-206 as a single enantiomer has been achieved. It has been carried out on a 30 mmol scale, with an overall yield of 26 % after 7 steps in 98 % e.e. This means a number of potentially very interesting

enantiomerically pure ligands can be synthesised and complexed onto transition metals can be investigated.

- The displacement of the secondary mesylate **335** by indene proved to be very successful with enantiomeric purity being maintained.
- The displacement of triflate group with $\text{Li}^+\text{PPh}_2\text{BH}_3$, results in the synthesis of borane-adduct (*S*)-**208**. Deprotection gives the enantiomerically pure free phosphine (*S*)-**201** with no need for purification by column chromatography under argon.

Chapter 4: The optimisation and synthesis of novel ruthenium complexes.

4.1 Background and aims

The optimised and novel synthesis of indene-phosphorus linked ligands has been discussed in chapters 2 and 3. These ligands contain a bidentate cyclopentadienyl-‘anchor’ structure, specifically designed for complexation to transition metals (Figure 4.1).

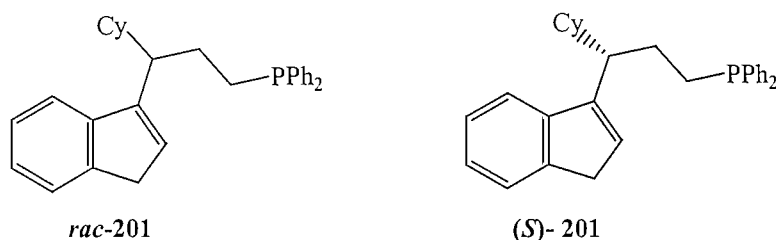
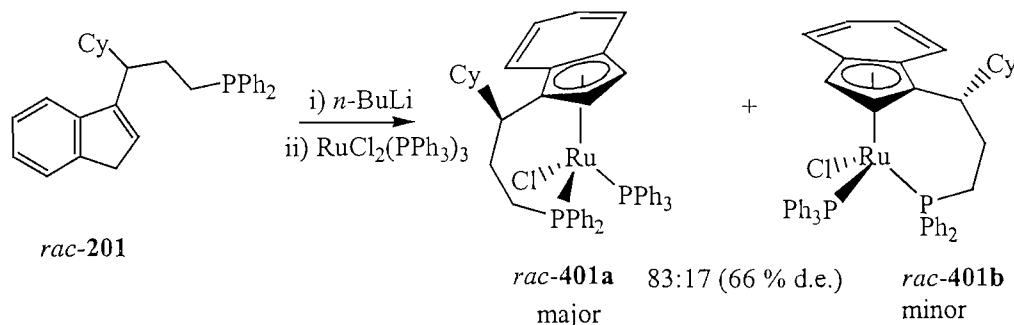


Figure 4.1

Ligands *rac*-201 and (*S*)-201 contain a chiral centre on the cyclopentadienyl -‘anchor’ chain, positioned *alpha* to the indene group, in order to fulfil the requirements of the ‘favoured rotamer’ complexation model (Section 1.2.2). Harrison has shown that reaction of lithiated *rac*-201 with $\text{RuCl}_2(\text{PPh}_3)_3$ in toluene, refluxing for 24 h, and isolation by column chromatography through neutral Al_2O_3 under oxygen free conditions, afforded complexes *rac*-401a and *rac*-401b in 55 % and 9 % yield respectively (Scheme 4.1).¹³ The complete control of metal centred chirality is notable.



Scheme 4.1

With large amounts of *rac*-**201** and samples of (*S*)-**201** in hand, our aim was now to:

- Produce large amounts of complex *rac*-**401** for catalytic studies
- Synthesise the single enantiomer form of **401**
- Synthesise the cationic and tetrahydroindenyl derivatives of **401**
- Investigate the induction of metal centred asymmetry in derivatives of *rac*-**401** obtained by ligand exchange.

4.2 The optimisation and synthesis of complexes.

4.2.1 Optimised synthesis of *rac*-**401**.

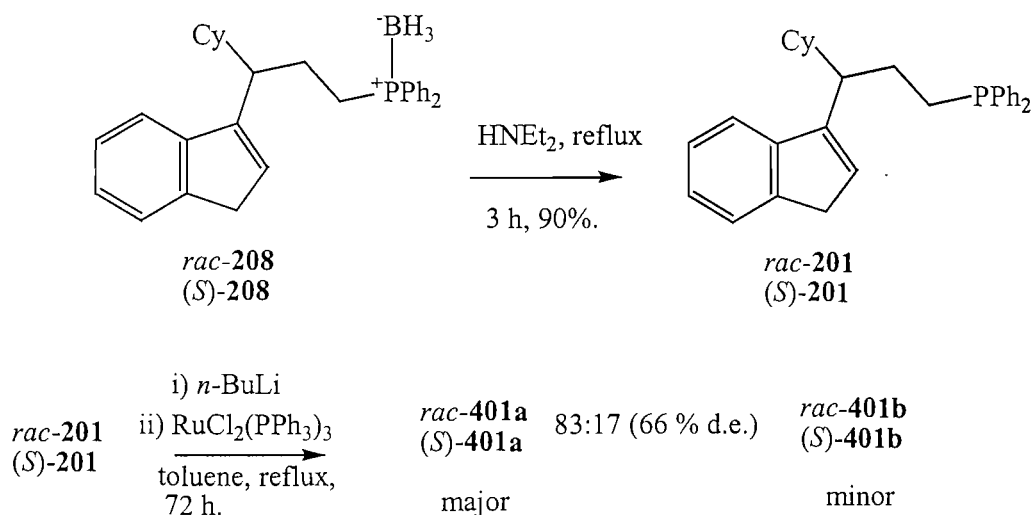
On a 1 mmol scale, *rac*-**201**, produced immediately before use by deprotection of *rac*-**208**, was deprotonated using *n*-BuLi at -78 °C in toluene, then treated with a solution of RuCl₂(PPh₃)₃ and warmed to reflux. After refluxing for 24 h, ¹H NMR of the crude material showed an 84:16 ratio of two diastereoisomers (68 % d.e.). Two separate components were visible by TLC, therefore the reaction was cooled and careful chromatography through Al₂O₃ in air allowed isolation of the major isomer *rac*-**401a**, and the minor isomer *rac*-**401b** in 38 % and 5 % yield respectively. This suggested that purification under inert conditions was not needed although the yields were lower than expected. The reaction was repeated on a similar scale and on a 5 mmol scale and both reactions were refluxed for a longer period of time (Table 4.1).

Scale of reaction	Time reflux (h)	Major isomer (%)	Minor isomer (%)	Ratio of diastereomers	d.e (%)
(1 mmol)	24	38	5	84:16	68
(1 mmol)	72	50	14	82:18	64
(5 mmol)	72	52	16	83:17	66

Table 4.1

It can be seen that increasing the length of time of the reaction increases isolated yield of both isomers. Chromatography was performed in air and seems to have had no detrimental effect with yields being comparable to those previously obtained (Scheme 4.2).¹³ This is encouraging and would be beneficial for large scale production of *rac*-**401**. It was found that the complexation required harsh reaction conditions, as no

reaction occurred at RT.



Scheme 4.2

The ^1H NMR of the planar-chiral diastereoisomers *rac-401a* and *rac-401b* show some major differences. The cyclopentadienyl protons of the major isomer *rac-401a*, are present at δ 4.65 and 3.36 ppm. The high field shift of one Cp-proton is a result of its close proximity to a phenyl ring of the triphenylphosphine ligand.³⁰ For the minor isomer *rac-401b*, both Cp-protons appear further downfield, at δ 4.90 and 4.38 ppm. This suggests a very different conformation of the ligand in this minor isomer. Upon complexation to ruthenium with *rac-201*, we have maintained complete control over the induction of chirality at the metal centre of complex *rac-401*. The high degree of induction of planar chirality (66 % d.e.) achieved with ligand *rac-401*, demonstrates the success of the ‘favoured rotamer’ complexation model and design of the *alpha*-substituted cyclopentadienyl-phosphine ligands.

4.2.2 Synthesis of enantiopure (S)-401

Please note that the chirality of the complexes has been derived from the chirality of the uncomplexed ligand.

With the successful optimisation of the synthesis of *rac-401*, (Section 4.2.1), complexation of the enantiopure three-carbon-tethered ligand (S)-201 to ruthenium was attempted. Following the same procedure as for ligand *rac-201*, the enantiopure three-carbon-tethered ligand (S)-201 was complexed with $\text{RuCl}_2(\text{PPh}_3)_3$ to form

complex (*S*)-**401** (Scheme 4.2). After refluxing for 72 h, ^1H NMR of the crude material showed an 83:17 ratio of two diastereomers (66 % d.e.). After the reaction was cooled, careful chromatography through Al_2O_3 under normal air conditions provided both isomers of complex (*S*)-**401**. The major isomer (*S*)-**401a** eluted first as a brown solid, 51 % yield and the minor isomer (*S*)-**401b** eluted second, as a red/brown solid in 16 % yield (Scheme 4.2).

Crystallisation of the major isomer (*S*)-**401a** was achieved by slow diffusion of hexane into a benzene solution of the complex and X-ray crystal analysis confirmed the structure was as shown, including the absolute stereochemistry (Figure 4.2).

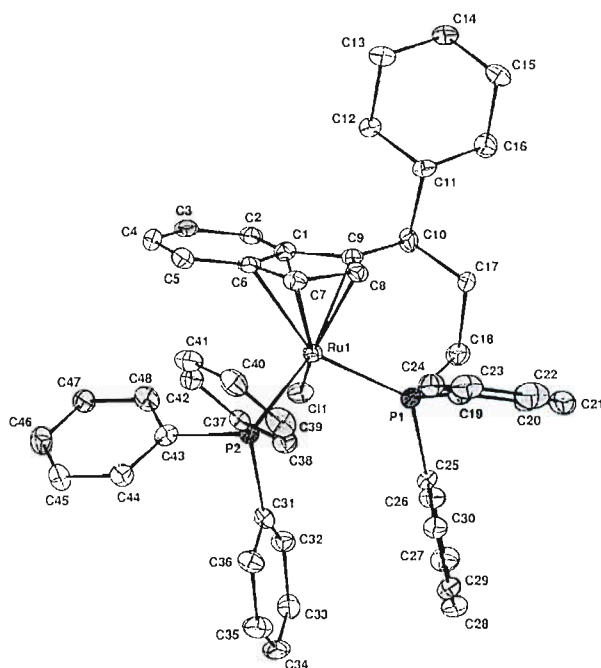


Figure 4.2

ORTEP view of major isomer (*S*)-**401a**. One of the two identical molecules in the asymmetric unit, thermal ellipsoids drawn at the 50 % probability level and hydrogens and solvent omitted for clarity See Appendix 5 for full details

The X-ray structure of (*S*)-**401a** shows a π -stacking arrangement between the phenyl rings of the triphenylphosphine group C31-C36 and the diphenylphosphine group, C25-C30. The benzene portion of the indenyl ring sits above and in between the Cl atom, which is to the right hand side as drawn, and the triphenylphosphine group C43-C48 which is to the left hand side. The ORTEP view also shows the close proximity

of Cp-proton H7 to the triphenylphosphine group C37-C42. This is the reason for the high-field shifted Cp resonance in the proton NMR.

Crystallisation of the minor isomer (*S*)-**401b** was achieved by slow diffusion of hexane into a benzene solution of the complex, and X-ray crystal analysis confirmed the structure was as shown (Figure 4.3).

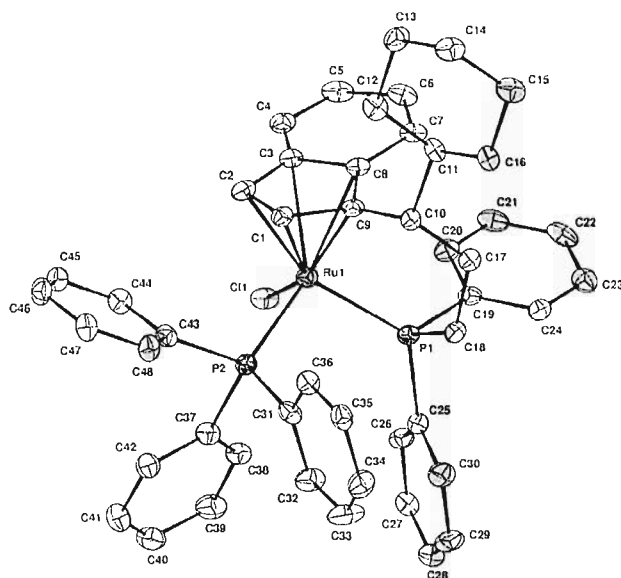


Figure 4.3

ORTEP view of major isomer (*S*)-**401b**. Thermal ellipsoids drawn at the 30% probability level, hydrogens and benzene solvent omitted for clarity.

See Appendix 6 for full details

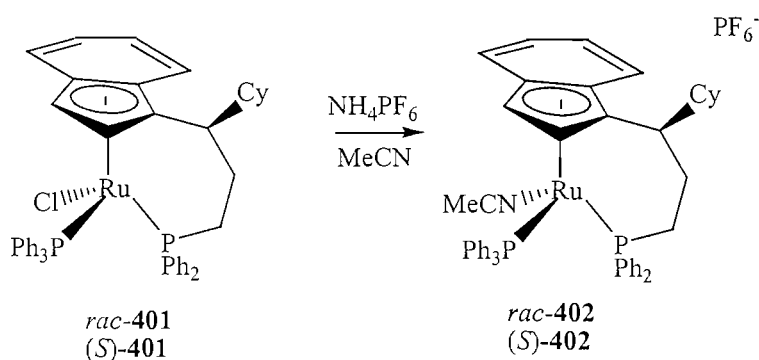
The structures of the major and minor isomers of complex (*S*)-**401** are very different. This is expected due to the inversion in planar chirality. There is less π -stacking in the X-ray structure of (*S*)-**401b**. The benzene portion of the indenyl ring sits above and in between the Cl atom, which is to the left hand side as drawn, and the diphenylphosphine group C19-C24 which is to the right hand side. The ^1H NMR of (*S*)-**401b** does not show a characteristic high field Cp-proton shift that is present in (*S*)-**401a**. The X-ray structure of (*S*)-**401b** shows the reason for this is that neither Cp-proton - H2 or H3 - is directed towards the centre of a proximal ring. The closest phenyl ring is the triphenylphosphine group C43-C48, and this is positioned between H2 and H3, so any interaction is reduced.

4.3 Synthesis of cationic complexes.

Ruthenium cationic complexes are of great interest due to their range of catalytic activity. Enantioselective allylic amination and alkylations,³⁵ hetero Diels-Alder reactions¹⁰⁵ and the reconstructive condensation of acetylenes and allyl alcohols¹⁰⁶ are examples of reactions catalysed by ruthenium cationic complexes. It was hoped that the cationic versions of *rac*- and (*S*)-**401** would be active catalysts in future catalytic trials.

The cationic complex is formed by abstraction of the chloride, using a 'chloride scavenger' reagent in the presence of a neutral ligand. Two such scavengers investigated were silver hexafluorophosphate in tetrahydrofuran,¹⁰⁷ and ammonium hexafluorophosphate in acetonitrile.¹⁰⁸ The acetonitrile ligand was chosen due to the ease of handling ammonium hexafluorophosphate compared to silver hexafluorophosphate, which is air-, light- and moisture sensitive.

Following the procedure of Slugovc, to a mixture of *rac*-**401** and ammonium hexafluorophosphate was added acetonitrile and the reaction was warmed to reflux (Scheme 4.3).¹⁰⁸ After 2 h, the reaction mixture had changed colour from brown to red and TLC indicated no starting material was present. Crude ¹H NMR indicated the presence of two sharp Cp-H signals at δ 4.41 and 4.12 ppm. Both the Cp-protons appear further downfield and this suggests a different structure to the neutral complex *rac*-**401a**. Purification was not possible by column chromatography, however recrystallisation from hot acetonitrile gave the cationic complex *rac*-**402** as a yellow solid in quantitative yield (Scheme 4.3).



Scheme 4.3

Crystallisation of the minor isomer *rac*-402 was achieved by slow diffusion of hexane into a benzene solution of the complex, and X-ray crystal analysis confirmed the structure was as shown (Figure 4.4).

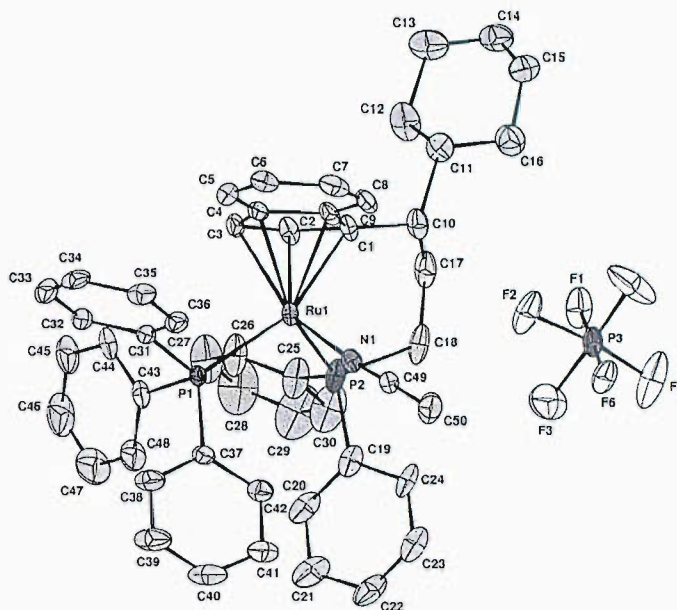


Figure 4.4

ORTEP view of major isomer *rac*-402, thermal ellipsoids drawn at the 30 % probability level and hydrogens and benzene solvent omitted for clarity. See Appendix 7 for full details

The X-ray structure of *rac*-402 has some interesting features. There is a π -stacking arrangement between the phenyl ring of the triphenylphosphine group C37-C42 and diphenylphosphine group, C19-C24. The PF_6^- counter ion sits very closely to the MeCN ligand, which sits underneath the indene ring. The ORTEP view also shows that neither Cp-proton lies in close proximity to a phenyl ring, therefore any shielding interaction by a phenyl ring's electron cloud on either proton is much reduced.

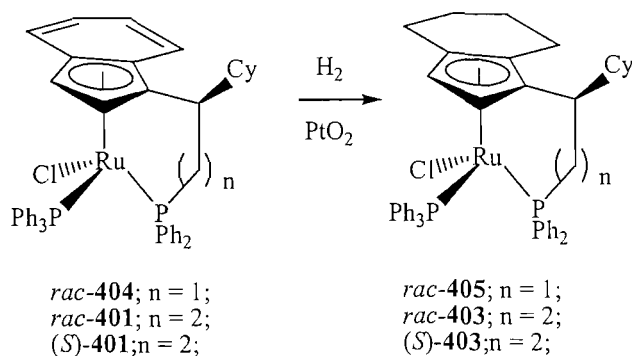
The slip parameter, Δ , of complex *rac*-402 is discussed later (See section 4.5.1)

By the same method as for *rac*-402, the single enantiomer complex (*S*)-402 was synthesised as a yellow solid in quantitative yield

4.4 Attempted synthesis of Ruthenium tetrahydroindenyl complexes.

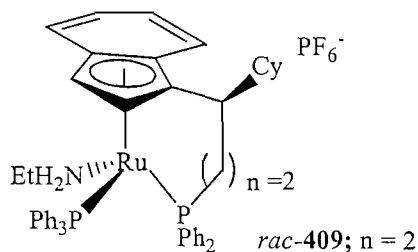
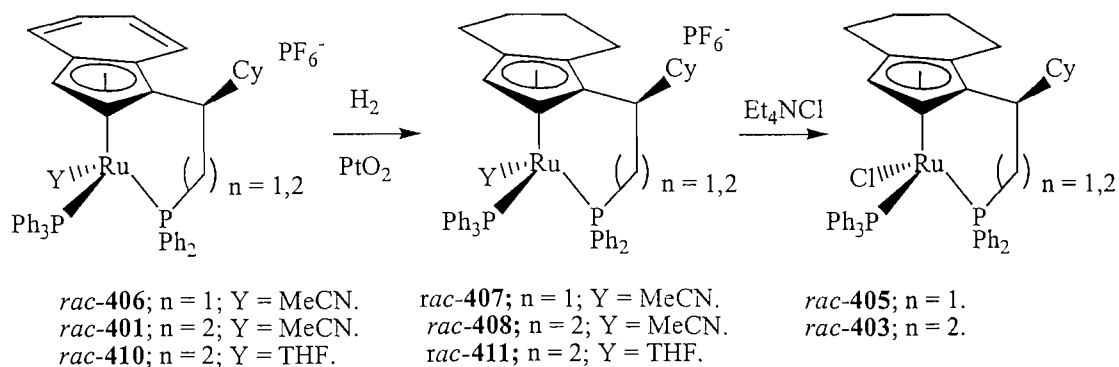
Indenyl complexes such as *rac*-**401** have different electronic properties to their analogous cyclopentadienyl complexes. The η^5 - η^3 ring slippage in some indenyl complexes is known to allow greater catalytic activity when compared to their analogous cyclopentadienyl complexes.¹⁰⁹ Hydrogenation of *rac*-**401** would provide us with a tetrahydroindenyl complex *rac*-**403**, giving an opportunity to directly compare their catalytic activities.

Hydrogenation of indenyl ligands complexed to early transition metals such as zirconium and titanium is known.² There are very few examples of hydrogenation of indenyl ligands complexed to ruthenium and other late transition metals. Gansow have reported the hydrogenation of a dinuclear indenyl-ruthenium carbonyl complex using Adams' catalyst, although no experimental details are given.¹¹⁰ Results within the group have shown that successful hydrogenation of complex *rac*-**404** occurs to give *rac*-**405** (Scheme 4.4).⁷⁴ The first attempt to form the tetrahydroindenyl complex *rac*-**403**, involved reaction of *rac*-**401** with 10 mol% PtO₂ and 1600 psi hydrogen at 65 °C over three days (Scheme 4.4). Analysis by ¹H and ³¹P NMR indicated the reaction was unsuccessful. A second attempt was made at forming *rac*-**403** involved 20 mol% PtO₂ and 1600 psi hydrogen at 80 °C. After three days, analysis by ¹H and ³¹P NMR indicated the reaction was unsuccessful. Electronically and structurally, *rac*-**401** and *rac*-**404** are very similar with the only difference being in *rac*-**404** the tether chain is two carbon atoms long, and in *rac*-**401**, it is three carbon atoms long. A reason for the different reactivities of *rac*-**401** and *rac*-**404** could be that the two-carbon tether complex *rac*-**404** is more strained, thus making it more reactive.



Scheme 4.4

An alternative method of synthesising the tetrahydroindenyl complex *rac-403* was thought to be hydrogenation of cationic complex *rac-402*, as it was believed that *rac-402* would be more reactive than *rac-401*. Results within the group have shown that successful hydrogenation of *rac-406* occurs to give the tetrahydroindenyl cationic complex *rac-407* (Scheme 4.5).⁷⁴ Subsequent treatment with *tetra*-butylammonium chloride regenerated the neutral complex *rac-405*.^{74,111} The first attempt involved reaction of *rac-402* with 10 mol% PtO₂ and 1600 psi hydrogen at 65 °C. (Scheme 4.5) After three days, analysis by mass spectrometry suggested that hydrogenation had occurred, with an increase in mass of 4 atomic mass units giving *rac-408*. After reaction with *tetra*-butylammonium chloride in refluxing acetone for 48 h, crude ¹H and ³¹P NMR revealed none of the desired hydrogenated complex *rac-403*. Reaction of *rac-403* with *tetra*-butylammonium chloride does regenerate the neutral complex *rac-401* in quantitative yield.¹¹¹ This suggests it is the hydrogenation of *rac-402* that is problematic. The increase in mass of 4 atomic mass units may have been caused by the hydrogenation of the acetonitrile group, giving the diethylamine complex *rac-409* but this was never isolated. The lack of hydrogenation was disappointing.

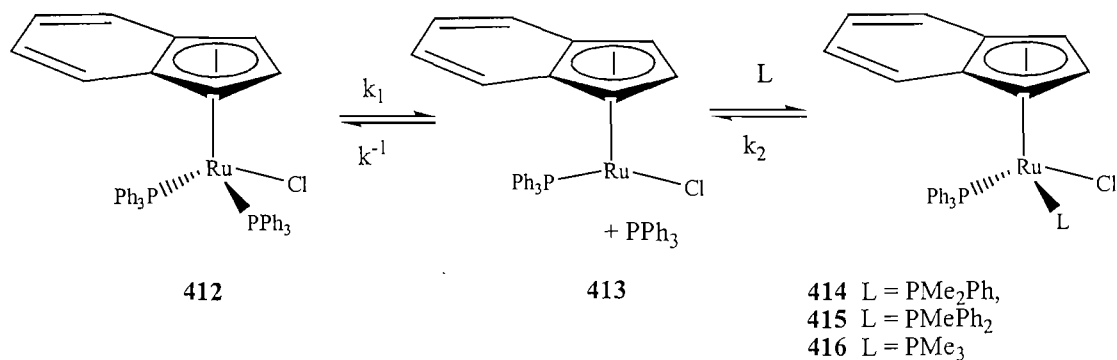


Scheme 4.5

An alternative method of synthesising the tetrahydroindenyl complex *rac*-**403**, involved initial hydrogenation of the tetrahydrofuran cationic complex, *rac*-**410**.¹⁰⁷ It was believed that with *rac*-**410** the coordinating ligand, would be impossible to hydrogenate, thus increasing the chance of successfully hydrogenating the indene ring. After initial formation of *rac*-**410**, and hydrogenation with 10 mol% PtO₂ and 1600 psi hydrogen at 65 °C over three days.^{74,107} and subsequent reaction with *tetra*-butylammonium chloride,¹¹¹ crude ¹H and ³¹P NMR revealed none of the desired hydrogenated complex *rac*-**403** (Scheme 4.5). Due to time constraints, this work was abandoned.

4.5 Ligand substitution reactions

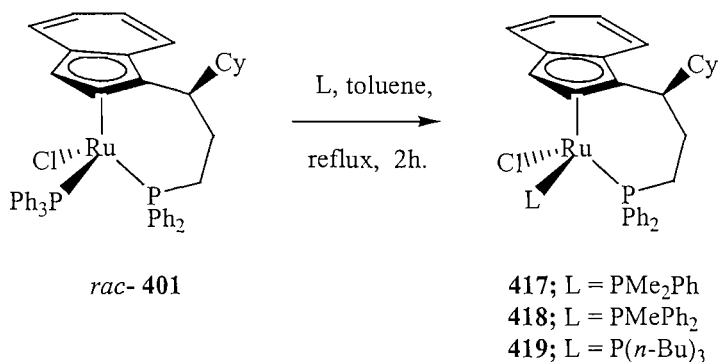
Ligand substitution reactions in indenyl transition metal complexes proceed at faster rates than in their corresponding cyclopentadienyl analogues. The higher reactivity has been explained as the result of the facile indenyl ring slippage from η^5 - η^3 coordination and the subsequent creation of a vacant coordination site for the entering ligand (Section 1.5.1).^{65,66,112} The reactions generally proceed by associative pathways for complexes of the metals rhodium,⁶⁶ iridium,¹¹³ and rhenium.¹¹⁴ On the other hand, carbonyl substitutions in [MoX(η^5 -Ind)(CO)₃] (X = Cl, Br, I) and [WCl(η^5 -Ind)(CO)₃] proceed by a mixed associative and dissociative mechanism and are still orders of magnitude faster than those of the Cp complexes.^{112,115} Gamasa has studied phosphine substitution in indenyl and cyclopentadienyl ruthenium complexes (Scheme 4.6).¹¹⁶



Scheme 4.6

The indenyl complex $[\text{RuCl}(\eta^5\text{-C}_9\text{H}_7(\text{PPh}_3)_2)]$, **412** reacts with monodentate (L: PMe_2Ph , PMePh_2 and PMe_3) to give monosubstituted $[\text{RuCl}(\eta^5\text{-C}_9\text{H}_7(\text{PPh}_3)\text{L})]$ complexes **414**, **415** and **416** in toluene or tetrahydrofuran (Scheme 4.6).¹¹⁶ Complex **412** can also react with bidentate (L-L: $\text{Ph}_2\text{PCH}_2\text{PPh}_2$) phosphines.¹¹⁶ The corresponding cyclopentadienyl complex reacts similarly at higher temps or longer reaction times.

Complex *rac*-**401** was reacted with a number of phosphines to see whether displacement of PPh_3 would occur. A mixture of *rac*-**401** and 2 equivalents of monodentate phosphine - dimethylphenylphosphine, methylphenylphosphine and tri-*n*-butylphosphine - were dissolved in toluene and the reactions were warmed to reflux. After 2 h, each reaction mixture had changed colour from brown to red (Scheme 4.7). Crude ^1H and ^{31}P NMR indicated no ruthenium starting material was present in all reactions. There was no reaction when *rac*-**401** was treated with tricyclohexylphosphine.



Scheme 4.7

One component was visible by TLC in each case. The reactions were cooled and careful chromatography through Al_2O_3 under normal air conditions provided complexes **417-418** in moderate to high yields. The successful displacement of triphenylphosphine had occurred in each case (Table 4.2).

Phosphine	Yield (%)	^1H (δ/ppm)		^{31}P (δ/ppm)	
417	40	4.25	4.21	51.4	12.0
418	58	4.28	4.19	49.4	29.5
419	65	4.68	4.36	51.4	17.9

Table 4.2: Isolated yields, the Cp-proton shifts and the peaks seen in the ^{31}P NMR.

Crystallisation of the dimethylphenylphosphine complex **417** was achieved by slow diffusion of hexane into a benzene solution of the complex and X-ray crystal analysis confirmed the structure was as shown (Figure 4.5).

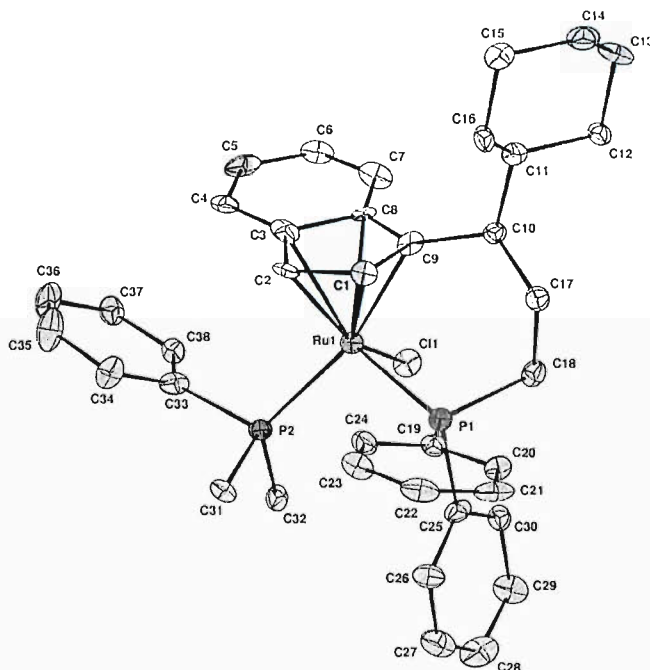


Figure 4.5

ORTEP view of *rac*-**417**, thermal ellipsoids drawn at the 50 % probability level, hydrogen atoms omitted for clarity. See appendix 8 for full details.

There is clearly π -stacking between the indene ring the phenyl ring C33-C38 of the dimethylphenylphosphine group and this is enhanced by the two methyl groups forcing this phenyl ring upwards underneath the indene group. The Cl atom is to the right hand side of the indene ring as drawn.

Crystallisation of the methylphenylphosphine complex **418** was achieved by slow diffusion of hexane into a benzene solution of the complex and X-ray crystal analysis confirmed the structure was as shown (Figure 4.6).

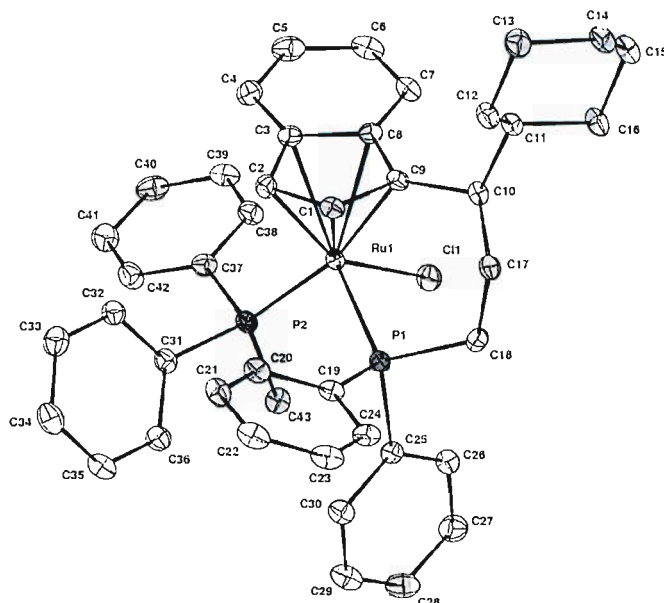


Figure 4.6

ORTEP view of *rac*-**418**, One of the two identical molecules in the asymmetric unit, solvent omitted for clarity and thermal ellipsoids drawn at the 35 % probability level.

See appendix 9 for full details.

The X-ray structure of **418** has some interesting features. There is clearly π -stacking between the indene and ring the phenyl ring C37-C42, of the diphenylmethylphosphine group. The Cl atom is to the right hand side of the indene ring as drawn. The methyl group sits directly below the Ru atom, almost forcing the two phenyl rings upwards towards the indene ring.

Crystallisation of the tri-*n*-butylphosphine complex **419** has so far resisted all attempts from a variety of solvents and conditions. On examination of the x-ray structures of *rac*-**417** and *rac*-**418**, it appears that the phosphine group is occupying the same position that the PPh₃ ligand was in *rac*-**401**. This indicates the thermodynamic product was formed in these displacement reactions, and that the displacement is probably a dissociative process. An inversion of configuration at the metal centre

would indicate an associative process.

4.5.1 Slip parameter of ruthenium complexes

Indenyl-transition metal complexes are known to display some degree of η^5 to η^3 distortion.¹⁰⁹ For complexes *rac-402*, *rac-417* and *rac-418* the bond lengths between ruthenium and the Cp-bridgehead carbons C3a and C7a, are slightly longer when compared to the bond lengths of the ruthenium-Cp-carbons C1, C2, C3. The degree of η^3 distortion can be expressed by the ‘slip parameter’ Δ , which is calculated as the difference between the average bond lengths of the metal/bridgehead (C3a, C7a) carbons, and the average bond lengths of the metal/cyclopentadienyl carbons C1-C3.

117

Table 4.3 shows a comparison of selected bond lengths for complex *rac-403*, *rac-417* and *rac-418*. These are compared to *rac-401*.¹³

	Complex <i>rac- 401</i>	Complex <i>rac- 403</i>	Complex <i>rac- 417</i>	Complex <i>rac- 418</i>
Ru – C1	2.198(4)	2.209(5)	2.157(10)	2.198(2)
Ru – C2	2.156(3)	2.192(5)	2.162(10)	2.163(2)
Ru – C3	2.184(3)	2.210(5)	2.182(10)	2.186(2)
Ru – C3a	2.345(4)	2.359(5)	2.309(12)	2.349(2)
Ru – C7a	2.335(4)	2.319(5)	2.308(12)	2.332(2)
Ru – P1	2.260(1)	2.339(12)	2.252(5)	2.238(6)
Ru – P2	2.318(1)	2.270(15)	2.272(3)	2.306(7)

Table 4.3

For complex *rac- 401*: $\Delta = (2.340 - 2.179) = 0.160 \text{ \AA}$.

For complex *rac- 403*: $\Delta = (2.339 - 2.204) = 0.135 \text{ \AA}$.

For complex *rac- 417*: $\Delta = (2.309 - 2.167) = 0.142 \text{ \AA}$.

For complex *rac- 418*: $\Delta = (2.354 - 2.182) = 0.172 \text{ \AA}$.

Values of the slip parameter vary from ≤ 0.03 Å for true η^5 complexes to ≥ 0.42 Å for true η^3 complexes.¹⁵ In the case of complexes *rac*-**403**, *rac*-**417**, and *rac*-**418**, these all indicate a slight distortion towards η^3 co-ordination of the indenyl ligand.

4.6 Conclusions

- Synthesis of *rac*-($\eta^5:\eta^1$)-Indenyl-CH(Cy)CH₂CH₂PPh₂)Ru^{II}(PPh₃)Cl, **401** has been optimised. The need for purification by column chromatography under argon is not required. The isolated yields of both isomers, 52 % and 16 %, are comparable to previous yields with high induction of planar-chirality and complete induction of metal-centred chirality being maintained.
- Complexation of enantiopure ligand (*S*)-**201** with RuCl₂(PPh₃)₃ has been achieved to form (*S*)-**401**. Both isomers have been isolated in 51 % and 16 % respectively with high induction of planar-chirality (66 %) and complete induction of metal-centred chirality.
- The cationic complexes *rac*-**402** and (*S*)-**402** have been synthesised in quantitative yield. However, the tetrahydroindenyl complex was not synthesised.
- Displacement of PPh₃ from *rac*-($\eta^5:\eta^1$)-Indenyl-CH(Cy)CH₂CH₂PPh₂)Ru^{II}(PPh₃)Cl, **401** has been successful with a number of phosphine ligands yielding complexes *rac*-**417-419**, with the retention of planar-chirality and metal-centred chirality.

Chapter 5: Catalytic studies of ruthenium complexes.

5.1 Background and aims

With large amounts of complexes *rac*-401 and *rac*-402 in hand it was now time to perform catalytic studies in a number of synthetic transformations (Figure 5.1). Once catalytic activity had been found, enantiopure complexes (*S*)-401 and (*S*)-402 would have been utilised to ascertain an e.e.

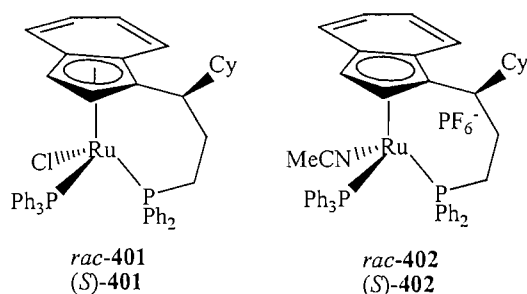
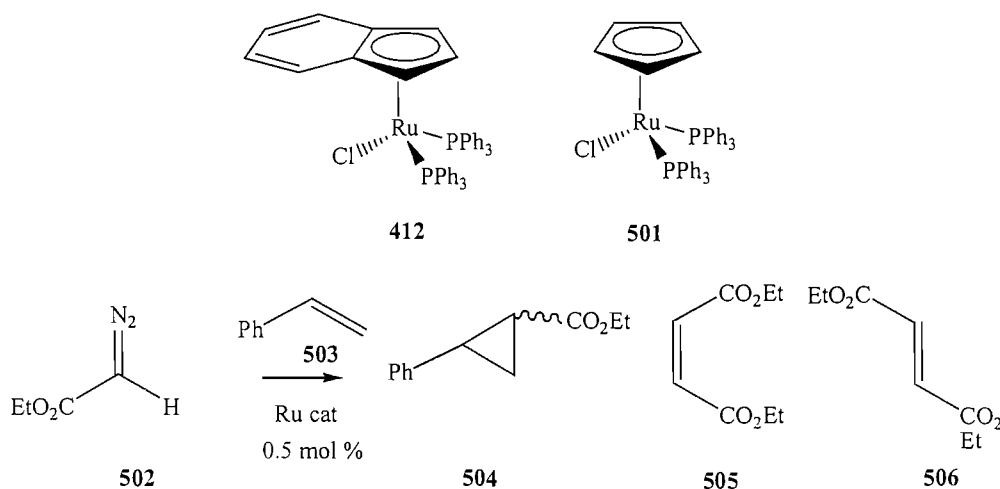


Figure 5.1

5.1.1 Olefin cyclopropanation and ROMP

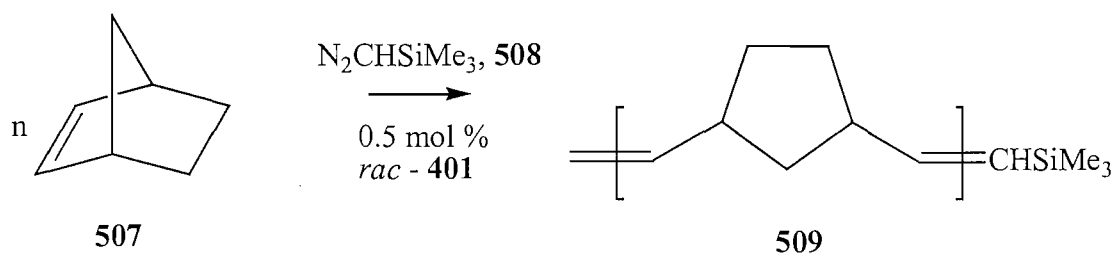
Demonceau's investigations of olefin cyclopropanations have shown that complexes 412 and 501 efficiently catalyse the cyclopropanation of styrenics with diazoesters.¹¹⁸ This was our first choice due to the structural similarities between the literature catalyst 412, and *rac*-401 (Scheme 5.1).¹¹⁸



Scheme 5.1

Complex **501** proved to be an effective catalyst for cyclopropanation of styrene. Cyclopropane products were obtained in high yield and with predominantly *cis* stereoselectivity. Compared to **501**, complex **412** led to the reversed stereoselectivity, with the *trans* isomer as the main product.¹¹⁸ Investigation involved studies of the reaction of ethyl diazoacetate **502** with styrene **503**. After dissolving *rac*-**401** in styrene at 40 °C, ethyl diazoacetate **502** was added over a 4 h period and the reaction was monitored by GC. The ratio of **504** to by-products **505** (diethyl maleate) and **506** (diethylfumarate) was encouraging. When **502** was added to **503** without any *rac*-**401** present, the same ratio of products was seen by GC. This suggests the complexes were inactive in this reaction, and the products were a result of a background reaction.

It is reasonable to assume that the initial stage of the catalytic cyclopropanation of olefins implies the generation of the carbene intermediate [RuCl(=CHCO₂Et)(Cp')-(PAR₃)], by reaction of the diazo compound with the 16 electron complex [RuCl(Cp')-(PAR₃)], formed by displacement of one of the phosphine ligands.¹¹⁹ Metathesis was then attempted using *rac*-**401**. A catalytic amount *rac*-**401** and norbornylene **507** were dissolved in chlorobenzene under argon, and a catalytic amount trimethylsilyldiazomethane **508** was added at 60 °C (Scheme 5.2).¹¹⁸



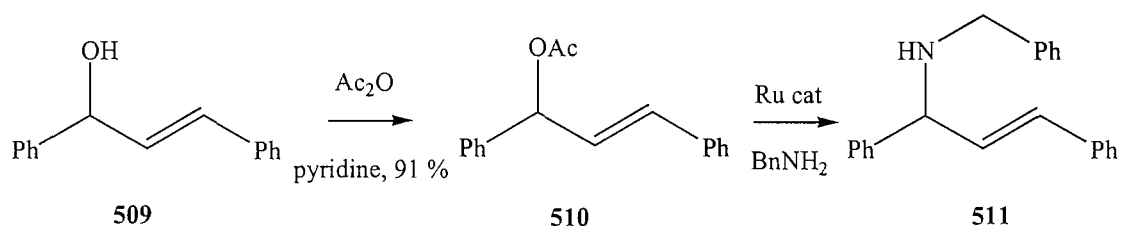
Scheme 5.2

After 16 h heating, addition of methanol precipitated ROMP product. When a reaction was carried out without the presence of *rac*-**401**, no ROMP occurred. It is not known why ROMP succeeded whilst the cyclopropanation reaction failed.

5.1.2 Ruthenium-catalysed allylic substitution.

Some ruthenium complexes show high catalytic activity for allylic substitutions.¹²⁰ The displacement of an allylic acetate by a nucleophile was chosen to test the catalytic

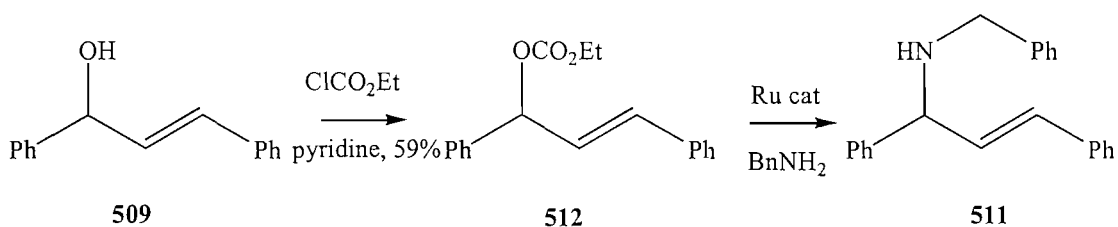
of *rac*-401 and *rac*-402. Most examples in the literature use 3-acetoxy-1,3-diphenylpropene **510** as a starting material. Reduction of chalcone using LiAlH_4 gave **509**. Subsequent reaction with Ac_2O gave **510** in 91% yield (Scheme 5.3).¹²⁰



Scheme 5.3

When allylic acetate **510** and benzylamine were reacted in the presence of *rac*-401 and *rac*-402, no reaction was observed. Even upon heating to 60 °C, no loss of starting material was observed by GC, although free PPh_3 was observed.

Takahashi used an allylic carbonate instead of an allylic acetate for his displacement reaction.³⁵ The allylic carbonate was synthesised by reaction of **509** with ethylchloroformate, which gave **512** in 59% yield (Scheme 5.4).³⁵

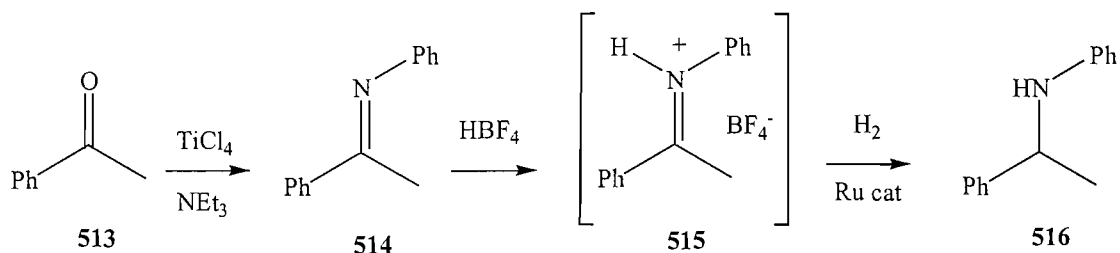


Scheme 5.4

When allylic acetate **512** and benzylamine were reacted in the presence of *rac*-401 and *rac*-402, no reaction was observed. Even upon heating to 60 °C, no loss of starting material was observed by GC, although free PPh_3 was observed. A stronger nucleophile was not tried in these reactions. Due to lack of activity and time constraints, this work was abandoned.

5.1.3 Hydrogenation

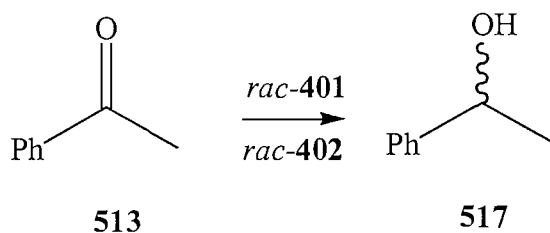
Another reaction chosen to test for catalytic activity of *rac*-401 and *rac*-402 was the hydrogenation of iminium salts under Norton's conditions.¹²¹ The iminium salt was generated *in-situ* from the corresponding imine (Scheme 5.5).



Initially the reactions were conducted at RT and the pressure was kept constant at 6 bar. Norton had observed no difference when the pressure was increased.¹²¹ After 24 h, GC suggested a yield of < 5%, and no increase in reaction was seen when the temperature was raised to 60 °C.

5.1.4 Transfer hydrogenation

The reduction of acetophenone **513** *via* transfer hydrogenation was chosen to test complexes *rac*-401 and *rac*-402 for activity (Scheme 5.6). All reactions were run overnight in an inert atmosphere and at 60 °C, to remove any acetone formed. Table 5.1 summarises the results.



Complex	Base	Solvent	Additive	Yield ^a (%)
<i>rac</i> -401	KOH	IPA	-	21
<i>rac</i> -402	KOH	IPA	-	-
<i>rac</i> -401	NaO ^{<i>i</i>} Pr	IPA	-	5
<i>rac</i> -401	NaO ^{<i>i</i>} Pr	IPA	1 eq. O ₂	19
<i>rac</i> -401	NaO ^{<i>i</i>} Pr	MeOH	-	-
<i>rac</i> -401	NaO ^{<i>i</i>} Pr	IPA	CyNH ₂	43

Table 5.1

^aYield calculated by GC

Initially the reactions were tried in IPA with KOH as base, however only slight reduction was observed. When the conditions were varied, it was found that the best conditions were in the presence of an excess of dicyclohexylamine and NaO^{*i*}Pr as base. When (*S*)-401 was reacted with NaO^{*i*}Pr in the presence of an excess of dicyclohexylamine and oxygen and the e.e. measured on a chiral GC. Unfortunately, despite many repeat measurements, the reduction product was racemic. It is possible that loss of the indenyl ring is the step, which forms the catalytically active species. This would result in the loss of the chirality at the metal centre and a racemic product. With time running out, no more catalytic studies were carried out.

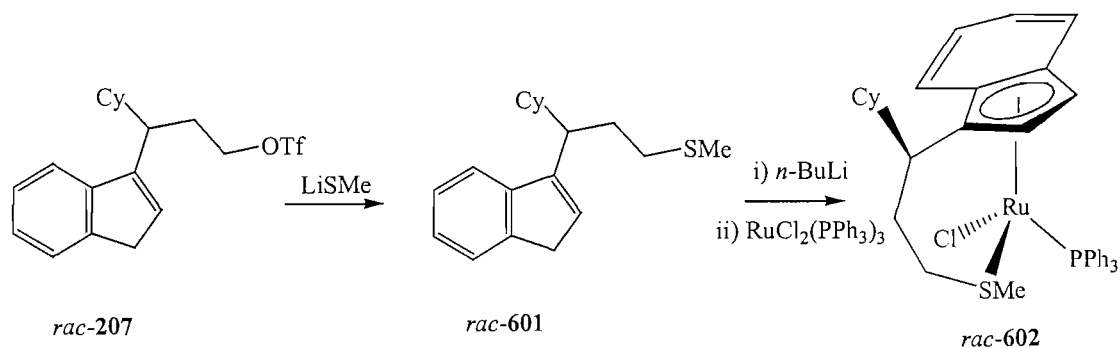
5.2 Conclusion

The lack of catalytic activity is disappointing with the polymerisation of norbornylene being the only transformation being successfully affected by *rac*-401. Due to time constraints a limited number of catalytic studies were performed. However, there are many more synthetic transformations on which to perform further catalytic studies.^{105,122,123}

Chapter 6: The synthesis of a chiral bidentate indenyl ligand containing a three-carbon bridge and co-ordinating amine ‘anchor’ group and subsequent complexation onto transition metals

6.1 Background and aims

With the optimised synthesis of the racemic three-carbon tethered alcohol, *rac*-**206** and the novel synthesis of the enantiopure three-carbon tethered alcohol (*S*)-**206**, there was the opportunity to investigate alternative tethered ‘anchor’ groups. This would lead to a number of interesting new ligands, which could be complexed with transition metals. Harrison has synthesised the thiomethyl-containing ligand *rac*-**601** (Scheme 6.1).¹³ Reaction of dimethyl sulphide with *n*-butyllithium in THF provided a suspension of LiSMe. Subsequent reaction with triflate *rac*-**207** at $-78\text{ }^{\circ}\text{C}$ gave thiomethyl ligand *rac*-**601** in 79 % yield as a pale orange oil after column chromatography (Scheme 6.1).¹³



Scheme 6.1

Subsequent deprotonation of *rac*-**601** with *n*-butyllithium in toluene, then treatment with a solution of RuCl₂(PPh₃)₃ gave two sharp Cp-H signals at δ 4.89 and 2.98 ppm. (Scheme 6.1).¹³ No minor Cp-H signals were seen by ¹H NMR suggesting very good induction of planar chirality and metal centred stereocontrol. Unfortunately, column chromatography of the resultant complex *rac*-**602** failed to give clean material and all crystallisation attempts failed.¹³

This proves that modification of the coordinating group is possible. Incorporation of a nitrogen coordinating group would be very interesting and allow the complexes to become involved in interesting catalytic cycles. Avecia have developed (pre)catalysts such as **603** for the reduction of imines and ketones consisting of a cyclopentadienyl rhodium or iridium complexed to a chiral bidentate amine-sulfonamide, diamine or aminoalcohol.^{40,41,124-126}

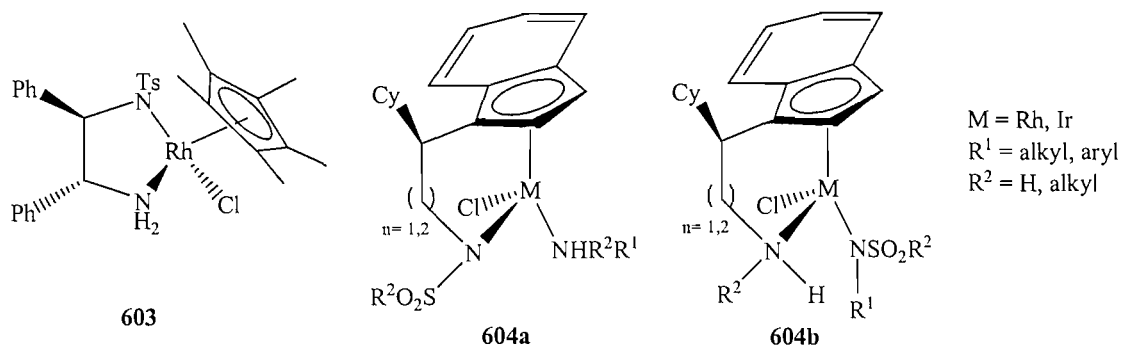


Figure 6.1

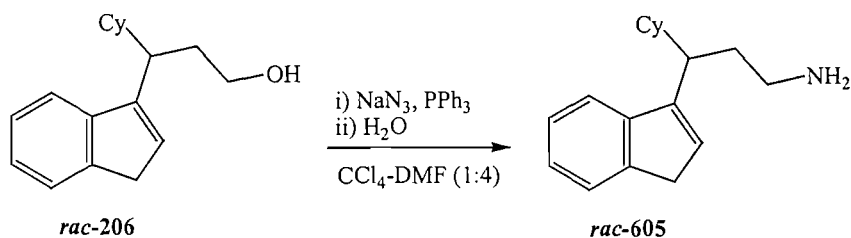
When the three-carbon tethered ligand with a nitrogen-coordinating group is complexed to a transition metal, the planar chirality of the complexed indene should provide control over the metal centred chirality in **604**. Therefore we can synthesise nitrogen coordinating complexes incorporating the ‘favoured rotamer’ design and bring them close in structure to the successful cyclopentadienyl-rhodium and cyclopentadienyl -iridium asymmetric hydrogenation catalysts.^{40,41}

The aim was to synthesise a racemic and the enantiopure three carbon primary amine ligand, as well as ligands with alternative coordinating amine groups. Complex these novel amine ligands with ruthenium and/or rhodium and test their applications as an asymmetric hydrogenation transfer catalyst.

6.2 Synthesis of amine ligands

6.2.1 Synthesis of racemic ligands with a substituent *alpha* to the indene ring.

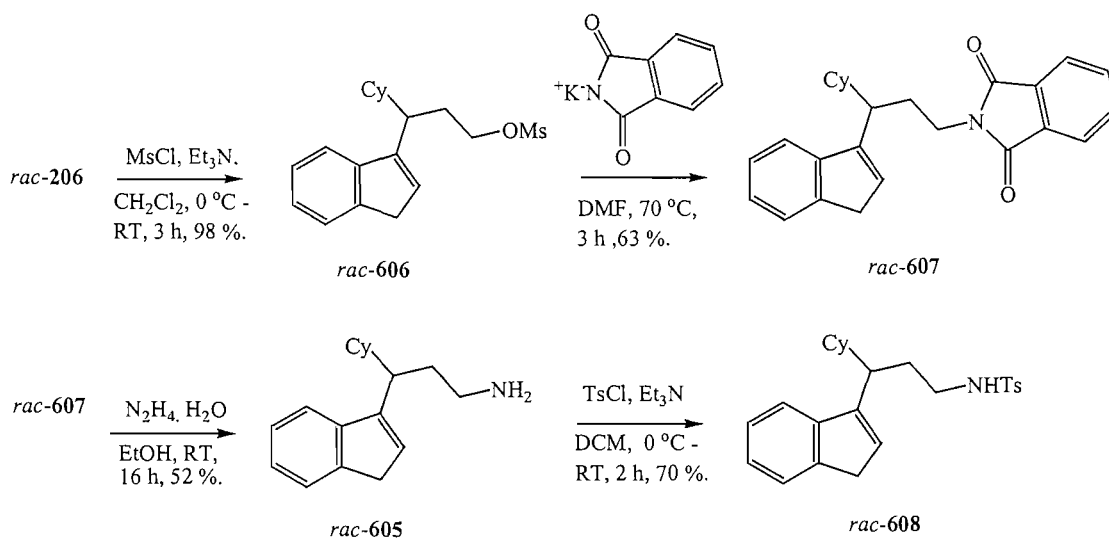
The three-carbon tethered ligand with a primary amine coordinating group, *rac*-**605** is a very interesting molecule. Once complexed to a transition metal, it has the potential of being an asymmetric hydrogenation transfer catalyst. The first attempt of forming *rac*-**605** was an attractive one-pot method devised by Reddy (Scheme 6.2).¹²⁷



Scheme 6.2

This involved treatment of *rac-206* with 1.4 equivalents of sodium azide and 2.1 equivalents of triphenylphosphine. The formation of the amine may be explained by initial formation of the azide. Reaction with the second equivalent of Ph_3P gives an iminophosphorane, which is converted to the primary amine upon treatment with water.¹²⁷ The driving force for the reaction is the formation of triphenylphosphine oxide. Unfortunately, this attempted synthesis failed on two occasions. An alternative synthesis of forming a primary amine from the alcohol was a three-step synthesis as described by Meyers (Scheme 6.3).¹²⁸

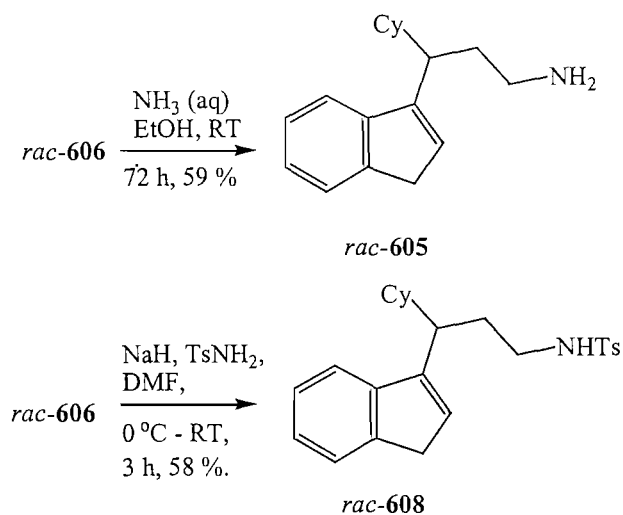
This involved the initial reaction of *rac-206* with triethylamine and methanesulfonyl chloride resulting in the isolation of mesylate *rac-606* in quantitative yield. Subsequent nucleophilic displacement of the mesylate by potassium phthalimide gave *rac-607* in good yield (Scheme 6.3).¹²⁸



Scheme 6.3

Removal of the phthalimide protecting group by the method of Meyers, involved the addition of hydrazine hydrate to *rac*-**608** refluxing in *t*-butanol.¹²⁸ This afforded the primary amine *rac*-**605** in 32 % yield. By the alternative method of Teubner, reaction of *rac*-**607** with hydrazine hydrate in ethanol gave *rac*-**605** in 52 % yield (Scheme 6.3).¹²⁹ Sulfonamide ligand *rac*-**608** very interesting as it is similar to other catalyst precursors.¹²⁴ Subsequent treatment of *rac*-**605** with triethylamine and *p*-toluenesulfonyl chloride, afforded *rac*-**608** in good yield. This route is not ideal if large-scale production of *rac*-**605** and *rac*-**608** is to be carried out.

It was found that reaction of mesylate *rac*-**606** and an excess of aqueous ammonia in ethanol gave *rac*-**605** after 72 h at RT (Scheme 6.4). This is a more attractive route as it omits the formation and removal of the phthalimide protecting group (Scheme 6.3). It was found that an alkyl bromide could be displaced by the Na salt of *p*-toluenesulfonamide in dimethylformamide, giving the respective alkyl sulfonamide in reasonable yield.¹³⁰ The reaction of the sodium salt of *p*-toluenesulfonamide with *rac*-**606** was successful with *rac*-**608** being synthesised in modest yield (Scheme 6.4).¹³⁰ This is an improvement on the previous synthetic route with modest yielding steps being omitted (Scheme 6.3). A striking feature of the ¹H NMR spectrum of *rac*-**608** is the very clear triplet of the NH at δ 4.30 ppm. This signal will give an indication of whether or not the sulfonamide ligand is complexed to a transition metal.



Scheme 6.4

Purification of *rac*-**608** was achieved by recrystallisation and X-ray crystal analysis has confirmed the structure is as shown (Figure 6.2).

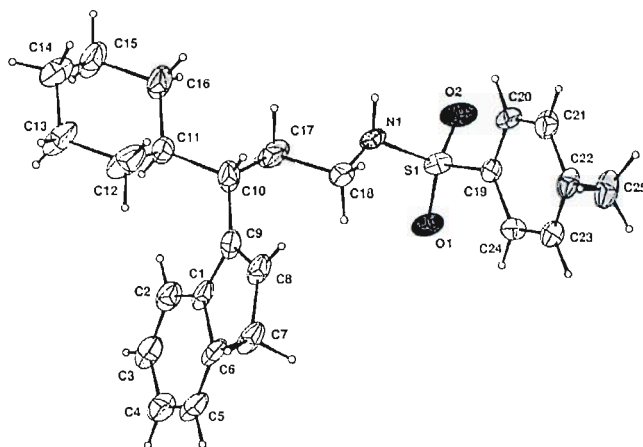


Figure 6.2

ORTEP view of *rac*-**608**, thermal ellipsoids drawn at the 30 % probability level. All hydrogen atoms were placed in idealised positions and refined using a riding model. There is a considerable amount of thermal motion within the crystal. See Appendix 10 for full details.

There is extensive hydrogen bonding between molecules lying adjacent to each other. The bond lengths are N-H 0.89(6) Å; H-O 2.08(6) Å and N-O 2.93(6) Å. The bond angle N-H-O is 160(6)°. Figure 6.3 shows a hydrogen-bonded chain of *rac*-**608** that extends down an axis.

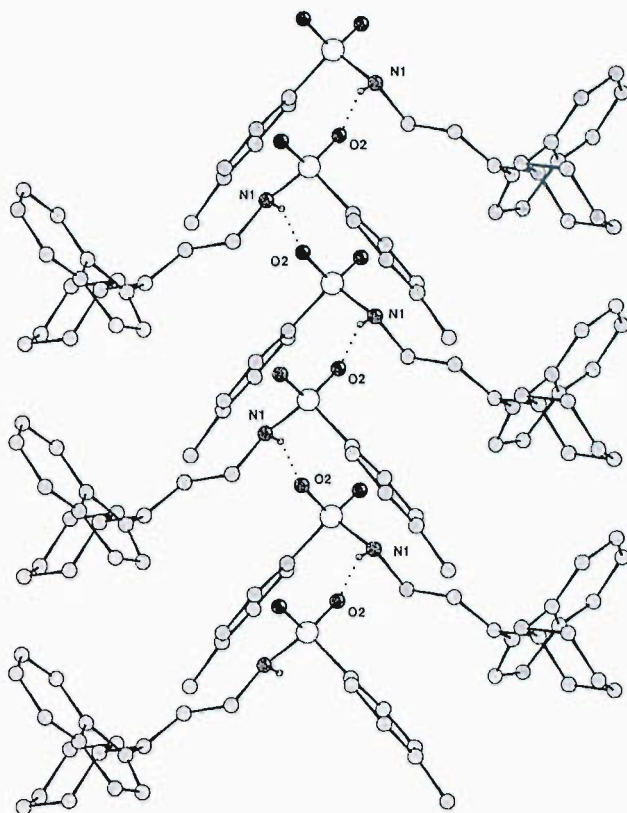
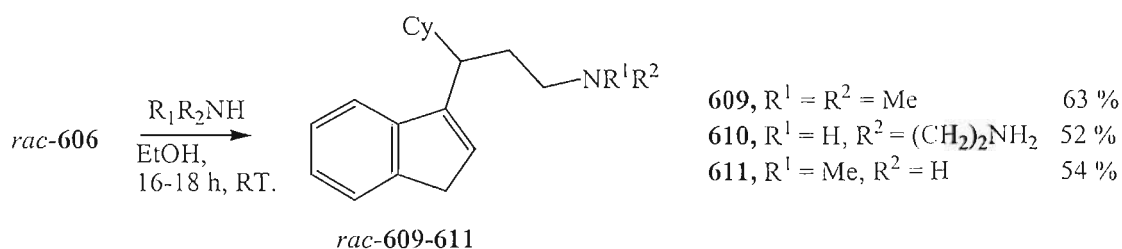


Figure 6.3

ORTEP view of *rac*-608, thermal ellipsoids drawn at the 30 % probability level. Part of one of the hydrogen bonded chains that extend down the *b* axis.

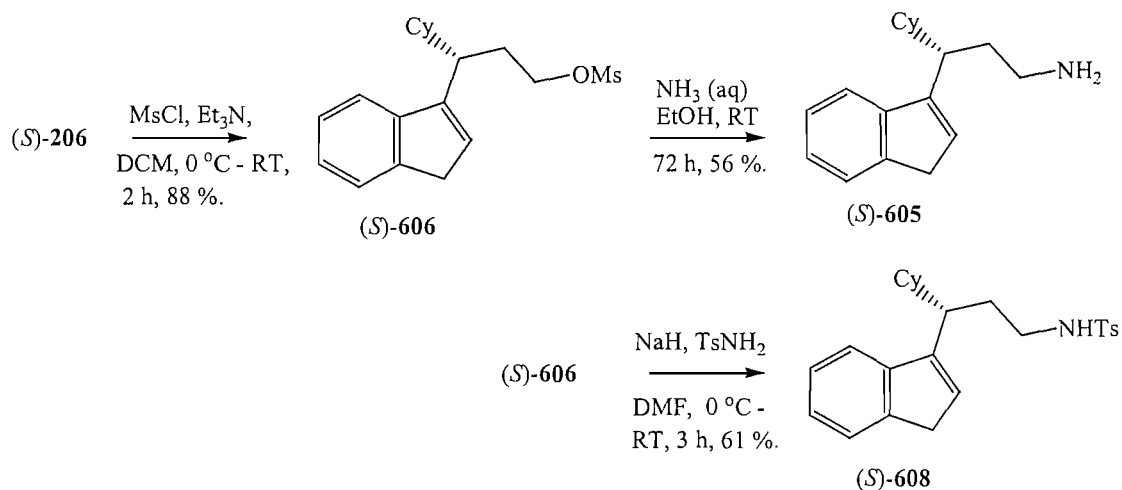
A number of other three-carbon tethered ligands with a nitrogen coordinating group, *rac*-609-611, were also synthesised. Racemic amine 609-611 ligands were synthesised by stirring *rac*-606 with dimethylamine, ethylenediamine, and methylamine respectively in ethanol at room temperature for 16-18 h (Scheme 6.5).¹²⁹ After acid/base work up, the amine products were isolated in 63 %, 52 % and 54 % yield respectively. *Rac*-610 is a particularly interesting, as it has the potential of being a tridentate ligand when complexed to a transition metal.



Scheme 6.5

6.2.2 Synthesis of chiral ligands with a substituent *alpha* to the indene ring.

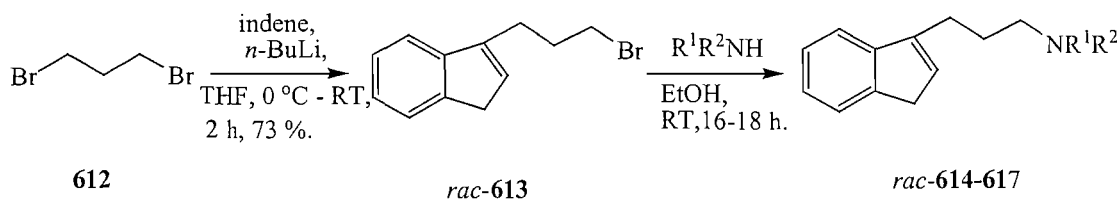
The chiral amine ligands (*S*)-**605** and (*S*)-**608**, with a cyclohexyl ring substituent *alpha* to the indene ring were synthesised by the optimised route as used to synthesise the racemic ligands (Scheme 6.6). These were isolated in reasonable yields. Complexation of these ligands was not attempted.



Scheme 6.6

6.2.3 Synthesis of ligands without a substituent *alpha* to the indene ring.

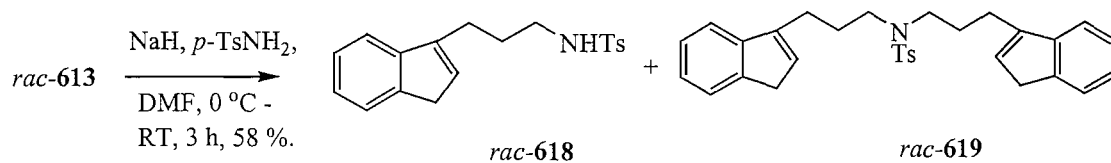
In order to avoid complications arising from diastereoisomer formation on complexation to metals, and due to lower cost of synthesis, model ligands lacking the cyclohexyl substituent α -to the indenyl ring were synthesised.¹³¹ Reaction of 1,3-dibromopropane, **612** with indenyl lithium on a 70 mmol scale, gave *rac*-**613** in good yield (Scheme 6.7).



614 , R ¹ = R ² = H	55 %
615 , R ¹ = H, R ² = (CH ₂) ₂ NH ₂	77 %
616 , R ¹ = R ² = Me	88 %
617 , R ¹ = Me, R ² = H	53 %

Scheme 6.7

Ligands **615-617** were synthesised by nucleophilic displacement of the bromine in *rac-613* by the respective amine in ethanol in reasonable yield (Scheme 6.7).¹²⁹ For the synthesis of *rac-614*, literature precedent suggested nucleophilic displacement of the bromine by potassium phthalimide followed by deprotection with hydrazine hydrate giving the primary amine.¹²⁹ It has been proven that such displacement and subsequent removal of the phthalimide protecting groups does not give high, reliable yields (Section 6.2.1). Reaction of *rac-613* with aqueous ammonia in ethanol afforded *rac-614* in 55 % yield (Scheme 6.7). This is ideal for large-scale production. Reaction of *rac-613* with an excess of the Na salt of *p*-toluenesulfonamide in dimethylformamide yielded **618** in 37 % yield (Scheme 6.8).¹³⁰ The racemic *bis*-sulfonamide, *rac-619* was isolated as a by-product in 15 % yield. It was found that using an equivalent amount of NaH compared to *p*-toluenesulfonylamide prevented the formation of *rac-619* and the isolated yield of *rac-618* increased to 58 % (Scheme 6.8).



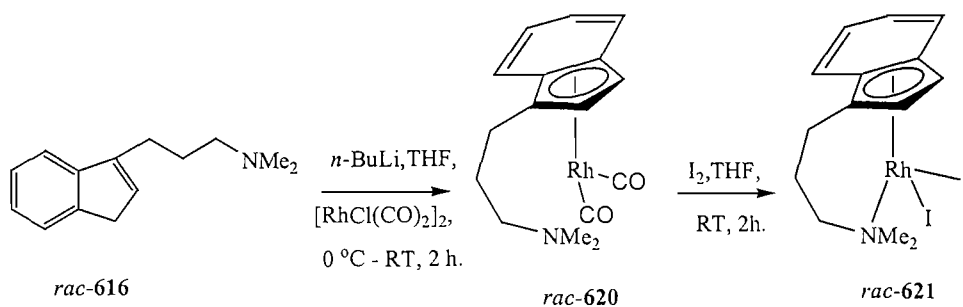
Scheme 6.8

6.3 Complexation of amine ligands without a substituent *alpha* to the indene ring to rhodium.

6.3.1 Complexation of the dimethylamine ligand, **616**.

In order to effect complexation to the rhodium source [RhCl(CO)₂]₂, *rac-616* was deprotonated using an equimolar amount of *n*-butyllithium at 0 °C in THF, then treated with a solution of [RhCl(CO)₂]₂ and left to stir for 2 h at RT (Scheme 6.9). ¹H NMR of the crude material suggested that complexation had occurred by the presence of two sharp Cp-H signals at δ 5.70 and 5.16 ppm, giving crude Rh(I) complex *rac-620*. Crude ¹H NMR also suggested no coordination between the NMe₂ and the rhodium metal centre had occurred as there had been no shift in the ¹H NMR scale of the NMe₂ signal (Figure 6.4). Crude IR spectra showed two strong absorptions at 1954 and 1960 cm⁻¹. Purification of complex **620** by column chromatography proved

impossible through both silica and neutral alumina and attempts at growing crystals have so far failed from a variety of solvents and conditions.



Scheme 6.9

With the aim of stabilising *rac-620* and coordinating the NMe₂ to the metal centre, crude *rac-620* was treated with 1 equivalent of iodine.¹³² After 2 h at RT, analysis by ¹H NMR suggested that oxidation to the Rh(III) complex **621** had occurred. The Cp-H signals had shifted to δ 6.25 and 5.81 ppm. The signal for the CH₂ next to the NMe₂ has shifted from δ 2.40 to 3.70 ppm. The presence of 2 singlets at δ 2.53 and 2.40 ppm, strongly suggested coordination of the NMe₂ group to the metal centre (Figure 6.5). Crude IR spectra indicated the disappearance of the two CO absorptions. Purification of complex *rac-621* by column chromatography proved impossible through both silica and neutral alumina and attempts at growing crystals have so failed from a variety of solvents and conditions.

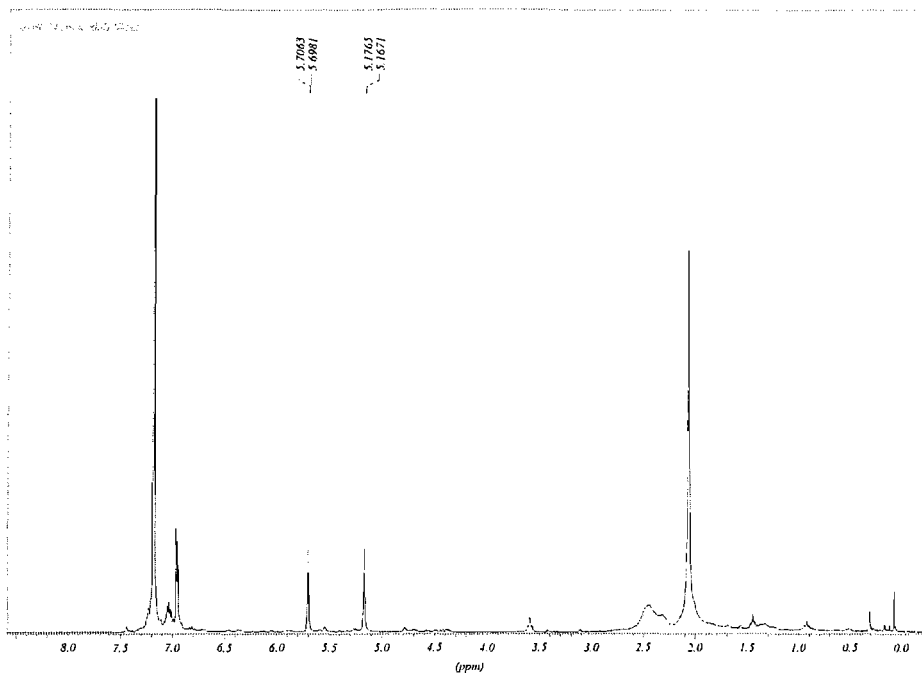


Figure 6.4: Crude ^1H NMR of Rh(I) NMe_2 complex, *rac*-**620**

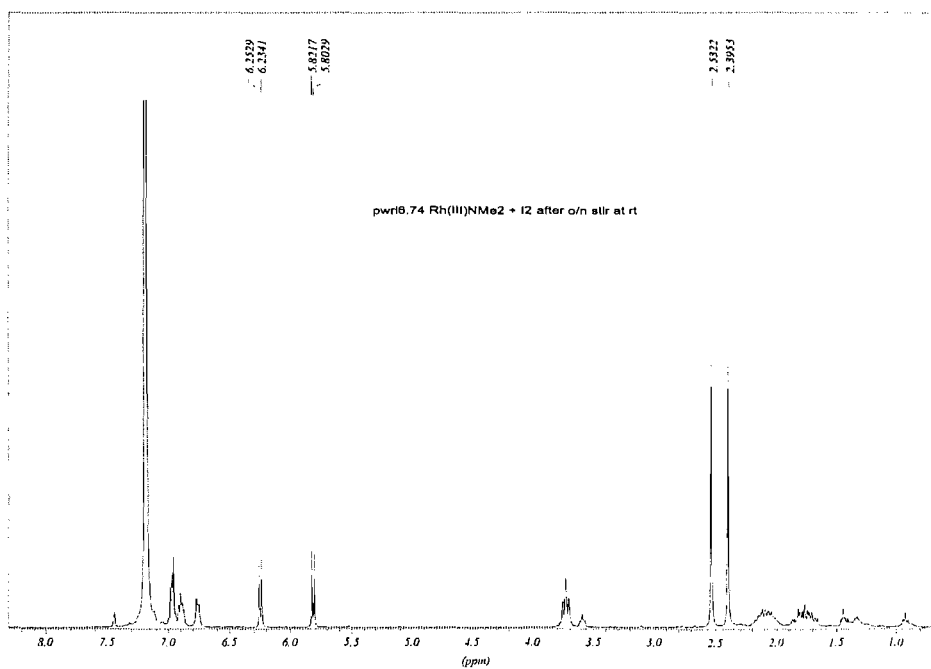
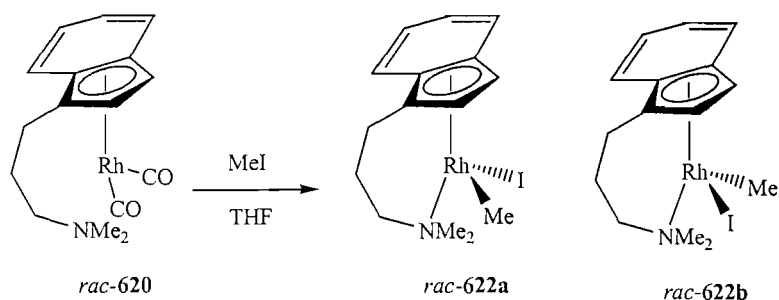


Figure 6.5: Crude ^1H NMR of Rh(III) NMe_2 complex, *rac*-**621**.

Oxidation from Rh(I) to Rh(III) was also attempted by reaction of crude *rac*-**620** with 1 equivalent of MeI.¹³¹ After 16 h at RT, ^1H NMR suggested that the reaction had occurred with a 1:1 mixture of diastereoisomers **622a** and **622b** being formed due to the appearance of one set of Cp-H protons at δ 5.61 and 5.11 ppm and another at δ 5.75 and 5.25 ppm (Scheme 6.10).¹³² There were two sets of NMe_2 signals at δ 2.45

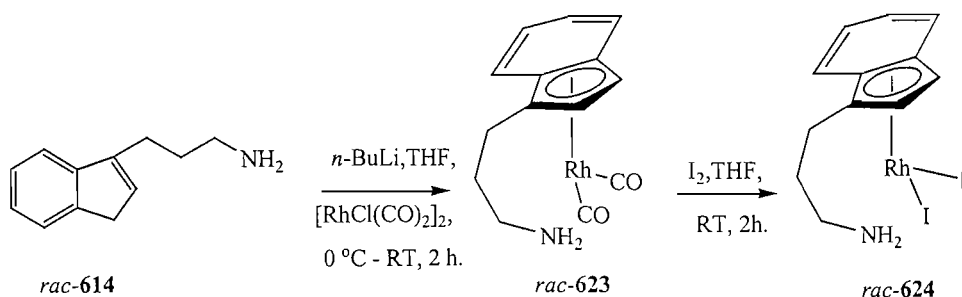
and 2.70 ppm. The mixtures of diastereoisomers suggested oxidation with I₂ was cleaner so the use of MeI was abandoned.



Scheme 6.10

6.3.2 Complexation of the primary amine ligand, 614.

In order to affect complexation to the rhodium source [RhCl(CO)₂]₂, ligand *rac-614* was deprotonated using an equimolar amount of *n*-butyllithium at 0 °C in THF, then treated with a solution of [RhCl(CO)₂]₂ and left to stir for 2 h at RT (Scheme 6.11). ¹H NMR of the crude material suggested that complexation had occurred by the presence of two sharp Cp-H signals at δ 5.60 and 5.17 ppm, giving crude Rh(I) complex *rac-623*. Crude ¹H NMR also suggested no coordination between the NH₂ and the rhodium metal centre (Figure 6.6) Crude IR spectra showed two strong absorptions at 1948 and 1956 cm⁻¹. Purification of complex *rac-623* by column chromatography proved impossible through both silica and neutral alumina and attempts at growing crystals have so far failed from a variety of solvents and conditions.



Scheme 6.11

With the hope of stabilising *rac-623*, it was decided to oxidise it from Rh(I) to Rh(III). This was done by reaction of *rac-623* with 1 equivalent of iodine (Scheme 6.12).¹³² After 2 h at RT, ¹H NMR of the crude suggested that oxidation had occurred,

giving crude Rh(III) complex *rac-624*, by the presence of two sharp Cp-H signals at δ 4.95 and 5.17 ppm. ^1H NMR also suggested no coordination between the NH_2 and the rhodium metal centre had occurred, although crude IR spectra indicated the disappearance of the two CO absorptions (Figure 6.7). Purification of complex *rac-624* by column chromatography proved impossible through both silica and neutral alumina and attempts at growing crystals have so far failed from a variety of solvents and conditions.

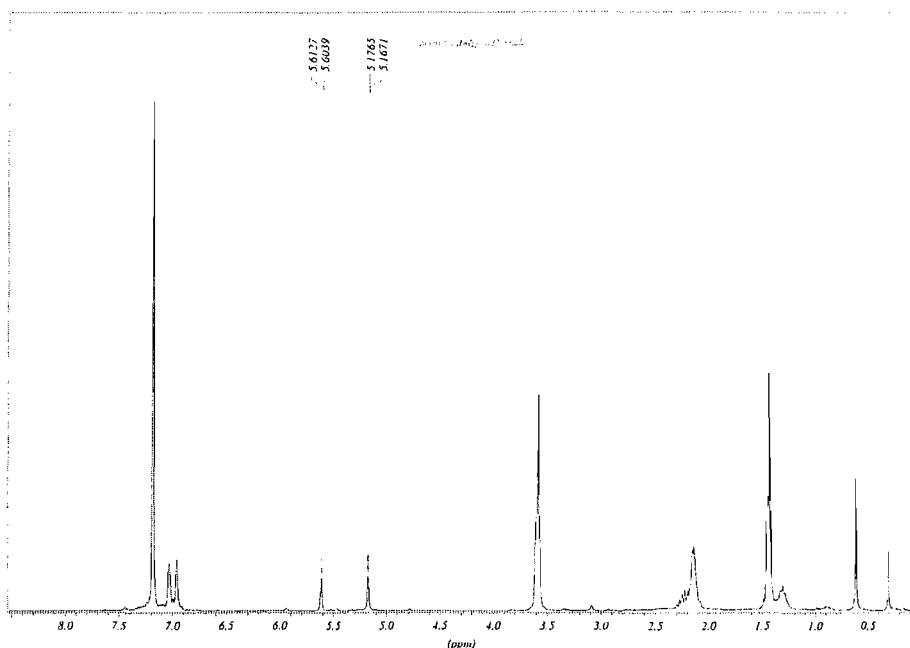


Figure 6.6: Crude ^1H nmr of Rh(I) NH_2 complex, *rac-623*.

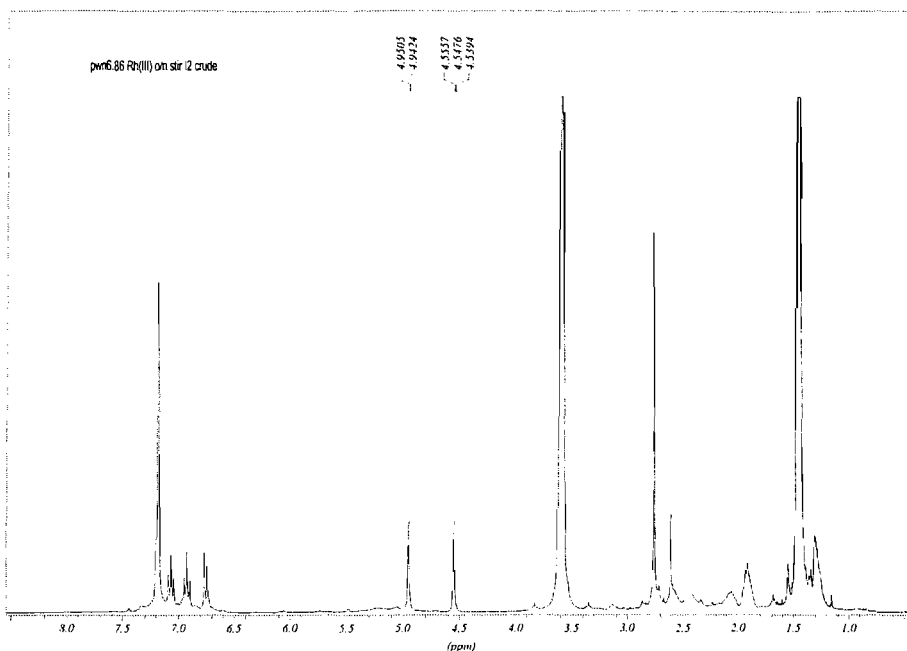
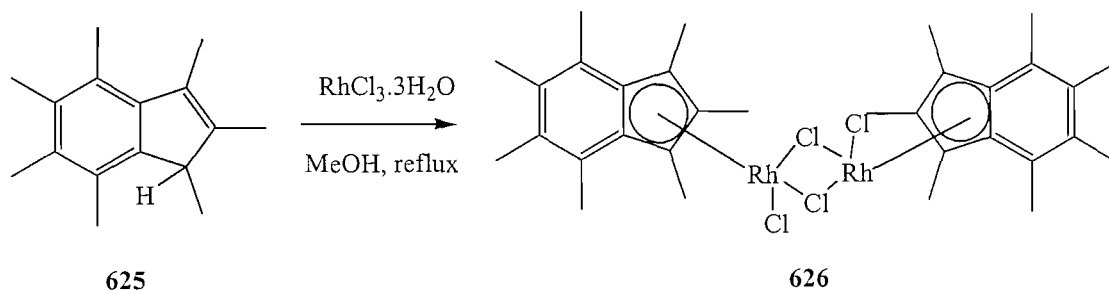


Figure 6.7: Crude ^1H nmr of Rh(III) NH_2 complex, *rac*-**624**.

6.3.3 Complexation of the tosylamine ligand, **618**.

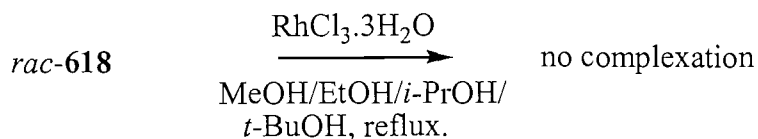
Initial attempts to complex the ligand *rac*-**618** to rhodium focused on the formation of the Rh(III) chloride bridged dimers as described by Marder.¹³³ Refluxing heptamethylindene **625** with $\text{RhCl}_3 \cdot 3\text{H}_2\text{O}$ in methanol and water for 48 h gave the rhodium(III) dimer **626** (Scheme 6.12). The bridging Rh-Cl bonds are cleaved by reaction with tertiary phosphines giving the monomeric complexes in quantitative yields.¹³³



Scheme 6.12

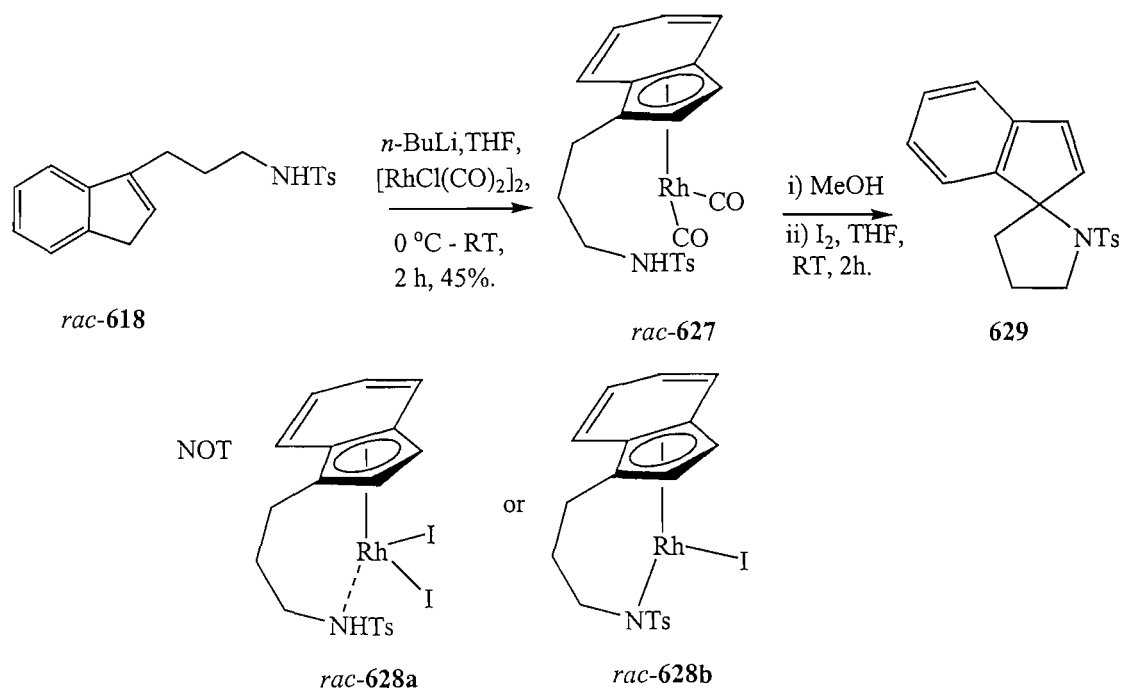
Refluxing *rac*-**618** and $\text{RhCl}_3 \cdot 3\text{H}_2\text{O}$ in methanol and water for up to 48 h resulted in the precipitation of a black solid in a red solution. After extraction into toluene, ^1H NMR suggested the recovery of unreacted *rac*-**618** (Scheme 6.13). The indene was

probably insufficiently reactive and dehydration of the rhodium trichloride was occurring. In order to increase the reactivity of the indene ligand, *rac*-**618** was reacted with RhCl₃·3H₂O in refluxing ethanol, *iso*-propanol and *tert*-butanol for up to 48 h. Again, unreacted *rac*-**618** was recovered.



Scheme 6.13

In order to effect complexation to the rhodium source [RhCl(CO)₂]₂, *rac*-**618** was deprotonated using 1 equivalent of *n*-butyl lithium at 0 °C in THF. The anion was then treated with a solution of [RhCl(CO)₂]₂ and left to stir for 2 h at RT (Scheme 6.14) ¹H NMR of the crude material indicated complexation had occurred giving crude Rh(I) complex **627**, by the presence of two sharp Cp-H signals at δ 5.89 and 5.52 ppm. The triplet signal present at δ 4.60 ppm suggested that the tosylamine group was not coordinated to the rhodium metal centre. Two strong IR absorption peaks at 2035 and 1974 cm⁻¹ also suggested the formation of the Rh(I) complex. The reaction was then warmed to reflux for a further 16 h with the hope of coordination of the tosylamine group to the Rh metal centre. ¹H NMR of the crude material proved this attempt was unsuccessful. The reaction was subsequently cooled. It was found that one spot was visible by TLC, and column chromatography through silica provided the complex, *rac*-**627** in 45 % yield (Scheme 6.14). Unfortunately all attempts at growing crystals have failed from a variety of solvents and conditions.



Scheme 6.14

Reaction of crude *rac-627* with 1 equivalent of I_2 was performed with the aim of coordinating the NH group to the rhodium metal centre (Scheme 6.14).¹³² After 2 hours at RT, crude ^1H NMR showed that the Cp-H signals had shifted downfield to δ 6.66 and 6.29 ppm. The disappearance of the triplet signal at δ 4.60 ppm suggested that the amine group was now coordinated to the Rh metal (Scheme 6.14). There had also been a shift down field of the 2H signal due to the diastereotopic protons next to the NH group from δ 2.72 to 3.72 ppm. One spot was visible by TLC, and column chromatography through silica provided the spiro compound **629** in 35 % yield, rather than the hoped for Rh(III) complexes *rac-628a* or *628b* (Scheme 6.14). This was confirmed by X-ray crystallography (Figure 6.8).

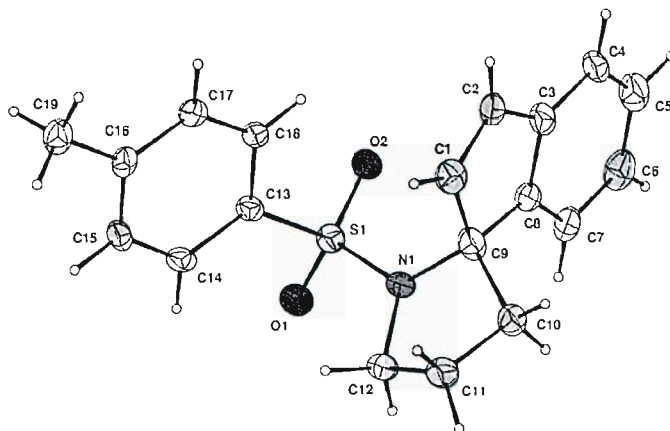
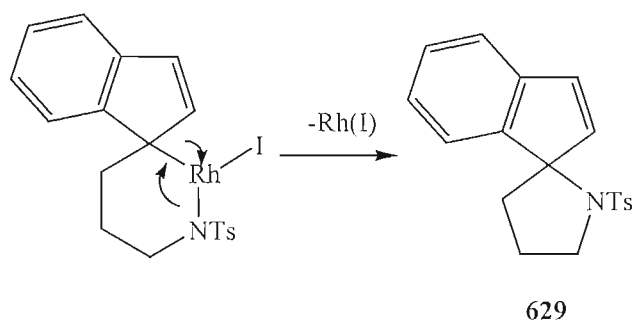


Figure 6.8

ORTEP view of *rac*-**629**, thermal ellipsoids drawn at the 35% probability level.

Solvent omitted for clarity See Appendix 11 for full details

It was thought that the cyclisation to form **629** might be induced by any hydrogen iodide that may have been generated. Therefore, the addition of I₂ was carried out in the presence of triethylamine or potassium carbonate, but clean formation of **629** was observed. It can be assumed that a reductive elimination reaction is occurring to yield **629** (Scheme 6.15).



Scheme 6.15

Unfortunately time constraints meant this work had to be abandoned.

6.4 Conclusions

- A number of novel of racemic amine ligands, **605**, **608** and **609-611**, with a cyclohexyl ring substituent *alpha* to the indene ring, have been synthesised in good yield. Ligands **605** and **608** are very interesting and large scale-production methods are reported.
- Chiral amine ligands, (*S*)-**605**, and (*S*)-**608**, with a cyclohexyl ring substituent *alpha* to the indene ring, have been synthesised in good yield.
- A number of novel of racemic amine ligands, **614-618**, with no substituent *alpha* to the indene ring have been synthesised in good yield.
- The Rh(I) complex *rac*-**627** has been synthesised, however the structure has not be proven by X-ray crystallography. Oxidation of Rh(I) *rac*-**627** to Rh(III) *rac*-**628** did not occur. X-ray crystallography proved spiro compound **629** was isolated instead.
- A number of amine complexes may have been synthesised. However isolation and purification of such amine complexes has proved difficult.

Chapter 7: Conclusions and further work.

7.1 Conclusions

At the beginning of my Ph.D., research aims were to develop a series of chiral ligands based on the successful ‘favoured rotamer’ complexation model (Chapters 2 and 3). This model allows the design of ligands, which induce planar- chirality upon complexation to transition metals *via* face selectivity and hence form diastereomerically pure complexes without the need for resolution. The ligands were targeted at late transition metals such as ruthenium and rhodium, with the intention of applying their complexes as novel catalysts of organic transformations.

Over the course of this research, the syntheses of novel ligand *rac*-**201** and complex *rac*-**401** have been optimised. Technically challenging column chromatography under inert atmosphere is no longer needed. A novel 1,4-catalytic addition of indenyl lithium to an α,β -unsaturated ester has been devised. The enantiopure alcohol (*S*)-**206** has been synthesised via asymmetric hydrogenation of a β -keto ester using a chiral bidentate phosphine-ruthenium complex. (*S*)-**206** has been converted to the enantiopure diphenylphosphine ligand (*S*)-**201**, and subsequently complexed to ruthenium with high induction of planar chirality and complete control of metal centred chirality yielding (*S*)-**401**. Although cationic complexes *rac* and (*S*)-**402** have been synthesised, the failure to synthesise the tetrahydroindenyl analogues of *rac*-**401** and (*S*)-**401** is disappointing. Complexes **417-419** were synthesised by displacement of PPh_3 in *rac*-**401** via a dissociative process.

The novel amine ligands based upon the ‘favoured rotamer’ and ‘roof and wall’ models *rac*- and (*S*)-**605**, *rac*- and (*S*)-**608** and **609-611** have been synthesised. Complexation of the amine ligands **614-618** to ruthenium and rhodium has been successful according to NMR spectroscopic evidence, however isolation of such complexes has proven difficult. The formation of the chloride salts of amine complexes *rac*-**621** and *rac*-**624** may have aided the isolation of such compounds. This is something that should be considered in the future.

Although the applications of ruthenium complexes *rac*-**401** and *rac*-**402**, have been

disappointing, the increasing number of reported reactions of closely related complexes give hope that catalytic applications will be found in the not too distant future.

7.2 Further work

The optimised synthesis of *rac*-**206** and the synthesis of enantiopure three-carbon tethered ligand (*S*)-**206**, offers the opportunity to a whole range of interesting novel ligands. The chiral amine ligands (*S*)-**605** and (*S*)-**608**, as well as the racemic amine ligands *rac*-**605** and **614**, could provide a very interesting set of complexes once complexed onto rhodium and/or iridium. These are similar to the CATHy catalyst (Section 6.1). The CATHy catalyst **603** is a highly efficient in the asymmetric transfer hydrogenation of a broad range of ketones and imines to chiral alcohols and amines. The catalyst is prepared in situ by combining a chiral bidentate nitrogen ligand with Rh(III) or Ir(III) metal complex containing a substituted cyclopentadienyl ligand. Our system will contain examples with a link between the cyclopentadienyl group and the amine group and the tosylamine group. They also give the option of having alternative amine groups. Using the CATHy catalyst as a precedent, it is believed our complexes will be active in catalytic processes such as asymmetric transfer hydrogenation (Figure 7.1).^{40,41,124-126}

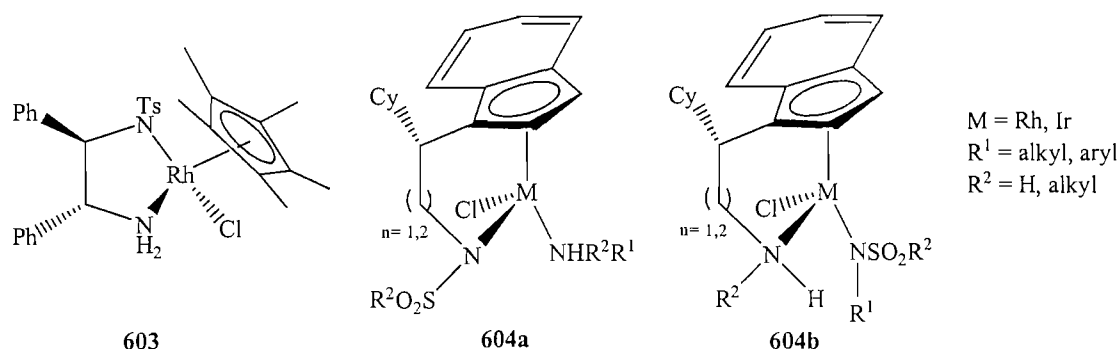


Figure 7.1

The disappointing results in the catalytic studies using complexes *rac*-**401** and *rac*-**402** causes much concern. The addition of a chloride scavenger, e.g silver hexafluorophosphate, may be advantageous in helping the creation of a second vacant

coordination site on the metal centre, thus increasing the chances of catalytic activity. (Figure 7.2).¹³⁴ Replacing the triphenylphosphine group with a more labile alternative (e.g. alkene, chlorine) should also help.

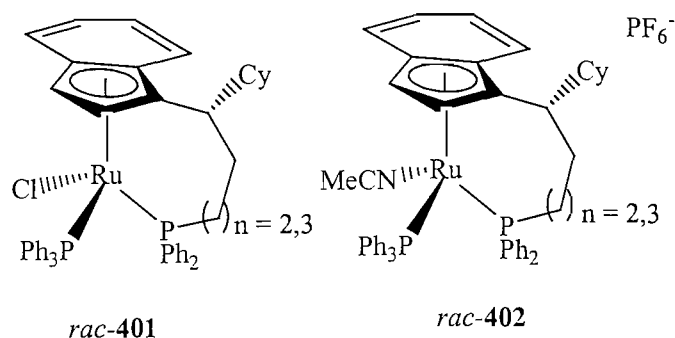


Figure 7.2

It has been reported that the catalytic activity and asymmetric induction of many ruthenium Cp-phosphine bidentate complexes can vary considerably depending on the length of the Cp-phosphine tether chain.^{29,35,67} Extension of the carbon tether to four or five atoms is another important long-term target for this series of ligands (Figure 7.2). In summary, the research detailed in this Ph.D. thesis has led to many new ideas, many of which have yet to be investigated. These should offer a stimulating basis for future research in this area.

Chapter 8: Experimental

8.1 General Techniques

8.1.1 Air and moisture sensitive manipulations

All reactions and manipulations involving organometallic and phosphorus-containing compounds were performed under an argon atmosphere, using standard Schlenk, syringe and vacuum-line techniques. Reaction flasks, syringes, needles and cannula were dried in a hot oven (>160 °C) for 12 hours prior to use and allowed to cool in a sealed desiccator, over silica gel.

8.1.2 Spectroscopic techniques

^1H , ^{13}C , ^{31}P and ^{19}F NMR spectra were recorded on Brüker AM300, Brüker AC300 or Brüker DPX400 Fourier Transform spectrometers. The NMR spectra of moisture sensitive organometallics were recorded in deuterobenzene (stored over 4 Å molecular sieves) and referenced to the residual benzene signals at 7.18 ppm (^1H , NMR) and 128.7 (^{13}C NMR). Unless otherwise stated all other spectra were recorded in deuteriochloroform (stored over K_2CO_3) and referenced to the residual benzene signals at 7.27 ppm (^1H , NMR) and 77.2 (^{13}C NMR). Phosphorus-31 and Fluorine-19 spectra were referenced to external H_3PO_4 and CFCl_3 standard solutions respectively. Chemical shifts are given in units of ppm on the δ scale. The following abbreviations are used to denote multiplicity and the shape of signal and may be compounded: s = singlet, d = doublet, t = triplet, q = quartet, m = multiplet, br = broad, fs = fine splitting. Coupling constants J are recorded in Hz. Carbon-13 spectra were proton decoupled and signals reported as C, CH, CH_2 , CH_3 depending on the number of directly attached protons (0, 1, 2, 3 respectively), this being determined by DEPT experiments. Assignments of ^{13}C spectra containing carbon signals split by nuclei other than hydrogen e.g. boron, rhodium and/or phosphorus, include multiplicities and coupling constants, reported using the same system of 's', 'd', 't', etc. abbreviations used for the proton assignments. 2D COSY spectra (H-H and C-H correlation) were routinely used to conclusively assign signals from ^1H and ^{13}C spectra and have not been specifically documented. Assignments of ^1H and ^{13}C NMR resonances are listed

using the numbering schemes in the title diagrams of the compounds (unless otherwise stated).

Mass spectra, including accurate masses, were recorded on a VG Analytical 70-250-SE double focusing mass spectrometer using, Electron Impact Ionisation (EI⁺) at 70eV. Electrospray (ES⁺) was recorded on a VG platform quadropole spectrometer in acetonitrile. M/z values are reported as values in atomic mass units followed by peak intensity relative to the base peak.

Infra-red spectra were recorded on a Perkin Elmer 1600 FT-IR spectrometer as films between sodium chloride plates, dichloromethane solutions, or directly. Absorptions are given in wavenumbers (cm⁻¹) and peaks are described as 's' (strong), 'm' (medium), 'w' (weak) and may be compounded with 'br' (broad).

Optical rotations were measured in an AA-100 Polarimeter (Optical Activity Limited).

8.1.3 Reagent purification

Unless otherwise indicated materials were obtained from commercial sources and used without further purification. Specific purifications were carried out according to standard procedures.¹³⁵ *n*-butyllithium (2.5M solution in cyclohexane) and *sec*-butyllithium (1.4M solution in cyclohexane) were purchased from Aldrich and their titre checked regularly. Dimethylphenylphosphine (4.0 M solution in toluene) was made freshly.

Diethyl ether, tetrahydrofuran and toluene were freshly distilled from dark purple solutions of sodium/benzophenone ketyl under an argon atmosphere. Dichloromethane, pyridine, triethylamine, diethylamine, dimethylformamide, and HMPA were dried over, and distilled from, calcium hydride. Petrol refers to the fraction of petroleum ether, which boils between 40 and 60 °C.

Tetracarbonylbis(μ -chloro)dirhodium(I) was prepared from rhodium trichloride trihydrate and resublimed prior to use in 69% yield.¹³⁶

Tris(triphenylphosphine)dichlororuthenium(II) was prepared from ruthenium trichloride trihydrate and triphenylphosphine in 95% yield.¹⁰⁵ Borane complexes of diphenylphosphine and methyl-diphenylphosphine were obtained by reacting a solution of the free phosphine in THF with DMS-borane in 75% yield, after recrystallisation from diethyl ether.⁷²

8.1.4 Chromatography

Thin layer chromatography was carried out using 0.25 mm POLYGRAM[®] SIL G / UV₂₅₄ and 0.20 mm POLYGRAM[®] ALOX N / UV₂₅₄ pre-coated plates and were visualised with a 254 nm UV lamp, followed by phosphomolybdinic acid (12 g in 150 mL ethanol), sulphuric (5 % v/v in methanol), potassium permanganate (10 % w/v in water) or iodine (on SiO₂). Column chromatography of organic compounds was performed on silica 60 (230-400 mesh), under slightly positive pressure. Chromatography of organometallic complexes was performed on neutral alumina (Brockman grade III, prepared from commercial grade I deactivated with 6% w/w distilled water). Chromatography solvent mixtures are described as % volumes prior to mixing.

Routine monitoring of reactions were carried out using gas chromatography on a Hewlett Packard 6890 instrument with auto-sampler, passing through a 5% phenyl methyl siloxane column using helium as the carrier gas.

Method A: 80-250 °C at 25 °C/min, then held at 250 °C for 4.2 mins.

Method B: 40 °C at 2 mins, then 60-130 °C at 10 °C/min, then 25 °C/min to 200 °C

Chiral HPLC was carried out using a Hewlett Packard 1050 series instrument, with UV detection at 210 nm, using normal phase elution through 250 mm x 4.6 mm Chiracel OD-H or OB-H column. GC and HPLC peak size analysis was carried out using HP ChemStation software.

8.1.5 Miscellaneous

Elemental analyses were performed by MEDAC Ltd., Egham, Surrey.

Melting points were performed on a Kolfer hotstage and are uncorrected.

8.2 Experimental for Chapter 2

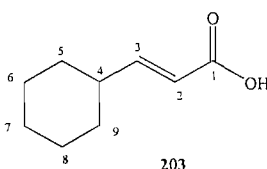
8.2.1. Optimised synthesis of *rac*-[3-cyclohexyl-3-(3*H*-inden-1-yl)-propyl]diphenyl-phosphane, 201.

8.2.1.1. 3-Cyclohexylacrylic acid, 203.

To a solution of malonic acid (52.0 g, 0.5 mol, 1.0 eq), in pyridine (65 mL, 0.8 mol, 1.6 eq), was added cyclohexanecarboxaldehyde (73 mL, 0.625 mol, 1.25 eq), and piperidine (cat. 4 mL, 42 mmol). The reaction was stirred for 5 days at RT, after which time the reaction was poured cautiously onto cold H₂SO₄ (50% solution, 150 mL). Diethyl ether (60 mL) was then added. The aqueous layer was separated and extracted with diethyl ether (3 x 40 mL) and the combined organics were washed with water (20 mL), brine (20 mL) and the solvents removed. The off white solid was dissolved in K₂CO₃ solution (10wt%, 300 ml) and washed with diethyl ether (2 x 100 mL). The basic aqueous phase was acidified with 2M HCl and then extracted with diethyl ether (3 x 50 mL). The combined organics were then washed with brine (20 mL), then dried over MgSO₄ and the solvents removed yielding the product as an off-white solid. Recrystallisation from ethanol at 5 °C gave white crystals (66 g, 0.43 mol, 85%).

NMR data were consistent with literature values.¹³

m.p. 57-58 °C. lit. m.p. 58-59 °C.



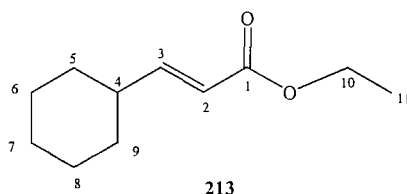
¹H NMR (300 MHz, CDCl₃): δ / ppm = 10.10 (1H, s, OH), 7.11 (1H, dd, *J* = 15.8, 7.0 Hz, H3), 5.81 (1H, dd, *J* = 15.8, 1.1 Hz, H2), 2.10 (1H, m, H4), 1.63–1.79 (5H, m, Cy), 0.9–1.3 (5H, m, Cy).

8.2.1.2. Ethyl (*E*)-3-cyclohexyl-1,2-propanoate, 213.

To a stirred solution of 3-cyclohexylacrylic acid, **203** (9.2 g, 60 mmol, 1.0 eq) in ethanol (100 mL) at 0 °C was added slowly dropwise thionyl chloride (6.5 mL, 90 mmol, 1.5 eq) over 10 mins. After 1 h at reflux the reaction was cooled to RT and the

solvents removed. Water (50 mL) and diethyl ether (80 mL) were added and the aqueous phase was separated and extracted with diethyl ether (3 x 50 mL). The combined organics were washed with NaHCO₃ (30 mL), dried over MgSO₄, and the solvents removed yielding the product as a yellow oil (8.2 g, 45 mmol, 75 %). The title compound was used without further purification.⁶⁹

NMR data were consistent with literature values.⁶⁸



IR (cm⁻¹ thin film): 2979 (m), 2927 (s), 2852 (m), 1721 (s), 1649 (m), 1449 (m), 1368 (m), 1170 (m), 1045 (w), 1368 (m), 852 (w), 708 (w).

¹H NMR (300 MHz, CDCl₃): δ / ppm = 6.85 (1H, dd, J = 15.8, 7.0 Hz, H3), 5.72 (1H, dd, J = 15.8, 1.0 Hz, H2), 4.13 (2H, q, J = 7.2 Hz, H10), 2.10 (1H, m, H4), 1.58-1.70 (5H, m, Cy), 1.25 (3H, t, J = 7.2 Hz, H11), 0.95-1.15 (5H, m, Cy).

¹³C NMR (75 MHz, CDCl₃): δ / ppm = 166.06 (C, C1), 154.20 (CH, C3), 118.82 (CH, C2), 60.06 (CH₂, C10), 40.35 (CH, C4), 31.64 (2 x CH₂, C5/9), 25.58 (CH₂, C7), 25.70 (2 x CH₂, C6/8), 14.22 (CH₃, C11).

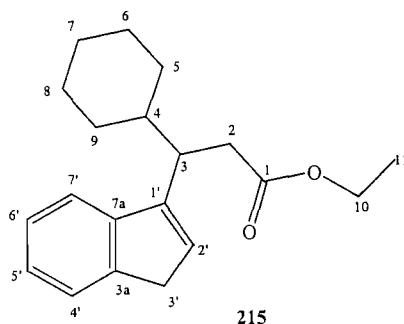
LRMS (CI): m/z = 183, ([M+H]⁺, 100%).

8.2.1.3. *rac*-Ethyl- 3-cyclohexyl-3-(1*H*-3-indenyl) propanoate, 215.

To a stirred solution of indene (8 mL, 68 mmol, 1.5 eq) and **213** (8 g, 45 mmol, 1.0 eq) in THF (50 mL) and in the dark, was added *sec*-BuLi (1.4 M in cyclohexane, 3.2 mL, 4.5 mmol, 10 mol%) dropwise over 10 min at RT. The reaction mixture was cooled to 0 °C and left to stir for 15 min, then allowed to warm to RT. After 3 h the reaction was quenched with water (50 mL) and then diethyl ether (50 mL) was added. The aqueous layer was separated and extracted with diethyl ether (3 x 50 mL) and the combined organics were washed with brine (30 mL), dried over MgSO₄, and the

solvents removed yielding a brown oil (~13 g). The crude mixture still containing excess indene was used without further purification in the reduction to alcohol **206** below (Section 8.2.1.6.)

On a 4.5 mmol (scaled down) reaction, the title compound was isolated from the crude mixture by first applying high vacuum (1 mmHg) to remove excess indene, then performing flash column chromatography (SiO₂, 5% diethyl ether/petrol, R_f = 0.35) to yield the title compound as a yellow oil. (1.04 g, 3.5 mmol, 78 %).



IR (cm⁻¹ thin film): 3068 (w), 2925 (s), 2851 (s), 1734 (s), 1606 (w), 1449 (m), 1248 (m), 1158 (m), 1034 (w), 769 (s), 720 (m).

¹H NMR (300 MHz, CDCl₃): δ / ppm = 7.46 (1H, d, J = 7.4 Hz, H7'/4'), 7.44 (1H, d, J = 7.4 Hz, H7'/4'), 7.31 (1H, td, J = 7.4, 1.1 Hz, H5'/6'), 7.20 (1H, td, J = 7.4, 1.1 Hz, H5'/6'), 6.23 (1H, t, J = 1.6 Hz, H2'), 4.03 (2H, q, J = 7.4 Hz, H10), 3.35 (2H, d, J = 1.6 Hz, H3'), 3.21 (1H, ddd, J = 10.0, 5.5, 5.5 Hz, H3) 2.75 (1H, dd, J = 15.0, 5.5 Hz, H2-a), 2.65 (1H, dd, J = 15.0, 10.0 Hz, H2-b) 1.36-1.72 (6H, m, Cy ring) 1.10 (3H, t, J = 7.4 Hz, H11), 0.75-1.20 (5H, m, Cy ring).

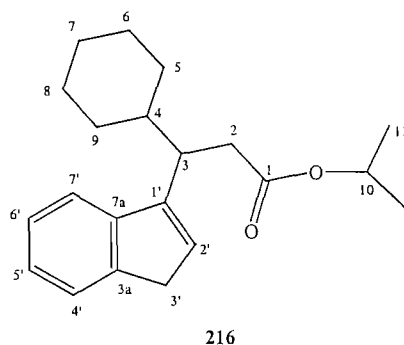
¹³C NMR (75 MHz, CDCl₃): δ / ppm = 173.16 (C, C1), 146.01 (C, C1'/3a/7a), 145.35 (C, C1'/3a/7a), 144.40 (C, C1'/3a/7a), 128.55 (CH, C4'/5'/6'/7'), 125.88 (CH, C4'/5'/6'/7'), 124.44 (CH, C4'/5'/6'/7'), 123.71 (CH, C4'/5'/6'/7'), 119.62 (CH, C2'), 60.16 (CH₂, C10), 41.26 (CH, C3/4), 40.13 (CH, C3/4), 37.75 (CH₂, C3'), 36.53 (CH₂, C2), 31.12 (CH₂, C5/9), 30.18 (CH₂, C5/9), 26.57, (CH₂, C6/7/8), 26.53 (CH₂, C6/7/8), 26.45 (CH₂, C6/7/8), 14.08 (CH₃, C11).

LRMS (CI): m/z = 299, ([M+H]⁺, 100%); 253, ([M-C₂H₅O]⁺, 18%).

HRMS (CI): C₂₀H₂₆O₂ requires *m/z* 298.1933, found 298.1927[M].

8.2.1.4. *rac*-Isopropyl- 3-cyclohexyl-3-(1*H*-3-indenyl) propanoate, 216.

To a stirred solution of indene (0.52 mL, 4.5 mmol, 1.5 eq) and, *isopropyl*-(*E*)-3-cyclohexyl-2-propanoate **214** (0.6 g, 3.0 mmol, 1.0 eq) in THF (15 mL) and in the dark, was added *sec*-BuLi, (1.4M in cyclohexanes, 0.21 mL, 0.3 mmol 10 mol%) dropwise over 10 minutes. The reaction mixture was cooled to 0 °C and left for 15 min, then allowed to warm to RT. After 3 h the reaction was quenched with water (10 mL) and then diethyl ether (20 mL) was added. The aqueous layer was separated and extracted with diethyl ether (3 x 20 mL). The combined organics were washed with brine (10 mL), dried over MgSO₄, and the solvents removed yielding a yellow oil. (1.15 g) The title compound was isolated from the crude mixture by first applying high vacuum (1 mmHg) to remove excess indene, then performing flash column chromatography (SiO₂, 5 % diethyl ether/petrol, R_f = 0.4) to yield the title compound as a yellow oil. (0.765 g, 2.4 mmol, 82 %).



IR (cm⁻¹ thin film): 3068 (w), 2977 (s), 2925 (s), 2852 (s), 1732 (s), 1606 (w), 1449 (m), 1258 (m), 1163 (m), 1022 (w), 769 (s), 720 (m).

¹H NMR (300 MHz, CDCl₃): δ / ppm = 7.46 (1H, d, *J* = 7.4 Hz, H7'/4'), 7.44 (1H, d, *J* = 7.4 Hz, H7'/4'), 7.30 (1H, td, *J* = 7.4, 1.1 Hz, H5'/6'), 7.20 (1H, td, *J* = 7.4, 1.1 Hz, H5'/6'), 6.22 (1H, t, *J* = 2.0 Hz, H2'), 4.88 (1H, septet, *J* = 6.2 Hz, H10), 3.37 (1H, dd, *J* = 21.0, 2.0 Hz, H3'-a), 3.31 (1H, dd, *J* = 21.0, 2.0 Hz, H3'-b), 3.20 (1H, ddd, *J* = 10.8, 6.0, 5.5 Hz, H3) 2.73 (1H, dd, *J* = 15.0 5.5 Hz, H2-a), 2.62 (1H, dd, *J* = 15.0, 10.0 Hz, H2-b) 1.46–1.72 (6H, m, Cy) 1.07 (3H, d, *J* = 6.2 Hz, H11), 1.02 (3H, t, *J* = 6.2 Hz, H11), 0.75-1.18 (5H, m, Cy).

¹³C NMR (75 MHz, CDCl₃): δ / ppm = 172.66 (C, C1), 146.06 (C, C1'/3a/7a), 145.47 (C, C1'/3a/7a), 144.32 (C, C1'/3a/7a), 128.53 (CH, C4'/5'/6'/7'), 125.85 (CH, C4'/5'/6'/7'), 124.42 (CH, C4'/5'/6'/7'), 123.66 (CH, C4'/5'/6'/7'), 119.65 (CH, C2'), 67.32 (CH, C10), 41.42 (CH, C3/4), 40.16 (CH, C3/4), 37.72 (CH₂, C3'), 36.96 (CH₂, C2), 31.09 (CH₂, C5/9), 30.29 (CH₂, C5/9), 26.57, (CH₂, C6/7/8), 26.54 (CH₂, C6/7/8), 26.45 (CH₂, C6/7/8), 21.67 (CH₃, C11), 21.52 (CH₃, C11),

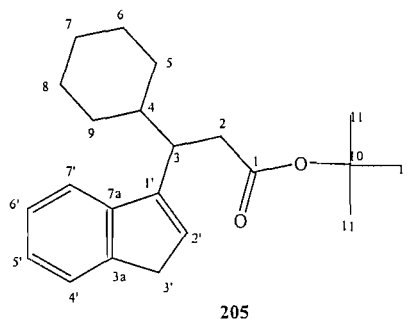
LRMS (CI): m/z = 313, ([M+H]⁺, 100%); 271, ([M-C₃H₆]⁺, 45%); 253, ([M-C₃H₇O]⁺, 36%);

HRMS (CI): C₂₁H₂₈O₂ requires m/z 312.2809, found 312.2806[M]

8.2.1.5. *rac*-*Tert*-butyl 3-cyclohexyl-3-(1*H*-3-indenyl) propanoate, 205.

To a stirred solution of indene (0.34 mL, 3.0 mmol, 1.5 eq) and *tert*-butyl (*E*)-3-cyclohexyl-2-propanoate, **204** (0.42 g, 2.0 mmol, 1.0 eq) in THF (15 mL) and in the dark, was added *sec*-BuLi, (1.4M in cyclohexanes, 0.21 mL, 0.3 mmol, 10 mol%) dropwise over 10 minutes. The reaction mixture was cooled to 0 °C and left for 15 min, then allowed to warm to RT. After 3 h the reaction was quenched with water (10 mL) and diethyl ether (20 mL) was added. The aqueous layer was separated and extracted with diethyl ether (3 x 50 mL). The combined organics were washed with brine (10 mL), dried over MgSO₄, and the solvents removed yielding a yellow oil. The title compound was isolated from the crude mixture by first applying high vacuum (1 mmHg) to remove excess indene, then performing flash column chromatography (SiO₂, 5 % ethyl acetate/petrol, R_f = 0.3) to yield the title compound as a yellow oil. (0.51 g, 2.4 mmol, 78 %).

NMR data were consistent with literature values.¹³



IR (cm⁻¹ thin film): 3070 (w), 2975 (s), 2923 (s), 2851 (s), 1728 (s), 1603 (w), 1450 (m), 1257 (m), 1150 (m), 972 (w), 769 (s), 720 (m).

¹H NMR (300 MHz, CDCl₃): δ / ppm = 7.48 (1H, d, J = 7.4 Hz, H7'/4'), 7.41 (1H, d, J = 7.4 Hz, H7'/4'), 7.33 (1H, td, J = 7.4, 1.1 Hz, H5'/6'), 7.31 (1H, td, J = 7.4, 1.1 Hz, H5'/6'), 6.26 (1H, t, J = 2.2 Hz, H2'), 3.42 (1H, dd, J = 23.5, 2.2 Hz, H3'-a), 3.33 (1H, dd, J = 23.5, 2.2 Hz, H3'-b), 3.19 (1H, ddd, J = 10.0, 6.6, 5.0 Hz, H3) 2.73 (1H, dd, J = 15.0 5.0 Hz, H2-a), 2.60 (1H, dd, J = 15.0, 10.0 Hz, H2-b) 1.46–1.69 (6H, m, Cy) 1.09 (9H, s, *t*-Bu), 0.71-1.23 (5H, m, Cy).

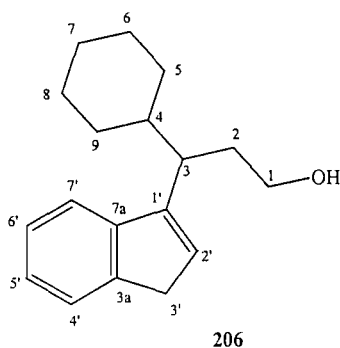
¹³C NMR (300 MHz, CDCl₃): δ / ppm = 172.42 (C, C1), 146.27 (C, C1'/3a/7a), 145.62 (C, C1'/3a/7a), 144.31 (C, C1'/3a'/7a'), 128.50 (CH, C4'/5'/6'/7'), 125.88 (CH, C4'/5'/6'/7'), 124.44 (CH, C4'/5'/6'/7'), 123.68 (CH, C4'/5'/6'/7'), 119.72 (CH, C2'), 79.94 (C, C10), 41.58 (CH, C3/4), 40.33 (CH, C3/4), 38.04 (CH₂, C3'), 37.73 (CH₂, C2), 31.18 (CH₂, C5/9), 30.41 (CH₂, C5/9), 27.86, (3 x CH₃, C11), 26.61 (CH₂, C7), 26.51 (2 x CH₂, C6/8).

8.2.1.6. *rac*-3-Cyclohexyl-3-(1*H*-3-indenyl)-1-propanol, 206.

Crude *rac*-Ethyl- 3-cyclohexyl-3-(1*H*-3-indenyl) propanoate, **215** (13 g, ~44 mmol, 1.0 eq), still containing excess indene from the previous 1,4-addition reaction (Section 8.2.1.3) was dissolved in diethyl ether (80 mL) and added carefully, *via* cannula, to a solution of lithium aluminium hydride (2.0 g, 53 mmol, 1.2 eq) in diethyl ether (80 mL) at 0 °C. After the addition was complete, the reaction was warmed to RT, and after 4 h, the reaction was cooled to 0 °C. Water (5 mL) was added very carefully (vigorous evolution of hydrogen gas). Sodium hydroxide (15 % aqueous solution, 10 mL) was then added slowly followed by further water (20 mL). The quenched reaction mixture was stirred at RT for 30 minutes, resulting in a pale yellow suspension. The suspension was filtered through celite (washed thoroughly with diethyl ether), then dried over MgSO₄, and the solvents removed yielding a yellow oil. The title compound was isolated using flash column chromatography (SiO₂, 40 % diethyl ether/petrol, R_f = 0.35) as a yellow oil which solidified on standing (8.2 g, 32 mmol, 73%). Recrystallisation from hot hexane gave **206** as white crystals.

NMR data were consistent with literature values.¹³

m.p. = 61-62 °C. lit. m.p. = 62-63 °C. ¹³



IR (cm⁻¹ thin film): 3275 (br), 3010 (w), 2920 (s), 2848 (s), 1686 (w), 1604 (w), 1450 (m), 1385 (m), 1019 (m), 720 (w, CH₂).

¹H NMR (300 MHz, CDCl₃): δ / ppm = 7.48 (1H, d, J = 7.4 Hz, H4'/7'), 7.43 (1H, d, J = 7.4 Hz, H4'/7'), 7.30 (1H, td, J = 7.4, 1.1 Hz, H5'/6'), 7.22 (1H, td, J = 7.4, 1.1 Hz, H5'/6'), 6.23 (1H, t, J = 2.2 Hz, H2'), 3.45-3.67 (2H, m, H1'), 3.35 (2H, d, J = 2.2 Hz, H3'), 2.70 (1H, ddd, J = 10.6, 6.6, 4.2 Hz, H3), 1.96-2.10 (2H, m, H2), 1.54-1.78 (6H, m, Cy), 0.91-1.29 (5H, m, Cy). The OH signal was not observed

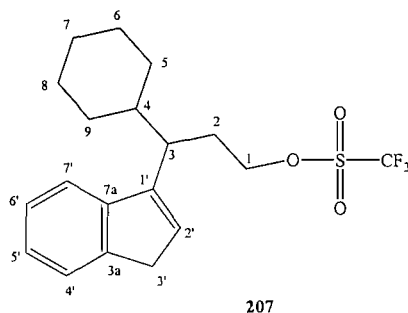
¹³C NMR (75 MHz, CDCl₃): δ / ppm = 146.28 (C, C1'/3a/7a), 145.44 (C, C1'/3a/7a), 144.76 (C, C1'/3a/7a), 128.86 (CH, C4'/5'/6'/7'), 125.89 (CH, C4'/5'/6'/7'), 124.51 (CH, C4'/5'/6'/7'), 123.86 (CH, C4'/5'/6'/7'), 119.72 (CH, C2'), 61.94 (CH₂, C1), 41.35 (CH, C3/4), 40.89 (CH, C3/4), 37.70 (CH₂, C3'), 33.59 (CH₂, C2), 31.33 (CH₂, C5/9), 30.65 (CH₂, C5/9), 26.60 (CH₂, C7), 26.57 (2 x CH₂, C6/8).

8.2.1.7. *rac*-Trifluoromethanesulfonic acid 3-cyclohexyl-3-(3*H*-indenyl-1)-propyl ester, **207**.

To a stirred solution of trifluoromethanesulfonic anhydride (2.2 mL, 13.8 mmol, 1.15 eq) in dichloromethane (40 mL) at 0 °C was added a solution of *rac*-3-cyclohexyl-3-(1*H*-3-indenyl)-1-propanol, **206** (3.1 g, 12.0 mmol, 1.0 eq) and pyridine (1.1 mL, 13.2 mmol, 1.1 eq) in dichloromethane (20 mL), slowly. After 90 mins stirring at 0 °C, the reaction was then quenched with water (10 mL) and dichloromethane (15 mL). The aqueous layer was separated and extracted with dichloromethane (3 x 20 mL). The

combined organics were dried over MgSO_4 and the solvents removed yielding the product as a light green oil (4.2 g, 11.0 mmol, 90 %) The title compound was used without further purification.

NMR data were consistent with literature values.¹³



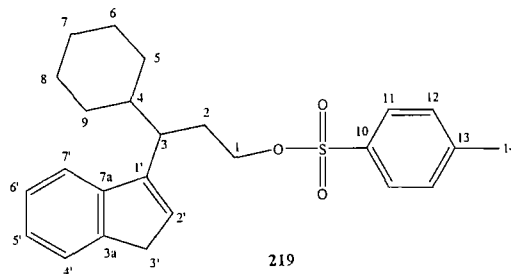
^1H NMR (300 MHz, CDCl_3): δ / ppm = 7.40 (1H, d, J = 7.4 Hz, H4'/7'), 7.30 (1H, d, J = 7.4 Hz, H4'/7'), 7.21 (1H, td, J = 7.4, 1.1 Hz, H5'/6'), 7.14 (1H, td, J = 7.4, 1.1 Hz, H5'/6'), 6.15 (1H, t, J = 2.2 Hz, H2'), 4.43 (1H, ddd, J = 9.9, 7.5, 4.4 Hz, H1-a), 4.30 (1H, ddd, J = 9.8, 7.4, 4.4 Hz, H1-a), 3.35 (2H, d, J = 2.2 Hz, 3'), 2.70 (1H, ddd, J = 10.6, 6.6, 4.2 Hz, H3), 2.33 (1H, ddd, J = 14.0, 8.5, 3.8 Hz, H2-a), 2.19 (1H, dddd, J = 14.1, 11.0, 6.3, 4.4 Hz, H2-b), 1.61-1.79 (6H, m, Cy), 0.91-1.29 (5H, m, Cy).

^{13}C NMR (75 MHz, CDCl_3): δ / ppm = 144.94 (C, C1'/3a/7a), 144.68 (C, C1'/3a/7a), 144.58 (C, C1'/3a/7a), 130.08 (CH, C4'/5'/6'/7'), 126.20 (CH, C4'/5'/6'/7'), 125.04 (CH, C4'/5'/6'/7'), 124.21 (CH, C4'/5'/6'/7'), 119.76 (CH, C2'), 76.78 (CH_2 , C1), 41.48 (CH, C3/4), 40.74 (CH, C3/4), 37.94 (CH_2 , C3'), 31.42 (CH_2 , C2), 30.73 (CH_2 , C5/9), 30.43 (CH_2 , C5/9), 26.59 (CH_2 , C7), 26.57 (2 x CH_2 , C6/8).

8.2.1.8. *rac*-toluene-4-sulfonic acid 3-cyclohexyl-3-(3*H*-inden-1-yl)-propyl ester, 219.

To a stirred solution of *rac*-3-cyclohexyl-3-(1*H*-3-indenyl) propanol, **206** (0.25 g, 1.0 mmol, 1.0 eq) in dichloromethane (3 mL) at 0 °C was added pyridine (0.13 g, 1.6 mmol, 1.6 eq). *p*-toluenesulfonylchloride (0.27 g, 1.4 mmol, 1.4 eq) was then added portionwise at 0 °C. The reaction was left to warm to RT, and after 2 h the reaction was quenched with water (10 mL) and dichloromethane (5 mL). The aqueous phase was separated and extracted with dichloromethane (3 x 10 mL). The combined

organics were washed with brine (10 mL), dried over MgSO₄ and the solvents removed. Purification was achieved by flash column chromatography (SiO₂, 10 % ether/petrol, R_f = 0.18) to yield a clear oil (0.21 g, 0.5 mmol, 51 %). The title compound was light/temperature sensitive, and seen to decompose to a black oil when left standing at room temperature for 2 h.



IR (cm⁻¹): 3057 (w), 2924 (s), 2850 (m), 1597 (w), 1449 (m), 1361 (m), 1176(s), 962 (m), 772 (m), 722 (m).

¹H NMR (400 MHz, CDCl₃): δ / ppm 7.64 (2H, d, *J* = 8.0 Hz, H11), 7.45 (1H, d, *J* = 7.0 Hz, CH), 7.14–7.31 (5H, m, CH), 6.22 (1H, t, *J* = 2.2 Hz, H2'), 4.04 (1H, ddd, *J* = 9.6, 7.0, 4.0 Hz, H1-a), 3.82 (1H, td, *J* = 9.2, 6.6 Hz, H1-b), 3.29 (1H, dd, *J* = 21.3, 1.8 Hz, H3'-a), 3.21 (1H, dd, *J* = 21.3, 1.8 Hz, H3'-b), 2.40 (3H, s, H17), 2.64 (1H, ddd, *J* = 10.6, 6.6, 4.0 Hz, H3), 2.16 (1H, dddd, *J* = 13.9, 8.5, 4.4, 3.7 Hz, H2-a), 1.95 (1H, dddd, *J* = 14.4, 11.4, 6.3, 4.4 Hz, H2-b), 1.61-1.79 (6H, m, Cy), 0.9-1.18 (5H, m, Cy).

¹³C NMR (100 MHz, CDCl₃): δ / ppm 144.93 (C, C1'/3a/7a/13), 144.74 (C, C1'/3a/7a/13), 144.64 (C, C1'/3a/7a/13), 144.40 (C, C1'/3a/7a/13), 132.85 (C, C10), 129.60 (2 x CH, C12), 129.28 (CH, C4'/5'/6'/7'), 127.11 (2 x CH, C11), 125.91 (CH, C4'/5'/6'/7'), 124.56 (CH, C4'/5'/6'/7'), 123.80 (CH, C4'/5'/6'/7'), 119.65 (CH, C2'), 69.58 (CH₂, C1), 41.03 (CH, C3/4), 40.21 (CH, C3/4), 37.63 (CH₂, C3'), 31.17 (CH₂, C2), 30.35 (CH₂, C5/9), 29.46 (CH₂, C5/9), 26.50 (CH₂, C7), 26.45 (2 x CH₂, C6/8), 21.61 (CH₃, C14).

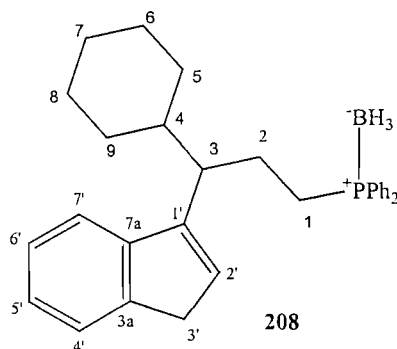
LRMS (ES⁺): *m/z* = 428, ([M+NH₄]⁺ 45 %); 144, ([M-C₁₇H₂₀O₃]⁺, 100%).

HRMS (ES⁺): C₂₅H₃₀O₃S₁ requires *m/z* 433.1807, found 433.1799. (M+Na)⁺

8.2.1.9. *rac*-[3-cyclohexyl-3-(3*H*-inden-1-yl)-propyl]diphenyl-phosphine-borane complex, **208**.

To a stirred solution of diphenylphosphine borane, **218** (1.95 g, 9.7 mmol, 1.0 eq) in THF (15 mL) at 0 °C was added *n*-BuLi (2.5M soln in cyclohexanes, 3.9 mL, 9.7 mmol, 1.0 eq). This was left to warm to RT. After 2h, it was added dropwise *via* cannula to a stirred solution of *rac*-trifluoromethanesulfonic acid 3-cyclohexyl-3-(3*H*-indenyl-1)-propyl ester, **207** (3.8 g, 9.7 mmol, 1.0 eq) in THF (10 mL) at 0 °C. This was left to warm to RT. After 2 h the reaction was quenched with water (20 mL) and diethyl ether (20 mL). The aqueous phase was separated and extracted with diethyl ether (3 x 20 mL). The combined organics were washed with brine (20 mL), dried over MgSO₄ and the solvents removed. The title compound was isolated by flash column chromatography (SiO₂, 5 % diethyl ether/petrol, R_f = 0.30) as a yellow solid. (3.20 g) Recrystallisation from hot hexanes gave the title compound as a white solid (2.97 g, 6.8 mmol, 70 %).

NMR data were identical to literature values.¹³



IR (cm⁻¹ thin film): 3072 (m), 3054 (m), 3011 (w), 2924 (s), 2851 (s), 2378 (s), 2340 (s), 1449 (m), 1105 (m), 906 (m), 770 (m).

¹H NMR (300 MHz, CDCl₃): δ / ppm = 7.04-7.41 (14H, m, Ar), 6.01 (1H, v.br.t, *J* = 1.7 Hz, H2'), 3.29 (2H, v.br.d, *J* = 2.2 Hz, H3'), 2.50 (1H, ddd, *J* = 9.9, 6.4, 3.1 Hz, H3), 1.51-2.21 (10H, m, Cy+H1+ H2), 0.91-1.25 (8H, m, Cy+BH₃).

¹³C NMR (75 MHz, CDCl₃): δ / ppm = 145.45 (C, s, C1'/3a/7a), 145.41 (C, s, C1'/3a/7a), 144.73 (C, s, C1'/3a/7a), 132.27 (2 x CH, d, *J* = 8.9 Hz, *o*-Ph), 131.91 (2 x CH, d, *J* = 8.9 Hz, *o*-Ph), 131.47 (C, d, *J* = 2.0 Hz, *i*-Ph), 130.93 (C, d, *J* = 2.0 Hz, *i*-

Ph), 129.66 (CH, s, *p*-Ph), 129.53 (CH, s, *p*-Ph), 129.30 (CH, s, C4'/5'/6'/7'), 128.76 (2 x CH, s, *m*-Ph), 128.63 (2 x CH, s, *m*-Ph), 125.95 (CH, s, C2'), 124.57 (CH, s, C4'/5'/6'/7'), 123.86 (CH, s, C4'/5'/6'/7'), 119.67 (CH, s, C4'/5'/6'/7'), 45.73 (CH, d, $J = 13.4$ Hz), 41.42 (CH, s), 37.77 (CH₂, s), 31.22 (CH₂, s), 30.63 (CH₂, s), 26.56 (CH₂, s), 26.52 (CH₂, s), 26.47 (CH₂, s), 23.88 (CH₂, d, $J = 37.7$ Hz), 23.85 (CH₂, s).

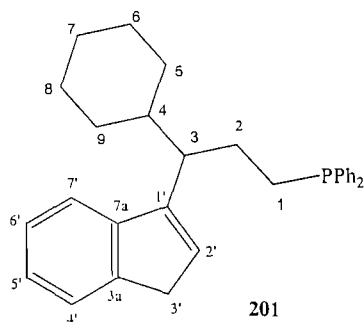
³¹P NMR (121 MHz, CDCl₃): δ / ppm = 16.80 (br. s) ppm.

Deprotection of borane complex

8.2.1.10. *rac*-[3-cyclohexyl-3-(3*H*-inden-1-yl)-propyl]diphenyl-phosphane, **201**.

rac-[3-cyclohexyl-3-(3*H*-inden-1-yl)-propyl]diphenyl-phosphine-borane complex, **208** (2.3 g, 5.2 mmol, 1.0 eq) was treated with an excess of neat diethylamine (10 mL), and warmed to reflux. After 3 h, TLC (10 % ether/petrol) indicated no borane protected phosphine and only free phosphine present. The reaction was then cooled and the solvent removed, leaving **201** as an air-sensitive oil (2.0 g, 4.7 mmol, 90 %). The title compound was used without further purification.

NMR data were identical to literature values.¹³



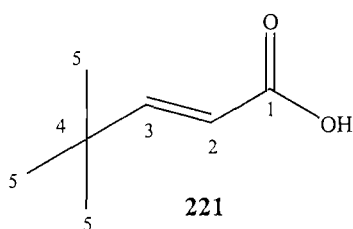
¹H NMR (400 MHz, CDCl₃): δ / ppm = 7.19–7.45 (14H, m, Ar), 6.10 (1H, t, $J = 2.0$ Hz, H2'), 3.32 (2H, d, $J = 1.8$ Hz, H3'), 2.52–2.63 (1H, m, H3), 1.81–2.01 (4H, m, H1+H2), 1.52–1.77 (6H, m, Cy), 1.02–1.31 (5H, m, Cy).

³¹P NMR (121 MHz, CDCl₃): δ / ppm = –14.98 (s) ppm.

8.2.1.11. (*E*)-3-*tert*-butyl propenoic acid, 221.

To a solution of malonic acid (0.42 g, 4 mmol, 1.0 eq) in pyridine (0.5 g, 6.4 mmol, 1.6 eq) was added pivaldehyde (0.43 g, 5 mmol, 1.25 eq) and piperidine (0.12 g, 1.33 mmol, 0.3 eq). A condenser was attached and the reagents were refluxed overnight. After 16 h, the reaction was cooled poured cautiously onto cold H₂SO₄ (50 % solution, 10 mL). Diethyl ether (20 mL) and water (10 mL) were added and the aqueous layer was separated and extracted with diethyl ether (3 x 20 mL). The combined organics were washed with water (10 mL), brine (10 mL), and the solvents removed. The resulting yellow oil was dissolved in K₂CO₃ (10 % wt, 20 mL) and washed with diethyl ether (3 x 20 mL). The aqueous basic solution was acidified with 2M HCl (30 mL) and then extracted with diethyl ether (3 x 20 mL). The combined organics were washed with brine (10 mL), dried over MgSO₄ and the solvents removed yielding the product as an oily clear solid (0.37 g, 3.0 mmol, 67 %).

NMR data were identical to literature values.¹³⁷



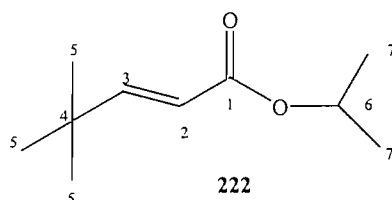
¹H NMR (300 MHz, CDCl₃): δ / ppm = 9.93 (1H, s, OH), 7.01 (1H, d, *J* = 15.8 Hz, H3), 5.69 (1H, d, *J* = 15.8 Hz, H2), 1.03 (9H, s, *t*-Bu).

¹³C NMR (300 MHz, CDCl₃): δ / ppm = 172.89 (C, C1), 162.08 (CH, C3), 116.2 (CH, C2), 34.16 (C, C4), 28.64 ((CH₃)₃, *t*-Bu).

8.2.1.12. *Iso*-propyl (*E*)-3-*tert* butyl-2-propanoate, 222.

To a stirred solution of (*E*)-3-*tert* butyl propenoic acid **221**, (0.25 g, 2.0 mmol, 1.0 eq) in dichloromethane (5 mL) at 0 °C under an argon atmosphere was added oxalyl chloride (0.26 mL, 3 mmol, 1.5 eq) slowly and DMF (5 drops). The reaction was allowed to warm to RT. After 2 h, the reaction had gone to completion and the solvent was removed yielding the acid chloride. (0.29 g, 2.0 mmol, 100 %). To a stirred

solution of acid chloride in benzene (5 mL) was added isopropanol (0.17 mL, 2.2 mmol, 1.1 eq) and pyridine (0.13 mL, 1.6 mmol, 0.8 eq) dropwise. The reaction was warmed to reflux. After 16 h, the reaction was cooled to RT and solvent was removed. The resulting residue was dissolved in dichloromethane (20 mL) and washed with 5 % NaHCO₃ (aq) soln (2 x 10 mL), 5 % HCl (aq) soln (2 x 10 mL) and the combined organics were dried over MgSO₄, and the solvents removed yielding the product as a clear oil (0.22 g, 1.3 mmol, 65 %).⁶⁸



IR (cm⁻¹ thin film): 2950 (s), 2893 (m), 2855 (m), 1715 (s), 1649 (m), 1469 (w), 1299 (m), 1162 (m), 987 (w), 706 (w).

¹H NMR (300 MHz, CDCl₃): δ / ppm = 6.94 (1H, d, J = 15.8 Hz, H3), 5.70 (1H, d, J = 15.8, H2), 5.04 (1H, septet, J = 6.3 Hz, H6), 1.24 (6H, d, J = 6.3 Hz, H7), 1.09 (9H, H5).

¹³C NMR (75 MHz, CDCl₃): δ / ppm = 166.87 (C, C1), 158.91 (CH, C3), 117.09 (CH, C2), 67.38 (CH, C6), 33.71 (C, C4), 28.63 ((CH₃)₃, C5), 21.89, (2 x CH₃, C7).

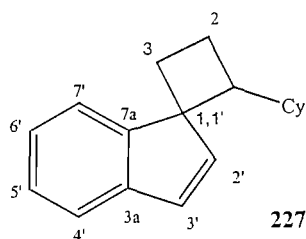
LRMS (CI): m/z = 170 ([M]⁺, 77%); 128, ([M]-C₃H₆)⁺, 100%); 83, ([M-C₄H₇O₂]⁺, 90%);

HRMS (CI): C₁₀H₁₈O₂ requires m/z 170.13103, found 170.13068 [M]

8.2.1.13. *rac*-Spiro-[(2-cyclohexylcyclobutane)-1,1'-indene], **227**.

To a stirred solution of methyldiphenyl phosphine borane, **226** (0.21 g, 1.0 mmol, 1.0 eq) in THF (2 mL) cooled to -78 °C was added *sec*-BuLi (1.4M in cyclohexanes, 0.71 mL, 1.0 mmol, 1.0 eq) and TMEDA (0.12 g, 1.0 mmol, 1.0 eq) dropwise. After stirring at -78 °C for 1 h, *rac*-trifluoromethanesulfonic acid 3-cyclohexyl-3-(3*H*-inden-1-yl)-propyl ester, **207** (0.35 g, 1.0 mmol, 1.0 eq) in THF (2 mL) was added

dropwise. The reaction was stirred at $-78\text{ }^{\circ}\text{C}$ for 1 h then left to warm to RT. After 2 h, the reaction was quenched with water (5 mL) and diethyl ether (10 mL). The aqueous phase was separated and extracted with diethyl ether (3 x 15 mL). The combined organics were combined, washed with brine (10 mL), dried over MgSO_4 and the solvents removed. The title compound was isolated using flash column chromatography (SiO_2 , 100 % petrol) as a white solid (0.16 g, 0.7 mmol, 65 %). NMR data were identical to literature values.¹³



^1H NMR (note: complicated by 2:1 mixture of diastereomers – only clearly identifiable major and minor resonances identified, 400 MHz, CDCl_3): δ / ppm = 7.71 (1H, d, $J = 6.6$ Hz, Ar), 7.51 (2H, dd, $J = 5.5, 5.5$ Hz, Ar), 7.21-7.38 (5H, m, Ar), 6.92 (1H, d, $J = 5.5$ Hz, CH, major), 6.80 (1H, d, $J = 5.5$ Hz, CH, major) 6.61 (1H, d, $J = 5.5$ Hz, CH, minor) 6.92 (1H, d, $J = 5.5$ Hz, CH, minor), 1.97-2.34 (4H, m, cyclobutyl ring), 0.61-1.82 (11H, m, Cy),

^{13}C NMR (major isomer – all resonances clearly identified from the spectrum of the 2:1 mixture, 100 MHz, CDCl_3): δ / ppm = 150.59 (C), 142.97 (C), 140.27 (CH), 129.58 (CH), 126.47 (CH), 125.00 (CH), 121.58 (CH), 120.87 (CH), 58.87 (C), 49.60 (CH), 42.72 (CH), 30.41 (CH_2), 29.97 (CH_2), 26.92 (CH_2), 26.67 (CH_2), 26.09 (CH_2), 25.73 (CH_2), 22.62 (CH_2).

^{13}C NMR (minor isomer – all resonances clearly identified from the spectrum of the 2:1 mixture, 100 MHz, CDCl_3): δ / ppm = 149.15 (C), 145.21 (CH), 144.51 (C), 128.08 (CH), 126.35 (CH), 124.54 (CH), 122.86 (CH), 121.07 (CH), 58.55 (C), 47.15 (CH), 40.79 (CH), 30.01 (CH_2), 29.45 (CH_2), 26.67 (CH_2), 26.49 (CH_2), 26.00 (CH_2), 25.48 (CH_2), 23.95 (CH_2).

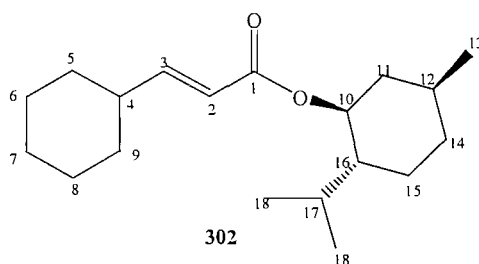
8.3 Experimental for Chapter 3

8.3.1 Synthesis of (*S*)-[3-Cyclohexyl-3-(3*H*-inden-1-yl)-propyl] diphenyl-phosphane, 201.

8.3.1.1. (*E*)-3-Cyclohexyl-acrylic acid 2-isopropyl-5-methyl-cyclohexyl ester, 302.

To a stirred solution of **203** (2.4 g, 16 mmol, 1.0 eq) in dichloromethane (15 mL) at 0 °C and was added oxalyl chloride (2.1 mL, 24 mmol, 1.5 eq) and DMF (3 drops). The reaction was allowed to warm RT. After 2 h the solvents were removed yielding the acid chloride. (2.7 g, 16 mmol, 100 %). To a stirred solution of acid chloride (2.7 g, 16 mmol, 1.0 eq) in benzene (20 mL) was added (1*S*, 2*S*, 5*S*)-(-)-menthol **301** (2.7 g, 18 mmol, 1.1 eq), pyridine (1 mL, 13 mmol, 0.8 eq) dropwise. After refluxing for 16 h, the reaction was cooled and the solvents were removed. The resulting residue was dissolved in dichloromethane (20 mL) and washed with 5 % NaHCO₃ (aq) soln (2 x 20 mL) and 5 % HCl (aq) soln (2 x 20 mL). The combined organics were dried over MgSO₄, and the solvents were removed. The title compound was isolated using flash column chromatography (SiO₂, 2 % diethyl ether/petrol, R_f = 0.2) as a clear oil (2.6 g, 8.9 mmol, 56 %).⁶⁸

$[\alpha]_D^{22} = -88^\circ$ (c = 0.08, CHCl₃).



IR (cm⁻¹ thin film): 2955 (m), 2927 (s), 2855 (m), 1715 (s), 1649 (m), 1450 (m), 1371 (m), 1133 (m), 982 (m), 845 (m).

¹H NMR (300 MHz, CDCl₃): δ / ppm = 6.82 (1H, dd, *J* = 15.8, 6.5 Hz, H3), 5.67 (1H, dd, *J* = 15.8, 1.2 Hz, H2), 4.66 (1H, td, *J* = 10.8, 4.5 Hz, H10), 2.01-2.04 (1H, m, H4), 1.91-1.98 (1H, m, H16), 1.71 (1H, septetd, *J* = 7.0, 2.5 Hz, H17), 1.54-1.74 (8H, m, Cy), 0.91-1.47 (9H, m, Cy), 0.85 (6H, dd, *J* = 7.0, 7.0 Hz, H18), 0.61 (3H, d, *J* = 6.8 Hz, H13).

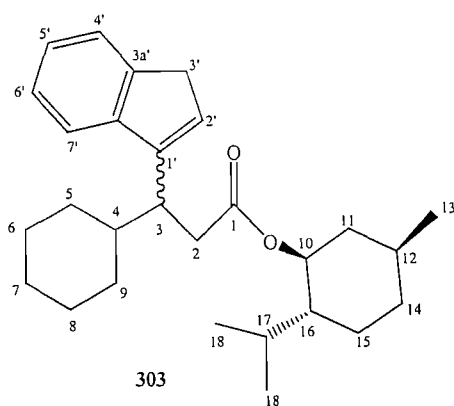
^{13}C NMR (75 MHz, CDCl_3): δ / ppm = 166.46 (C, C1), 153.72 (CH, C3), 118.93 (CH, C2), 75.73 (CH, C10), 46.86 (CH, C16), 41.42 (CH_2 , C11), 40.72 (CH, C4), 34.03 (CH_2 , C14), 31.44 (CH_2 , C5), 31.39 (CH_2 , C9), 31.10 (CH, C17), 26.04 (CH, C12), 25.67 (CH_2 , C7), 25.46 (CH_2 , C15), 23.31 (2 x CH_2 , C6/8), 21.73 (CH_3 , C18), 20.43 (CH_3 , C18), 16.17 (CH_3 , C13).

LRMS (EI): m/z = 293 ($[\text{MH}]^+$, 6%); 154, ($[\text{M}-\text{C}_{10}\text{H}_{18}]^+$, 86%); 81, ($[\text{M}-\text{C}_{13}\text{H}_{22}\text{O}_2]^+$, 100%)

HRMS (EI): $\text{C}_{19}\text{H}_{32}\text{O}_2$ requires 292.2397; found 292.2402.

8.3.1.2. 3-Cyclohexyl-3-(3*H*-inden-1-yl)-propanoyl (1*R*,2*S*,5*R*)-2-isopropyl-5-methyl-cyclohexyl ester, 303.

To a stirred solution of **302**, (0.88 g, 3.0 mmol, 1 eq) and indene (0.7 mL, 6 mmol, 2.0 eq) in THF (5 mL) at 0 °C, and in the dark, was added *sec*-BuLi (1.4M soln in cyclohexanes, 0.21 mL, 0.3 mmol, 10 mol%) dropwise. The reaction was left to warm to RT while stirring. After 1 h, the reaction was quenched with water (5 mL) and diethyl ether (10 mL). The aqueous layer was separated and extracted with diethyl ether (3 x 20 mL). The combined organics were washed with brine (10 mL), dried over MgSO_4 and the solvents removed. The title compound was isolated using flash column chromatography (SiO_2 , 7.5 % diethyl ether/petrol, R_f = 0.23) as a yellow oil and as a 1:1 mixture of diastereomers (0.52 g, 1.3 mmol, 43 %).



IR (cm^{-1} thin film): 2955 (m), 2927 (s), 2855 (m), 1715 (s), 1649 (m), 1450 (m), 1371 (m), 1133 (m), 982 (m), 845 (m).

¹H NMR (note: complicated by 1:1 mixture of diastereomers – only clearly identifiable resonances identified, 300 MHz, CDCl₃): δ / ppm = 7.41-7.45 (3H, m, Ar), 7.29 (3H, m Ar), 7.18 (2H, tt, $J = 7.5, 1.2$ Hz, Ar), 6.23 (1H, t, $J = 2.0$ Hz, H2'), 6.21 (1H, t, $J = 2.0$ Hz, H2'), 4.54 (1H, td, $J = 7.8, 4.2$ Hz, H10), 4.53 (1H, td, $J = 7.8, 4.5$ Hz, H10), 3.32 (2H, d, $J = 2.0$ Hz, H2'), 3.30 (2H, d, $J = 2.0$ Hz, H2'), 3.15-3.26 (2H, m), 2.72 (2H, ddd, $J = 14.8, 10.5, 5.3$ Hz, H2-a), 2.64 (2H, ddd, $J = 15.0, 10.0, 6.5$ Hz, H2-b), 0.83 (3H, d, $J = 6.5$ Hz, H13/18/19), 0.78 (3H, d, $J = 6.5$ Hz, H13/18/19), 0.76 (3H, d, $J = 6.5$ Hz, H13/18/19), 0.63 (3H, d, $J = 6.5$ Hz, H13/18/19), 0.52 (3H, d, $J = 6.5$ Hz, H13/18/19), 0.45 (3H, d, $J = 6.5$ Hz, H13/18/19).

¹³C NMR (note: all resonances clearly identified from the 1:1 mixture, 75 MHz, CDCl₃): δ / ppm = 172.85 (C), 146.10 (C), 145.64 (C), 144.56 (C), 128.86 (CH), 126.05 (CH), 124.62 (CH), 123.83 (CH), 119.89 (CH), 74.12 (CH), 45.85 (CH), 40.50 (CH), 39.74 (CH), 39.29 (CH), 36.73 (CH₂), 36.19 (CH₂), 33.21 (CH₂), 30.27 (CH), 30.14 (CH₂), 29.55 (CH₂), 25.63 (CH₂), 25.52 (CH₂), 25.00 (CH₂), 24.54 (CH₂), 22.26 (CH₂), 20.95 (CH₃), 19.68 (CH₃), 14.99 (CH₃).

¹³C NMR (note: all resonances clearly identified from the 1:1 mixture, 75 MHz, CDCl₃): δ / ppm = 172.85 (C), 146.03 (C), 144.58 (C), 144.52 (C), 128.6 (CH), 126.05 (CH), 124.62 (CH), 123.82 (CH), 119.76 (CH), 74.08 (CH), 45.81 (CH), 40.31 (CH), 39.52 (CH), 38.26 (CH), 36.69 (CH₂), 35.64 (CH₂), 33.19 (CH₂), 30.20 (CH), 29.98 (CH₂), 28.91 (CH₂), 25.57 (CH₂), 25.45 (CH₂), 24.73 (CH₂), 24.49 (CH₂), 21.98 (CH₂), 20.92 (CH₃), 19.57 (CH₃), 14.53 (CH₃).

LRMS (ES): $m/z = 409$ ($[MH]^+$, 8%); 254 , ($[M-C_{10}H_{18}O]^+$, 100%).

HRMS (ES): C₂₈H₄₀O₂ requires 408.6160; found 408.6166.

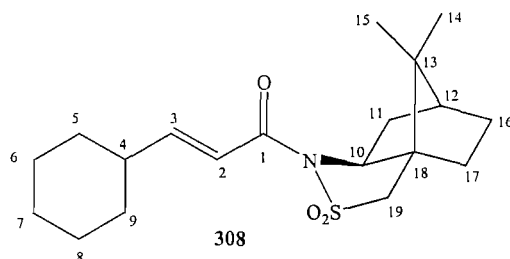
8.3.1.3. N-((*E*)-3-cyclohexyl-acryloyl)-C-(7,7-dimethyl-bicyclo[2.2.1]hept-1-yl)-N-methyl-methanesulfonamide, 308.

To a stirred solution of **203**, (1.2 g, 8 mmol, 1.0 eq) in dichloromethane (15 mL) at 0 °C and under argon was added oxalyl chloride (1.1 g, 12 mmol, 1.5 eq) and DMF (3 drops). The reaction was allowed to warm RT and after 3 h the solvent was removed to yield the acid chloride (1.38 g, 8 mmol, 100 %). To a stirred solution of 60 %

dispersion NaH (0.29 g, 12 mmol, 1.5 eq) in dichloromethane (10 mL) at 0 °C was added sulfonamide, **304** (2.15 g, 10 mmol, 1.25 eq) in dichloromethane (10 mL) dropwise. After stirring for 30 mins acid chloride (1.38 g, 8 mmol, 1.0 eq) in dichloromethane (10 mL) was added slowly at 0 °C. After 12 h at RT the reaction was quenched with NH₄Cl (aq) sat (10 mL) and dichloromethane (20 mL). The aqueous layer was separated and extracted with dichloromethane (3 x 20 mL). The combined organics were dried over MgSO₄ and the solvents removed. The title compound was isolated using flash column chromatography (SiO₂, 25 % diethyl ether/ petrol R_f = 0.3) as a white solid (1.54 g, 4.9 mmol, 55 %).⁷⁶

m.p. = 128-130 °C

X-ray quality crystals were obtained by slow evaporation of an ethanol solution of **308**. Crystallographic analysis has confirmed the structure is as shown (Appendix 1).



IR (cm⁻¹ thin film): 2931 (s), 2855 (m), 1678 (s), 1630 (s), 1450 (m), 1380 (m), 1157 (m), 1053 (m), 780 (m).

¹H NMR (400 MHz, CDCl₃): δ / ppm = 6.95 (1H, dd, *J* = 15.3, 7.0 Hz, H3), 6.42 (1H, dd, *J* = 15.3, 1.5 Hz, H2), 3.83 (1H, dd, *J* = 7.4, 5.3 Hz, H10), 3.40 (2H, dd, *J* = 28.4, 13.8 Hz, H19), 1.98-2.28 (4H, m), 1.75-1.91 (3H, m), 1.62-1.73 (5H, m, Cy), 1.53-1.60 (1H, m) 1.13-1.4 (5H, m, Cy), 1.13 (3H, s, H14/15), 0.92 (3H, s, H14/15).

¹³C NMR (100 MHz, CDCl₃): δ / ppm = 163.07 (C, C1), 154.20 (CH, C3), 117.12 (CH, C2), 63.71 (CH, C10), 51.70 (CH₂, C19), 46.95 (C, C13/18), 46.31 (C, C13/18), 43.26 (CH, C4/12), 39.30 (CH, C4/12), 37.06 (CH₂, C11/17), 31.42 (CH₂, C11/17), 30.17 (CH₂, C5/9), 30.07 (CH₂, C5/9), 25.03 (CH₂, C16), 24.41 (CH₂, C6/7/8), 24.17 (CH₂, C6/7/8), 24.16 (CH₂, C6/7/8), 19.41 (CH₃, C14/15), 18.44 (CH₃, C14/15).

LRMS (CI): *m/z* = 351, ([M]⁺, 42%); 152, ([M-C₉H₁₃NO₂S]⁺, 30%); 137, ([M-C₉H₁₆NO₂S]⁺, 100%);

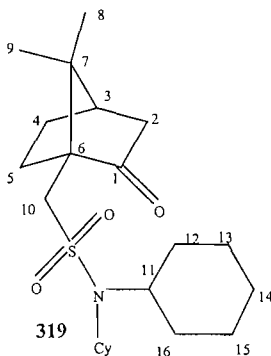
Anal. Calcd. For C₁₉H₂₉NO₃S : C, 64.92; H, 8.32; N, 3.98; Found: C, 64.61; H, 8.65; N, 3.78.

8.3.1.4. (+)-10[(Dicyclohexylamino) sulfonyl]-bornan-6-one, **319**.

To a stirred solution of dicyclohexylamine (8.0 g, 44 mmol, 2.0 eq), pyridine (3.5 g, 44 mmol, 2.0 eq) and DMAP (0.54 g, 4.4 mmol, 0.2 eq) in DMF (50 mL) at 0 °C, was added (1*R*)-(+)-camphor-10-sulfonyl chloride **318** (5.5 g, 22 mmol, 1.0 eq) in DMF (50 mL) slowly. After 12 h at RT the reaction was quenched with 5 % HCl (aq) (20 mL) and dichloromethane (30 mL). The separated aqueous phase was extracted with dichloromethane (3 x 30 mL). The combined organics were dried over MgSO₄ and the solvents removed. The title compound was isolated using flash column chromatography (SiO₂, 30% ether/petrol R_f = 0.3) as a white crystalline solid (4.2 g, 10.6 mmol, 48 %).⁸⁰

m.p. = 133-134 °C; lit. m.p. = 134-135 °C.⁸⁰

Although the synthesis of this compound has been reported previously,⁸⁰ full analysis and detailed NMR assignments have now been obtained and are given here.



IR (cm⁻¹ thin film): 2931 (s), 2860 (m), 1743 (s), 1455 (m), 1389 (w), 1323 (s), 1162 (m), 1049 (m), 850 (m), 741 (m).

¹H NMR (300 MHz, CDCl₃): δ / ppm = 3.30 (1H, d, *J* = 14.2 Hz, H10-a), 3.25-3.33 (2H, m, H11), 2.78 (1H, d, *J* = 14.2 Hz, H10-b), 2.60 (1H, m), 2.36 (1H, 2x t, *J* = 4.0 Hz, 4.0, H3), 1.97-2.06 (2H, m), 1.90 (1H, m), 1.71-1.84 (12H, m, Cy), 1.54-1.62 (3H, m), 1.29-1.39 (5H, m), 1.15 (3H, s, H8/9), 1.08-1.13 (2H, m), 0.8 (3H, s, H8/9).

^{13}C NMR (75 MHz, CDCl_3): δ / ppm = 215.74 (C, C1), 58.98 (C, C6), 57.61 (CH, C11), 52.18 (CH_2 , C10), 47.50 (C, C7), 42.94 (CH, C3), 42.58 (CH_2 , C2), 32.98 (CH_2 , C12/16), 32.52 (CH_2 , C12/16), 26.84 (CH_2 , C5), 26.43 (2 x CH_2 , C13/15), 25.28 (CH_2 , C4), 25.18 (CH_2 , C14), 20.29 (CH_3 , C8/9), 19.87 (CH_3 , C8/9).

LRMS (EI): m/z = 395 ($[\text{M}]^+$, 10%); 215, ($[\text{M}-\text{C}_{12}\text{H}_{22}\text{N}]^+$, 95%); 138, ($[\text{M}-\text{C}_{13}\text{H}_{23}\text{NO}_2\text{S}]^+$, 100%).

HRMS (EI): $\text{C}_{22}\text{H}_{37}\text{NO}_3\text{S}$ requires m/z 395.2493, found 395.2494.

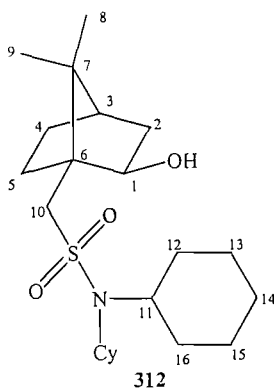
8.3.1.5.(+)-10[(Dicyclohexylamino)sulfonyl]-bornan-6-ol, **312**.

To a stirred solution of **319**, (3.77 g, 8.9 mmol, 1.0 eq) in THF (15 mL) at $-78\text{ }^\circ\text{C}$ was added 1M L-selectride in THF (9.9 mL, 9.9 mmol, 1.1 eq) dropwise. The reaction was stirred at $-78\text{ }^\circ\text{C}$ for 30 mins then left to warm to RT. After 12 h the reaction was cooled to $0\text{ }^\circ\text{C}$ and quenched with slow addition of water (10 mL), ethanol (20 mL), 3M NaOH (10 mL) and 30 % H_2O_2 (aq) (10 mL), followed by saturation of the aqueous phase with K_2CO_3 . The aqueous phase was separated and extracted with diethyl ether:THF (1:1) (3 x 40 mL). The combined organics were then dried over MgSO_4 and the solvents removed yielding title compound as a white solid (3.48 g, 8.8 mmol, 92 %).⁸⁰

m.p. = $162\text{-}163\text{ }^\circ\text{C}$; lit. m.p. = $163\text{-}164\text{ }^\circ\text{C}$.⁸⁰

Although the synthesis of this compound has been reported previously,⁸⁰ full analysis and detailed NMR assignments have now been obtained and are given here.

X-ray quality crystals were obtained by slow evaporation of an ethanol solution of **312**. Crystallographic analysis has confirmed the structure is as shown (Appendix 2).



IR (cm⁻¹ thin film): 3518 (br), 2932 (s), 2850 (m), 1460 (m), 1389 (w), 1313 (s), 1162 (m), 1048 (m), 982 (m).

¹H NMR (300 MHz, CDCl₃): δ / ppm = 4.11 (1H, ddd, J = 8.0, 4.0, 4.0 Hz, H1), 3.50 (1H, d, J = 4.0 Hz, OH), 3.26 (1H, d, J = 13.3 Hz, H10-a), 3.25-3.31 (2H, m, H11), 2.67 (1H, d, J = 13.3 Hz, H10-b), 1.71-1.85 (18H, m), 1.58-1.69 (3H, m), 1.32-1.39 (4H, m), 1.19-1.29 (2H, m), 1.05 (3H, s, H8/9), 0.82 (3H, s, H8/9).

¹³C NMR (75 MHz, CDCl₃): δ / ppm = 76.54 (CH, C1), 57.77 (CH, C11), 55.26 (CH₂, C10), 50.87 (C, C6), 48.47 (C, C7), 44.46 (CH, C3), 38.80 (CH₂, C2), 32.90 (CH₂, C12/16), 32.69 (CH₂, C12/16), 31.00 (CH₂, C5), 27.34 (CH₂, C4), 26.42 (2 x CH₂, C13/15), 25.14 (CH₂, C14), 20.62 (CH₃, C8/9), 19.97 (CH₃, C8/9).

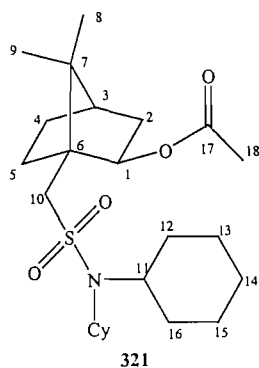
LRMS (EI): m/z = 380 ([M-OH], 8%); 181, ([M-C₁₀H₁₆O₃S]⁺, 92%⁺); 395 ([M], 10%); 138, ([M-C₁₃H₂₃NO₂S]⁺, 100%).

HRMS (EI): C₂₂H₃₉NO₃S requires m/z 397.2650, found 397.2650.

8.3.1.6. (+)-10[(Dicyclohexylamino) sulfonyl]-bornan-6-olmethyl ester, **321**.

To a stirred solution of **312** (0.2 g, 0.5 mmol, 1.0 eq) in pyridine (1 mL) at 0 °C was added DMAP (0.0061 g, 0.05 mol, 10 mol %) and Ac₂O (0.1 g, 1 mmol, 2.0 eq) slowly. The reaction was left to stir while warming to RT. After 16 h, the solvent was removed and the residue was dissolved in water (5 mL) and diethyl ether was added (10 mL). The aqueous layer was separated and extracted with diethyl ether (3 x 10 mL). The combined organics were washed with brine (10 mL), dried over MgSO₄ and the solvents removed. The title compound was isolated using flash column chromatography (SiO₂, 25 % ether/petrol R_f = 0.25) as a white solid. Recrystallization from ethanol afforded the compound as colourless crystals (0.12 g 0.3 mmol, 56 %).
m.p. = 178-179 °C.

X-ray quality crystals were obtained by slow evaporation of an ethanol solution of **321**. Crystallographic analysis has confirmed the structure is as shown (Appendix 3).



IR (cm⁻¹ thin film): 2940 (m), 2855 (s), 1735 (s), 1323 (m) 1143 (m), 1043 (m).

¹H NMR (300 MHz, CDCl₃): δ / ppm = 4.96 (1H, dd, J = 9.2, 3.0 Hz, H1), 3.25 (1H, d, J = 13.2 Hz, H10-a), 3.21-3.31 (2H, m, H11), 2.68 (1H, d, J = 13.2 Hz, H10-b), 2.09 (3H, s, H18), 1.96-2.04 (2H, m), 1.71-1.86 (16H, m), 1.59-1.66 (4H, m), 1.19-1.39 (5H, m), 0.99 (3H, s, H8/9), 0.89 (3H, s, H8/9).

¹³C NMR (75 MHz, CDCl₃): δ / ppm = 169.48 (C, C17), 76.64 (CH, C1), 57.48 (CH, C11), 53.69 (CH₂, C10), 49.31 (C, C6/7), 49.14 (C, C6/7), 44.48 (CH, C3), 39.51 (CH₂, C2), 32.80 (CH₂, C12/16), 32.73 (CH₂, C12/16), 30.08 (CH₂, C5), 27.00 (CH₂, C4), 26.53 (CH₂, C13/15), 26.50 (CH₂, 13/15), 25.20 (CH₂, C14), 21.34 (CH₃, C18), 20.45 (CH₃, C8/9), 20.02 (CH₃, C8/9).

LRMS (CI): m/z = 439 ([M]⁺, 6%); 38 ([M-C₁₅H₂₃NO₄S]⁺, 100%).

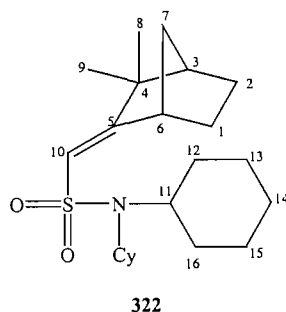
Anal. Calcd. For C₂₄H₄₁NO₄S : C, 65.57; H, 9.40; N, 3.18; Found: C, 65.32; H, 9.53; N, 3.21.

8.3.1.7. N, N-Dicyclohexy-C-[3,3-dimethyl-bicyclo[2.2.1]hept-(2E)-ylidene]methansulfonamide, 322.

To a stirred solution of **203** (0.16 g, 1.0 mmol, 1 eq) in dichloromethane (5 mL) at 0 °C was added oxalyl chloride (0.14 g, 1.52 mmol, 1.5 eq) and DMF (5 drops) slowly. After 2 h the solvent was removed to yield the acid chloride (0.17 g, 1.04 mmol, 100%). To a stirred solution of **312** (0.2 g, 0.5 mmol, 1 eq) in toluene (3 mL) was added AgCN (0.1 g, 0.75 mmol, 1.4 eq), a solution of acid chloride (0.17 g, 1.04 mmol, 2.05 eq) in toluene (1 mL) was added dropwise. After 12 h at reflux, the

reaction was cooled to 0 °C, diethyl ether (10 mL) and 2M NaOH (8 mL) were added and the precipitate collected. The precipitate was then washed with diethyl ether (3 x 20 mL) and the combined organics were washed with brine (10 mL), dried over MgSO₄ and the solvents removed. The title compound was isolated using flash column chromatography (SiO₂, 15 % diethyl ether/petrol, R_f = 0.3) as a white solid (0.15 g, 0.34 mmol, 67 %).

m.p. = 141-142 °C.



IR (cm⁻¹ thin film): 2931 (s), 2855 (s), 1637 (m), 1452 (m), 1315 (m) 1142 (m), 1047 (m), 893 (m), 703 (w).

¹H NMR (300 MHz, CDCl₃): δ / ppm = 5.62 (1H, s, H10), 3.94 (1H, d, *J* = 5.0 Hz, H6), 3.20 (2H, tt, *J* = 9.3, 7.5 Hz, H11), 1.96 (1H, m), 1.71-1.82 (15H, m), 1.63-1.69 (3H, m), 1.61 (1H, 2 x t, *J* = 3.0 Hz, H3), 1.25-1.39 (5H, m), 1.09-1.18 (2H, m) 0.96 (3H, s, H8/9), 0.94 (3H, s, H8/9).

¹³C NMR (75 MHz, CDCl₃): δ / ppm = 169.44 (C, C5), 119.54 (CH, C10), 57.54 (CH, C11), 47.12 (C, C4), 44.22 (CH, 3/6), 42.75 (CH, C3/6), 37.50 (CH₂, C7), 32.91 (CH₂, C12/16), 32.77 (CH₂, C12/16), 28.52 (CH₃, C8/9), 27.58 (CH₂, C1/2/4), 26.73 (2 x CH₂, C13/15), 25.59 (CH₃, C8/9), 25.47 (CH₂, C1/2/4), 23.56 (CH₂, C1/2/4).

LRMS (CI): *m/z* = 380 ([MH]⁺, 22%); 259, ([M-C₉H₁₂]⁺, 100%).

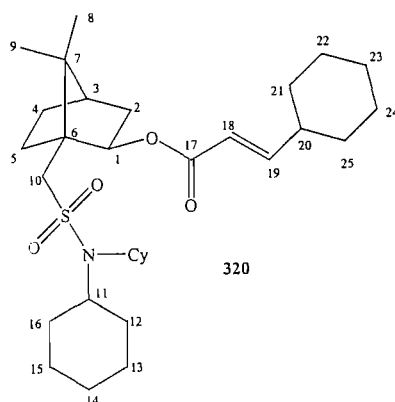
Anal. Calcd. For C₂₂H₃₇NO₂S : C, 69.61; H, 9.82; N, 3.69; Found: C, 69.68; H, 10.09; N, 3.59.

8.3.1.8. (*E*)-3-cyclohexyl-acrylic acid 1-[(dicyclohexylsulfonamyl)-methyl]-7,7-dimethyl-bicyclo[2.2.1]hept-2-yl ester, 320.

To a stirred solution of **203** (0.16 g, 1.04 mmol, 1 eq) in dichloromethane (5 mL) 0 °C was added oxalyl chloride (0.14 g, 1.52 mmol, 1.5 eq) and DMF (5 drops) slowly. The reaction was allowed to warm RT and after 2 h solvent was removed yielding the acid chloride (0.17 g, 1.04 mmol, 100 %). To a stirred solution of **312** (0.2 g, 0.5 mmol, 1 eq) in toluene (3 mL) was added AgCN (0.31 g, 2.29 mmol, 2.2 eq). A solution of acid chloride (0.17 g, 1.04 mmol, 2.05 eq) in toluene (1 mL) was added dropwise. After 2 h at reflux the reaction was cooled to 0 °C. Diethyl ether (10 mL) and 2M NaOH (8 mL) were added and the precipitate was filtered off. The precipitate was then washed with diethyl ether (3 x 20 mL) and the combined organics were washed with brine (10 mL), dried over MgSO₄ and the solvents removed. The title compound was isolated using flash column chromatography (SiO₂, 10 % diethyl ether/petrol, R_f = 0.1) as a white solid (0.12 g, 0.21 mmol, 55 %).

m.p. = 141-142 °C.

X-ray quality crystals were obtained by slow evaporation of an ethanol solution of **320**. Crystallographic analysis has confirmed the structure is as shown (Appendix 4).



IR (cm⁻¹ thin film): 2926 (s), 2851 (m), 1720 (m), 1654 (m), 1445 (m), 1328 (m), 1167 (m), 1134 (m), 1049 (m), 892 (w), 731 (m).

¹H NMR (400 MHz, CDCl₃): δ / ppm = 6.86 (1H, dd, *J* = 15.8, 6.3 Hz, H19), 5.66 (1H, dd, *J* = 15.8, 1.2, H18), 4.98 (1H, dd, *J* = 8.8, 5.6 Hz, H1), 3.21 (1H, d, *J* = 13.3 Hz, H10-a), 3.16 (2H, tt, *J* = 9.3, 7.5, Hz, H11), 2.61 (1H, d, *J* = 13.3 Hz, H10-b),

2.01-2.09 (1H, m), 1.87-1.97 (2H, m), 1.61-1.72 (20H, CH on Cy), 1.51-1.59 (3H, m), 1.04-1.15 (12H, m, CH on Cy), 0.95 (3H, s, CH₃ on C8/9), 0.82 (3H, s, CH₃ on C8/9).

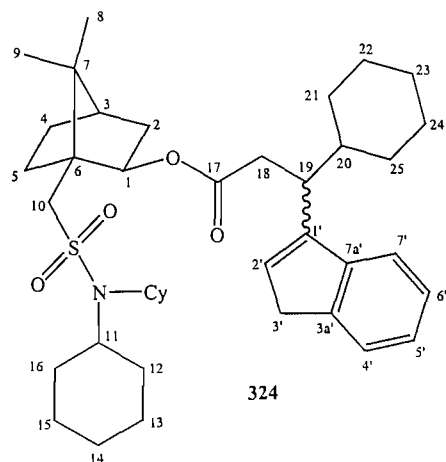
¹³C NMR (100 MHz, CDCl₃): δ / ppm = 164.50 (C, C17), 153.09 (CH, C19), 117.98 (CH, C18), 77.10 (CH, C1), 56.45 (CH, C11), 52.61 (CH₂, C10), 48.41 (C, C6/7), 48.10 (C, C6/7), 43.58 (CH, C3), 39.50 (CH, C20), 38.52 (CH₂, C2), 31.82 (CH₂, C12/16), 31.75 (CH₂, C12/16), 30.81 (CH₂, C21/25), 30.59 (CH₂, C21/25), 28.85 (CH₂, C5), 26.02 (CH₂, C4), 25.51 (2 x CH₂, C13/15), 24.95 (CH₂, C22/23/24), 24.78 (CH₂, C22/23/24), 24.73 (CH₂, 22/23/24), 24.19 (CH₂, C14), 19.50 (CH₃, C8/9), 19.09 (CH₃, C8/9).

LRMS (CI): *m/z* = 533 ([M]⁺, 12%); 138, ([M-C₂₁H₃₇O₃S]⁺, 100%).

Anal. Calcd. For C₃₁H₅₁NO₄S : C, 69.75; H, 9.63; N, 2.62; Found: C, 69.44; H, 9.82; N, 2.64.

8.3.1.9. 3-Cyclohexyl-3-(3*H*-inden-1-yl)-propionic acid 1-[(dicyclohexylsulfamoyl)-methyl]-7,7-dimethyl-bicyclo[2.2.1]hept-2-yl ester, 324.

To a stirred solution of **320** (0.24 g, 0.5 mmol, 1 eq) and indene (0.17 g, 1.5 mmol, 3.0 eq) in THF (4 mL) at 0°C and in the dark, was added *sec*-BuLi (1.4M soln in cyclohexanes, 0.1 mL, 0.1 mmol, 20 mol%) was added slowly. The reaction was cooled to 0 °C for 15 mins then left to warm to RT while stirring. After 3 h, the reaction was quenched with water (5 mL) and diethyl ether (10 mL). The aqueous layer was separated and extracted with diethyl ether (3 x 20 mL). The combined organics were washed with brine (10 mL), dried over MgSO₄ and the solvents removed. The title compound was isolated using flash column chromatography (SiO₂, 5 % diethyl ether/petrol, R_f = 0.15) as a yellow oil (0.11 g, 0.2 mmol, 37 %).



IR (cm⁻¹ thin film): 3057 (w), 2931 (s), 2859 (m), 1714 (m), 1654 (m), 1445 (m), 1328 (m), 1175 (m), 1123 (m), 1057 (m), 724 (m).

¹H NMR (note: complicated by 1:1 mixture of diastereomers – only clearly identifiable resonances identified, 300 MHz, CDCl₃): δ / ppm = 7.38-7.46 (3H, m, Ar), 7.28 (3H, t, J = 7.5 Hz, Ar), 7.19 (2H, t, J = 7.5 Hz, Ar), 6.24 (1H, br. s, H2'), 6.18 (1H, br. s, H2'), 4.86 (2H, 2x dd, J = 9.0, 6.0 Hz, H1), 3.24 (2H, br. s, H3'), 3.30 (2H, br s, H3'), 3.15-3.26 (2H, m), 2.61-2.79 (4H, m, H18).

¹³C NMR (note: all resonances clearly identified from the 1:1 mixture, 75 MHz, CDCl₃): δ / ppm = 171.65 (C), 146.05 (C), 145.18 (C), 144.49 (C), 128.61 (CH), 125.88 (CH), 124.50 (CH), 123.74 (CH), 119.83 (CH), 78.45 (CH), 57.51 (2 x CH), 53.74 (CH₂), 49.26 (C), 48.99 (C), 44.90 (CH), 41.01 (CH), 40.89 (CH₂), 39.95 (CH₂), 37.71 (CH₂), 36.32 (CH₂), 32.86 (2 x CH₂), 32.77 (2 x CH₂), 31.24 (CH₂), 30.29 (CH₂), 30.03 (CH₂), 25.23 (CH₂), 20.40 (CH₃), 19.89 (CH₃).

Note: 3 x CH₂ carbons (*ca.* 26.5 ppm) could not be unambiguously distinguished owing to broadening of their signals in this compound.

¹³C NMR (note: all resonances clearly identified from the 1:1 mixture, 75 MHz, CDCl₃): δ / ppm = 171.42 (C), 145.66 (C), 144.93 (C), 144.46 (C), 128.59 (CH), 125.75 (CH), 124.42 (CH), 123.70 (CH), 119.58 (CH), 78.42 (CH), 57.51 (2 x CH), 53.69 (CH₂), 49.18 (C), 48.97 (C), 44.30 (CH), 40.97 (CH), 40.86 (CH₂), 39.32 (CH₂), 37.60 (CH₂), 36.32 (CH₂), 32.81 (2 x CH₂), 32.70 (2 x CH₂), 31.18 (CH₂), 30.19 (CH₂), 29.87 (CH₂), 25.18 (CH₂), 20.37 (CH₃), 19.64 (CH₃).

Note: 3 x CH₂ carbons (*ca.* 26.5 ppm) could not be unambiguously distinguished owing to broadening of their signals in this compound.

LRMS (ES⁺): *m/z* = 650 (M+H, 100 %); 672 (M+Na, 39%)⁺;

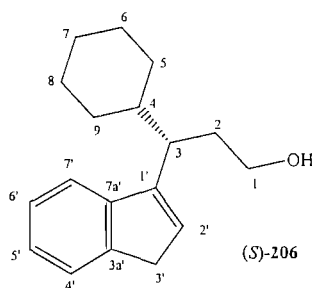
HRMS (ES): C₄₀H₅₉NO₄S requires *m/z* 650.4245, found 650.4250. (MH)⁺

8.3.1.10. (*S*)-3-cyclohexyl-3-(1*H*-3-indenyl) propanol, 206.

To a stirred solution of LiAlH₄ (0.2 g, 0.45 mmol, 3.0 eq) in diethyl ether (3 mL) at 0 °C was added **324** (0.1 g, 0.15 mmol, 1.0 eq) in diethyl ether (5 mL) slowly. The reaction was left to warm to RT. After 4 h, the reaction was cooled to 0 °C, and water (5 mL) was added very carefully (vigorous evolution of hydrogen gas). Diethyl ether (10 mL) was added slowly followed by further water (5 mL). The quenched reaction mixture was stirred at RT for 30 mins, resulting in a pale yellow suspension. The suspension was filtered through celite (washed thoroughly with diethyl ether), then dried over MgSO₄, and the solvents removed. The title compound was isolated using flash column chromatography (SiO₂, 40 % diethyl ether/petrol, R_f = 0.35) as a yellow oil which solidified on standing (0.03 g, 0.12 mmol, 78 %).

NMR data were identical to literature values (Section 8.2.1.6).¹³

HPLC analysis of the alcohol, Chiracel OD-H column 10% IPA / hexanes, 1 mL / min with retention times 27.7 and 31.9 (major enantiomer) minutes gave a 6% e.e.

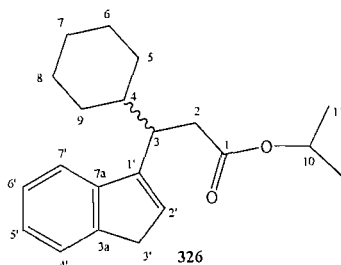


8.3.1.11. (*S*) or (*R*) Isopropyl 3-cyclohexyl-3-(1*H*-3-indenyl) propanoate, 326.

To a stirred solution of indene (0.23 mL, 2 mmol, 2.0 eq), and **214** (0.2 g, 1 mmol, 1.0 eq) in THF (4 mL), at 0 °C and in the dark was added (-)-sparteine (0.11 mL, 0.5 mmol, 0.5 eq) and *sec*-BuLi (1.4M soln in cyclohexanes, 0.14 mL, 0.2 mmol, 10 mol%) dropwise. The reaction was left to warm to RT. After 4 h the reaction was quenched with water (10 mL) and diethyl ether (20 mL) was added. The aqueous

layer was separated and extracted with diethyl ether (3 x 20 mL). The combined organics were washed with brine (10 mL), dried over MgSO₄, and the solvents removed. The title compound was isolated from the crude mixture by first applying high vacuum (1 mmHg) to remove excess indene, then performing flash column chromatography (SiO₂, 5 % diethyl ether/petrol, R_f = 0.4) to yield the title compound as a yellow oil (0.18 g, 0.6 mmol, 58 %).

NMR data were identical to literature values (Section 8.2.1.4).

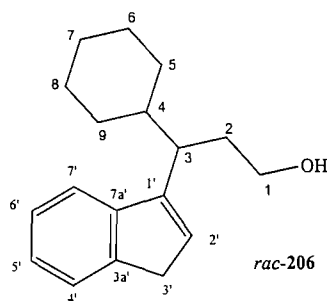


8.3.1.12. *rac*- 3-Cyclohexyl-3-(1*H*-3-indenyl) propanol, 206.

To a stirred solution of LiAlH₄ (0.07 g, 1.8 mmol, 3.0 eq) in diethyl ether (3 mL) at 0 °C and under argon was added **326** (0.18 g, 0.6 mmol, 1.0 eq) in diethyl ether (5 mL) slowly. The reaction was left to warm to RT while stirring. After 2 h, the reaction was cooled to 0 °C, and water (5 mL) was added very carefully (vigorous evolution of hydrogen gas). Diethyl ether (10 mL) was added slowly followed by further water (5 mL). The quenched reaction mixture was stirred at RT for 30 minutes, resulting in a pale yellow suspension. The suspension was filtered through celite (washed thoroughly with diethyl ether), dried over MgSO₄, and the solvents removed. The title compound was isolated using flash column chromatography (SiO₂, 40 % diethyl ether/petrol, R_f = 0.35) as a yellow oil which solidified on standing (0.12 g, 0.5 mmol 80 %).

NMR data was identical to literature values (Section 8.2.1.6).¹³

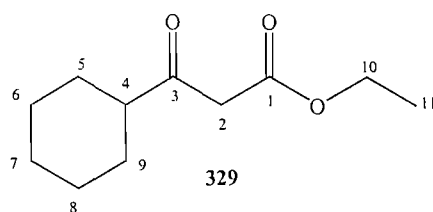
HPLC analysis of the alcohol, Chiracel OD-H column 10% IPA / hexanes, 1 mL / min with retention times 27.7 and 31.9 minutes gave a 0% e.e.



8.3.1.13. 3-Cyclohexyl-3-oxo-propionic acid ethyl ester, 329.

To a stirred solution of 2,2-dimethyl-1,3-dioxane-4,6-dione (30.0 g, 0.21 mol, 1.0 eq) in dichloromethane (100 mL) at 0 °C was added pyridine (32.9 g, 0.42 mol, 2.0 eq) slowly, and the reaction was stirred for 10 minutes. Cyclohexane carbonyl chloride (33.3 mL, 0.25 mol, 1.2 eq) was then added dropwise and the reaction was left to stir at 0 °C for 1 h and then at RT. After 2 h the reaction was then quenched with water (50 mL) and 2M HCl (50 mL). The aqueous phase was separated and extracted with dichloromethane (3 x 50 mL). The combined organics were dried over MgSO₄ and the solvents removed. The residue was then dissolved in ethanol (100 mL) and heated to reflux. After 14 h the reaction was cool to RT and the solvents removed. The title compound was isolated by flash column chromatography (SiO₂, 10 % ether/petrol, R_f = 0.15) and Kugelrohr distillation (80 °C, 11 mmHg) as a yellow oil (23.60 g, 0.12 mol, 57 %).⁶⁸

NMR data were identical to literature values.¹³⁸



IR (cm⁻¹): 2983 (m), 2932 (s), 2586 (s), 1743 (s), 1708 (s), 1646 (m), 1623 (m), 1450 (m), 1220 (s), 733 (w).

¹H NMR (300 MHz, CDCl₃): δ / ppm = 4.17 (2H, q, *J* = 7.1 Hz, H10), 3.30 (2H, s, H2), 2.44 (1H, m, H4), 1.51-1.79 (5H, m, Cy), 1.08-1.21 (5H, m, Cy), 1.16 (3H, t, *J* = 7.1 Hz, H11).

^{13}C NMR (75 MHz, CDCl_3): δ / ppm = 205.85 (C, C3), 167.46 (C, C1), 61.20 (CH_2 , C10), 50.84 (CH, C4), 47.31 (CH_2 , C2), 28.15 (2 x CH_2 , C5/9), 25.69 (CH_2 , C7), 25.44 (2 x CH_2 , C6/8), 14.06 (CH_3 , C11).

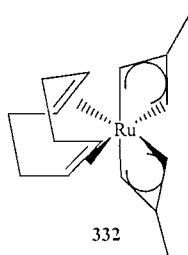
LR-MS (CI): m/z = 199 ($[\text{M}+\text{H}]^+$, 100%); 111 ($[\text{M}-\text{C}_4\text{H}_6\text{O}_2]^+$, 43%).

8.3.1.14. (η^4 -1,5-cyclooctadiene)bis(η^3 -2-methylallyl)ruthenium(II), 332.

To a stirred solution of $[\text{RuCl}_2(\text{COD})]_x$ (0.5 g, 1.8 mmol, 1.0 eq) in diethyl ether (5mL) was added 2-methylallylmagnesium chloride (0.5 M, 20 mL, 10.8 mmol, 6.0 eq) slowly. After stirring at RT for 2 h, diethyl ether (15 mL) was added and the reaction mixture was filtered through celite (washed thoroughly with diethyl ether). The filtrate was then hydrolysed in ice-water (50 mL). The aqueous layer was separated and extracted with diethyl ether (3 x 30 mL). The combined organics were dried over MgSO_4 , filtered through a short column of neutral alumina and the solvents removed. Recrystallisation from methanol and petrol (1:1) gave the title compound as a brown solid (0.42 g, 1.3 mmol, 74 %).⁹⁹

m.p. = 82-83°C; lit. m.p. = 80-85°C.⁹⁹

NMR data were identical to literature values.⁹⁹



^1H NMR (300 MHz, C_6D_6): δ / ppm = 4.01 (2H, dd, J = 8.9, 5.5 Hz, CH- of COD), 3.52 (2H, d, J = 2.1 Hz, syn-H of Me-allyl), 2.90 (2H, s, anti H of Me-allyl), 2.65-3.0 (4H, m, CH_2 of COD), 1.72 (6H, s, CH_3 of Me-allyl), 1.59 (2H, s, syn- H of Me-allyl), 1.45-1.70 (4H, m, CH_2 of COD), 1.11-1.26 (2H, m, CH of COD), 0.25 (2H, s, anti-H of Me-allyl).

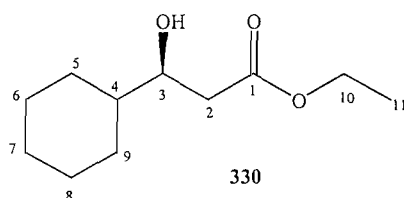
8.3.1.15. (*R*)-3-Cyclohexyl-3-hydroxy-propionic acid ethyl ester, 330.

R-(+)-BINAP (6 mg, 0.01 mmol, 1 mol %) and RuCl₃.nH₂O (2 mg, 0.01 mmol, 1 mol%) were placed in a bomb, and degassed by three cycles of vacuum/argon at RT. 3-Cyclohexyl-3-oxo-propionic acid ethyl ester **329**, (0.2 g 1 mmol, 1.0 eq) in degassed EtOH (2 mL) was then added. After 20 h at 50 °C, and 4-5 atm H₂, the reaction was cooled to RT. The title compound was isolated by flash column chromatography (SiO₂, 25 % ether/petrol, R_f = 0.15) a yellow oil (0.13 g, 0.65 mmol, 65%).⁹³

[α]²²_D = -27.8 ° (c = 0.01, CHCl₃). Lit [α]¹⁹_D = +27.8 (c = 0.01, CHCl₃)(opposite enantiomer).¹³⁹

HPLC analysis of the hydroxy ester, Chiracel OD-H column 5 % IPA / hexanes, 1 mL / min with retention times 7.3 (major enantiomer) and 11.2 (minor enantiomer) minutes gave a 99 % e.e.

NMR data were identical to literature values.¹⁴⁰



IR (cm⁻¹): 3489 (br), 2988 (m), 2921 (s), 2855 (s), 1729 (s), 1445 (m).

¹H NMR (300 MHz, CDCl₃): δ / ppm = 4.11 (2H, q, *J* = 7.1 Hz, H10), 3.70 (1H, ddd, *J* = 9.0, 6.0, 3.1 Hz, H3), 2.85 (1H, br s, OH), 2.44 (1H, dd, *J* = 16.3, 3.1 Hz, H2-a), 2.33 (1H, dd, *J* = 16.3, 9.0 Hz, H2-b), 1.51-1.69 (5H, m, Cy), 0.95-1.19 (6H, m, Cy), 1.19 (3H, t, *J* = 7.1 Hz, H11).

¹³C NMR (75 MHz, CDCl₃): δ / ppm = 173.66 (C, C1), 72.27 (CH, C3), 60.76 (CH₂, C10), 43.19 (CH, C4), 38.71 (CH₂, C2), 28.91 (CH₂, C5/9), 28.37 (CH₂, C5/9), 26.53 (CH₂, C6/7/8), 26.27 (CH₂, C6/7/8), 26.16 (CH₂, C6/7/8), 14.28 (CH₃, C11).

LR-MS (EI): *m/z* = 201 ([M+H]⁺, 88%⁺); 183 ([MH-OH]⁺, 100%).

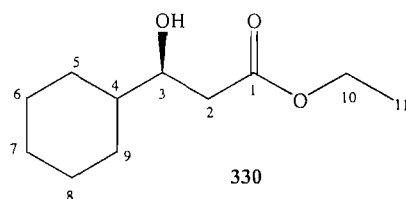
8.1.3.16. (*R*)-3-Cyclohexyl-3-hydroxy-propionic acid ethyl ester, 330.

To a mixture of *R*-(+)-BINAP (0.075 g, 0.12 mmol, 0.4 mol%) and (Cod)Ru(2-methylallyl)₂ **332**, (0.04 g, 0.12 mmol, 0.4 mol%) was added degassed acetone (2 mL). Methanolic HBr solution (1.1 mL, 0.27 M, 0.3 mmol) was then added and after 30 mins at RT a yellow solid precipitated. The solvent was removed and the catalyst used immediately. Degassed ethanol (2 mL) was added and the catalyst was transferred to the bomb and degassed by three cycles of vacuum/argon at RT. A solution of 3-Cyclohexyl-3-oxo-propionic acid ethyl ester, **329** (6 g, 0.03 mol, 1.0 eq) in degassed ethanol (2 mL) was added dropwise to the bomb. After 20 h at 50 °C, and 4-5 atm H₂, the reaction was cooled to RT. The title compound was isolated by flash column chromatography (SiO₂, 25% ether/petrol, R_f = 0.15) a yellow oil (4.85 g, 0.024 mol, 81 %).¹⁰²

$[\alpha]_{\text{D}}^{22} = -27.8^{\circ}$ (c = 0.01, CHCl₃). Lit $[\alpha]_{\text{D}}^{19} = +27.8^{\circ}$ (c = 0.01, CHCl₃)(opposite enantiomer).¹³⁹

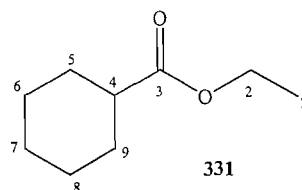
HPLC analysis of the hydroxy ester, Chiracel OD-H column 5 % IPA / hexanes, 1 mL / min with retention times 7.3 (major enantiomer) and 11.2 (minor enantiomer) minutes gave a 99 % e.e.

NMR data were identical to literature values (Section 8.3.1.15).¹⁴⁰



8.3.1.17 Cyclohexanecarboxylic acid ethyl ester, 331.

The product from the ruthenium catalysed aldol condensation.



NMR data were identical to literature values.¹⁴¹

$^1\text{H NMR}$ (300 MHz, CDCl_3): δ / ppm = 4.06 (2H, q, $J = 7.0$ Hz, H2), 2.20 (1H, tt, $J = 11.3, 7.3$ Hz, H4), 1.76-1.72 (1H, m), 1.48-1.56 (1H, m), 1.25-1.42 (2H, m), 1.07-1.21 (6H, m), 1.08 (3H, t, $J = 7.0$ Hz, H1).

$^{13}\text{C NMR}$ (75 MHz, CDCl_3): δ / ppm = 176.53 (C, C3), 60.40 (CH_2 , C2), 43.65 (CH, C4), 29.43 (2 x CH_2 , C5/9), 26.19 (CH_2 , C7), 25.86 (2 x CH_2 , C6/8), 14.63 (CH_3 , C1).

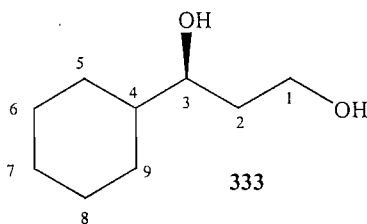
LR-MS (EI): $m/z = 157$ ($[\text{MH}]^+$, 100% $^+$); 141 ($[\text{M}-\text{CH}_3]^+$, 18%).

8.3.1.18. (*R*)-Cyclohexyl-propane-1,3-diol, 333.

To a stirred solution of LiAlH_4 (1.2 g, 31 mmol, 1.5 eq) in diethyl ether (20 mL) at 0 °C was added, (*R*)-3-Cyclohexyl-3-hydroxy-propionic acid ethyl ester, 330 (4.2 g, 21 mmol, 1.0 eq) in diethyl ether (20 mL) dropwise. The reaction was then left to stir at 0 °C then allowed to warm to RT. After 1 h the reaction was cooled to 0 °C, and water (10 mL) was added very carefully (vigorous evolution of hydrogen gas). Diethyl ether (20 mL) was then added and the mixture was left to stir for a further 30 mins. The white precipitate formed was filtered off and washed with diethyl ether (3 x 50 mL). The combined organics were then dried over MgSO_4 and the solvents removed. The title compound was isolated using flash column chromatography (SiO_2 , 80 % diethyl ether/petrol, $R_f = 0.2$) as a colourless oil (2.9 g, 18 mmol, 87 %).

$[\alpha]_{\text{D}}^{22} = -8.25^\circ$ ($c = 0.05$, CHCl_3) Lit $[\alpha]_{\text{D}}^{19} = 8.25$ ($c = 0.01$, CHCl_3).¹⁴²

NMR data were identical to literature values.¹⁴³



IR (cm^{-1} thin film): 3352 (br), 2922 (s), 2851 (s), 1451 (m), 1086 (w), 968 (w), 888 (m).

¹H NMR (300 MHz, CDCl₃): δ / ppm = 3.83 (1H, ddd, *J* = 23.0, 11.0, 5.0, H1-a), 3.82 (1H, ddd, *J* = 23.0, 11.0, 5.0, H1-b), 3.58 (1H, ddd, *J* = 9.0, 5.9, 3.1, H3), 3.30 (2H, br s, 2x OH), 1.61-1.89 (8H, m), 1.03-1.49 (5H, m, Cy).

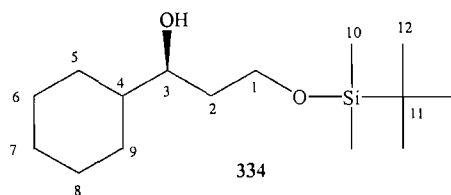
¹³C NMR (75 MHz, CDCl₃): δ / ppm = 76.45 (CH, C3), 61.95 (CH₂, C1), 43.98 (CH, C4), 35.05 (CH₂, C2), 28.84 (CH₂, C5/9), 28.15 (CH₂, C5/9), 26.78 (CH₂, C6/7/8), 26.21 (CH₂, C6/7/8), 26.11 (CH₂, C6/7/8).

LRMS (EI): *m/z* = 159, ([M+H]⁺, 38%); 141, ([M-OH]⁺, 100%); 123, ([M-(OH)₂]⁺, 21%).

8.3.1.19. (*R*)- 3-(*tert*-Butyl-dimethyl-silanloxy)-1-cyclohexyl-propan-1-ol, 334.

To a stirred solution of imidazole (4.9 g, 72 mmol, 4.0 eq) in THF (20 mL) at 0 °C was added *tert*-butyldimethylsilyltrifluoromethanesulphonate (4.13 mL, 18 mmol, 1.0 eq) slowly. (*R*)-Cyclohexyl-propane-1,3-diol, **333** (2.9 g, 18 mmol, 1.0 eq) in THF (20 mL) was then added dropwise. The reaction was then left to stir at 0 °C and after 1 h the reaction was quenched with water (10 mL) and left to stir for 30 minutes. Diethyl ether (20 mL) was then added and the aqueous phase was separated and extracted with diethyl ether (3 x 20 mL). The combined organics were then washed with brine (10 mL), dried over MgSO₄ and the solvents removed. The title compound was isolated by flash column chromatography (SiO₂, 10 % diethyl ether/petrol, *R_f* = 0.2) as a colourless oil (4.2 g, 15 mmol, 86 %).

[α]²²_D = -6.67 ° (*c* = 0.06, CHCl₃).



IR (cm⁻¹ thin film): 3456 (br), 2954 (m), 2931 (s), 2855 (m), 1450 (m), 1252 (m), 1091 (s), 935 (m), 774 (m).

¹H NMR (300 MHz, CDCl₃): δ / ppm = 3.82 (1H, ddd, *J* = 10.0, 6.0, 5.0 Hz, H1-a), 3.72 (1H, ddd, *J* = 10.0, 7.3, 5.0 Hz, H1-b), 3.48 (1H, dtd, *J* = 6.0, 6.0, 2.0 Hz, H3),

3.20 (1H, d, $J = 2.0$ Hz, OH), 1.73-1.82 (2H, m, H2), 1.53-1.69 (5H, m, Cy), 0.95-1.25 (6H, m, Cy), 0.82 (9H, s, H12), 0.01 (6H, s, H10).

^{13}C NMR (75 MHz, CDCl_3): δ / ppm = 75.38 (CH, C3), 62.19 (CH_2 , C1), 42.87 (CH, C4), 34.38 (CH_2 , C2), 27.94 (CH_2 , C5/9), 27.25 (CH_2 , C5/9), 25.63 (CH_2 , C6/7/8), 25.37 (CH_2 , C6/7/8), 25.26 (CH_2 , C6/7/8), 24.87 ($(\text{CH}_3)_3$, C12), 17.12 (C, C11), -6.53 (CH_3 , C10), -6.54 (CH_3 , C10).

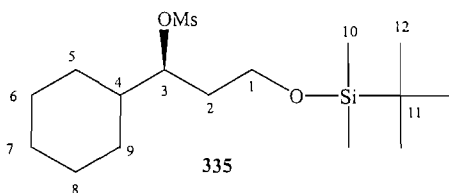
LRMS (CI): $m/z = 273$, ($[\text{M}+\text{H}]^+$, 34%); 189, ($[\text{MH}-\text{C}_6\text{H}_{10}]^+$, 89%); 123, ($[\text{M}+\text{H}-\text{C}_6\text{H}_{17}\text{O}_2\text{Si}]^+$, 100%).

HRMS (CI): $\text{C}_{15}\text{H}_{32}\text{O}_2\text{Si}$ requires m/z 273.2251, found 273.2250 ($\text{M}+\text{H}$) $^+$

8.3.1.20 Methansulfonic acid (*R*)-3-(*tert*-butyl-dimethyl-silanoxy)-1-cyclohexyl-propyl ester, 335.

To a stirred solution of (*R*)-3-(*tert*-Butyl-dimethyl-silanoxy)-1-cyclohexyl-propan-1-ol, **334** (4.2 g, 15 mmol, 1.0 eq) in dichloromethane (30 mL) at 0 °C was added triethylamine (3.3 mL, 24 mmol, 1.6 eq). After 15 mins, methanesulfonyl chloride (1.6 mL, 21 mmol, 1.4 eq) was added dropwise and the reaction was left to stir while warming to RT. After 3 h the reaction was quenched with water (10 mL) and dichloromethane (30 mL). The organic phase was separated and extracted with NaHCO_3 (aq. sat) (3 x 30 mL). The combined organics were then washed with brine (10 mL), dried over MgSO_4 and the solvents removed yielding the title compound as a colourless oil. (5.10 g, 14 mmol, 97 %). No further purification was attempted, as this intermediate was found to be unstable to silica gel chromatography, and was found to be unstable to storage at -20 °C for more than 24 h.

$[\alpha]_D^{22} = -33.6^\circ$ ($c = 0.06$, CHCl_3).

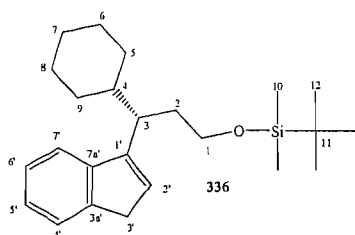


¹H NMR (300 MHz, CDCl₃): δ / ppm = 4.72 (1H, dt, *J* = 5.5, 5.5 Hz, H3), 3.71 (2H, m, H1), 3.03 (3H, s, CH₃ on OMs), 1.61-1.89 (8H, m), 1.03-1.23 (5H, m), 0.82 (9H, s, H12), 0.01 (6H, s, H10).

¹³C NMR (75 MHz, CDCl₃): δ / ppm = 85.15 (CH, C3), 58.77 (CH₂, C1), 41.85 (CH, C4), 38.20 (CH₃, OMs), 33.89 (CH₂, C2), 28.17 (CH₂, C5/9), 28.03 (CH₂, C5/9), 25.67 (CH₂, C6/7/8), 26.05 (CH₂, C6/7/8), 25.99 (CH₂, C6/7/8), 25.85 ((CH₃)₃, C12), 18.16 (C, C11), -5.34 (CH₃, C10), -5.39 (CH₃, C10).

8.3.1.21. *tert*-Butyl-[(*S*)-3-cyclohexyl-3-(3H-inden-1-yl)-propoxy]-dimethyl-silane, 336.

To a stirred solution of indene (4.0 mL, 35 mmol, 2.5 eq) in THF (30 mL) at -78 °C was added *n*-BuLi (2.5M soln in cyclohexanes, 10 mL, 25 mmol, 1.8 eq) slowly. HMPA (8.7 mL, 50 mmol, 3.6 eq) was added dropwise and the reaction was left to stir at -78 °C for 30 mins. Methansulfonic acid (*R*)-3-(*tert*-butyl-dimethyl-silanloxy)-1-cyclohexyl-propyl ester, **335** (5.0 g, 14 mmol, 1.0 eq) in THF (20 mL) was added dropwise and the reaction left to stir at -78 °C for 30 mins then left to warm to RT. After 2 h the reaction was quenched with water (20 mL) and diethyl ether (30 mL). The aqueous phase was separated and extracted with diethyl ether (3 x 30 mL). The combined organics were then washed with brine (10 mL), dried over MgSO₄ and the solvents removed. The title compound was isolated by flash column chromatography (SiO₂, 30 % diethyl ether/petrol, *R*_f = 0.25) as a yellow oil (3.9 g, 10 mmol, 77 %). [α]_D²² = +45 ° (c = 0.06, CHCl₃).



IR (cm⁻¹ thin film): 3058 (w), 2950 (m), 2931 (s), 2851 (m), 1604 (w), 1455 (w), 1256 (m), 1095 (s), 831 (m), 764 (m).

¹H NMR (300 MHz, CDCl₃): δ / ppm = 7.47 (1H, d, J = 7.4 Hz, H4'/7'), 7.41 (1H, d, J = 7.4 Hz, H4'/7'), 7.30 (1H, td, J = 7.4, 1.1 Hz, H5'/6'), 7.21 (1H, td, J = 7.4, 1.1 Hz, H5'/6'), 6.10 (1H, t, J = 2.2 Hz, H2'), 3.58 (1H, ddd, J = 10.0, 8.8, 4.8. H1-a), 3.47 (1H, m, H1-b), 3.36 (2H, d, J = 2.2 Hz, H2'), 2.70 (1H, ddd, J = 10.0, 5.5, 3.4 Hz, H3), 1.82-2.01 (2H, m, H2), 1.53-1.72 (6H, m, Cy), 1.09-1.21 (5H, m, Cy), 0.95 (9H, s, t-Bu), -0.02 (3H, s, H10), -0.10 (3H, s, H10).

¹³C NMR (75 MHz, CDCl₃): δ / ppm = 146.35 (C, C1'/3a/7a), 145.75 (C, C1'/3a/7a), 144.70 (C, C1'/3a/7a), 128.47 (CH, 4'/5'/6'/7'), 124.29 (CH, C4'/5'/6'/7'), 124.44 (CH, C4'/5'/6'/7'), 123.71 (CH, C4'/5'/6'/7'), 119.77 (CH, C2'), 62.06 (CH₂, C1), 41.35 (CH, C3/4), 40.35 (CH, C3/4), 37.65 (CH₂, C3'), 33.66 (CH₂, C2), 31.26 (CH₂, C5/9), 30.53 (CH₂, C5/9), 26.69 (CH₂, C6/7/8), 26.63 (2 x CH₂, C6/7/8), 25.97 ((CH₃)₃, C12), 18.29 (C, C11), -5.33 (2 x CH₃, C10).

LRMS (CI): m/z = 371 ([M+H]⁺, 72%); 313 ([M+H-C₄H₉]⁺, 38%); 239 ([M+H-C₆H₁₅OSi]⁺, 100%).

HRMS (CI): C₂₄H₃₈OSi requires m/z 371.2765; found 371.2770.[M+H]⁺

8.3.1.22. (*S*)-3-cyclohexyl-3-(3H-inden-1-yl) propanol, 206.

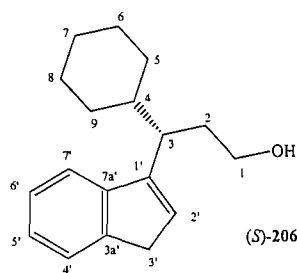
To a stirred solution of *tert*-Butyl-[(*S*)-3-cyclohexyl-3-(3H-inden-1-yl)-propoxy]-dimethyl-silane, **336**, (3.9 g, 10 mmol, 1.0 eq) in THF (10 mL) was added TBAF (1M in THF (10 mL, 10 mmol, 1.0 eq) dropwise at RT. After 2 h the reaction was quenched with water (10 mL) and diethyl ether (20 mL). The aqueous phase was separated and extracted with diethyl ether (3 x 20 mL). The combined organics were washed with brine (10 mL), dried over MgSO₄ and solvents removed. The title compound was isolated by flash column chromatography (SiO₂, 40 % diethyl ether/petrol, R_f = 0.35) as a yellow oil which solidified on standing (2.0 g, 7.7 mmol, 77 %). Recrystallisation from hot hexanes gave white crystals.

NMR data were identical to literature values (Section 8.2.1.6).¹³

m.p. = 61-62 °C lit. m.p. = 62-63 °C.¹³

$[\alpha]_D^{22} = +28.2^\circ$ (c = 0.01, CHCl₃).

HPLC analysis, Chiracel OD-H column 2% IPA / hexanes, 1 mL / min with retention times 31.1 (minor enantiomer) and 35.6 (major enantiomer) gave a 98 % e.e.

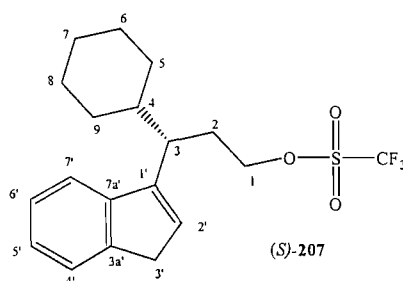


8.3.1.23. (S)-Trifluoro-methansulfonic acid (S)-3-cyclohexyl-3-(3*H*-inden-1-yl)-propyl, 207.

To a stirred solution of trifluoromethanesulfonic anhydride (1.2 mL, 7.2 mmol, 1.15 eq) in dichloromethane (25 mL) at 0°C was added a solution of (S)- 3-cyclohexyl-3-(3*H*-inden-1-yl) propanol, **206** (1.60 g, 6.2 mmol, 1 eq) and pyridine (0.5 g, 6.25 mmol, 1 eq) in dichloromethane (15 mL) dropwise. After 2 h the reaction was quenched with the addition of water (10 mL) and dichloromethane (15 mL). The aqueous layer was separated and extracted with dichloromethane (3 x 20 mL). The combined organics were combined, dried over MgSO₄ and the solvents removed yielding the product as a light green oil (2.00 g, 5.2 mmol, 85 %) The title compound was used without further purification.

NMR data were identical to literature values (Section 8.2.1.7).¹³

$[\alpha]_D^{22} = +48.9^\circ$ (c = 0.01, CHCl₃).



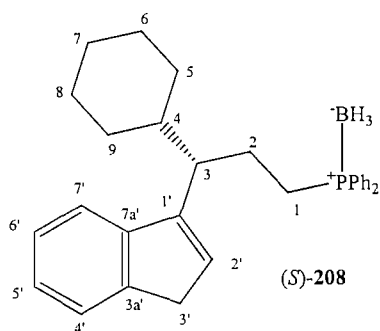
8.3.1.24. (S)-[3-Cyclohexyl-3-(3*H*-inden-1-yl)-propyl]diphenyl-phosphine-borane complex, 208.

To a stirred solution of diphenylphosphineborane **218** (1.25 g, 6.25 mmol, 1.0 eq) in THF (5 mL) at 0 °C was added *n*-BuLi (2.5M soln in cyclohexanes, 2.5 mL, 6.25 mmol, 1.0 eq) dropwise and then left to warm to RT. After 2 h, it was added dropwise

via cannula to a stirred solution of trifluoromethanesulfonic acid (*S*)-3-cyclohexyl-3-(3*H*-inden-1-yl)-propyl, (*S*)-**207**, (2.00 g, 5.2 mmol, 1.0 eq) in THF (10 mL) at 0 °C. After 2 h the reaction was quenched with water (10 mL) and diethyl ether (30 mL). The aqueous phase was separated and extracted with diethyl ether (3 x 20 mL). The combined organic phases were washed with brine (20 mL), dried over MgSO₄ and the solvents removed. The title compound was isolated by flash column chromatography (SiO₂, 5 % diethyl ether/petrol, R_f = 0.3) as a yellow solid. Recrystallisation from hot hexanes gave the title compound as a white solid (1.78 g, 4 mmol, 65 %).

NMR data were identical to literature values (Section 8.2.1.9).¹³

$[\alpha]_D^{22} = +22.2^\circ$ (c = 0.01, CHCl₃).

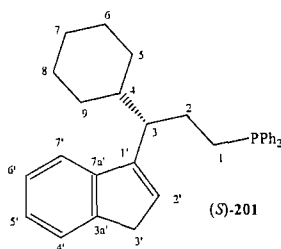


8.3.1.25. (*S*)-[3-Cyclohexyl-3-(3*H*-inden-1-yl)-propyl]diphenyl-phosphine, **201**.

(*S*)-[3-Cyclohexyl-3-(3*H*-inden-1-yl)-propyl]diphenyl-phosphine-borane complex, (*S*)-**208** (1.9 g, 4.3 mmol, 1.0 eq) was treated with an excess of neat diethylamine (10 mL), and warmed to reflux. After 3 h, TLC indicated no borane protected phosphine and only free phosphine present. The reaction was then cooled and evacuated to dryness, leaving (*S*)-**201** as an air-sensitive oil. (1.65 g, 3.9 mmol, 90 %). The title compound was used without further purification.

NMR data were identical to literature values (Section 8.2.1.10).¹³

$[\alpha]_D^{22} = +26^\circ$ (c = 0.02, CHCl₃).



8.4. Experimental for Chapter 4

8.4.1. Synthesis of Ruthenium complexes

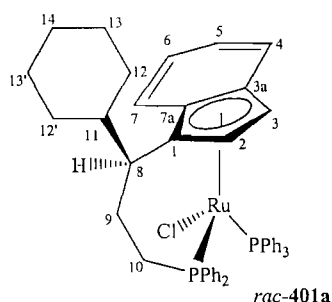
8.4.1.1. *rac*-($\eta^5:\eta^1$)-Indenyl-CH(Cy)CH₂CH₂PPh₂Ru^{II} (PPh₃)Cl, 401 .

rac-3-Cyclohexyl-3-(3*H*-inden-1-yl)-propyl]diphenyl-phosphane **201** (1.6 g, 4.5 mmol, 1.0 eq) was dissolved in toluene (10 mL) and cooled to -78 °C. *n*-BuLi (2.5 M solution in cyclohexanes, 2.0 mL, 4.9 mmol, 1.1 eq) was added dropwise, in the dark, and the reaction was stirred at -78 °C for 15 mins. The reaction was then allowed to warm to RT and stirred for 2 h. This was then added *via* cannula to a suspension of dichlorotris(triphenylphosphine)ruthenium(II) (5.1 g, 5.4 mmol, 1.2 eq) in toluene at -60 °C.

The dark mixture was stirred at -60 °C for 15 mins and then warmed to reflux. After 72 h, the reaction was cooled to room temperature and the solvents removed. Purification of the complex was achieved by column chromatography (45 % ether/petrol, neutral Al₂O₃), which provided both diastereomers of the complex. The major isomer was collected as a dark-red solid (1.9 g, 2.3 mmol, 52 %, $R_f = 0.5$) m.p. 170-172 °C(dec). lit. m.p. 168-171 °C.¹³ The minor diastereomer was collected as a red/brown solid (0.6 g, 0.72 mmol, 16 %, $R_f = 0.1$). m.p. 179-181 °C (dec). lit. m.p. 179-182 °C.¹³

NMR data were identical to literature values.¹³

Major diastereomer: *rac*-401a



IR (cm⁻¹ thin film): 3034 (m), 2914 (m), 2850 (s), 1479 (m), 1433 (s), 1329 (w), 1262 (w), 1092 (m), 812 (s).

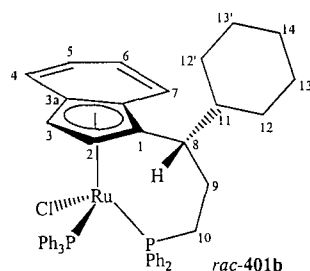
¹H NMR (400 MHz, C₆D₆): δ / ppm = 7.75 (1H, d, $J = 8.8$ Hz, Ar), 7.54-7.63 (7H, m, Ar), 7.33 (2H, dd, $J = 8.0, 7.0$ Hz, Ar), 7.21-7.31 (2H, m, Ar), 7.19 (3H, dd +

fs, $J = 7.0, 7.0$ Hz, Ar), 6.98-7.04 (10H, m, Ar), 6.87 (1H, dd, $J = 7.0, 7.0$ Hz, Ar), 6.83 (1H, d + fs, $J = 7.0$ Hz, Ar), 6.71 (2H, dd + fs, $J = 7.5, 7.5$ Hz, Ar), 4.65 (1H, dd, $J = 5.0, 2.2$ Hz, Cp-H), 3.90 (1H, dddd, $J = 13.0, 13.0, 7.0, 2.0$ Hz, H9-a), 3.60 (1H, br. d, $J = 12.0$ Hz, H9-b), 3.36 (1H, br. s, Cp-H), 2.65 (1H, ddd, $J = 14.8, 14.8, 5.5$ Hz, H10-a), 2.10 (1H, dddd, $J = 36.4, 14.8, 3.0, 3.0$ Hz, H10-b), 1.46-1.55 (6H, m, Cy), 0.95-1.16 (6H, m, Cy).

^{13}C NMR (100 MHz, C_6D_6): δ / ppm = 139.29 (C, d, $J = 35.0$ Hz, *i*-Ph), 137.90 (C, d, $J = 43.2$ Hz, *i*-Ph(PPh_3)₃), 137.46 (C, d, $J = 39.0$ Hz, *i*-Ph), 134.09 (CH, d, $J = 10.9$ Hz, *o*-Ph (PPh_3)₃), 133.67 (CH, d, $J = 7.8$ Hz, *o*-Ph), 133.33 (CH, d, $J = 10.1$ Hz, *o*-Ph), 130.34 (CH, d, $J = 2.4$ Hz, *p*-Ph), 128.77 (CH, d, $J = 2.4$ Hz, *p*-Ph), 128.67 (CH, s, C4/5/6/7), 128.56 (CH, d, $J = 1.2$ Hz, *p*-Ph (PPh_3)₃), 128.27 (CH, d, $J = 9.0$ Hz, *m*-Ph), 128.00 (CH, d, $J = 9.0$ Hz, *m*-Ph (PPh_3)₃), 127.59 (CH, d, $J = 9.0$ Hz, *m*-Ph), 126.21 (CH, s, C4/5/6/7), 126.11 (CH, s, C4/5/6/7), 124.33 (CH, s, C4/5/6/7), 111.05 (C, s, C3a), 105.93 (C, d, $J = 7.3$ Hz, C7a), 84.57 (CH, s, C2), 75.46 (C, d, $J = 13.6$ Hz, C1), 64.77 (CH, s, C3), 46.08 (CH, d, $J = 5.0$ Hz, C11), 40.46 (CH, d, $J = 2.4$ Hz, C8), 30.98 (CH_2 , s, C12/12'), 30.87 (CH_2 , s, C12/12'), 30.31 (CH_2 , d, $J = 34.5$ Hz, C10), 27.47 (CH_2 , s, C13/13'/14), 27.41 (CH_2 , s, C13/13'/14), 27.10 (CH_2 , s, C13/13'/14), 26.62 (CH_2 , s, C9).

^{31}P NMR (121 MHz, C_6D_6): 48.02 (d, $J = 35.6$ Hz), 38.12 (d, $J = 35.6$ Hz).

Minor diastereomer: *rac*-401b



IR (cm^{-1} thin film): 3031 (m), 2924 (s), 2851 (m), 1478 (m), 1430 (s), 1337 (w), 1261 (w), 1089 (m), 816 (s).

^1H NMR (400 MHz, C_6D_6): δ / ppm = 7.49-7.62 (7H, m, Ar), 7.40 (1H, d, $J = 8.5$ Hz, Ar), 7.18 (1H, dd, $J = 7.0, 7.0$ Hz, Ar), 7.09-7.16 (6H, m, Ar), 6.81-6.92 (10H,

Ar), 6.42 (2H, dd, $J = 8.5, 7.8$ Hz, Ar), 6.38 (2H, dd, $J = 8.5, 7.0$ Hz, Ar), 4.73 (1H, dd, $J = 5.0, 2.2$ Hz, Cp-H), 4.21 (1H, dd, $J = 5.0, 2.2$ Hz, Cp-H), 2.54 (1H, ddd, $J = 13.8, 13.8, 5.3$ Hz, H9-a), 1.97 (1H, dddd, $J = 35.0, 13.8, 2.4, 2.4$ Hz, H9-b), 1.81 (1H, dd, $J = 12.5, 12.3$ Hz, H10-a), 1.72 (1H, br. d, $J = 13.2$ Hz, H8), 1.62 (1H, dddd, $J = 13.5, 13.5, 2.5, 2.5$ Hz, H10-b), 1.43 (1H, br. d, $J = 14.0$ Hz, H11), 1.06-1.39 (5H, m, Cy), 0.71-1.01 (5H, m, Cy).

^{13}C NMR (100 MHz, C_6D_6): δ / ppm = 140.01 (C, d $J = 31.0$ Hz, *i*-Ph), 138.95 (C, d, $J = 43.0$ Hz, *i*-Ph), 138.46 (C, d, $J = 39.2$ Hz, *i*-Ph (PPh_3)₃), 135.64 (CH, d, $J = 9.4$ Hz, *o*-Ph), 135.08 (CH, d, $J = 9.7$ Hz, *o*-Ph (PPh_3)₃), 132.33 (CH, d, $J = 8.7$ Hz, *o*-Ph), 129.53 (CH, d, $J = 2.4$ Hz, *p*-Ph (PPh_3)₃), 129.25 (CH, d, $J = 4.0$ Hz, *p*-Ph), 128.68 (CH, s, C4/5/6/7), 128.63 (CH, d, $J = 4.3$ Hz, *p*-Ph), 128.49 (CH, d, $J = 9.7$ Hz, *m*-Ph), 128.18 (CH, d, $J = 8.3$ Hz, *m*-Ph), 127.84 (CH, d, $J = 9.7$ Hz, *m*-Ph (PPh_3)₃), 124.46 (CH, s, C4/5/6/7), 123.82 (CH, s, C4/5/6/7), 123.23 (CH, s, C4/5/6/7), 117.95 (C, d, $J = 2.8$ Hz, C3a), 100.98 (C, d, $J = 8.5$ Hz, C7a), 81.87 (CH, s, C2), 71.30 (CH, d, $J = 2.9$ Hz, C3), 69.42 (C, d, $J = 14.1$ Hz, C1), 42.95 (CH, s, C11), 41.30 (CH, s, C8), 30.78 (CH₂, s, C12/12'), 30.43 (CH₂, s, C12/12'), 29.10 (CH₂, d, $J = 36.1$ Hz, C10), 25.33 (CH₂, s, C13/13'/14), 25.27 (CH₂, s, C13/13'/14), 25.21 (CH₂, s, C13/13'/14), 24.20 (CH₂, s, C9).

^{31}P NMR (121 MHz, C_6D_6): 56.63 (d, $J = 42.2$ Hz), 26.10 (d, $J = 41.2$ Hz)

8.4.1.2. (*S*)-(η^5 : η^1)-Indenyl-CH(Cy)CH₂CH₂PPh₂Ru^{II} (PPh₃)Cl, 401.

(*S*)-3-Cyclohexyl-3-(3*H*-inden-1-yl)-propyl]diphenyl-phosphane **201** (1.6 g, 3.7 mmol, 1.0 eq) was dissolved on toluene (5 mL) and cooled to -78 °C. *n*-BuLi (2.5 M solution in cyclohexanes, 1.7 mL, 4.2 mmol, 1.1 eq) was added dropwise, in the dark, and the reaction was stirred at -78 °C for 15 mins. The reaction was then allowed to warm to RT and stirred for 2 h. This was then added *via* cannula to a suspension of dichlorotris(triphenylphosphine)ruthenium(II) (4.34 g, 4.5 mmol, 1.2 eq) in toluene at -60 °C.

The dark mixture was stirred at -60 °C for 15 mins and then warmed to reflux. After 72 h, the reaction was cooled to RT and the solvents removed.

Purification of the complex was achieved by column chromatography (45 % ether/petrol, neutral Al₂O₃), which provided both diastereomers of the complex. The major isomer was collected as a dark-red solid (1.55 g, 1.9 mmol, 51 %, R_f = 0.5). m.p. 169-171 °C (dec). The minor diastereomer was collected as a red/brown solid (0.49 g, 0.6 mmol, 16 %, R_f = 0.1) m.p. 179-181 °C (dec).

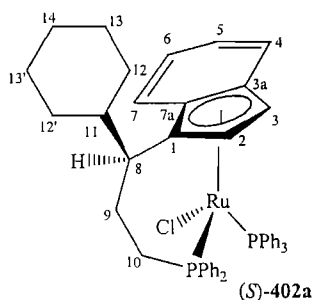
NMR data were identical to literature values (Section 8.4.1.1).¹³

The major isomer was crystallised by slow diffusion of hexane into a solution in benzene, over 2 weeks at RT and in the dark. The minor isomer was crystallised by slow diffusion of pentane into a solution in benzene, over 16 h at RT and in the dark. X-ray crystallography has confirmed the structures of the major and minor isomers (See appendices 5 and 6).

Major diastereomer: (*S*)-401a

$[\alpha]_D^{22} = -6.28^\circ$ (c = 0.05, CHCl₃).

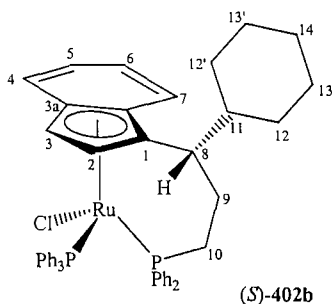
Anal. Calcd. For C₄₈H₄₇ClP₂Ru: C, 70.11; H, 5.76. Found C, 70.22; H, 6.02



Minor diastereomer: (*S*)-401b

$[\alpha]_D^{22} = -6.33^\circ$ (c = 0.045, CHCl₃).

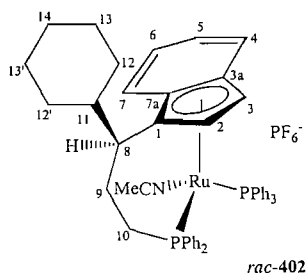
Anal. Obtained for major isomer, see above.



8.4.1.3. *rac*-($\eta^5:\eta^1$)-Indenyl-CH(Cy)CH₂CH₂PPh₂)Ru^{II} (PPh₃)MeCN⁻[PF₆⁻], 402.

To a mixture of *rac*-($\eta^5:\eta^1$)-1-(1-cyclohexyl-3-diphenylphosphinopropyl)(chloro)(triphenylphosphine)ruthenium, **401a** (1.57 g, 1.9 mmol, 1.0 eq) and ammonium hexafluorophosphate (0.37 g, 2.3 mmol, 1.2 eq) was added acetonitrile (10 mL). The brown reaction was heated to reflux for 3 h, after which it had turned red. The reaction was cooled to RT and the solvents removed. The crude was dissolved in fresh acetonitrile and filtered through a plug of cotton wool under argon. The solvents were then removed giving a bright red solid. Recrystallisation from hot acetonitrile gave the title complex as yellow crystals (1.62 g, 1.66 mmol, 87 %).¹⁰⁸
m.p. 221-223 °C (dec)

X-ray quality crystals were obtained by slow diffusion of hexane into a solution in acetonitrile, over 48 h at RT and in the dark. Crystallographic analysis has confirmed the structure is as shown (Appendix 7).



IR (cm⁻¹ thin film): 3237 (w), 3060 (w), 2925 (m), 2581 (m), 1611 (w), 1481 (m), 1434 (s), 1268 (w), 1092 (m), 840 (s), 740 (m), 697 (m).

¹H NMR (400 MHz, CD₃CN): δ / ppm = 7.46 (1H, dd+fs, J = 8.5, 6.5 Hz, Ar), 7.36 (1H, dddd+fs, J = 6.8, 6.8, 2.2, 2.2 Hz, Ar), 7.33 (1H, d, J = 8.5 Hz, Ar), 7.17-7.23 (5H, m, Ar), 7.03-7.13 (9H, m, Ar), 6.95 (2H, ddd, J = 7.5, 7.5, 2.5 Hz, Ar), 6.75-6.85 (7H, m, Ar), 6.69 (2H, dd+fs, J = 8.0, 8.0 Hz, Ar), 6.38 (1H, d, J = 8.5 Hz, Ar), 4.42 (1H, dd, J = 2.7, 2.7 Hz, Cp-H), 4.14 (1H, dd, J = 2.0, 2.0 Hz, Cp-H), 3.01 (1H, br.d, J = 12.0 Hz, H8), 2.83 (1H, ddd, J = 14.8, 14.8, 6.0 Hz, H9-a), 2.75 (1H, dddd, J = 27.1, 14.8, 2.5, 2.5 Hz, H9-b), 2.09-2.21 (2H, H10), 1.88 (3H, s, CH₃), 1.32-1.59 (5H, m, Cy), 0.75-1.09 (6H, m, Cy).

¹³C NMR (100 MHz, CD₃CN): δ / ppm = 137.52 (C, d, J = 39.9 Hz, *i*-Ph), 135.85 (C, d, J = 39.4 Hz, *i*-Ph(PPh₃)₃), 133.79 (CH, d, J = 11.2 Hz, *o*-Ph), 132.86 (C, d, J = 48.1 Hz, *i*-Ph), 132.38 (CH, d, J = 10.7 Hz, *o*-Ph (PPh₃)₃), 130.85 (CH, d, J = 8.3 Hz, *o*-Ph), 130.58 (CH, d, J = 2.4 Hz, *p*-Ph), 129.62 (CH, s, C4/5/6/7), 129.47 (CH, d, J = 2.4 Hz, *p*-Ph), 128.97 (CH, d, J = 1.9 Hz, *p*-Ph (PPh₃)₃), 128.14 (C, d, J = 9.7 Hz, *m*-Ph), 128.04 (C, d, J = 10.2 Hz, *m*-Ph), 127.87 (CH, d, J = Hz, *m*-Ph(PPh₃)), 126.34 (CH, s, C4/5/6/7), 126.32 (CH, s, C4/5/6/7), 120.16 (CH, s, C4/5/6/7), 117.01 (CN), 108.81 (C, d, J = 2.9 Hz, C3a), 102.69 (C, d, J = 2.9 Hz, C7a), 84.28 (CH, s, C2), 77.10 (C, d, J = 11.7 Hz, C1), 68.48 (CH, s, C3), 44.78 (CH, d, J = 3.9 Hz, C11), 39.73 (CH, s, C8), 29.93 (CH₂, s, C12/12'), 29.70 (CH₂, s, C12/12'), 29.64 (CH₂, d, J = 34.5 Hz, C10), 26.03 (CH₂, s, C13/13'/14), 26.00 (CH₂, s, C13/13'/14), 28.83 (CH₂, s, C13/13'/14), 24.47 (CH₂, s, C9), 2.8 (CH₃, s, CH₃).

³¹P NMR (121 MHz, CD₃CN): 44.15 (d, J = 30.0 Hz), 40.41 (d, J = 30.0 Hz), -144.39 (heptet, J = 707 Hz).

¹⁹F NMR (282 MHz, CD₃CN): -72.86 (d, J = 707 Hz).

LRMS (ES⁺): (MeCN): m/z = 828, ([M-PF₆]⁺, 30%); 787, ([M-PF₆-MeCN]⁺, 100%).

Anal. Calcd. For C₅₀H₅₀P₂RuNPF₆: C, 61.73; H, 5.18; N, 1.44. Found C, 61.97; H, 5.54; N, 1.42.

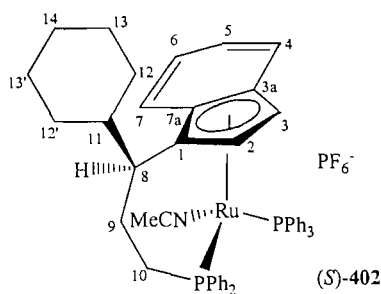
8.4.1.4. (*S*)-(η⁵:η¹)-Indenyl-CH(Cy)CH₂CH₂PPh₂Ru¹¹(PPh₃) MeCN⁻[PF₆⁻], 402.

A mixture of (*S*)-(η⁵:η¹)-Indenyl-CH(Cy)CH₂CH₂PPh₂Ru¹¹(PPh₃)Cl, **401a**, (0.07 g, 0.08 mmol, 1.0 eq) and ammonium hexafluorophosphate (0.016 g, 0.1 mmol, 1.2 eq) was added acetonitrile (4 mL). The brown reaction was heated to reflux for 3 h, after which it had turned red. The reaction was cooled to RT and the solvents removed. The crude was dissolved in fresh acetonitrile and filtered through a plug of cotton wool under argon. The solvents were then removed giving a bright red solid. Recrystallisation from hot acetonitrile gave the title complex as yellow crystals (0.078 g, 0.08 mmol, 95 %).

$[\alpha]_D^{22} = -6.85^\circ$ ($c = 0.02$, CHCl₃).

m.p. 220-222 °C (dec).

NMR data were identical to previous values (Section 8.4.1.3).

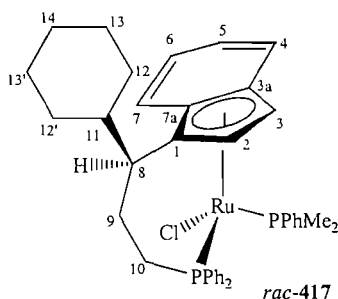


8.4.1.5. *rac*-($\eta^5:\eta^1$)-Indenyl-CH(Cy)CH₂CH₂PPh₂Ru^{II} (Me₂PPh)Cl, 417.

To a stirred solution of *rac*-($\eta^5:\eta^1$)-1-(1-cyclohexyl-3-diphenylphosphinopropyl)(chloro)(triphenylphosphine)ruthenium, **401a** (0.1 g, 0.12 mmol, 1 eq) in toluene (5 mL) was added dimethylphenylphosphine (0.09 mL, 0.36 mmol, 3 eq) dropwise and the reaction heated to reflux. After 2 h, the reaction was cooled to RT and the solvent removed. The title complex was isolated using flash column chromatography (Al₂O₃, 40% ether/ petrol, R_f = 0.26) as a red solid (0.4 g, 0.6 mmol, 40 %).

m.p. = 125-127 °C.

X-ray quality crystals were obtained by slow diffusion of hexane into a solution in benzene, over 72 h at RT and in the dark. Crystallographic analysis has confirmed the structure is as shown (Appendix 8).



IR (cm⁻¹ thin film): 3051 (w), 2922 (m), 2581 (m), 1604 (w), 1454 (w), 1433 (m), 1275 (w), 1096 (m), 940 (s), 904 (s), 810 (s).

¹H NMR (400 MHz, C₆D₆): δ / ppm = 7.59-7.64 (2H, m, Ar), 7.39-7.51 (6H, m, Ar), 7.22-7.31 (6H, m, Ar), 7.06-7.10 (3H, m, Ar), 6.80 (2H, d, *J* = 8.6 Hz, Ar), 4.25 (1H, s, Cp-H), 4.21 (1H, s, Cp-H), 3.24-3.33 (2H, m, H9), 2.70 (1H, td, *J* = 14.6, 5.7, H10-a), 2.08 (1H, dddd, *J* = 34.0, 14.5, 2.8, 2.8 Hz, H10-a), 1.78 (1H, br.d, *J* = 12.0

Hz, H8), 1.51-1.64 (6H, m, Cy), 1.35 (3H, d, $J = 8.3$ Hz, CH₃), 1.16 (3H, d, $J = 8.3$ Hz, CH₃), 0.95-1.09 (5H, m, Cy).

¹³C NMR (100 MHz, C₆D₆): δ / ppm = 145.13 (C, d, $J = 34.9$ Hz, *i*-Ph), 141.19 (C, d, $J = 39.1$ Hz, *i*-Ph), 137.34 (C, d, $J = 43.0$ Hz, *i*-Ph), 135.05 (CH, d, $J = 8.3$ Hz, *o*-Ph), 133.85 (2 x CH, d, $J = 8.7$ Hz, *o*-Ph), 129.77 (CH, s, *p*-Ph), 129.69 (CH, s, *p*-Ph), 129.32 (CH, s, *p*-Ph), 128.62 (CH, d, $J = 9.2$ Hz, *m*-Ph), 128.54 (CH, d, $J = 7.8$ Hz, *m*-Ph), 128.31 (CH, s, C4/5/6/7), 128.00 (CH, d, $J = 8.3$ Hz, *m*-Ph), 126.32 (CH, s, C4/5/6/7), 124.40 (CH, s, C4/5/6/7), 132.12 (CH, s, C4/5/6/7), 112.57 (C, d, $J = 3.3$ Hz, C3a), 104.39 (C, d, $J = 7.1$ Hz, C7a), 82.21 (CH, s, C2), 75.84 (C, d, $J = 12.9$ Hz, C1), 61.12 (CH, s, C3), 46.22 (CH, d, $J = 5.0$ Hz, C11), 41.06 (CH, d, $J = 2.0$ Hz, C8), 31.50 (CH₂, s, C12/12'), 30.80 (CH₂, s, C12/12'), 30.10 (CH₂, d, $J = 32.6$ Hz, C10), 27.40 (CH₂, s, C13/13'/14), 27.38 (CH₂, s, C13/13'/14), 27.11 (CH₂, s, C13/13'/14), 26.92 (CH₂, s, C9), 17.69 (CH₃, d, $J = 29.2$ Hz, CH₃), 16.01 (CH₃, d, $J = 25.3$ Hz, CH₃).

³¹P NMR (121 MHz, C₆D₆): 51.35 (d, $J = 39.0$ Hz), 11.97 (d, $J = 39.0$ Hz).

LRMS (ES⁺): (MeCN): $m/z = 698$, ([M]⁺, 100 %).

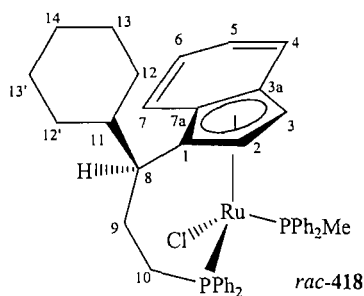
Anal. Calcd. For C₃₈H₄₃P₂RuCl: C, 65.37; H, 6.21. Found C, 65.04; H, 6.57.

8.4.1.6. *rac*-(η^5 : η^1)-Indenyl-CH(Cy)CH₂CH₂PPh₂Ru^{II} (MePPh₂)Cl, 418.

To a stirred solution of *rac*-(η^5 : η^1)-1-(1-cyclohexyl-3-diphenylphosphinopropyl)(chloro)(triphenylphosphine)ruthenium, **401** (0.125 g, 0.15 mmol, 1.0 eq) in toluene (5 mL) was added methyldiphenyl phosphine (0.09 g, 0.46 mmol, 3.0 eq) dropwise and the reaction was heated to reflux. After 2 h, the reaction was cooled to RT and the solvent removed. The title complex was isolated using flash column chromatography (Al₂O₃, 30% ether/ petrol, $R_f = 0.32$) as a red solid (0.07 g, 0.09 mmol, 58 %).

m.p. = 143-144 °C.

X-ray quality crystals were obtained by slow diffusion of hexane into a solution in benzene, over 36 h at RT and in the dark. Crystallographic analysis has confirmed the structure is as shown (Appendix 9).



IR (cm⁻¹ thin film): 3051 (w), 2923 (m), 2582 (m), 1605 (w), 1482 (w), 1433 (s), 1265 (w), 1096 (m), 889 (m), 808 (w), 702 (s).

¹H NMR (400 MHz, C₆D₆): δ / ppm = 7.62-7.69 (3H, m, Ar), 7.52-7.57 (3H, m, Ar), 7.26-7.34 (5H, m, Ar), 7.01-7.19 (11H, m, Ar), 6.80 (1H, dd, J = 7.5, 7.5 Hz, Ar), 6.67 (1H, d = fs, J = 8.0 Hz, Ar), 4.28 (1H, dd, J = 5.3, 2.1 Hz, Cp-H), 4.19 (1H, d = fs, J = 1.5 Hz, Cp-H), 3.59-3.64 (2H, H10), 2.70 (1H, ddd, J = 14.8, 14.8, 5.7 Hz, H-10a), 2.12 (1H, dddd, J = 36.0, 14.3, 3.0, 3.0 Hz, H10-b), 1.55-1.70 (7H, m), 1.01-1.11 (5H, m), 1.00 (3H, d, J = 8.5 Hz, CH₃).

¹³C NMR (100 MHz, C₆D₆): δ / ppm = 141.57 (C, d, J = 39.4 Hz, *i*-Ph), 139.64 (C, d, J = 36.9 Hz, *i*-Ph), 137.70 (C, d, J = 32.6 Hz, *i*-Ph), 135.05 (C, d, J = 45.7 Hz, *i*-Ph), 133.00 (CH, d, J = 9.2 Hz, *o*-Ph), 132.04 (CH, d, J = 7.8 Hz, *o*-Ph), 131.18 (CH, d, J = 10.7 Hz, *o*-Ph), 130.41 (CH, d, J = 10.2 Hz, *o*-Ph), 128.50 (CH, d, J = 2.0 Hz, *m*-Ph), 127.70 (CH, d, J = 1.9 Hz, *m*-Ph), 127.19 (CH, s, C4/5/6/7), 126.93 (CH, s, *m*-Ph), 126.84 (CH, s, *m*-Ph), 126.76 (CH, s, *p*-Ph), 126.66 (CH, s, *p*-Ph), 126.64 (CH, s, *p*-Ph), 126.57 (CH, s, *p*-Ph), 124.81 (CH, s, C4/5/6/7), 123.61 (CH, s, C4/5/6/7), 121.88 (CH, s, C4/5/6/7), 110.08 (C, d, J = 3.4 Hz, C3a), 103.36 (C, d, J = 6.8 Hz, C7a), 82.44 (CH, s, C2/3), 73.90 (C, d, J = 13.1 Hz, C1), 60.30 (CH, s, C2/3), 44.62 (CH, d, J = 4.8 Hz, C11), 39.06 (CH, d, J = 2.0 Hz, C8), 29.47 (CH₂, s, C12/12'), 29.05 (CH₂, s, C12/12'), 28.02 (CH₂, d, J = 34.0 Hz, C10), 25.73 (CH₂, s, C13/13'/14), 25.40 (CH₂, s, C13/13'/14), 25.15 (CH₂, s, C13/13'/14), 24.81 (CH₂, s, C9), 11.60 (CH₃, d, J = 25.2 Hz, Me).

³¹P NMR (121 MHz, C₆D₆): 49.41 (d, J = 38.1 Hz), 29.50 (d, J = 38.1 Hz).

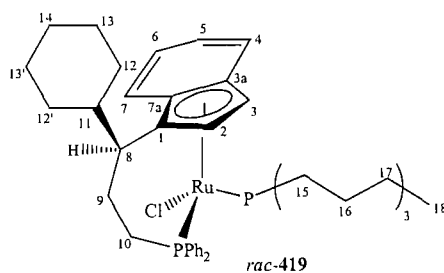
LRMS (ES⁺): (MeCN): m/z = 760, ([MH]⁺, 100 %).

Anal. Calcd. For C₃₈H₄₅P₂RuCl: C, 67.93; H, 5.97. Found C, 68.20; H, 6.19.

8.4.1.7. *rac*-($\eta^5:\eta^1$)-Indenyl-CH(Cy)CH₂CH₂PPh₂)Ru^{II} (P(*n*-Bu)₃)Cl, 419.

To a stirred solution of *rac*-($\eta^5:\eta^1$)-1-(1-cyclohexyl-3-diphenylphosphinopropyl)(chloro)(triphenylphosphine)ruthenium, **401a** (0.10 g, 0.12 mmol, 1.0 eq) in toluene (5 mL) was added tri-*n*-butylphosphine (0.08 g, 0.37 mmol, 3.0 eq) dropwise and the reaction was heated to reflux. After 2 h, the reaction was cooled to RT and the solvent removed. The title complex was isolated using flash column chromatography (Al₂O₃, 20% ether/ petrol, R_f = 0.35) as a red solid (0.063 g, 0.08 mmol, 65 %).

m.p. = 96-97 °C.



IR (cm⁻¹ thin film): 3052 (w), 2954 (m), 2925 (m), 2583 (m), 1604 (w), 1462 (w), 1434 (m), 1261 (w), 1093 (m), 901 (s), 805 (s), 701 (s).

¹H NMR (400 MHz, C₆D₆): δ / ppm = 7.65 (3H, dd, *J* = 8.0, 7.0, Hz, Ar), 7.59 (3H, d, *J* = 8.5 Hz, Ar), 7.48 (1H, d, *J* = 6.7 Hz, Ar), 7.44 (1H, d, *J* = 8.3 Hz, Ar), 7.26-7.36 (4H, m, Ar), 7.02-7.06 (3H, m, Ar), 6.97 (1H, dd, *J* = 7.8, 7.3 Hz, Ar), 4.68 (1H, s, Cp-H), 4.36 (1H, dd, *J* = 5.0, 2.3 Hz, Cp-H), 3.64 (1H, dddd, *J* = 13.8, 13.8, 7.0, 2.3 Hz, H9-a), 3.56 (1H, br. d, *J* = 12.3 Hz, H9-b), 2.68 (1H, ddd, *J* = 14.1, 14.1, 5.5 Hz, H10-a), 2.09 (1H, dddd, *J* = 36.1, 14.3, 3.0, 3.0 Hz, H10-b), 1.84-1.95 (3H, m), 1.74-1.79 (1H, m, H8), 1.55-1.69 (6H, m), 1.25-1.39 (8H, m), 1.04-1.17 (10H, m), 0.98 (9H, t, *J* = 7.0 Hz, CH₃).

¹³C NMR (75 MHz, C₆D₆): δ / ppm = 140.53 (C, d, *J* = 36.0 Hz, *i*-Ph), 135.54 (C, d, *J* = 42.8 Hz, *i*-Ph), 132.22 (2 x CH, d, *J* = 7.8 Hz, *o*-Ph), 128.81 (CH, d, *J* = 2.2 Hz, *p*-Ph), 127.40 (CH, d, *J* = 2.0 Hz, *p*-Ph), 127.69 (CH, d, *J* = 2.2 Hz, *m*-Ph), 126.17 (CH, d, *J* = 2.2 Hz, *m*-Ph), 126.09 (CH, s, C4/5/6/7), 123.88 (CH, s, C4/5/6/7), 122.36 (CH, s, C4/5/6/7), 122.26 (CH, s, C4/5/6/7), 110.76 (C, d, *J* = 3.4 Hz, C3a/7a), 103.67 (C,

d, $J = 7.2$ Hz, C3a/7a), 81.04 (CH, s, C2/3), 74.95 (C, d, $J = 13.2$ Hz, C1), 54.72 (CH, s, C2/3), 44.67 (CH, d, $J = 4.6$ Hz, C11), 39.90 (CH, s, C8), 29.53 (CH₂, s, C12/12'), 29.02 (CH₂, s, C12/12'), 28.57 (CH₂, d, $J = 34.0$ Hz, C10), 27.01 (CH₂, d, $J = 20.9$ Hz, C15), 25.73 (CH₂, s, C13/13'), 25.41 (CH₂, s, C13/13'), 25.34 (CH₂, s, C14), 24.75 (CH₂, s, C9), 23.66 (CH₂, s, C16), 23.54 (CH₂, s, C17), 12.99 (CH₃, s, C18).

³¹P NMR (121 MHz, C₆D₆): 51.39 (d, $J = 38.8$ Hz), 17.94 (d, $J = 38.8$ Hz).

LRMS (ES⁺): (MeCN): $m/z = 762$, ([M]⁺, 100 %).

Anal. Calcd. For C₄₂H₅₉P₂RuCl: C, 66.17; H, 7.80. Found C, 66.01; H, 7.99.

8.5 Experimental for chapter 5

8.5.1. Catalytic reaction details

8.5.1.1 Reaction procedure for the cyclopropanation of styrene

To a solution of catalyst *rac*-401 (4 mg) in styrene (2 mL) 40 °C was added ethyl diazoacetate (0.11 g) in styrene (1 mL) over 4 h. The reaction was monitored by GC (Method A). A blank reaction with no catalyst was also performed.

8.5.1.2 Reaction procedure for ROMP

Norbonylene (0.5 g) and catalyst *rac*-401 (6 mg) were dissolved in chlorobenzene (10 mL) and heated to 60 °C. After 20 mins, trimethylsilyldiazomethane (0.01 g) diluted in chlorobenzene (1 mL) was added dropwise. The reaction was heated at 60 °C for 16 h, then cooled to RT and the product was precipitated with the addition of MeOH.

8.5.1.3 General procedure for the allylic displacement reaction

To a solution of catalyst (3 mg) in THF (2 mL) was added the allylic acetate, followed by benzylamine dropwise at RT. The reactions were monitored by GC (method A),

Reaction	Catalyst	510	512	PhCH ₂ NH ₂
A	<i>rac</i> -401	19 mg	-	9 mg
B	<i>rac</i> -402	19 mg	-	9 mg
C	<i>rac</i> -401	-	20 mg	10 mg
D	<i>rac</i> -402	-	20 mg	10 mg

Table 8.1 Allylic displacement details

8.5.1.4 General procedure for the hydrogenation reaction

Catalyst *rac*-401 (3 mg), imine 514 (40 mg), HBF₄ (10 μL) and dichloromethane (3 mL) were placed in a bomb stainless-steel hydrogenation bomb under an inert atmosphere. The bomb was purged with hydrogen and pressurised to 6 bar, then

stirred for 60 h at RT. After this time, the reaction was analysed by GC (method A). Another reaction was performed with *rac*-402 at 50 °C.

8.5.1.5 General procedure for the transfer hydrogenation

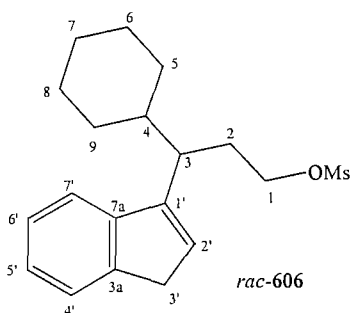
IPA system: To a solution of catalyst *rac*-401 (3mg) in IPA (4 mL) was added base, acetophenone and any other additives. The reactions were stirred with GC monitoring (method B). See Table 5.1 (Section 5.1.4) for results.

8.6 Experimental for Chapter 6

8.6.1. Synthesis of amine ligands and complex

8.6.1.1 *rac*-3-cyclohexyl-3-(1*H*-3-indenyl) propyl methansulfonate, 606.

To a stirred solution of *rac*-3-cyclohexyl-3-(1*H*-3-indenyl) propanol **206** (3.8 g, 15 mmol, 1.0 eq), in dichloromethane (30 mL) and at 0 °C was added triethylamine (3.3 mL, 24 mmol, 1.6 eq) dropwise. Methanesulfonyl chloride (1.62 mL, 21 mmol, 1.4 eq) was then added slowly and the reaction mixture was stirred as it warmed RT. After 2 h the reaction was quenched with water (20 mL) and diluted with dichloromethane (30 mL). The aqueous layer was separated and extracted with dichloromethane (3 x 30 mL). The combined organics were washed with brine (10 mL), dried over MgSO₄, and the solvents removed, yielding the crude mesylate (5 g, 15 mmol, 98 %). The title compound was used without further purification.¹²⁸



IR (cm⁻¹ thin film): 3066(w), 2922 (m), 2850 (m), 1605 (w) 1450 (w), 1351 (s), 1171 (s), 968 (m), 916 (m), 877 (w).

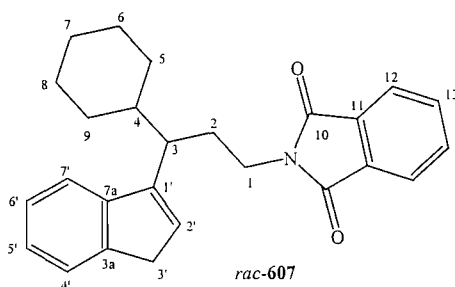
¹H NMR (300 MHz, CDCl₃): δ / ppm = 7.49 (1H, d, J = 7.0 Hz, H4'/7'), 7.40 (1H, d, J = 7.0 Hz, H4'/7'), 7.30 (1H, td, J = 7.4, 1.1 Hz, H5'/6'), 7.20 (1H, t, J = 7.4 Hz, H5'/6'), 6.24 (1H, t, J = 2.0 Hz, H2'), 4.21 (1H, ddd, J = 9.6, 7.4, 4.4 Hz, H1-a), 4.05 (1H, ddd, J = 9.6, 8.4, 4.4 Hz, H1-b), 3.40 (2H, d, J = 2.0 Hz, H3'), 2.82 (3H, s, OMs), 2.72 (1H, ddd, J = 11.0, 7.0, 3.7 Hz, H3), 2.27 (1H, dddd, J = 13.6, 8.5, 6.0, 3.7 Hz, H2-a), 2.09 (1H, dddd, J = 13.3, 11.4, 6.6, 4.4 Hz, H2-b), 1.56-1.87 (6H, m, Cy), 0.92-1.12 (5H, m, Cy).

¹³C NMR (75 MHz, CDCl₃): δ / ppm = 145.04 (C, C1'/3a/7a), 145.00 (C, C1'/3a/7a), 144.69 (C, C1/3a/7a), 129.49 (CH, C4'/5'/6'/7'), 126.00 (CH,

C4'/5'/6'/7'), 124.75 (CH, C4'/5'/6'/7'), 124.00 (CH, C4'/5'/6'/7'), 119.58 (CH, C2'), 64.91 (CH₂, C1), 41.30 (CH, C3/4), 40.52 (CH, C3/4), 37.80 (CH₂, C3'), 37.04 (CH₃, OMs), 31.22 (CH₂, C2), 30.60 (CH₂, C5/9), 30.18, (CH₂, C5/9), 26.48 (CH₂, C7), 26.45 (2 x CH₂, C6/8).

8.6.1.2. *rac*-[3-cyclohexyl-3-(1*H*-3-indenyl) propyl]-1,3-isoindolinedione, 607.

To a stirred solution of *rac*-3-cyclohexyl-3-(1*H*-3-indenyl) propyl methansulfonate, **606** (4.2 g, 12.6 mmol, 1.0 eq) in DMF (40 mL) was added potassium phthalimide (2.4 g, 13.2 mmol, 1.05 eq) slowly. The reaction mixture was heated at 70 °C and after 3 h was allowed to cool to RT, quenched with water (30 mL) and diluted with diethyl ether (30 mL). The aqueous layer was separated and extracted with diethyl ether (3 x 30 mL). The combined organics were dried over MgSO₄, the solvents removed. The title compound was isolated by flash column chromatography (SiO₂, 45 % diethyl ether/petrol, R_f = 0.4) as a yellow oil (3.06 g, 7.9 mmol, 63 %).¹²⁸



IR (cm⁻¹ thin film): 3051 (w), 2922 (m), 2850 (m), 1772 (w), 1706 (s), 1439 (m), 1394 (m), 1363 (m), 1007 (w), 870 (m), 714 (m).

¹H NMR (300 MHz, CDCl₃): δ / ppm = 7.60-7.67 (2H, m, Ar), 7.52-7.58 (2H, m, Ar), 7.25-7.30 (2H, m, Ar), 7.18 (1H, td, J = 7.3, 1.1 Hz, Ar), 7.05 (1H, td, J = 7.5, 1.1 Hz, Ar), 6.22 (1H, t, J = 2.0 Hz, H2'), 3.61 (1H, ddd, J = 13.5, 8.6, 6.8 Hz, H1-a), 3.51 (1H, ddd, J = 13.5, 8.6, 5.9 Hz, H1-b), 3.24 (1H, dd, J = 23.5, 2.2 Hz, H3'-a), 3.15 (1H, dd, J = 23.5, 2.2 Hz, H3'-b), 2.59 (1H, ddd, J = 10.8, 4.9, 4.9 Hz, H3), 1.98-2.08 (2H, m, H2), 1.69-1.73 (1H, m, Cy), 1.46-1.61 (5H, m, Cy), 0.8-1.11 (5H, m, Cy).

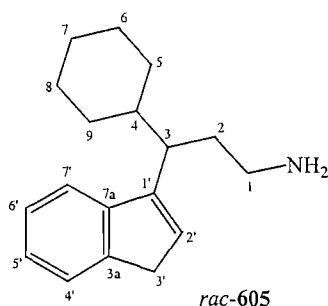
¹³C NMR (75 MHz, CDCl₃): δ / ppm = 168.31 (C, C10), 145.54 (C, C1'/3a/7a), 145.50 (C, C1'/3a/7a), 144.74 (C, C1'/3a/7a), 133.62 (2 x CH, C13), 132.07 (C, C11), 129.05 (CH, C4'/5'/6'/7'), 125.81 (CH, C4'/5'/6'/7'), 124.39 (CH, C4'/5'/6'/7'), 123.62 (CH, C4'/5'/6'/7'), 122.86 (2 x CH, C12), 119.72 (CH, C2'), 42.10 (CH, C3/4), 41.78 (CH, C3/4), 37.77 (CH₂, C1), 37.43 (CH₂, C3'), 31.02 (CH₂, C5/9), 30.33 (CH₂, C5/9), 29.23 (CH₂, C2), 26.61 (CH₂, C6/7/8), 26.76 (CH₂, C6/7/8), 26.70 (CH₂, C6/7/8).

LRMS (CI): m/z = 386, ([M]⁺, 100%); 270, ([M-C₇O₂]⁺, 42%).

HRMS (ES⁺): C₂₆H₂₇NO₂ requires m/z 408.1939, found 408.1933 [M+Na]⁺.

8.6.1.3. *rac*-3-Cyclohexyl-3-(3*H*-inden-1-yl)-propylamine, 605.

To a stirred solution of 2[3-cyclohexyl-3-(1*H*-3-indenyl) propyl]-1,3-isoindolinedione, **607** (0.39 g, 1 mmol, 1.0 eq) in *t*-butanol (8 mL) was added hydrazine hydrate (0.12 mL, 4 mmol, 4.0 eq) dropwise. After refluxing for 90 mins, the reaction was diluted with the addition of diethyl ether (15 mL) and 2.0 M HCl (20 mL), The organic layer was separated and extracted with 2.0 M HCl (3 x 20 mL). The aqueous acidic layer was made basic *via* addition of NaOH pellets. The aqueous layer was extracted with diethyl ether (3 x 20 mL), and the combined organics were washed with brine (10 mL), dried over MgSO₄ and the solvents removed. Kugelrohr distillation (110 °C, 11 mmHg) yielded the title compound as a yellow oil (0.1 g, 0.3 mmol, 32%).¹²⁸



IR (cm⁻¹ thin film): 3365 (m), 3283 (m), 3065 (m), 3015 (m), 2923 (s), 2850 (s), 2663 (w), 1604 (m), 1448 (m), 1261 (m), 968 (m), 720 (m).

¹H NMR (300 MHz, CDCl₃): δ / ppm = 7.38 (1H, d, J = 7.3 Hz, H4'/7'), 7.32 (1H, d, J = 7.3 Hz, H4'/7'), 7.24 (1H, td, J = 7.3, 1.1 Hz, H5'/6'), 7.21 (1H, td, J = 7.4, 1.1 Hz, H5'/6'), 6.10 (1H, t, J = 2.0 Hz, H2'), 3.27 (2H, d, J = 2.0 Hz, H3'), 2.42-2.59 (2H, m, H1), 2.24 (2H, m, NH₂), 1.68-1.75 (1H, m, H3), 1.41-1.62 (2H, m, H2), 1.29-1.35 (6H, m, Cy), 0.91-1.25 (5H, m, Cy).

¹³C NMR (75 MHz, CDCl₃): δ / ppm = 146.51 (C, C1'/3a/7a), 145.75 (C, C1'/3a/7a), 144.92 (C, C1'/3a/7a), 128.83 (CH, C4'/5'/6'/7'), 125.99 (CH, C4'/5'/6'/7'), 124.54 (CH, C4'/5'/6'/7'), 123.97 (CH, C4'/5'/6'/7'), 119.80 (CH, C2), 42.26 (CH₂, C1), 41.53 (CH, C3/4), 41.07 (CH, C3/4), 37.82 (CH₂, C3'), 34.87 (CH₂, C2), 31.52 (CH₂, C5/9), 31.46 (CH₂, C5/9), 30.88 (CH₂, C7), 26.76, (2 x CH₂, C6/8).

LRMS (ES⁺): m/z = 256, ([MH]⁺, 100%).

HRMS (ES⁺): C₁₉H₂₅N requires m/z 256.2056, found 256.2060[M+H]⁺

8.6.1.4. 3-Cyclohexyl-3-(3*H*-inden-1-yl)-propylamine, 605.

To a stirred solution of 2-[3-cyclohexyl-3-(1*H*-3-indenyl)propyl]-1,3-isoindolinedione, **607** (3.0 g, 7.8 mmol, 1 eq) in ethanol (20 mL) was added hydrazine hydrate (0.5 mL, 15.6 mmol, 2.0 eq) dropwise. After 16 h at RT, diethyl ether (25 mL) and 2.0 M HCl (20 mL) were added. The organic layer was separated and extracted with 2.0 M HCl (3 x 40 mL). The acidic aqueous layer was then made basic *via* addition of NaOH pellets. The aqueous layer was extracted with diethyl ether (3 x 50 mL) and the combined organics were washed with brine (20 mL), dried over MgSO₄ and the solvents removed. Kugelrohr distillation (110 °C, 11 mmHg) yielded the title compound as a yellow oil (1.0 g, 4 mmol, 52 %).¹²⁹

NMR data were identical to previous values (see section 8.6.1.3).

8.6.1.5. 3-Cyclohexyl-3-(3*H*-inden-1-yl)-propylamine, 605.

To a stirred solution of 3-cyclohexyl-3-(1*H*-3-indenyl) propyl methansulfonate, **606** (1 g, 3 mmol, 1.0 eq) in ethanol (10 mL) was added aqueous NH₃ 880 (12 mL) dropwise at 0 °C and the reaction was left to warm to RT. After 72 h the reaction was diluted with the addition of diethyl ether (20 mL) and 2.0 M HCl (30 mL). The organic

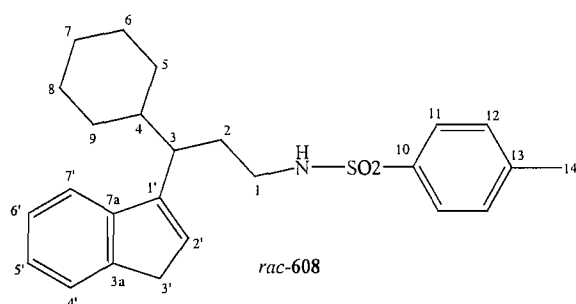
layer was separated and extracted with 2.0 M HCl (3 x 40 mL). The acidic layer was then made basic *via* the addition of NaOH pellets and aqueous layer was then extracted with diethyl ether (3 x 30 mL). The combined organics were washed with brine (20 mL), dried over MgSO₄ and the solvents removed. Kugelrohr distillation (110 °C, 11 mmHg) yielded the title compound as a yellow oil (0.45 g, 1.8 mmol, 59 %). NMR data were identical to previous values (see section 8.6.1.3).

8.6.1.6. *N*-[3-cyclohexyl-3-(3*H*-inden-1-yl)-propyl]-4-methyl-benzenesulfonamide, **608**.

To a stirred solution of 3-cyclohexyl-3-(3*H*-inden-1-yl)-propylamine, **605** (0.8 g, 3.1 mmol, 1.0 eq), in dichloromethane (10 mL) at 0 °C, was added triethylamine (0.7 mL, 5 mmol, 1.6 eq) dropwise. After 15 mins *p*-toluenesulfonylchloride (0.84 g, 4.4 mmol, 1.4 eq) was added portionwise. After 2 h, the reaction was quenched with sat NH₄Cl (aq) soln. (10 mL) and dichloromethane (10 mL) was added. The aqueous layer was separated which was extracted with dichloromethane (3 x 20 mL). The combined organics were washed with brine (10 mL), dried over MgSO₄ and the solvents removed. The title compound was isolated by flash chromatography (SiO₂, 50 % diethyl ether/petrol, R_f = 0.3) as a white solid (0.89 g, 2.1 mmol, 70 %).

m.p. = 142-143 °C.

X-ray quality crystals were obtained by slow evaporation of an ethanol solution of **608**. Crystallographic analysis has confirmed the structure is as shown. (Appendix 10).



IR (cm⁻¹ thin film): 3065 (w), 2926 (s), 2851 (s), 1611 (w) 1458 (w), 1325 (s), 1160 (s), 1093 (m), 813 (m), 733 (m).

¹H NMR (300 MHz, CDCl₃): δ / ppm = 7.61 (2H, d, J = 8.3 Hz, H12), 7.46 (1H, d, J = 6.6 Hz, H4'/7'), 7.22 (1H, d, J = 7.0 Hz, H4'/7'), 7.13 (1H, td, J = 7.5, 1.3 Hz, H5'/6'), 7.11 (2H, d, J = 7.8 Hz, H11), 7.10 (1H, td, J = 7.0, 1.5 Hz, H5'/6'), 6.10 (1H, t, J = 2.2 Hz, H2'), 4.30 (1H, t, J = 6.3 Hz, NH), 3.35 (2H, d, J = 2.2 Hz, H3'), 2.83 (1H, dddd, J = 12.9, 8.1, 7.8, 5.9 Hz, H1-a), 2.66 (1H, dddd, J = 12.8, 8.1, 7.7, 5.9 Hz, H1-b), 2.51 (1H, ddd, J = 10.6, 6.5, 4.0 Hz, H3), 2.41 (3H, s, H14), 1.45-1.86 (8H, m, H2, H4, Cy), 0.55-1.18 (5H, m, Cy).

¹³C NMR (75 MHz, CDCl₃): δ / ppm = 145.32 (C, C1'/3a/7a), 145.05 (C, C1'/3a/7a), 144.73 (C, C1'/3a/7a), 143.18 (C, C13), 136.88 (C, C10), 129.59 (2 x CH, C12), 129.28 (CH, C4'/5'/6'/7'), 127.06 (2 x CH, C11), 125.93 (CH, C4'/5'/6'/7'), 124.57 (CH, C4'/5'/6'/7'), 123.88 (CH C4'/5'/6'/7'), 119.63 (CH, C2'), 42.07 (CH₂, C1), 41.76 (CH, C3/4), 41.09 (CH, C3/4), 37.69 (CH₂, C3'), 31.24 (CH₂, C2), 30.47 (CH₂, C5/9), 30.34 (CH₂, C5/9), 26.52 (CH₂, C7), 26.49 (2 x CH₂, C6/8), 21.52 (CH₃, C14).

LRMS (CI): m/z = 410 ([MH]⁺, 100%); 254 ([MH-C₇H₇SO₂]⁺, 90 %).

Anal. Calcd. For C₂₅H₃₁NO₂S : C, 73.31; H, 7.63, N, 3.42; Found: C, 73.16; H, 7.64; N, 3.41.

8.6.1.7. *N*-[3-cyclohexyl-3-(3*H*-inden-1-yl)-propyl]-4-methyl-benzenesulfonamide, 608.

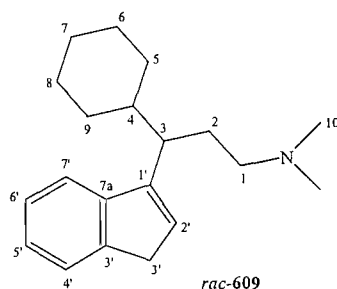
To a stirred solution of NaH (60% dispersion in mineral oil, 0.32 g, 8 mmol, 4.0 eq) in dry DMF (15 mL) at 0 °C was added *p*-toluenesulfonamide (1.4 g, 8 mmol, 4.0 eq) in dry DMF (15 mL) dropwise. (with evolution of gas) After 15 mins stirring, 3-cyclohexyl-3-(1*H*-3-indenyl) propyl methansulfonate, **606** (0.65 g, 2 mmol, 1.0 eq) in dry DMF (10 mL) was added slowly. After 3 h at RT, the reaction was quenched with the addition of methanol (10 mL) and water (5 mL). Diethyl ether (15 mL) was added and the aqueous phase was separated and extracted with diethyl ether (3 x 20 mL). The combined organics were then extracted with 2.0 M NaOH (3 x 20 mL), washed with water (20 mL), dried over MgSO₄ and the solvents removed yielding a yellow oil. The title compound was isolated by flash chromatography (SiO₂, 50% diethyl ether/petrol, R_f = 0.3) as a white solid (0.47 g, 1.2 mmol, 58%).¹³⁰

m.p. = 142-143 °C.

NMR data were identical to previous values. (Section 8.6.1.6).

8.6.1.8. [3-cyclohexyl-3-(1*H*-3-indenyl) propyl]-dimethyl-amine, 609.

To a stirred solution of 3-cyclohexyl-3-(1*H*-3-indenyl) propyl methanesulfonate, **606** (0.33 g, 1 mmol, 1.0 eq) in ethanol (10 mL) was added dimethylamine (2.0 M soln. in MeOH, 1.5 mL, 3 mmol, 3.0 eq) via syringe. After 16 h at RT, the reaction was diluted with diethyl ether (20 mL) and 2.0 M HCl (20 mL) was also added. The organic layer was separated and extracted with 2.0 M HCl (3 x 25 mL). The acidic aqueous layer was made basic with addition of NaOH pellets. The aqueous layer was extracted with diethyl ether (3 x 20 mL), dried over MgSO₄ and the solvents removed. Kugelrohr distillation (115 °C, 11 mmHg) yielded the title compound as a yellow oil (0.18 g, 0.64 mmol, 63 %).¹²⁹



IR (cm⁻¹ thin film): 3064 (w), 2921 (s), 2851 (m), 2855 (m), 2817 (m), 2760 (m), 1608 (w), 1450 (w), 1039 (w), 765 (m).

¹H NMR (300 MHz, CDCl₃): δ / ppm = 7.48 (1H, d, J = 7.4 Hz, H4'/7'), 7.41 (1H, d, J = 7.4 Hz, H4'/7'), 7.29 (1H, td, J = 7.4, 1.1 Hz, H5'/67'), 7.20 (1H, td, J = 7.4, 1.1 Hz, H5'/6'), 6.20 (1H, t, J = 2.0 Hz, H2'), 3.37 (2H, d, J = 2.0 Hz, H3'), 2.57 (1H, ddd, J = 10.7, 6.0, 4.0 Hz, H3), 2.19 (6H, s, H10), 1.73-1.94 (2H, m, H1), 1.59-1.73 (8H, m, H2/Cy) 1.09-1.30 (5H, m, Cy).

¹³C NMR (75 MHz, CDCl₃): δ / ppm = 146.47 (C, C1'/3a/7a), 145.82 (C, C1'/3a/7a), 144.72 (C, C1'/3a/7a), 128.48 (CH, C4'/5'/6'/7'), 125.81 (CH, C4'/5'/6'/7'), 124.30 (CH, C4'/5'/6'/7'), 123.74 (CH, C4'/5'/6'/7'), 119.63 (CH, C18), 58.68 (CH₂, C1), 45.59 (2 x CH₃, C10), 42.42 (CH, C3/4), 41.56 (CH, C3/4),

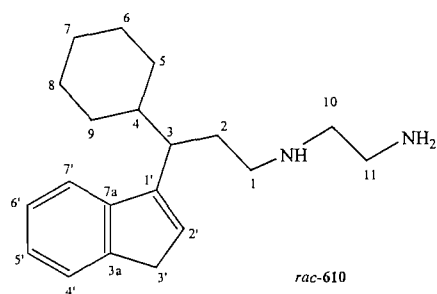
37.69 (CH₂, C3'), 31.22 (CH₂, C5/9), 30.58 (CH₂, C5/9), 28.85, (CH₂, C2), 26.66 (CH₂, C6/7/8), 26.63 (CH₂, C6/7/8), 26.60 (CH₂, C6/7/8).

LRMS (EI): $m/z = 283$, ($[M]^+$, 10%); 58, (M-C₁₇H₂₀)⁺, 100%.

HRMS (EI⁺): C₂₀H₂₉N requires m/z 283.2295, found 283.2300 [M].

8.6.1.9. *N*-[3-cyclohexyl-3-(3*H*-inden-1-yl)-propyl]-ethane-1,2-diamine, **610**.

Using the same procedure as for **8.6.1.8**, **8.6.1.9** was obtained by reaction of *rac*-3-cyclohexyl-3-(1*H*-3-indenyl) propyl methansulfonate, **606**, (0.5 g, 1.5 mmol, 1.0 eq) with ethylenediamine (0.3 mL, 4.5 mmol, 3.0 eq) as a yellow (0.23 g, 0.8 mmol, 52%). Kugelrohr distillation (140 °C, 11 mmHg) yielded the title compound.¹²⁹



IR (cm⁻¹ thin film): 3299 (w), 3062 (w), 2923 (s), 2850 (m), 1604 (w), 1574 (w), 1449 (m), 1395 (w), 963 (w), 769 (m).

¹H NMR (300 MHz, CDCl₃): δ / ppm = 7.48 (1H, d, $J = 7.5$ Hz, H4'/7'), 7.40 (1H, d, $J = 7.4$ Hz, H4'7'), 7.28 (1H, td, $J = 7.4$ 1.5 Hz, H5'/6'), 7.20 (1H, td, $J = 7.2$, 1.5 Hz, H4'/5'/6'/7'), 6.19 (1H, t, $J = 1.8$ Hz, H2'), 3.36 (2H, d, $J = 1.8$ Hz, H3'), 2.72 (2H, t, $J = 6.25$ Hz, H10), 2.44-2.56 (5H, m), 1.81-1.99 (2H, m), 1.40-1.56 (5H, m, Cy), 1.30 (3H, br. s, NH), 0.99-1.05 (6H, m, Cy).

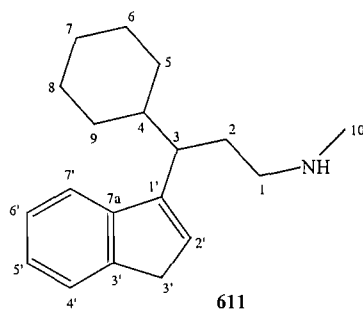
¹³C NMR (75 MHz, CDCl₃): δ / ppm = 145.49 (C, C1'/3a/7a), 144.66 (C, C1'/3a/7a), 143.72 (C, C1'/3a/7a), 127.57 (CH, C4'/5'/6'/7'), 124.83 (CH, C4'/5'/6'/7'), 123.37 (CH, C4'/5'/6'/7'), 122.79 (CH, C4'/5'/6'/7'), 118.63 (CH, C2'), 51.49 (CH₂, C10), 47.64 (CH₂, C1), 41.49 (CH, C3/4), 40.66 (CH₂, C11), 40.55 (CH, C3/4), 36.66 (CH₂, C3'), 30.34 (CH₂, C5/9), 30.22 (CH₂, C2), 29.73 (CH₂, C5/9), 25.60 (3 x CH₂, C6/7/8).

LRMS (EI): $m/z = 299$, ($[\text{MH}]^+$, 100%);

HRMS (EI⁺): $\text{C}_{20}\text{H}_{30}\text{N}_2$ requires m/z 299.2482, found 299.2485 (MH).

8.6.1.10. N-[3-cyclohexyl-3-(3*H*-inden-1-yl)propyl]-methyl-amine, 611.

8.6.1.10 was prepared using the same procedure as for 8.6.1.8 and 8.6.1.9 by reaction of *rac*-3-cyclohexyl-3-(1*H*-3-indenyl) propyl methansulfonate, 606, (0.28 g, 0.79 mmol, 1.0 eq) methylamine (6 mL, 33 % in EtOH) as a yellow (0.12 g, 0.43 mmol, 54%).¹²⁹



IR (cm⁻¹ thin film): 3443 (w), 3060 (w), 2928 (s), 2851 (s), 2798 (s), 1604 (w) 1449 (w), 1380 (w), 1003 (w), 775 (m).

¹H NMR (300 MHz, CDCl₃): δ / ppm = 7.48 (1H, d, $J = 7.4$ Hz, H4'/7'), 7.41 (1H, d, $J = 7.4$ Hz, H4'/7'), 7.29 (1H, d, $J = 7.4$ Hz, H5'/6'), 7.20 (1H, td, $J = 7.4, 1.1$ Hz, H5'/6'), 6.20 (1H, t, $J = 2.2$ Hz, H2'), 3.26 (2H, d, $J = 2.2$ Hz, H3'), 2.59 (1H, ddd, $J = 10.7, 6.3, 4.0$ Hz, H3), 2.39-2.53 (2H, m, H1), 2.35 (3H, s, H10), 1.80-2.0 (3H, m, H2 and H4), 1.40-1.60 (5H, m, Cy), 0.9-1.30 (5H, m, Cy).

(NH proton not observed)

¹³C NMR (75 MHz, CDCl₃): δ / ppm = 146.60 (C, C1'/3a/7a), 145.85 (C, C1'/3a/7a), 144.91 (C, C1'/3a/7a), 128.73 (CH, C4'/5'/6'/7'), 125.99 (CH, C4'/5'/6'/7'), 124.51 (CH, C4'/5'/6'/7'), 123.95 (CH, C4'/5'/6'/7'), 119.80 (CH, C2'), 51.12 (CH₂, C1), 42.58 (CH, C3/4), 41.62 (CH, C3/4), 37.83 (CH₂, C3'), 36.70 (CH₃, C10), 31.48 (CH₂, C2), 31.12 (CH₂, C5/9), 30.80 (CH₂, C5/9), 30.48 (CH₂, C7), 26.77 (2 x CH₂, C6/8).

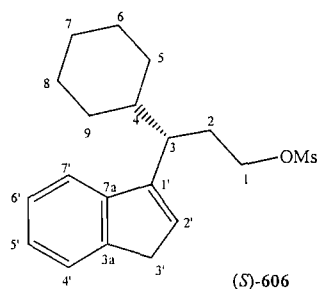
LRMS (CI): $m/z = 270$ ($[M+H]^+$, 100%), 212 ($[M+HC_3H_7N]^+$, 30%), 130 ($[M+H-C_3H_7N]^+$, 18 %)

HRMS (ES⁺): $C_{19}H_{27}N$ requires m/z 270.2214, found 270.2216 $[M+H]^+$.

8.6.1.11 (*S*)-3-cyclohexyl-3-(1*H*-3-indenyl) propyl methansulfonate, 606.

To a stirred solution of (*S*)-3-cyclohexyl-3-(1*H*-3-indenyl) propanol **206** (0.67 g, 2 mmol, 1.0 eq), in dichloromethane (20 mL) and at 0 °C was added triethylamine (0.47 mL, 3.2 mmol, 1.6 eq) dropwise. Methanesulfonyl chloride (0.22 mL, 2.8 mmol, 1.4 eq), was then added slowly and the reaction mixture was stirred as it warmed RT. After 2 h, the reaction was quenched with water (10 mL) and diluted with dichloromethane (10 mL). The aqueous layer was separated and extracted with dichloromethane (3 x 10 mL). The combined organics were washed with brine (10 mL), dried over $MgSO_4$, and the solvents removed, yielding the crude mesylate (0.59 g, 1.76 mmol, 88%). The title compound was used without further purification.¹²⁸

NMR data were identical previous literature values (Section 8.6.1.1).

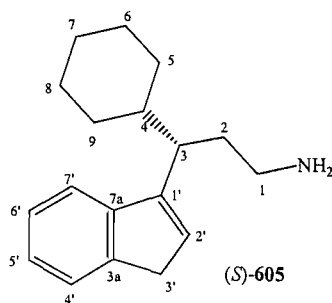


8.6.1.12. (*S*)-3-Cyclohexyl-3-(3*H*-inden-1-yl)-propylamine, 605.

8.6.1.12 was prepared according to the procedure described for **8.6.1.5** by reaction of (*S*)-3-cyclohexyl-3-(1*H*-3-indenyl) propyl methansulfonate, **206**, (0.28 g, 0.79 mmol, 1.0 eq) with aqueous NH_3 880 (10 mL). Kugelrohr distillation (109 °C, 11 mmHg) yielded the title compound as a yellow oil (0.12 g, 0.48 mmol, 56%).

$[\alpha]_D^{23} = +29.0^\circ$ ($c = 0.02$, $CHCl_3$).

NMR data were identical to previous values (Section 8.6.1.3).



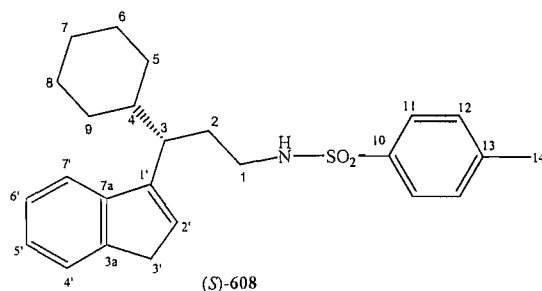
8.6.1.13 (S)-N-[3-cyclohexyl-3-(3*H*-inden-1-yl)-propyl]-4-methylbenzenesulfonamide, 608.

To a stirred solution of NaH (60% dispersion in mineral oil, 0.14 g, 3.56 mmol, 4.0 eq) in dry DMF (10 mL) at 0 °C was added *p*-toluenesulfonamide (0.6 g, 3.56 mmol, 4.0 eq) in dry DMF (10 mL) dropwise. (with evolution of gas) After 15 mins stirring, (S)-3-cyclohexyl-3-(1*H*-3-indenyl) propyl methansulfonate, **606** (0.28 g, 0.89 mmol, 1.0 eq) in dry DMF (10 mL) was added slowly. After 3 h at RT, the reaction was quenched with the addition of methanol (5 mL) and water (5 mL). Diethyl ether (10 mL) was added and the aqueous phase was separated and extracted with diethyl ether (3 x 10 mL). The combined organics were then extracted with 2.0 M NaOH (3 x 10 mL), washed with water (10 mL), dried over MgSO₄ and the solvents removed yielding a yellow oil. The title compound was isolated by flash chromatography (SiO₂, 50 % diethyl ether/petrol, R_f = 0.3) as a white solid (0.49 g, 1.25 mmol, 61%).¹³⁰

m.p. = 142-143 °C.

$[\alpha]_D^{23} = +32.2^\circ$ (c = 0.02, CHCl₃).

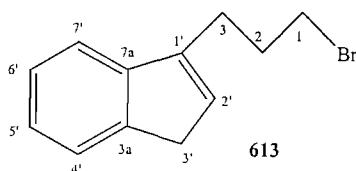
NMR data were identical to previous values (Section 8.6.1.6).



8.6.1.14. 3-(3-bromo-propyl)-1*H*-indene, 613.

To a stirred solution of indene (8.0 mL, 69 mmol, 1.0 eq) in THF (40 mL) at 0 °C was added *n*-BuLi (2.5 M soln in cyclohexanes, 27.6 mL, 69 mmol, 1.0 eq) dropwise in the dark. The reaction was stirred at 0 °C for 15 mins then left to warm to RT and stirred for 90 mins. The anion was then added via cannula to a stirred solution of 1,3-*di*bromopropane (21 mL, 207 mmol, 3.0 eq) in THF (40 mL) at 0 °C and in the dark. After 30 mins the reaction was quenched with water (30 mL) and diluted with diethyl ether (30 mL). The aqueous phase was extracted with diethyl ether (3 x 50 ml). The combined organics were washed with brine (20 mL), dried over MgSO₄ and the solvents removed. Excess 1,3-*di*bromopropane was removed via distillation yielding the title compound as a yellow oil. (11.94g, 50 mmol, 73%).¹³¹

NMR data were identical to literature values.¹³¹



IR (cm⁻¹ thin film): 3063 (w), 3016 (s), 2931 (s), 2899 (s), 1608 (w) 1456 (w).

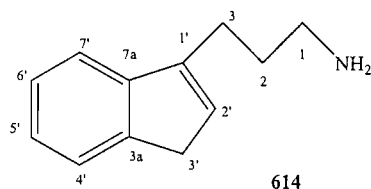
¹H NMR (300 MHz, CDCl₃): δ / ppm = 7.51 (1H, d, J = 7.4 Hz, H4'/7'), 7.41 (1H, d, J = 7.4 Hz, H4'/7'), 7.34 (1H, td, J = 7.4, 1.1 Hz, H5'/6), 7.24 (1H, td, J = 7.4, 1.1 Hz, H5'/6), 6.29 (1H, tt, J = 1.8, 1.8 Hz, H2'), 3.52 (2H, t, J = 6.6 Hz, H1), 3.37 (2H, dt, J = 2.2, 2.0 Hz, H3'), 2.77 (2H, m, H3), 2.29 (2H, pentet, J = 6.6 Hz, H2).

¹³C NMR (75 MHz, CDCl₃): δ / ppm = 145.00 (C, C1'/3a/7a), 144.49 (C, C1'/3a/7a), 142.62 (C, C1'/3a/7a), 128.82 (CH, C4'/5'/6'/7'), 126.09 (CH, C4'/5'/6'/7'), 124.72 (CH, C4'/5'/6'/7'), 123.86 (CH, C4'/5'/6'/7'), 118.92 (CH, C2'), 37.81 (CH₂, C3'), 33.63 (CH₂, C3), 30.95 (CH₂, C1), 26.10 (CH₂, C2).

[3-(3*H*-Inden-1-yl)-propyl]-amine, 614.

To a stirred solution of 3-(3-Bromo-propyl)-1*H*-indene, **613** (3.3 g, 14 mmol, 1.0 eq) in ethanol (20 mL) was added aqueous NH₃ 880 (20 mL) dropwise at 0 °C. The reaction was left to stir at RT and after 96 h, the reaction was diluted with diethyl ether (20 mL) and 2.0 M HCl (20 mL). The organic layer was separated and extracted with 2.0 M HCl (3 x 50 mL). The acidic layer was then basified with the addition of NaOH pellets and then extracted with diethyl ether (3 x 50 mL). The combined organics were washed with brine (20 mL), dried over MgSO₄ and the solvent removed Kugelrohr distillation (80 °C, 11 mmHg) yielded the title compound as a yellow oil (1.33 g, 7.7 mmol, 55 %).¹³¹

NMR data was identical to literature values.¹³¹



IR (cm⁻¹ thin film): 3067 (w), 2930 (s), 2880 (m), 1573 (m), 1460 (m), 1316 (m), 962 (m), 764 (s).

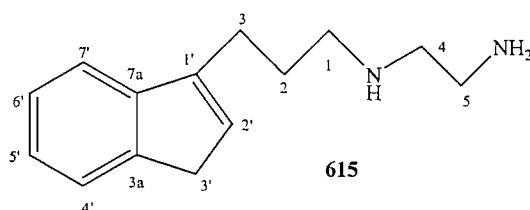
¹H NMR (300 MHz, CDCl₃): δ / ppm = 7.48 (1H, d, J = 7.4 Hz, H4'/7'), 7.40 (1H, d, J = 7.4 Hz, H4'/7'), 7.32 (1H, td, J = 7.4, 1.1 Hz, H5'/6'), 7.22 (1H, td, J = 7.4, 1.1 Hz, H5'/6'), 6.24 (1H, tt, J = 1.8, 1.8 Hz, H2'), 3.35 (2H, d, J = 1.8 Hz, H3'), 2.82 (2H, t, J = 7.0 Hz, H1), 2.62 (2H, m, H3), 1.86 (2H, pentet, J = 7.0 Hz, H2), 1.35 (2H, br s, NH₂).

¹³C NMR (75 MHz, CDCl₃): δ / ppm = 145.40 (C, C1'/3a/7a), 144.52 (C, C1'/3a/7a), 144.05 (C, C1'/3a/7a), 127.88 (CH, C4'/5'/6'/7'), 126.00 (CH, C4'/5'/6'/7'), 124.54 (CH, C4'/5'/6'/7'), 123.77 (CH, C4'/5'/6'/7'), 118.94 (CH, C2'), 42.15 (CH₂, C1), 37.72 (CH₂, C3'), 32.02 (CH₂, C3), 25.08 (CH₂, C2).

LRMS (ES⁺): m/z = 173 (M, 100%)⁺.

8.6.1.16 N'-[3-(3*H*-Inden-1-yl)-propyl]-ethane-1,2-diamine, 615.

To a stirred solution of 3-(3-bromo-propyl)-1*H*-indene, **613** (0.5 g, 2.1 mmol, 1.0 eq) in ethanol (10 mL) at °C was added ethylenediamine (0.42 mL, 6.3 mmol, 3.0 eq) dropwise. The reaction was left to stir at RT and after 16 h, the reaction was diluted with the addition of diethyl ether (10 mL) and 2.0 M HCl (10 mL) was added. The organic layer was separated and extracted with 2.0 M HCl (3 x 20 mL). The aqueous layer was then made basic with the addition of NaOH pellets and then extracted with diethyl ether (3 x 20 mL). The combined organics were washed with brine (15 mL), dried over MgSO₄ and the solvents removed. Kugelrohr distillation (105 °C, 11 mmHg) yielded the title compound as a yellow oil (0.35 g, 1.6 mmol, 77 %).



IR (cm⁻¹ thin film): 3070 (w), 2933 (s), 2882 (m), 1608 (w), 1574 (w), 1461 (m), 1395 (m), 962 (m), 767 (s).

¹H NMR (300 MHz, CDCl₃): δ / ppm = 7.45 (1H, d, J = 7.5 Hz, H4'/7'), 7.37 (1H, d, J = 7.4 Hz, H4'/7'), 7.30 (1H, td, J = 7.0, 1.3 Hz, H5'/6'), 7.20 (1H, td, J = 7.2, 1.3 Hz, H5'/6'), 6.23 (1H, tt, J = 2.0, 2.0 Hz, H2'), 3.35 (2H, dt, J = 2.0, 2.0 Hz, H3'), 2.78-2.87 (2H, m, H4), 2.66-2.76 (4H, m, H5, H1), 2.57-2.65 (2H, m, H3), 1.90 (2H, pentet, J = 6.0 Hz, H2), 1.55 (3H, s, NH).

¹³C NMR (75 MHz, CDCl₃): δ / ppm = 145.40 (C, C1'/3a/7a), 144.49 (C, C1'/3a/7a), 144.13 (C, C1'/3a/7a), 127.83 (CH, C4'/5'/6'/7'), 125.98 (CH, C4'/5'/6'/7'), 124.51 (CH, C4'/5'/6'/7'), 123.72 (CH, C4'/5'/6'/7'), 118.93 (CH, C2'), 52.52 (CH₂, C4), 49.70 (CH₂, C1), 41.78 (CH₂, C5), 37.70 (CH₂, C3'), 28.47 (CH₂, C2/3), 25.49 (CH₂, C2/3).

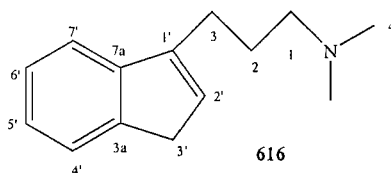
LRMS (ES⁺): m/z = 217 ([M+H]⁺, 100%);

HRMS (ES⁺): C₁₄H₂₀N requires *m/z* 217.1699, found 217.1701[M+H]⁺

8.6.1.17 [3-(3*H*-Inden-1-yl)-propyl]-dimethyl-amine, 616.

In the same manner as described above, **8.6.1.17** was obtained by reaction of 3-(3-bromo-propyl)-1*H*-indene, (4 g, 17 mmol, 1.0 eq) **613**, with added dimethylamine (2.0 M soln. in MeOH. 12 ml, 26 mmol, 1.5 eq). Kugelrohr distillation (97 °C, 11 mmHg) yielded the title compound as a yellow oil (3.03 g, 15 mmol, 88%).

NMR data were identical to literature values.¹⁴⁴



IR (cm⁻¹ thin film): 3064 (w), 2940 (s), 2883 (m), 2763 (s), 1609 (w) 1460 (s, CH₂) 1263 (m), 1097 (w), 914 (m), 718 (m).

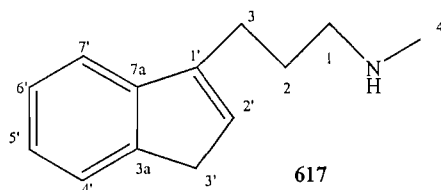
¹H NMR (300 MHz, CDCl₃): δ / ppm = 7.49 (1H, d, *J* = 7.4 Hz, H4'/7'), 7.41 (1H, d, *J* = 7.4 Hz, H4'/7'), 7.31 (1H, td, *J* = 7.4, 1.1 Hz, H5'/6'), 7.21 (1H, td, *J* = 7.4, 1.1 Hz, H5'/6'), 6.23 (1H, tt, *J* = 1.8, 1.8 Hz, H2'), 3.35 (2H, dt, *J* = 1.8, 1.8 Hz, H3'), 2.63-2.67 (2H, m, H1), 2.41 (2H, t, *J* = 7.0 Hz, H3), 2.28 (6H, s, H4), 1.90 (2H, pentet, *J* = 7.0 Hz, H2).

¹³C NMR (75 MHz, CDCl₃): δ / ppm = 145.47 (C, C1'/3a/7a), 144.50 (C, C1'/3a/7a), 142.27 (C, C1'/3a/7a), 127.74 (CH, C4'/5'/6'/7'), 126.00 (CH, C4'/5'/6'/7'), 124.50 (CH, C4'/5'/6'/7'), 123.73 (CH, C4'/5'/6'/7'), 118.97 (CH, C2'), 59.75 (CH₂, C1), 45.61 (2 x CH₃, C4), 37.72 (CH₂, C3'), 26.15 (CH₂, C2/3), 25.55 (CH₂, C2/3).

LRMS (CI): *m/z* = 202 ([M+H]⁺, 100%).

8.6.1.18 [3-(3*H*-Inden-1-yl)-propyl]-methyl-amine, 617.

8.6.1.18 was prepared according to the procedures described for 8.6.1.16 and 8.6.1.17 by reaction of 3-(3-bromo-propyl)-1*H*-indene, (0.236 g, 1 mmol, 1.0 eq) 613, was added methylamine (2.0 M soln. in MeOH. 0.75 ml, 1.5 mmol, 1.5 eq) dropwise. Kugelrohr distillation (90 °C, 11 mmHg) yielded the title compound as a yellow oil (0.099 g, 0.5 mmol, 53 %).



IR (cm⁻¹ thin film): 3035 (w), 2933 (m), 2880 (m), 2841 (m), 1609 (w) 1460 (m), 1304 (w), 962 (w), 796 (s), 718 (w).

¹H NMR (300 MHz, CDCl₃): δ / ppm = 7.47 (1H, d, J = 7.4 Hz, H4'/7'), 7.39 (1H, d, J = 7.4 Hz, H4'/7'), 7.31 (1H, td, J = 7.4, 1.1 Hz, H5'/6'), 7.21 (1H, td, J = 7.4, 1.1 Hz, H5'/6'), 6.23 (1H, tt, J = 1.8, 1.8 Hz, H2'), 3.35 (2H, dt, J = 1.8, 1.8 Hz, H3'), 2.70 (2H, t, J = 7.0 Hz, H1), 2.56-2.65 (2H, m, H3), 2.47 (3H, s, H4), 1.91 (2H, pentet, J = 7.0 Hz, H2), 1.62 (1H, br s, NH).

¹³C NMR (75 MHz, CDCl₃): δ / ppm = 145.39 (C, C1'/3a/7a), 144.49 (C, C1'/3a/7a), 144.09 (C, C1'/3a/7a), 127.84 (CH, C4'/5'/6'/7'), 125.98 (CH, C4'/5'/6'/7'), 124.51 (CH, C4'/5'/6'/7'), 123.74 (CH, C4'/5'/6'/7'), 118.94 (CH, C2'), 51.97 (CH₂, C1), 37.71 (CH₂, C3'), 36.50 (CH₃, C4), 28.13 (CH₂, C2/3), 25.47 (CH₂, C2/3).

LRMS (CI): m/z = 188 ([M+H]⁺, 100%).

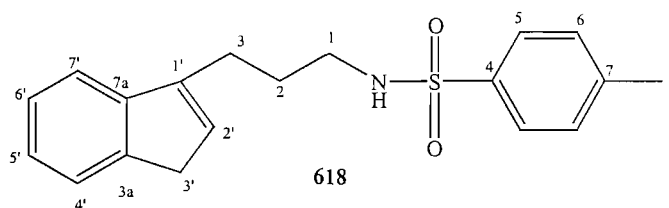
HRMS (ES⁺): C₁₃H₁₇N requires m/z 188.1434, found 188.1432 [M+H]⁺.

8.6.1.19 *N*-[3-(3*H*-Inden-1-yl)-propyl]-4-methyl-benzenesulfonamide, 618.

To a stirred solution of NaH (1.33 g, 39 mmol, 4.0 eq) in DMF (10 mL) 0 °C was added *p*-toluenesulfonamide (6.67 g, 39 mmol, 4.0 eq) in dry DMF (50 mL) dropwise.

The reaction was left to stir for 15 mins, then 3-(3-Bromo-propyl)-1H-indene, **613** (2.3 g, 9.75 mmol, 1.0 eq) in DMF (50 mL) was added dropwise. After 3 h, the reaction was quenched with of methanol (20 mL) and water (20 mL). Diethyl ether (50 mL) was then added and the aqueous phase was separated and extracted with diethyl ether (3 x 30 mL). The combined organics were then extracted with 2.0 M NaOH (3 x 20 mL), washed with water (20 mL), dried over MgSO₄ and the solvents removed. The title compound was isolated using flash column chromatography (SiO₂, 30% diethyl ether/petrol, R_f = 0.2) as a white solid (1.8 g, 5 mmol, 58%).¹³⁰

m.p. = 79-80 °C.



IR (cm⁻¹ thin film): 3281 (m), 3064 (w), 2940 (s), 2882 (s), 1598 (w) 1428 (w), 1325 (s), 1159 (s), 966 (m), 719 (w).

¹H NMR (300 MHz, CDCl₃): δ / ppm = 7.78 (2H, d, *J* = 8.5 Hz, H5), 7.46 (1H, d, *J* = 7.4 Hz, Ar), 7.16-7.31 (5H, m, Ar), 6.15 (1H, tt, *J* = 2.0, 2.0 Hz, H2'), 5.02 (1H, t, *J* = 6.3 Hz, NH), 3.31 (2H, d, *J* = 2.0 Hz, H3'), 3.04 (2H, dt, *J* = 7.0, 7.0 Hz, H1), 2.51-2.60 (2H, m, H3), 2.43 (3H, s, H8), 1.86 (2H, pentet, *J* = 7.4 Hz, H2).

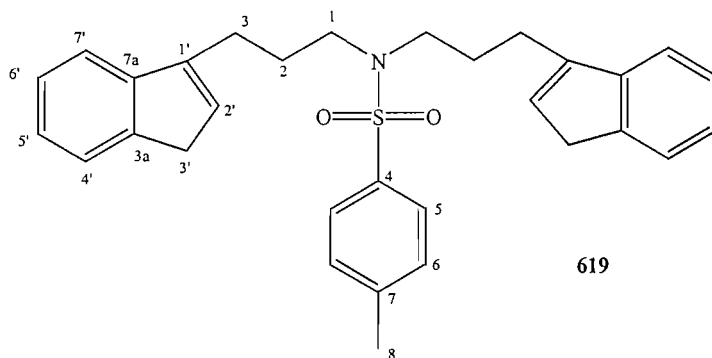
¹³C NMR (75 MHz, CDCl₃): δ / ppm = 144.98 (C, C1/3a/7a), 144.43 (C, C1'/3a/7a), 143.39 (C, C1'/3a/7a), 142.95 (C, C7), 136.89 (C, C4), 29.73 (2 x CH, C6), 128.44 (CH, C4'/5'/6'/7'), 127.11 (2 x CH, C5), 126.03 (CH, C4'/5'/6'/7'), 124.65 (CH, C4'/5'/6'/7'), 123.80 (CH, C4'/5'/6'/7'), 118.86 (CH, C2'), 42.94 (CH₂, C1), 37.72 (CH₂, C3'), 27.72 (CH₂, C2/3), 24.63 (CH₂, C2/3), 21.55 (CH₃, C8).

LRMS (CI): *m/z* = 328 ([MH]⁺, 100%); 172 ([MH-C₆H₅NO₂S], 90%)⁺

Anal. Calcd. For C₁₉H₂₁NO₂S : C, 69.69; H, 6.46; N, 4.28; Found: C, 69.50; H, 6.48; N, 4.17.

8.6.1.20. *N,N*-Bis-[3-(3*H*-inden-1-yl)-propyl]-4-methyl-benzenesulfonamide, 619.

The *bis*-indenyl ligand was also isolated as a white solid in 15 % yield (0.072 g, 1.5×10^{-4} mol).



IR (cm⁻¹ thin film): 3062 (w), 3016 (w), 2929 (s), 2879 (s), 1597 (w) 1460 (w), 1338 (s), 1158 (s).

¹H NMR (300 MHz, CDCl₃): δ / ppm = 7.68 (2H, d, J = 8.5 Hz, H5), 7.47 (2H, d, J = 7.4 Hz, Ar), 7.19-7.30 (8H, m, Ar), 6.19 (2H, tt, J = 1.8, 1.8 Hz, H2'), 3.33 (4H, 2 x dt, J = 1.8, 1.8 Hz, H3'), 3.26 (4H, t, J = 7.4 Hz, H1), 2.49-2.57 (4H, m, H3), 2.42 (3H, s, H8), 1.94 (4H, pentet, J = 7.4 Hz, H2).

¹³C NMR (100 MHz, CDCl₃): δ / ppm = 144.10 (2 x C, C1'/3a/7a), 143.42 (2 x C, C1'/3a/7a), 142.18 (2 x C, C1'/3a/7a), 141.89 (C, C7), 135.95 (C, C4), 128.59 (2 x CH, C6), 127.14 (2 x CH, C4'/5'/6'/7'), 126.10 (2 x CH, C5), 125.00 (2 x CH, C4'/5'/6'/7'), 123.61 (2 x CH, C4'/5'/6'/7'), 122.76 (2 x CH, C4'/5'/6'/7'), 117.81 (2 x CH, C2'), 47.05 (2 x CH₂, C1), 36.71 (2 x CH₂, C2'), 25.83 (2 x CH₂, C2/3), 23.79 (2 x CH₂, C2/3), 20.44 (CH₃, C8).

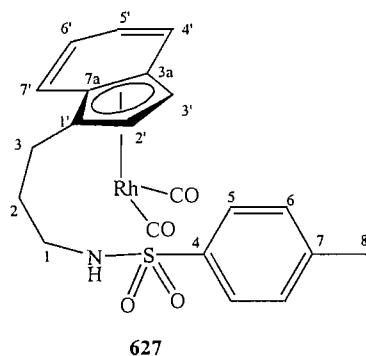
LRMS (ES⁺): m/z = 522.5 ([M+K]⁺, 25%); 284 ([M+K)-C₁₉H₁₀]⁺, 100%).

Anal. Calcd. For C₃₁H₃₃NO₂S : C, 76.98; H, 6.88, N, 2.89; Found: C, 76.64; H, 6.53; N, 2.59.

8.6.1.21. *rac*-(η^5 : η^1)-Indenyl-CH₂CH₂CH₂ NHTsRh^I (CO)₂, 627.

To a stirred solution of *N*-[3-(3*H*-Inden-1-yl)-propyl]-4-methyl-benzenesulfonamide, **618** (0.196 g, 0.6 mmol, 1.0 eq) in THF (2 mL) at 0 °C in the dark, was added *n*-BuLi

(0.24 mL, 0.6 mmol, 1.0 eq) dropwise. The reaction was stirred at 0 °C for 15 mins and then left to warm to RT. After 2 h, this solution was then transferred slowly *via* cannula, to a cooled solution of [RhCl(CO)₂]₂ (0.24 g, 0.6 mmol, 1.0 eq) in THF (2 mL) at 0 °C. The reaction was stirred at 0 °C for 15 mins and then left to warm to RT. After 2 h, solvents were removed and the title complex was isolated by flash column chromatography (SiO₂, 50% ether/petrol, R_f = 0.3) as a yellow oil (0.13 g, 0.36 mmol, 45%).



IR (cm⁻¹): 3271 (br), 3061 (w), 2921 (s), 2855 (s), 2035 (s), 1974 (s), 1597 (w), 1423 (w), 1323 (m), 1160 (s), 815 (w).

¹H NMR (400 MHz, C₆D₆): δ / ppm = 7.69 (2H, d, *J* = 8.4 Hz, H5), 6.96-7.11 (4H, m, Ar), 6.85 (2H, d, *J* = 8.0 Hz, Ar), 5.61 (1H, d, *J* = 3.0 Hz, Cp-H), 5.12 (1H, t, *J* = 3.0 Hz, Cp-H), 4.60 (1H, t, *J* = 6.0 Hz, NH), 2.72 (2H, dt, *J* = 6.5, 6.5 Hz, H3), 2.37 (1H, ddd, *J* = 14.8, 9.0, 6.0 Hz, H2-a), 2.30 (1H, ddd, *J* = 14.8, 9.0, 7.0 Hz, H2-b), 2.16 (3H, s, CH₃), 1.49 (1H, ddd, *J* = 13.8, 9.0, 7.0 Hz, H1-a), 1.41 (1H, ddd, *J* = 13.8, 9.0, 6.7 Hz, H1-b).

¹³C NMR (100 MHz, C₆D₆): δ / ppm = 192.07 (C, s, CO), 191.21 (C, s, CO), 143.68 (C, s, C7), 139.07 (C, s, C4), 130.14 (2 x CH, s, C6), 128.68 (C, s, C1'), 127.86 (2 x CH, s, C5), 125.87 (CH, s, C4'/5'/6'/7'), 125.687 (CH, s, C4'/5'/6'/7'), 118.71 (C, s, C3a/7a), 119.96 (CH, s, C4'/5'/6'/7'), 117.96 (CH, s, C4'/5'/6'/7'), 98.40 (C, d, *J* = 3.3 Hz, C3a/7a), 98.10 (CH, d, *J* = 6.3 Hz, C2/3), 72.62 (CH, d, *J* = 3.9 Hz, C2/3), 43.54 (CH₂, s, C1), 31.43 (CH₂, s, C2), 24.91 (CH₂, s, C3), 21.77 (CH₃, s, C8).

LR-MS (ES⁺): *m/z* = 428 ([M 2CO]⁺, 46%); 276 ([M-C₉H₇SO₄]⁺, 100%).

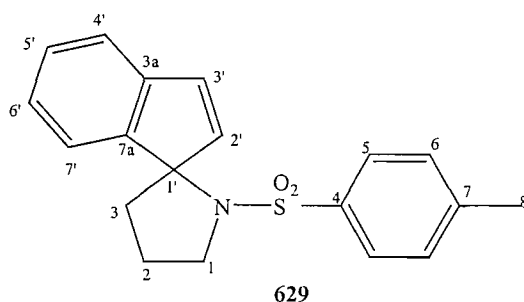
Anal. Calcd. For $C_{21}H_{20}NSO_4Rh$: C, 52.35; H, 4.18, N, 2.91; Found: C, 52.16; H, 4.30; N, 2.80.

8.6.1.22. N-[(4-methylphenyl)-sulfonyl]-2-spiro[1-indene-pyrrolidine], 629.

To a stirred solution of I_2 (0.05 g, 0.2 mmol, 1.0 eq) in THF (1 mL) at 0 °C and in the dark, was added **627** (0.1 g, 0.2 mmol, 1.0 eq) in THF (1 mL) dropwise. The reaction was stirred at 0 °C for 15 mins and then left to warm to RT. After 2 h, the solvents were removed and the title spirocycle was isolated by flash chromatography (SiO₂, 50 % ether/petrol, $R_f = 0.25$) as a yellow oil. Trituration from hexane gave a white solid. (0.02 g, 0.07 mmol, 35%).

m.p. = 135-137 °C

X-ray quality crystals were obtained by slow evaporation of an ethanol solution of **629**. Crystallographic analysis has confirmed the structure is as shown (Appendix 11).



IR (cm⁻¹): 3065 (w), 2975 (m), 2877 (m), 1598 (w), 1463 (w), 1342 (s), 1156 (s), 1096 (s), 751 (m).

¹H NMR (400 MHz, C₆D₆): δ / ppm = 7.60 (2H, d, $J = 8.4$ Hz, H6), 7.12 (2H, d, $J = 7.0$ Hz, Ar), 6.85-6.91 (1H, m, Ar), 6.76 (3H, m, Ar), 6.55 (1H, $J = 5.5$ Hz, H2'/3'), 6.29 (1H, t, $J = 5.5$ Hz, H2'/3'), 3.73 (1H, dt, $J = 7.8, 7.0$ Hz, H1-a), 3.69 (1H, dt, $J = 7.8, 7.0$ Hz, H1-b), 2.39 (3H, s, CH₃), 1.61-1.69 (2H, m, H3), 1.54-1.65 (2H, m, H2).

¹³C NMR (100 MHz, CDCl₃): δ / ppm = 148.35 (C, C3a/7a), 143.17 (C, C3a/7a), 142.37 (CH, C2'/3'), 138.67 (C, C7), 130.36 (CH, C2'/3'), 129.64 (2 x CH, C6), 138.67 (C, C4), 128.99 (CH, C4'/5'/6'/7'), 128.46 (2 x CH, C5), 126.23 (CH, C4'/5'/6'/7'), 123.05 (CH, C4'/5'/6'/7'), 122.36 (CH, C4'/5'/6'/7'), 76.72 (C, C1'), 50.58 (CH₂, C1), 38.72 (CH₂, C3), 24.01 (CH₂, C2), 21.70 (CH₃, C8).

LR-MS (ES⁺): $m/z = 326$ ([MH]⁺, 56%); 235 ([MH-C₇H₇]⁺, 100%).

Anal. Calcd. For C₁₉H₁₉NO₂S: C, 70.13; H, 5.88; N, 4.30; Found: C, 69.95; H, 5.71; N, 4.20.

Chapter 9:References.

- Kealy, T. J.; Pauson, P. L. *Nature* **1951**, 168, 1039-1040.
- (2) Halterman, R. L. *Chem. Rev.* **1992**, 92, 965-994.
- (3) Cessaroti, E.; Kagan, H. B.; Goddard, R.; Kruger, C. *J. Organomet. Chem.* **1978**, 178, 297-308.
- (4) Wild, F. W. R. P.; Wasiucionek, M.; Huttner, G.; Brintzinger, H. H. *J. Organomet. Chem.* **1985**, 288, 63-67.
- (5) Wild, F. W. R. P.; Zsolnai, L.; Huttner, G.; Brintzinger, H. H. *J. Organomet. Chem.* **1982**, 232, 233-247.
- (6) Morken, J. P.; Diduik, M. T.; Hoveyda, A. H. *J. Am. Chem. Soc.* **1993**, 115, 6997-6998.
- (7) Bell, L.; Brookings, D. C.; Dawson, G. J.; Whitby, R. J.; Jones, R. V. H.; Standen, M. C. H. *Tetrahedron.* **1998**, 54, 14617-14634.
- (8) Onitsuka, K.; Dodo, N.; Matsushima, Y.; Takahashi, S. *Chem. Comm.* **2001**, 521-522.
- (9) Bell, L.; Whitby, R. J.; Jones, R. V. H.; Standen, M. C. H. *Tetrahedron. Lett.* **1996**, 37, 7139-7142.
- (10) Dawson, G.; Durrant, C. A.; Kirk, G. G.; Whitby, R. J.; Jones, R. V. H.; Standen, M. C. H. *Tetrahedron. Lett.* **1997**, 38, 2335-2338.
- (11) Green, S. M. Ph.D. Thesis. The University of Southampton, **1999**.
- (12) Brookings, D. C.; Ph.D. Thesis. The University of Southampton, **1999**.
- (13) Harrison, S. A. Ph.D. Thesis, The University of Southampton, **2002**.
- (14) Jutzi, P.; Redeker, T. *Eur. J. Inorg. Chem.* **1998**, 663-674.
- (15) Jutzi, P.; Siemeling, U. *J. Organomet. Chem.* **1995**, 500, 175-185.
- (16) Siemeling, U. *Chem. Rev.* **2000**, 100, 1495-1526.
- (17) Butenschon, H. *Chem Rev.* **2000**, 100, 1527-1564.
- (18) Vollhardt, K. P. C.; Halterman, R. L.; *Organometallics* **1988**, 7, 883-892.
- (19) Vollhardt, K. P. C.; Halterman, R. L.; *Tetrahedron Lett.* **1986**, 27, 1461-1464.
- (20) McLaughlin, M. L.; McKinney, J. A.; Paquette, L. A. *Tetrahedron Lett.* **1986**, 27, 5595-5598.
- (21) Moriarty, K. J.; Rogers, R. D.; Paquette, L. A. *Organometallics* **1989**, 8, 1512-1517.

- (22) LoCoco, M.D.; Jordan, R.F. *J. Am. Chem. Soc.* **2004**, *126*, 13918-13919.
- (23) Zhang, X.; Zhu, Q.; Guzei, A.I.; Jordan, R.F. *J. Am. Chem. Soc.* **2000**, *122*, 8093-8094.
- (24) LoCoco, M.D.; Jordan, R.F. *Organometallics* **2003**, *22*, 5498-5503.
- (25) Price, D.; Simpkins, N. S. *Tetrahedron. Lett.* **1995**, *36*, 6135-6136.
- (26) Wang, T-F.; Juang, J-P.; Wen, Y-S. *J. Organomet. Chem.* **1995**, *503*, 117-128.
- (27) Esteruelas, M.A.; Lopez, A. N.; Onate, E.; Royo, E. *Organometallics* **2004**, *23*, 3021-3030.
- (28) Kauffmann, T.; Olbrich, J. *Tetrahedron Lett.* **1984**, *25*, 1967-1970.
- (29) Trost, B. M.; Vidal, B.; Thommen, M. *Chem. Eur. J.* **1999**, *5*, 1055-1069.
- (30) Slawin, A. M. Z.; Williams, D.L.; Crosby, J.; Ramsden, J. A.; White, C. J. *Chem. Soc. Dalton. Trans.* **1988**, 2491-2494.
- (31) Dodo, N.; Matsushima, Y.; Uno, M.; Onitsuka, K.; Takahashi, S. *J. Chem. Soc., Dalton Trans.*, **2000**, 35-41.
- (32) Komatsuzaki, N.; Uno, M.; Kikuchi, H.; Takahashi, S. *Chem. Lett.* **1996**, 677-678.
- (33) Matsushima, Y.; Onitsuka, K.; Takahashi, S. *Chem. Lett.* **2000**, 760-761.
- (34) Matsushima, Y.; Onitsuka, K.; Takahashi, S. *Organometallics* **2004**, *23*, 2439-2446.
- (35) Matsushima, Y.; Onitsuka, K.; Kondo, T.; Mitsudo, T.; Takahashi, S. *J. Am. Chem. Soc.* **2001**, *123*, 10405-10406.
- (36) Kataoka, Y.; Saito, Y.; Nagata, K.; Kitmura, K.; Shibahara, A.; Tani, K. *Chem. Lett.* **1995**, 833-834.
- (37) Gorman, J. S. T.; Lynch, V.; Pagenkopf, B. L.; Young, B. *Tetrahedron. Lett.* **2003**, *44*, 5435-5439.
- (38) Brookings, D. C.; Harrison, S. A.; Whitby, R. J.; Crombie, B.; Jones, R. V. H. *Organometallics* **2001**, *20*, 4574-4583.
- (39) Nakatsuji, Y.; Nakamura, T.; Yonetani, M.; Yuya, H.; Okahara, M. *J. A. Chem. Soc.* **1988**, *110*, 531-538.
- (40) Hoffmann, R.W. *Chem. Rev.* **1989**, *89*, 1841-1860.
- (41) Mao, J. M.; Baker, D.C.; *Org. Lett.* **1999**, *1*, 841-843.
- (42) Murata, K.; Ikariya, T.; Noyori, R. *J. Org. Chem.* **1999**, *64*, 2186-2187.
- (43) Jutzi, P.; Dalhaus, J.; Kristen, M. O. *J. Organomet. Chem.* **1993**, C1-C3.

- (44) Jiminez-Tenorio, M.; Puetra, M.C.; Valgera, P. *Eur. J. Inorg. Chem.* **2004**, 17-32.
- (45) Jonas, K.; Klusmann, P.; Goddard, R. *Z. Naturforsch., B; Chem. Sci.* **1995**, 50, 394-404.
- (46) Chu, H.S.; Lau, C.P.; Wong, K.Y. *Organometallics* **1998**, 17, 2768-2777.
- (47) Ayllon, J.A.; Sayers, S.F.; Sabo-Etienne, S.; Donnadiou, B.; Chaudret, B. *Organometallics* **1999**, 18, 3981-3990.
- (48) Esteruelas, M.A.; Lopez, A.M.; Onate, E.; Royo, E. *Organometallics* **2004**, 23, 5633-5636.
- (49) Jutzi, P.; Kristen, M. O.; Dahlhaus, J.; Neumann, B.; Stammler, H-G. *Organometallics* **1993**, 12, 2980-2985.
- (50) Jutzi, P.; Kristen, M. O.; Neumann, B.; Stammler, H-G. *Organometallics* **1994**, 13, 3854-3861.
- (51) Philippopoulos, A. I.; Poilblanc, R.; Hadjiliadis, N. *Inorg. Chim. Acta* **1998**, 283, 24-29.
- (52) McGowan, P.C.; Hart, C. E.; Donnadiou, B.; Poilblanc, R. *J. Organomet. Chem.* **1997**, 528, 191-194.
- (53) Philippopoulos, A. I.; Hadjiliadis, N.; Hart, C. E.; Donnadiou, B.; McGowan, P.C.; Poilblanc, R. *Inorg. Chim. Acta* **1997**, 36, 1842-1849.
- (54) Philippopoulos, A. I.; Bay, R.; Poilblanc, R.; Hadjiliadis, N. *Inorg. Chim. Acta* **1998**, 37, 4822-4827.
- (55) Enders, M.; Ludwig, G.; Pritzkow, H. *Organometallics* **2001**, 20, 827-833.
- (56) Enders, M.; Kohl, H.J.; Pritzkow, H. *J. Organomet. Chem.* **2004**, 689, 3024-3030.
- (57) Paisner, S. N.; Lavoie, G. G.; Bergman, R.G. *Inorg. Chim. Acta* **2002**, 334, 253-275.
- (58) Adams, H.; Bailey, N.A.; Colley, N.; Schofield, P.A.; White, C. *J. Chem. Soc. Dalton Trans.* **1994**, 1445-1451.
- (59) Kataoka, Y.; Nagakawa, Y.; Shibahara, A.; Yamagata, T.; Mashima, K.; Tani, K. *Organometallics* **2004**, 23, 2095-2099.
- (60) Blais, M.S.; Chien, J. C. W.; Rausch, M. D. *Organometallics* **1998**, 17, 3775-3783.
- (61) Leino, R.; H, Lehmus, P.; Lehtnon, A. *Eur. J. Inorg. Chem.* **2004**, 3201-3204.
- (62) Douglass, M. R.; Marks, T. J. *J. Am. Chem. Soc.* **2000**, 122, 1824-1825.

- (63) Sheng, E.; Wang, S.; Yang, G.; Zhou, S.; Cheng, L.; Zang, K.; Huang, Z. *Organometallics* **2003**, *22*, 684-692.
- (64) Rerek, M.E.; Ji, L.N.; Basolo, F. *J. Chem. Soc. Chem. Comm.* **1983**, 1208-1209.
- (65) Cramer, R.; Seiwel, L. P. *J. Organomet. Chem.* **1975**, *92*, 245-252.
- (66) Rerek, M. E.; Basolo, F. *J. Am. Chem. Soc.* **1984**, *106*, 5908-5912.
- (67) Kataoko, Y.; Shibahara, A.; Saito, Y.; Yamagata, T.; Tani, K. *Organometallics* **1998**, *17*, 4338-4340.
- (68) Arad Yellin, R.; Green, B. S.; Muszkat, K. A. *J. Org. Chem.* **48**, 2578-2583.
- (69) Hosangadi, B. D.; Dave, R. H. *Tetrahedron. Lett.* **1996**, *37*, 6375-6378.
- (70) Pellon, P. *Tetrahedron. Lett.* **1992**, *33*, 4451-4452.
- (71) Inamoto, T.; Oshiki, T.; Onozanwa, T.; Kusumoto, T.; Sato, K. *J. Org. Chem.* **1990**, *112*, 5244-5252.
- (72) Langer, F.; Puntener, K.; Sturmer, R.; Knochel, P. *Tetrahedron: Asym.* **1997**, *8*, 715-738.
- (73) Pellon, P.; Le. Goaster, C.; Toupet, L. *Tetrahedron Lett.* **1996**, *37*, 27, 4713-4716.
- (74) Pugh, D. C. M.Phil. Thesis, The University of Southampton, **2005**.
- (75) Crispiro, G. A.; Jeong, K-S.; Klob, H. C.; Wang, Z-M.; Xu, D.; Sharpless, K, B. *J. Org. Chem.* **1993**, *58*, 3785-3786.
- (76) Vandewalle, M. van der Eycken. J.; Oppolzer, W.; Vullioud, C. *Tetrahedron.* **1986**, *42*, 4035-4043.
- (77) Wu, M-J.; Wu, C-C.; Lee, P-C. *Tetrahedron Lett.* **1992**, *33*, 2547-2548.
- (78) Oppolzer, W.; Poli, G.; Kingma, A.J.; Starkemann, C.; Bernardinelli, G. *Helv. Chim. Acta.* **1987**, *70*, 2201-2214.
- (79) Oppolzer, W.; Chapuis, C.; Kelly, M. J. *Helv. Chim. Acta* **1983**, *66*, 2358-2361.
- (80) Oppolzer, W.; Chapuis, C.; Bernardinelli, G. *Tetrahedron Lett.* **1984**, *25*, 5885-5888.
- (81) Oppolzer, W.; Dudfield, P.; Stevenson, T.; Godel, T. *Helv. Chim. Acta.* **1985**, *68*, 212-215.
- (82) Oppolzer, W.; Dudfield, P. *Helv. Chim. Acta.* **1985**, *68*, 216-219.
- (83) Oppolzer, W.; Moretti, R.; Bernardinelli, G. *Tetrahedron. Lett.* **1986**, *27*, 39, 4713-4716.

- (84) Stoermer, D.; Caron, S.; Heathcock, C. H. *J. Org. Chem.* **1996**, 61, 9115-9125.
- (85) Hernanz, D.; Camps, F.; Guerrero, A.; Delgado, A. *Tetrahedron: Asym.* **1995**, 6, 9, 2291-2298.
- (86) Oppolzer, W.; Moretti, R. *Tetrahedron* **1988**, 44, 17, 5541-5552.
- (87) Oppolzer, W.; Dudfield, P. *Tetrahedron Lett.* **1985**, 26, 41, 5037-5040.
- (88) Davis, F.A.; Boyd, R.; Zhou, P.; Abdul-Malik, N.F.; Carroll, P, J. *Tetrahedron Lett.* **1996**, 37, 19, 3267-3270.
- (89) Corey, E.J.; Boaz, N.W. *Tetrahedron Lett.* **1984**, 25, 29, 3063-3066.
- (90) Yamamoto, Y.; Chounan, Y.; Nishii, S.; Ibuka, T.; Kitahara, H. *J. A. Chem. Soc.* **1992**, 114, 7652-7660.
- (91) Laqua, H.; Fröhlich, R.; Wibbeling, B.; Hoppe, D.; *J. Organomet. Chem.* **2001**, 624, 96-104.
- (92) Burk, M. J.; Harper, T.G.P.; Kalberg, C.S. *J. Am. Chem. Soc.* **1995**, 117, 4423-4424.
- (93) Madec, J.; Pfister, X.; Phansavath, P.; Ratovelomanana-Vidal, V.; Genet, J. P. *Tetrahedron* **2001**, 57, 2563-2568.
- (94) Genet, J. P.; Ratovelomanana-Vidal, V.; Cano de Andrade, M. C.; Pfister, X.; Guerreiro, P.; Lenoir, J. Y. *Tetrahedron Lett.* **1995**, 36, 27, 4801-4804.
- (95) Noyori, R. Ohkuma, T.; Kitamura, M.; Takaya, H.; Sayo, N.; Kumobayashi, H.; Akutagawa, S. *J. Am. Chem. Soc.* **1987**, 109, 5856-5858.
- (96) Oikawa, Y. Sugano, K.; Yonemitsu, O. *J. Org. Chem.* **1978**, 43, 2087-2088.
- (97) Fleming, I. Ramarao, C.; *Chem. Comm.* **1999**, 1113-1114.
- (98) Odenkirk, W.; Whelan, J.; Bosnich, B. *Tetrahedron Lett.* **1992**, 33, 39, 5729-5732.
- (99) MacFarlane, K. S.; Rettig, S. J.; Liu, Z.; James, B. R. *J. Organomet. Chem.* **1998**, 557, 213-219.
- (100) Genet, J. P.; Pinel, C.; Ratovelomanana-Vidal, V.; Mallart, S.; Pfister, X.; Cano de Andrade, M. C.; Laffitte, J. A. *Tetrahedron: Asym.* **1994**, 5, 4, 665-674
- (101) Genet, J. P.; Pinel, C.; Ratovelomanana-Vidal, V.; Mallart, S.; Pfister, X.; Bischoff, L.; Cano de Andrade, M.C.; Darses, S.; Galopin, C.; Laffitte, J. A. *Tetrahedron: Asym.* **1994**, 5, 4, 675-690.
- (102) Ratovelomanana-Vidal, V.; Girard, C.; Touati, R.; Tranchier, J. P.; Ben Hassine, B.; Genet, J. P.; *Adv. Synth. Catal.* **2003**, 345, 261-274.

- (103) Marshall, J. A.; Johns, B. A. *J. Org. Chem.* **2000**, 65, 1501-1510.
- (104) Sodeoka, M.; Yamada, H.; Shibasaki, M. *J. Org. Chem.* **1990**, 112, 4906-4911.
- (105) Faller, J. W.; Smart, C. J. *Tetrahedron Lett.* **1989**, 30, 1189-1192.
- (106) Trost, B. M.; Dyker, G.; Kulawiec, R. J. *J. Am. Chem. Soc.* **1990**, 112, 7809-7811.
- (107) Bruce, M. I.; Hinterding, P.; Low, P. J.; Skelton, B. W.; White, A. H. *J. Chem. Soc., Dalton. Trans.* **1998**, 467-473.
- (108) Slugovc, C. Ruba, E.; Schmid, R.; Kirchner, K. *Organometallics* **1999**, 18, 4230-4233.
- (109) Kakkar, A. K. Taylor, N. J.; Marder, T. B.; Shen, J. K.; Hallinan, N.; Basolo, F. *Inorg. Chim. Acta* **1992**, 200, 219-231.
- (110) Gansow, O. A. Burke, A.R.; Vernon, W. D. *J. Am. Chem. Soc.* **1976**, 98, 5817-5826.
- (111) Lindsay, C.; Cesarotti, E.; Adams, H.; Bailey, N. A.; White, C. *Organometallics* **1990**, 9, 2594-2602.
- (112) Hart-Davis, A. J. White, C.; Mawby, R.J. *Inorg. Chim. Acta* **1970**, 4, 441.
- (113) Habib, A.; Tanke, R. S.; Holt, E. M.; Crabtree, R. H. *Organometallics* **1989**, 8, 1225-1231.
- (114) Bang, H.; Lynch, T.J.; Basolo, F. *Organometallics* **1992**, 11, 40-48.
- (115) Turaki, N. N.; Huggins, J. M.; Lebioda, L. *Inorg. Chem.* **1988**, 27, 424-427.
- (116) Gamasa, M. P.; Gimeno, J.; Gonzalez-Bernardo, C.; Martin-Vaca, B. M.; Monti, D.; Bassetti, M. *Organometallics* **1996**, 15, 302-308.
- (117) Westcott, S. A. Kakkar, A. K.; Stringer, G.; Taylor, N. J.; Marder, T.B. *J. Organomet. Chem.* **1990**, 394, 777-794.
- (118) Tutusaus, O.; Delfosse, S.; Demonceau, A.; Noels, A.F.; Nunez, R.; Vinas, C.; Teixidor, F. *Tetrahedron Lett.* **2002**, 43, 983-987
- (119) Baratta, W.; Herrmann, W. A.; Kratzer, R.M.; Rigo, P. *Organometallics* **2000**, 19, 3664-3669.
- (120) Morisaki, Y.; Kondo, T.; Mitsudo, T. *Organometallics* **1999**, 18, 4742-4746.
- (121) Magee, M.P.; Norton, J.P. *J. Am. Chem. Soc.* **2001**, 123, 1778-1779.
- (122) Kundig, E.P.; Saudan, C.M.; Alezra, V.; Viton, F.; Bernardinelli, G. *Agnew. Chem. Int. Ed.* **2001**, 40, 4481-4485.

- (123) Lee, D.; Huh, E.A.; Kim, M.-J.; Jung, H.M.; Koh, J.H.; Park, J. *Org. Lett.* **2000**, *2*, 2377-2379.
- (124) Blacker, A. J.; Mellor, B. J. Zeneca, PCT WO 98/42643.
- (125) Thorpe, T.; Blacker, A. J.; Brown, S. M.; Bubert, C.; Crosby, J.; Fitzjohn, S.; Muxworthy, J. P.; Williams, J. M. J. *Tetrahedron. Lett.* **2001**, *42*, 4041-4043.
- (126) Cross, D. J.; Kenny, J. A.; Houson, I.; Campbell, L.; Walsgrove, T.; Wills, M. *Tetrahedron. Asymmetry.* **2001**, *12*, 1801-1806.
- (127) Vidya Sagar Reddy, G.; Venkat Rao, G.; Subramanyam, R. V. K.; Iyengar, D. S. *Synth. Commun.* **2000**, *30*, 12, 2233-2237.
- (128) Meyers, A. I.; Reuman, M.; Gabel, R. A.; *J. Org. Chem.* **1981**, *46*, 783-788.
- (129) Teubner, A.; Gerlach, H. *Liebigs. Ann. Chem.* **1993**, 161-165.
- (130) Schill, G.; Zuercher, C. *Chem. Ber.* **1997**, *116*, 2046-2066.
- (131) Plenio, H.; Diodone, R. *J. Org. Chem.* **1993**, *58*, 6650-6653.
- (132) Lefort, L.; Crane, T.W.; Farwell, M.D; Baruch, D.M.; Kaeuper, J.A.; Lachicotte, R.J.; Jones, W.D. *Organometallics* **1998**, *17*, 3889-3899.
- (133) Kakkar, A.K.; Stringer, G.; Taylor, N.J.; Marder, T.B. *Can. J. Chem.* **1995**, *73*, 981-988.
- (134) Naota, T.; Takaya, H.; Murahashi, S, I. *Chem. Rev.* **1998**, *98*, 2599-2660.
- (135) Perrin, D.D.; Armarego, W. L. F. *Purification of Laboratory Chemicals*; 3rd Edition ed.; Pergammon Press: Oxford, 1988.
- (136) McCleverty, J.A.; Wilkinson, G. *Inorg. Synth.* **1966**, *8*, 211-214.
- (137) Arnold, R. T.; Elmer, D. C.; Dobson, R. M. *J. Am. Chem. Soc.* **1950**, *72*, 4359.
- (138) Balaji, B. S.; Chanda, B. M. *Tetrahedron* **1998**, *54*, 13237-13252.
- (139) Carreira, E.M.; Singer R.A.; Lee, W. *J. Am. Chem. Soc.* **1994**, *116*, 8837-8838.
- (140) Lee, P.H.; Bang, K.; Lee, K.; Sung, S-Y.; Chang, S. *Synth. Commun.* **2001**, *31*, 3781-3790.
- (141) Kowalski, C. J.; Haque, M. S.; Fields, K. W. *J. Am. Chem. Soc.* **1985**, *107*, 1429-1430.
- (142) Corey, E. J. Choi, S. *Tetrahedron. Lett.* **1991**, *32*, 2857-2860.
- (143) Cohen, T. Jeong, I. H.; Mudryk, B.; Bhupathy, M.; Awad, M. M .A.; *J. Org. Chem.* **1990**, *55*, 1528-1536.

(144) Hagemeister, T.; Jutzi, P.; Stammer, A.; Stammer. *Can. J. Chem.* **2003**, *81*, 1255-1262.

The Appendices.

- Appendix 1 X-ray Structure of sultam **308**
- Appendix 2 X-ray Structure of alcohol **312**
- Appendix 3 X-ray Structure of ester **321**
- Appendix 4 X-ray Structure of Michael addition-precursor **320**
- Appendix 5 X-ray Structure of Ruthenium complex (*S*)-**401a**
- Appendix 6 X-ray Structure of Ruthenium complex (*S*)-**401a**
- Appendix 7 X-ray Structure of Ruthenium complex *rac*-**402**
- Appendix 8 X-ray Structure of Ruthenium complex *rac*-**417**
- Appendix 9 X-ray Structure of Ruthenium complex *rac*-**418**
- Appendix 10 X-ray Structure of tosamide *rac*-**608**
- Appendix 11 X-ray Structure of spiro cycle **629**

For appendices **1** and **2**, X-ray structure solutions by R. Whitby.

For appendices **3-11**, X-ray structure solutions by M.Light.

Thanks to Simon Coles and Mark Light for the collection of the X-ray crystal data.

Table 1. Crystal data and structure refinement for 03paw004.

Identification code	03paw004	
Empirical formula	C ₁₉ H ₂₉ N O ₃ S	
Formula weight	351.49	
Temperature	293(2) K	
Wavelength	0.71073 Å	
Crystal system	Orthorhombic	
Space group	P212121	
Unit cell dimensions	a = 7.85390(10) Å	α = 90°.
	b = 12.3204(3) Å	β = 90°.
	c = 18.9170(5) Å	γ = 90°.
Volume	1830.47(7) Å ³	
Z	4	
Density (calculated)	1.275 Mg/m ³	
Absorption coefficient	0.194 mm ⁻¹	
F(000)	760	
Crystal size	0.12 x 0.1 x 0.08 mm ³	
Theta range for data collection	3.26 to 27.48°.	
Index ranges	-10 ≤ h ≤ 9, -15 ≤ k ≤ 15, -24 ≤ l ≤ 24	
Reflections collected	20924	
Independent reflections	4153 [R(int) = 0.0693]	
Completeness to theta = 27.48°	99.4 %	
Absorption correction	None	
Refinement method	Full-matrix least-squares on F ²	
Data / restraints / parameters	4153 / 0 / 311	
Goodness-of-fit on F ²	1.028	
Final R indices [I > 2σ(I)]	R1 = 0.0351, wR2 = 0.0807	
R indices (all data)	R1 = 0.0428, wR2 = 0.0845	
Absolute structure parameter	-0.07(6)	
Largest diff. peak and hole	0.165 and -0.307 e.Å ⁻³	

Table 2. Atomic coordinates ($\times 10^4$) and equivalent isotropic displacement parameters ($\text{\AA}^2 \times 10^3$)

for 03paw004. $U(\text{eq})$ is defined as one third of the trace of the orthogonalized U_{ij} tensor.

	x	y	z	U(eq)
S(1)	4217(1)	6280(1)	9133(1)	30(1)
N(1)	2532(2)	6962(1)	8787(1)	27(1)
O(1)	-325(2)	7129(1)	8782(1)	39(1)
O(3)	4898(2)	5559(1)	8611(1)	41(1)
C(8)	755(2)	5327(1)	8694(1)	29(1)
C(2)	-1116(2)	3660(1)	8716(1)	28(1)
C(6)	-201(2)	1772(2)	8394(1)	32(1)
O(2)	3740(2)	5822(1)	9800(1)	46(1)
C(17)	5111(2)	8710(1)	8134(1)	28(1)
C(7)	-756(2)	4857(1)	8742(1)	31(1)
C(9)	893(2)	6518(1)	8762(1)	30(1)
C(10)	5526(2)	7453(1)	9262(1)	31(1)
C(13)	2066(2)	8847(2)	8253(1)	30(1)
C(11)	4633(2)	8403(1)	8912(1)	26(1)
C(19)	5035(2)	7783(2)	7592(1)	34(1)
C(1)	315(2)	2969(1)	8410(1)	30(1)
C(12)	2704(2)	8150(1)	8877(1)	26(1)
C(14)	3637(2)	9541(1)	8082(1)	30(1)
C(15)	3973(2)	10291(1)	8725(1)	33(1)
C(16)	4745(2)	9509(1)	9287(1)	31(1)
C(18)	6881(2)	9217(2)	8070(1)	37(1)
C(3)	-1613(2)	3262(2)	9459(1)	35(1)
C(4)	-2057(3)	2050(2)	9454(1)	39(1)
C(5)	-639(2)	1377(2)	9135(1)	36(1)

Table 3. Bond lengths [Å] and angles [°] for 03paw004.

S(1)-O(2)	1.4311(14)
S(1)-O(3)	1.4317(14)
S(1)-N(1)	1.6991(14)
S(1)-C(10)	1.7904(18)
N(1)-C(9)	1.400(2)
N(1)-C(12)	1.479(2)
O(1)-C(9)	1.218(2)
C(8)-C(7)	1.324(3)
C(8)-C(9)	1.477(2)
C(8)-H(8)	0.95(2)
C(2)-C(7)	1.503(2)
C(2)-C(1)	1.523(2)
C(2)-C(3)	1.540(2)
C(2)-H(2A)	1.079(19)
C(6)-C(5)	1.522(3)
C(6)-C(1)	1.530(2)
C(6)-H(6E)	1.01(2)
C(6)-H(6A)	0.97(2)
C(17)-C(18)	1.529(2)
C(17)-C(19)	1.537(2)
C(17)-C(14)	1.549(2)
C(17)-C(11)	1.565(2)
C(7)-H(7)	0.981(19)
C(10)-C(11)	1.517(2)
C(10)-H(10B)	0.96(2)
C(10)-H(10A)	0.94(2)
C(13)-C(14)	1.536(2)
C(13)-C(12)	1.543(2)
C(13)-H(13E)	1.01(2)
C(13)-H(13B)	0.969(19)
C(11)-C(16)	1.538(2)
C(11)-C(12)	1.548(2)
C(19)-H(19A)	0.9600
C(19)-H(19B)	0.9600
C(19)-H(19C)	0.9600
C(1)-H(1E)	1.01(2)

C(1)-H(1A)	0.98(2)
C(12)-H(12)	0.956(17)
C(14)-C(15)	1.549(2)
C(14)-H(14)	1.047(19)
C(15)-C(16)	1.558(2)
C(15)-H(15A)	1.00(2)
C(15)-H(15B)	1.01(2)
C(16)-H(16B)	0.97(2)
C(16)-H(16A)	1.012(19)
C(18)-H(18A)	0.9600
C(18)-H(18B)	0.9600
C(18)-H(18C)	0.9600
C(3)-C(4)	1.533(3)
C(3)-H(3E)	0.99(2)
C(3)-H(3A)	0.95(3)
C(4)-C(5)	1.514(3)
C(4)-H(4A)	0.99(2)
C(4)-H(4E)	0.95(2)
C(5)-H(5A)	1.02(2)
C(5)-H(5E)	1.00(2)

O(2)-S(1)-O(3)	117.50(9)
O(2)-S(1)-N(1)	109.33(8)
O(3)-S(1)-N(1)	109.38(8)
O(2)-S(1)-C(10)	110.37(9)
O(3)-S(1)-C(10)	112.30(9)
N(1)-S(1)-C(10)	95.75(8)
C(9)-N(1)-C(12)	118.33(13)
C(9)-N(1)-S(1)	122.38(11)
C(12)-N(1)-S(1)	111.99(11)
C(7)-C(8)-C(9)	119.64(16)
C(7)-C(8)-H(8)	123.0(13)
C(9)-C(8)-H(8)	117.4(13)
C(7)-C(2)-C(1)	114.95(14)
C(7)-C(2)-C(3)	109.29(14)
C(1)-C(2)-C(3)	110.84(15)
C(7)-C(2)-H(2A)	106.2(9)
C(1)-C(2)-H(2A)	109.0(9)

C(3)-C(2)-H(2A)	106.2(9)
C(5)-C(6)-C(1)	110.48(15)
C(5)-C(6)-H(6E)	112.3(12)
C(1)-C(6)-H(6E)	107.3(12)
C(5)-C(6)-H(6A)	109.1(12)
C(1)-C(6)-H(6A)	106.9(11)
H(6E)-C(6)-H(6A)	110.7(16)
C(18)-C(17)-C(19)	106.59(14)
C(18)-C(17)-C(14)	113.87(14)
C(19)-C(17)-C(14)	114.84(14)
C(18)-C(17)-C(11)	113.07(14)
C(19)-C(17)-C(11)	116.05(14)
C(14)-C(17)-C(11)	92.29(12)
C(8)-C(7)-C(2)	126.56(16)
C(8)-C(7)-H(7)	115.3(11)
C(2)-C(7)-H(7)	118.1(11)
O(1)-C(9)-N(1)	118.68(14)
O(1)-C(9)-C(8)	123.97(16)
N(1)-C(9)-C(8)	117.33(15)
C(11)-C(10)-S(1)	107.33(11)
C(11)-C(10)-H(10B)	109.7(13)
S(1)-C(10)-H(10B)	106.3(13)
C(11)-C(10)-H(10A)	114.6(12)
S(1)-C(10)-H(10A)	108.0(11)
H(10B)-C(10)-H(10A)	110.5(18)
C(14)-C(13)-C(12)	102.11(13)
C(14)-C(13)-H(13E)	113.8(11)
C(12)-C(13)-H(13E)	111.5(11)
C(14)-C(13)-H(13B)	112.2(11)
C(12)-C(13)-H(13B)	112.1(11)
H(13E)-C(13)-H(13B)	105.2(16)
C(10)-C(11)-C(16)	117.11(14)
C(10)-C(11)-C(12)	108.40(13)
C(16)-C(11)-C(12)	104.74(13)
C(10)-C(11)-C(17)	119.07(14)
C(16)-C(11)-C(17)	101.89(13)
C(12)-C(11)-C(17)	104.06(13)
C(17)-C(19)-H(19A)	109.5

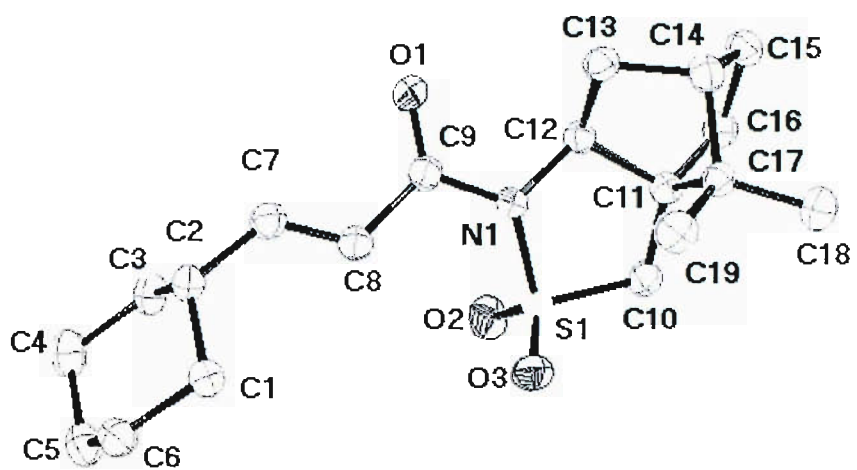
C(17)-C(19)-H(19B)	109.5
H(19A)-C(19)-H(19B)	109.5
C(17)-C(19)-H(19C)	109.5
H(19A)-C(19)-H(19C)	109.5
H(19B)-C(19)-H(19C)	109.5
C(2)-C(1)-C(6)	110.54(15)
C(2)-C(1)-H(1E)	109.8(11)
C(6)-C(1)-H(1E)	110.7(10)
C(2)-C(1)-H(1A)	109.6(11)
C(6)-C(1)-H(1A)	107.3(11)
H(1E)-C(1)-H(1A)	108.8(16)
N(1)-C(12)-C(13)	115.64(14)
N(1)-C(12)-C(11)	107.07(13)
C(13)-C(12)-C(11)	103.81(13)
N(1)-C(12)-H(12)	110.0(10)
C(13)-C(12)-H(12)	109.8(10)
C(11)-C(12)-H(12)	110.2(10)
C(13)-C(14)-C(17)	102.64(13)
C(13)-C(14)-C(15)	107.72(14)
C(17)-C(14)-C(15)	102.55(13)
C(13)-C(14)-H(14)	114.7(11)
C(17)-C(14)-H(14)	111.2(11)
C(15)-C(14)-H(14)	116.5(10)
C(14)-C(15)-C(16)	103.46(14)
C(14)-C(15)-H(15A)	107.5(12)
C(16)-C(15)-H(15A)	110.0(12)
C(14)-C(15)-H(15B)	111.1(11)
C(16)-C(15)-H(15B)	110.4(11)
H(15A)-C(15)-H(15B)	113.8(16)
C(11)-C(16)-C(15)	102.16(13)
C(11)-C(16)-H(16B)	109.7(11)
C(15)-C(16)-H(16B)	113.7(12)
C(11)-C(16)-H(16A)	110.7(11)
C(15)-C(16)-H(16A)	113.0(11)
H(16B)-C(16)-H(16A)	107.5(16)
C(17)-C(18)-H(18A)	109.5
C(17)-C(18)-H(18B)	109.5
H(18A)-C(18)-H(18B)	109.5

C(17)-C(18)-H(18C)	109.5
H(18A)-C(18)-H(18C)	109.5
H(18B)-C(18)-H(18C)	109.5
C(4)-C(3)-C(2)	111.21(15)
C(4)-C(3)-H(3E)	109.9(12)
C(2)-C(3)-H(3E)	108.3(11)
C(4)-C(3)-H(3A)	109.0(13)
C(2)-C(3)-H(3A)	107.2(14)
H(3E)-C(3)-H(3A)	111.2(18)
C(5)-C(4)-C(3)	111.65(16)
C(5)-C(4)-H(4A)	112.6(14)
C(3)-C(4)-H(4A)	107.5(13)
C(5)-C(4)-H(4E)	108.7(14)
C(3)-C(4)-H(4E)	109.9(13)
H(4A)-C(4)-H(4E)	106(2)
C(4)-C(5)-C(6)	110.99(15)
C(4)-C(5)-H(5A)	109.1(11)
C(6)-C(5)-H(5A)	107.3(12)
C(4)-C(5)-H(5E)	108.6(13)
C(6)-C(5)-H(5E)	112.0(12)
H(5A)-C(5)-H(5E)	108.7(17)

Symmetry transformations used to generate equivalent atoms:

Table 4. Anisotropic displacement parameters ($\text{\AA}^2 \times 10^3$) for 03paw004. The anisotropic displacement factor exponent takes the form: $-2 \sum [h^2 a^{*2} U^{11} + \dots + 2 h k a^* b^* U^{12}]$

	U11	U22	U33	U23	U13	U12
S(1)	27(1)	27(1)	35(1)	3(1)	-2(1)	1(1)
N(1)	26(1)	23(1)	33(1)	1(1)	0(1)	1(1)
O(1)	25(1)	32(1)	61(1)	-2(1)	4(1)	1(1)
O(3)	32(1)	34(1)	56(1)	-11(1)	-1(1)	5(1)
C(8)	28(1)	27(1)	33(1)	-2(1)	2(1)	1(1)
C(2)	26(1)	29(1)	30(1)	-1(1)	0(1)	-3(1)
C(6)	36(1)	30(1)	32(1)	0(1)	-6(1)	0(1)
O(2)	47(1)	47(1)	43(1)	19(1)	-3(1)	-5(1)
C(17)	27(1)	31(1)	26(1)	2(1)	1(1)	-1(1)
C(7)	29(1)	31(1)	32(1)	-2(1)	0(1)	1(1)
C(9)	27(1)	30(1)	32(1)	-2(1)	1(1)	-2(1)
C(10)	26(1)	33(1)	34(1)	1(1)	-3(1)	-1(1)
C(13)	27(1)	30(1)	32(1)	0(1)	-4(1)	2(1)
C(11)	26(1)	27(1)	25(1)	0(1)	0(1)	1(1)
C(19)	36(1)	39(1)	27(1)	-2(1)	4(1)	1(1)
C(1)	30(1)	28(1)	31(1)	-1(1)	0(1)	-2(1)
C(12)	26(1)	24(1)	27(1)	-1(1)	1(1)	0(1)
C(14)	32(1)	31(1)	29(1)	2(1)	-3(1)	-2(1)
C(15)	34(1)	27(1)	37(1)	-1(1)	-3(1)	0(1)
C(16)	31(1)	30(1)	32(1)	-4(1)	-4(1)	-2(1)
C(18)	32(1)	41(1)	37(1)	1(1)	5(1)	-4(1)
C(3)	33(1)	39(1)	32(1)	-2(1)	3(1)	-8(1)
C(4)	40(1)	41(1)	37(1)	4(1)	4(1)	-12(1)
C(5)	41(1)	31(1)	36(1)	5(1)	-6(1)	-7(1)



Thermal ellipsoids drawn at the 30% probability level

Table 1. Crystal data and structure refinement for 03paw001

Identification code	03paw001	
Empirical formula	C ₂₂ H ₃₉ N O ₃ S	
Formula weight	397.60	
Temperature	293(2) K	
Wavelength	0.71073 Å	
Crystal system	Monoclinic	
Space group	P2(1)	
Unit cell dimensions	a = 11.1625(8) Å	$\alpha = 90^\circ$.
	b = 17.9654(9) Å	$\beta = 116.947(3)^\circ$.
	c = 12.1670(8) Å	$\gamma = 90^\circ$.
Volume	2175.0(2) Å ³	
Z	4	
Density (calculated)	1.214 Mg/m ³	
Absorption coefficient	0.170 mm ⁻¹	
F(000)	872	
Crystal size	0.12 x 0.10 x 0.08 mm ³	
Theta range for data collection	2.94 to 27.44°.	
Index ranges	-14 ≤ h ≤ 12, -23 ≤ k ≤ 20, -14 ≤ l ≤ 15	
Reflections collected	17412	
Independent reflections	8634 [R(int) = 0.0959]	
Completeness to theta = 27.44°	97.5 %	
Absorption correction	None	
Refinement method	Full-matrix least-squares on F ²	
Data / restraints / parameters	8634 / 1 / 492	
Goodness-of-fit on F ²	1.010	
Final R indices [I > 2σ(I)]	R1 = 0.0662, wR2 = 0.1452	
R indices (all data)	R1 = 0.1041, wR2 = 0.1640	
Absolute structure parameter	-0.01(8)	
Largest diff. peak and hole	0.397 and -0.481 e.Å ⁻³	

Table 2. Atomic coordinates ($\times 10^4$) and equivalent isotropic displacement parameters ($\text{\AA}^2 \times 10^3$)

for 03paw001. $U(\text{eq})$ is defined as one third of the trace of the orthogonalized U^{ij} tensor.

	x	y	z	$U(\text{eq})$
N(1)	3052(3)	737(2)	2995(3)	28(1)
C(15)	-2071(4)	983(2)	2186(3)	31(1)
C(13)	423(4)	888(2)	2589(3)	25(1)
C(14)	-1041(4)	1019(2)	1642(3)	28(1)
C(17)	-1381(4)	1775(2)	929(4)	33(1)
C(16)	-1611(5)	422(2)	614(4)	37(1)
O(3)	1206(3)	695(2)	875(2)	32(1)
O(1)	-766(4)	2408(2)	1664(3)	41(1)
C(19)	-3291(4)	1102(3)	914(4)	40(1)
O(2)	1757(3)	1872(2)	2053(2)	33(1)
C(18)	-3150(5)	471(3)	145(4)	46(1)
C(21)	-1911(5)	1594(2)	3127(4)	35(1)
C(22)	-2077(5)	237(2)	2782(4)	36(1)
C(20)	-2906(5)	1826(3)	464(4)	40(1)
O(1')	-10886(3)	822(2)	-3795(2)	35(1)
O(2')	-9133(3)	814(2)	-4500(2)	32(1)
C(14')	-8670(4)	1976(2)	-2212(3)	30(1)
C(13')	-8393(4)	1150(2)	-2224(3)	30(1)
C(9')	-12297(6)	-1405(4)	-3708(7)	87(2)
C(11')	-11141(12)	-988(3)	-1545(9)	109(4)
C(10')	-12477(11)	-1150(5)	-2604(14)	143(5)
C(20')	-7477(4)	2423(2)	-1197(3)	31(1)
O(3')	-8246(6)	2286(3)	-4010(3)	103(2)
C(21')	-6210(5)	2459(3)	-1377(5)	54(1)
C(17')	-8251(5)	3154(3)	-1495(5)	57(2)
C(22')	-7008(7)	2135(3)	106(4)	59(2)
C(19')	-9032(7)	2434(3)	-3376(5)	79(2)
C(15')	-9802(6)	2130(4)	-1840(7)	89(2)
C(18')	-8751(10)	3244(3)	-2864(6)	133(4)
C(16')	-9448(7)	2914(4)	-1239(9)	123(4)

S(1)	1620(1)	1075(1)	2030(1)	27(1)
S(2)	-9530(1)	651(1)	-3553(1)	27(1)
N(2)	-9252(4)	-217(2)	-3234(3)	31(1)
C(7)	3867(4)	1146(2)	4156(3)	27(1)
C(7')	-10159(4)	-694(2)	-2934(3)	31(1)
C(1)	3486(4)	-22(2)	2855(4)	29(1)
C(1')	-7986(4)	-540(2)	-3131(3)	31(1)
C(12)	5264(4)	1325(2)	4288(4)	33(1)
C(8)	3960(4)	738(3)	5293(3)	36(1)
C(4)	3553(5)	-1467(2)	1764(4)	43(1)
C(5)	4512(5)	-838(3)	1838(4)	42(1)
C(4')	-5958(5)	-1688(3)	-2717(4)	40(1)
C(10)	6172(5)	1360(3)	6591(4)	48(1)
C(9)	4778(5)	1184(3)	6462(4)	48(1)
C(6)	3899(5)	-80(2)	1818(4)	34(1)
C(3')	-5709(5)	-1070(3)	-1800(4)	44(1)
C(6')	-8245(4)	-1156(2)	-4071(4)	36(1)
C(3)	3156(5)	-1399(2)	2792(4)	39(1)
C(5')	-6931(5)	-1446(3)	-4009(4)	43(1)
C(2)	2524(4)	-643(2)	2778(4)	31(1)
C(11)	6073(5)	1770(3)	5463(4)	41(1)
C(2')	-7018(5)	-796(3)	-1841(4)	42(1)
C(8')	-11500(5)	-851(3)	-4045(5)	50(1)
C(12')	-10311(7)	-427(3)	-1816(5)	65(2)

Table 3. Bond lengths [\AA] and angles [$^\circ$] for 03paw001.

N(1)-C(7)	1.483(5)
N(1)-C(1)	1.483(5)
N(1)-S(1)	1.613(3)
C(15)-C(22)	1.525(6)
C(15)-C(21)	1.538(6)
C(15)-C(19)	1.545(5)
C(15)-C(14)	1.566(6)
C(13)-C(14)	1.532(5)
C(13)-S(1)	1.784(4)
C(14)-C(16)	1.548(5)
C(14)-C(17)	1.563(5)
C(17)-O(1)	1.418(5)
C(17)-C(20)	1.533(6)
C(16)-C(18)	1.547(7)
O(3)-S(1)	1.437(3)
C(19)-C(18)	1.522(7)
C(19)-C(20)	1.546(6)
O(2)-S(1)	1.439(3)
O(1')-S(2)	1.439(3)
O(2')-S(2)	1.439(3)
C(14')-C(13')	1.518(6)
C(14')-C(19')	1.525(6)
C(14')-C(15')	1.549(7)
C(14')-C(20')	1.566(6)
C(13')-S(2)	1.780(4)
C(9')-C(8')	1.511(7)
C(9')-C(10')	1.517(14)
C(11')-C(10')	1.492(14)
C(11')-C(12')	1.502(10)
C(20')-C(22')	1.517(6)
C(20')-C(17')	1.523(6)
C(20')-C(21')	1.528(6)
O(3')-C(19')	1.432(9)
C(17')-C(18')	1.507(9)
C(17')-C(16')	1.563(10)
C(19')-C(18')	1.558(8)

C(15')-C(16')	1.553(8)
S(2)-N(2)	1.603(3)
N(2)-C(1')	1.479(6)
N(2)-C(7')	1.492(5)
C(7)-C(12)	1.527(6)
C(7)-C(8)	1.527(5)
C(7')-C(12')	1.522(6)
C(7')-C(8')	1.521(6)
C(1)-C(2)	1.522(6)
C(1)-C(6)	1.531(6)
C(1')-C(6')	1.522(5)
C(1')-C(2')	1.519(6)
C(12)-C(11)	1.526(6)
C(8)-C(9)	1.524(6)
C(4)-C(3)	1.509(7)
C(4)-C(5)	1.532(7)
C(5)-C(6)	1.519(6)
C(4')-C(3')	1.507(6)
C(4')-C(5')	1.515(6)
C(10)-C(11)	1.518(6)
C(10)-C(9)	1.524(7)
C(3')-C(2')	1.521(7)
C(6')-C(5')	1.526(6)
C(3)-C(2)	1.526(6)

C(7)-N(1)-C(1)	118.3(3)
C(7)-N(1)-S(1)	119.0(3)
C(1)-N(1)-S(1)	122.0(3)
C(22)-C(15)-C(21)	107.3(3)
C(22)-C(15)-C(19)	114.0(4)
C(21)-C(15)-C(19)	113.5(4)
C(22)-C(15)-C(14)	113.5(3)
C(21)-C(15)-C(14)	115.2(3)
C(19)-C(15)-C(14)	93.1(3)
C(14)-C(13)-S(1)	114.3(2)
C(13)-C(14)-C(16)	114.2(3)
C(13)-C(14)-C(17)	117.3(3)
C(16)-C(14)-C(17)	104.2(3)

C(13)-C(14)-C(15)	114.4(3)
C(16)-C(14)-C(15)	101.6(3)
C(17)-C(14)-C(15)	103.3(3)
O(1)-C(17)-C(20)	108.9(4)
O(1)-C(17)-C(14)	114.9(3)
C(20)-C(17)-C(14)	102.0(3)
C(18)-C(16)-C(14)	103.9(3)
C(18)-C(19)-C(20)	106.6(4)
C(18)-C(19)-C(15)	102.8(4)
C(20)-C(19)-C(15)	102.2(3)
C(19)-C(18)-C(16)	102.9(4)
C(17)-C(20)-C(19)	105.0(3)
C(13')-C(14')-C(19')	119.2(4)
C(13')-C(14')-C(15')	112.0(4)
C(19')-C(14')-C(15')	105.5(5)
C(13')-C(14')-C(20')	113.9(3)
C(19')-C(14')-C(20')	103.2(3)
C(15')-C(14')-C(20')	101.1(3)
C(14')-C(13')-S(2)	115.9(3)
C(8')-C(9')-C(10')	111.8(6)
C(10')-C(11')-C(12')	114.6(6)
C(11')-C(10')-C(9')	109.9(6)
C(22')-C(20')-C(17')	115.6(4)
C(22')-C(20')-C(21')	105.1(4)
C(17')-C(20')-C(21')	113.0(4)
C(22')-C(20')-C(14')	114.7(3)
C(17')-C(20')-C(14')	93.8(3)
C(21')-C(20')-C(14')	114.8(3)
C(18')-C(17')-C(20')	104.0(4)
C(18')-C(17')-C(16')	109.2(6)
C(20')-C(17')-C(16')	99.1(5)
O(3')-C(19')-C(14')	115.5(5)
O(3')-C(19')-C(18')	109.1(6)
C(14')-C(19')-C(18')	102.3(4)
C(14')-C(15')-C(16')	103.4(5)
C(17')-C(18')-C(19')	104.3(4)
C(15')-C(16')-C(17')	102.4(5)
O(3)-S(1)-O(2)	118.43(16)

O(3)-S(1)-N(1)	107.87(16)
O(2)-S(1)-N(1)	107.37(17)
O(3)-S(1)-C(13)	108.58(17)
O(2)-S(1)-C(13)	105.76(17)
N(1)-S(1)-C(13)	108.50(17)
O(1')-S(2)-O(2')	118.02(16)
O(1')-S(2)-N(2)	109.11(18)
O(2')-S(2)-N(2)	107.23(17)
O(1')-S(2)-C(13')	109.21(19)
O(2')-S(2)-C(13')	105.87(18)
N(2)-S(2)-C(13')	106.85(18)
C(1')-N(2)-C(7')	118.9(3)
C(1')-N(2)-S(2)	118.3(3)
C(7')-N(2)-S(2)	122.6(3)
N(1)-C(7)-C(12)	111.1(3)
N(1)-C(7)-C(8)	112.7(3)
C(12)-C(7)-C(8)	111.0(3)
N(2)-C(7')-C(12')	113.7(4)
N(2)-C(7')-C(8')	113.1(3)
C(12')-C(7')-C(8')	112.9(4)
N(1)-C(1)-C(2)	115.0(3)
N(1)-C(1)-C(6)	113.2(3)
C(2)-C(1)-C(6)	111.6(3)
N(2)-C(1')-C(6')	111.9(3)
N(2)-C(1')-C(2')	114.3(3)
C(6')-C(1')-C(2')	111.1(3)
C(11)-C(12)-C(7)	110.6(3)
C(9)-C(8)-C(7)	111.0(4)
C(3)-C(4)-C(5)	110.6(4)
C(6)-C(5)-C(4)	111.3(4)
C(3')-C(4')-C(5')	111.3(4)
C(11)-C(10)-C(9)	110.8(4)
C(10)-C(9)-C(8)	111.0(4)
C(5)-C(6)-C(1)	110.5(4)
C(4')-C(3')-C(2')	111.2(4)
C(1')-C(6')-C(5')	111.1(4)
C(4)-C(3)-C(2)	111.8(4)
C(4')-C(5')-C(6')	111.7(4)

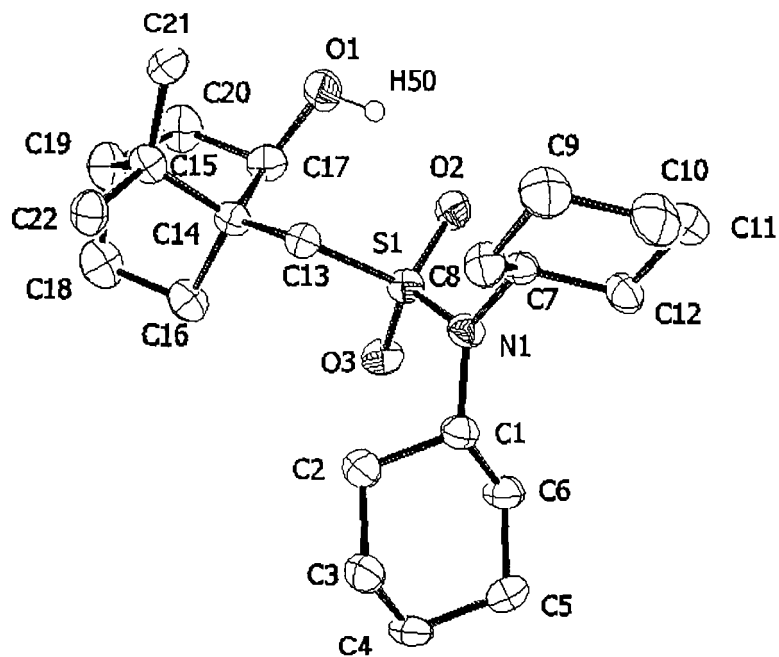
C(1)-C(2)-C(3)	110.0(4)
C(10)-C(11)-C(12)	111.2(4)
C(1')-C(2')-C(3')	110.8(4)
C(9')-C(8')-C(7')	110.1(4)
C(11')-C(12')-C(7')	108.3(5)

Symmetry transformations used to generate equivalent atoms:

Table 4. Anisotropic displacement parameters ($\text{\AA}^2 \times 10^3$) for 03paw004. The anisotropic displacement factor exponent takes the form: $-2 \sum [h^2 a^{*2} U^{11} + \dots + 2 h k a^* b^* U^{12}]$

	U11	U22	U33	U23	U13	U12
N(1)	28(2)	27(2)	24(2)	-5(1)	8(1)	1(1)
C(15)	32(2)	28(2)	28(2)	5(2)	10(2)	1(2)
C(13)	29(2)	26(2)	19(2)	3(1)	12(2)	0(2)
C(14)	33(2)	24(2)	24(2)	1(2)	12(2)	0(2)
C(17)	38(3)	31(2)	30(2)	4(2)	15(2)	5(2)
C(16)	36(3)	38(3)	26(2)	-1(2)	7(2)	-4(2)
O(3)	40(2)	37(2)	21(1)	-1(1)	15(1)	3(1)
O(1)	38(2)	28(2)	57(2)	9(1)	23(2)	2(1)
C(19)	31(2)	49(3)	32(2)	6(2)	7(2)	-1(2)
O(2)	36(2)	29(2)	37(2)	5(1)	20(1)	-1(1)
C(18)	44(3)	49(3)	34(2)	4(2)	8(2)	-5(2)
C(21)	33(2)	36(2)	39(2)	1(2)	19(2)	6(2)
C(22)	36(3)	37(2)	37(2)	7(2)	18(2)	-2(2)
C(20)	40(3)	39(3)	34(2)	20(2)	11(2)	7(2)
O(1')	34(2)	32(2)	38(1)	1(1)	17(1)	1(1)
O(2')	41(2)	31(2)	23(1)	1(1)	14(1)	4(1)
C(14')	29(2)	29(2)	29(2)	0(2)	11(2)	-1(2)
C(13')	37(2)	30(2)	20(2)	-1(2)	11(2)	-2(2)
C(9')	39(3)	62(4)	146(6)	46(4)	30(4)	-5(3)
C(11')	223(11)	41(4)	170(8)	43(4)	182(9)	49(5)
C(10')	139(9)	73(5)	317(15)	80(8)	191(11)	40(6)
C(20')	39(3)	24(2)	25(2)	-2(2)	10(2)	-7(2)
O(3')	187(6)	84(3)	30(2)	-10(2)	43(3)	-87(3)

C(21')	45(3)	60(3)	59(3)	-19(3)	26(3)	-23(3)
C(17')	44(3)	28(3)	71(3)	-16(2)	0(3)	7(2)
C(22')	95(5)	52(3)	27(2)	-8(2)	25(3)	-30(3)
C(19')	108(5)	33(3)	30(3)	9(2)	-25(3)	-4(3)
C(15')	45(4)	87(5)	136(6)	-76(4)	44(4)	-19(3)
C(18')	184(9)	23(3)	61(4)	7(3)	-59(5)	-2(4)
C(16')	39(4)	102(6)	207(9)	-109(6)	37(5)	-11(4)
S(1)	34(1)	27(1)	23(1)	2(1)	15(1)	2(1)
S(2)	34(1)	23(1)	22(1)	1(1)	10(1)	2(1)
N(2)	33(2)	26(2)	33(2)	2(1)	14(2)	4(2)
C(7)	31(2)	27(2)	25(2)	-4(2)	15(2)	1(2)
C(7')	39(3)	27(2)	31(2)	3(2)	19(2)	4(2)
C(1)	31(3)	27(2)	29(2)	-4(2)	12(2)	1(2)
C(1')	30(2)	27(2)	33(2)	-2(2)	11(2)	0(2)
C(12)	38(3)	27(2)	36(2)	-2(2)	19(2)	-7(2)
C(8)	40(2)	45(3)	28(2)	-1(2)	19(2)	-4(2)
C(4)	40(3)	28(2)	58(3)	-15(2)	21(2)	2(2)
C(5)	40(3)	41(3)	54(3)	-8(2)	29(2)	5(2)
C(4')	33(3)	37(3)	49(3)	5(2)	18(2)	3(2)
C(10)	46(3)	59(3)	31(2)	-12(2)	10(2)	-10(2)
C(9)	54(3)	58(3)	29(2)	-8(2)	18(2)	-5(2)
C(6)	41(3)	30(2)	37(2)	-5(2)	21(2)	2(2)
C(3')	36(3)	37(3)	46(2)	-2(2)	7(2)	1(2)
C(6')	34(2)	38(2)	30(2)	-8(2)	11(2)	-1(2)
C(3)	34(3)	28(2)	51(3)	-2(2)	16(2)	0(2)
C(5')	44(3)	46(3)	42(2)	-1(2)	22(2)	3(2)
C(2)	33(2)	29(2)	32(2)	-2(2)	15(2)	-2(2)
C(11)	43(3)	35(2)	43(2)	-10(2)	18(2)	-7(2)
C(2')	43(3)	37(3)	32(2)	-4(2)	5(2)	3(2)
C(8')	36(3)	42(3)	67(3)	14(2)	18(3)	-7(2)
C(12')	128(6)	36(3)	62(3)	11(2)	69(4)	21(3)



Thermal ellipsoids drawn at the 30% probability level



Table 1. Crystal data and structure refinement details for

Identification code	03sot089	
Empirical formula	C ₂₄ H _{41.67} NO _{4.33} S	
Formula weight	C ₂₄ H ₄₁ NO ₄ · (H ₂ O)	
Temperature	445.63	
Wavelength	120(2) K	
Crystal system	0.71069 Å	
Space group	Orthorhombic	
Unit cell dimensions	P2 ₁ 2 ₁ 2 ₁	
Volume	a = 9.2060(2) Å	
Z	b = 12.4220(2) Å	
Density (calculated)	c = 20.7190(3) Å	
Absorption coefficient	2369.36(7) Å ³	
F(000)	4	
Crystal	1.249 Mg / m ³	
Crystal size	0.168 mm ⁻¹	
θ range for data collection	Block; Colourless	
Index ranges	0.2 × 0.2 × 0.2 mm ³	
Reflections collected	2.92 – 27.66°	
Independent reflections	-11 ≤ h ≤ 12, -16 ≤ k ≤ 16, -26 ≤ l ≤ 25	
Completeness to θ = 27.50°	18588	
Absorption correction	5449 [R _{int} = 0.0415]	
Max. and min. transmission	99.4 %	
Refinement method	Semi-empirical from equivalents	
Data / restraints / parameters	0.9834 and 0.9834	
Goodness-of-fit on F ²	Full-matrix least-squares on F ²	
Final R indices [F ² > 2σ(F ²)]	5449 / 3 / 293	
R indices (all data)	1.047	
Absolute structure parameter	R1 = 0.0339, wR2 = 0.0840	
Extinction coefficient	R1 = 0.0397, wR2 = 0.0874	
Largest diff. peak and hole	-0.01(5)	
	0.0136(13)	
	0.250 and -0.295 e Å ⁻³	

Diffractometer: Nonius KappaCCD area detector (ϕ scans and ω scans to fill asymmetric unit). Cell determination: DirAx (Duisenberg, A.J.M.(1992). J. Appl. Cryst. 25, 92-96.) **Data collection:** Collect (Collect: Data collection software, R. Hoof, Nonius B.V., 1998). **Data reduction and cell refinement:** Denzo (Z. Otwinowski & W. Minor, *Methods in Enzymology* (1997) Vol. 276: *Macromolecular Crystallography*, part A, pp. 307-326; C. W. Carter, Jr. & R. M. Sweet, Eds., Academic Press). **Absorption correction:** Sheldrick, G. M. SADABS - Bruker Nonius area detector scaling and absorption correction - V2.10 **Structure solution:** SHELXS97 (G. M. Sheldrick, Acta Cryst. (1990) A46 467-473). **Structure refinement:** SHELXL97 (G. M. Sheldrick (1997), University of Göttingen, Germany). **Graphics:** Cameron - A Molecular Graphics Package. (D. M. Watkin, L. Pearce and C. K. Prout, Chemical Crystallography Laboratory, University of Oxford, 1993).

Special details: All hydrogen atoms were placed in idealised positions and refined using a riding model. C15=R, C17=R, C20=S

Table 2. Atomic coordinates [$\times 10^4$], equivalent isotropic displacement parameters [$\text{\AA}^2 \times 10^3$] and site occupancy factors. U_{eq} is defined as one third of the trace of the orthogonalized U^j tensor.

Atom	x	y	z	U_{eq}	$S.o.f.$
S1	3257(1)	9432(1)	2500(1)	16(1)	1
N1	4137(1)	8781(1)	3044(1)	17(1)	1
O1	-1305(1)	8333(1)	1405(1)	39(1)	1
O2	1064(1)	7955(1)	1360(1)	22(1)	1
O3	1742(1)	9240(1)	2590(1)	21(1)	1
O4	3767(1)	10521(1)	2505(1)	22(1)	1
C1	3568(2)	7789(1)	3343(1)	18(1)	1
C2	2378(2)	8016(1)	3829(1)	23(1)	1
C3	1999(2)	7002(1)	4201(1)	29(1)	1
C4	1543(2)	6117(1)	3741(1)	29(1)	1
C5	2684(2)	5907(1)	3232(1)	25(1)	1
C6	3104(2)	6921(1)	2871(1)	20(1)	1
C7	5634(2)	9124(1)	3217(1)	18(1)	1
C8	6768(2)	8308(1)	3005(1)	21(1)	1
C9	8289(2)	8656(1)	3209(1)	26(1)	1
C10	8370(2)	8892(2)	3925(1)	30(1)	1
C11	7251(2)	9729(1)	4118(1)	27(1)	1
C12	5729(2)	9374(2)	3933(1)	23(1)	1
C13	-476(2)	6610(2)	1746(1)	42(1)	1
C14	-321(2)	7719(2)	1492(1)	29(1)	1
C15	1332(2)	9040(1)	1129(1)	18(1)	1
C16	993(2)	9165(2)	406(1)	24(1)	1
C17	2421(2)	9568(1)	124(1)	22(1)	1
C18	2640(2)	10717(1)	370(1)	27(1)	1
C19	2996(2)	10541(1)	1090(1)	20(1)	1
C20	2958(2)	9306(1)	1171(1)	16(1)	1
C21	3555(2)	8920(1)	503(1)	21(1)	1
C22	3454(2)	7713(1)	390(1)	30(1)	1
C23	5117(2)	9260(2)	366(1)	30(1)	1
C24	3764(2)	8863(1)	1747(1)	17(1)	1
O5	3849(4)	11886(3)	3630(2)	29(1)	0.33

Table 3. Bond lengths [\AA] and angles [$^\circ$].

S1-O3	1.4270(11)
S1-O4	1.4318(11)
S1-N1	1.6059(13)
S1-C24	1.7752(14)
N1-C1	1.4748(19)
N1-C7	1.4855(19)
O1-C14	1.197(2)
O2-C14	1.338(2)
O2-C15	1.4505(18)
C1-C2	1.515(2)
C1-C6	1.517(2)
C2-C3	1.517(2)
C3-C4	1.514(2)
C4-C5	1.511(2)
C5-C6	1.515(2)
C7-C12	1.518(2)

C7-C8	1.520(2)
C8-C9	1.526(2)
C9-C10	1.514(2)
C10-C11	1.517(2)
C11-C12	1.517(2)
C13-C14	1.481(3)
C15-C20	1.536(2)
C15-C16	1.539(2)
C16-C17	1.523(2)
C17-C18	1.528(2)
C17-C21	1.535(2)
C18-C19	1.542(2)
C19-C20	1.543(2)
C20-C24	1.511(2)
C20-C21	1.564(2)
C21-C22	1.521(2)
C21-C23	1.525(2)

O3-S1-O4	118.48(7)
O3-S1-N1	108.51(7)
O4-S1-N1	107.78(7)
O3-S1-C24	107.78(7)
O4-S1-C24	107.22(7)
N1-S1-C24	106.48(7)
C1-N1-C7	117.89(12)
C1-N1-S1	122.36(10)
C7-N1-S1	119.52(10)
C14-O2-C15	115.72(13)
N1-C1-C2	112.39(13)
N1-C1-C6	115.12(12)
C2-C1-C6	110.90(13)
C1-C2-C3	110.48(14)
C4-C3-C2	110.38(13)
C5-C4-C3	111.77(14)
C4-C5-C6	112.25(14)
C5-C6-C1	110.19(12)
N1-C7-C12	110.35(12)
N1-C7-C8	112.11(12)
C12-C7-C8	112.26(13)
C7-C8-C9	111.16(13)
C10-C9-C8	111.86(13)
C9-C10-C11	110.87(14)
C10-C11-C12	111.18(14)
C11-C12-C7	111.12(13)
O1-C14-O2	123.36(16)
O1-C14-C13	124.96(17)
O2-C14-C13	111.67(17)
O2-C15-C20	110.31(12)
O2-C15-C16	112.35(13)
C20-C15-C16	103.31(12)
C17-C16-C15	103.43(12)
C16-C17-C18	107.02(13)
C16-C17-C21	102.61(13)
C18-C17-C21	103.23(13)

C17-C18-C19	102.64(12)
C18-C19-C20	103.93(12)
C24-C20-C15	116.41(12)
C24-C20-C19	115.91(12)
C15-C20-C19	103.27(12)
C24-C20-C21	114.56(12)
C15-C20-C21	103.11(11)
C19-C20-C21	101.59(12)
C22-C21-C23	107.58(14)
C22-C21-C17	113.39(14)
C23-C21-C17	113.63(14)
C22-C21-C20	114.66(13)
C23-C21-C20	114.25(13)
C17-C21-C20	93.04(12)
C20-C24-S1	114.90(10)

Table 4. Anisotropic displacement parameters [$\text{\AA}^2 \times 10^3$]. The anisotropic displacement factor exponent takes the form: $-2\pi^2[h^2 a^{*2} U^{11} + \dots + 2 h k a^* b^* U^{12}]$.

Atom	U^{11}	U^{22}	U^{33}	U^{23}	U^{13}	U^{12}
S1	16(1)	17(1)	14(1)	0(1)	0(1)	2(1)
N1	16(1)	18(1)	16(1)	2(1)	-1(1)	-1(1)
O1	25(1)	48(1)	44(1)	6(1)	4(1)	-10(1)
O2	26(1)	18(1)	23(1)	-2(1)	2(1)	-6(1)
O3	15(1)	29(1)	19(1)	-2(1)	-1(1)	3(1)
O4	28(1)	15(1)	21(1)	-1(1)	-3(1)	1(1)
C1	19(1)	18(1)	17(1)	2(1)	0(1)	-2(1)
C2	24(1)	25(1)	19(1)	-4(1)	5(1)	-4(1)
C3	34(1)	30(1)	24(1)	0(1)	9(1)	-7(1)
C4	30(1)	27(1)	31(1)	1(1)	5(1)	-10(1)
C5	29(1)	20(1)	26(1)	0(1)	0(1)	-3(1)
C6	23(1)	19(1)	20(1)	-2(1)	1(1)	0(1)
C7	15(1)	17(1)	20(1)	0(1)	0(1)	-1(1)
C8	20(1)	22(1)	21(1)	-3(1)	1(1)	2(1)
C9	18(1)	30(1)	29(1)	-3(1)	1(1)	2(1)
C10	19(1)	37(1)	34(1)	-2(1)	-6(1)	0(1)
C11	24(1)	33(1)	26(1)	-8(1)	-5(1)	-3(1)
C12	19(1)	30(1)	20(1)	-6(1)	0(1)	-1(1)
C13	49(1)	34(1)	42(1)	3(1)	8(1)	-19(1)
C14	31(1)	33(1)	22(1)	-4(1)	4(1)	-14(1)
C15	20(1)	16(1)	18(1)	0(1)	0(1)	-2(1)
C16	25(1)	31(1)	16(1)	-2(1)	-2(1)	-3(1)
C17	26(1)	27(1)	13(1)	0(1)	1(1)	-2(1)
C18	35(1)	25(1)	21(1)	5(1)	-5(1)	-2(1)
C19	24(1)	17(1)	20(1)	2(1)	-3(1)	-2(1)
C20	19(1)	16(1)	15(1)	1(1)	0(1)	0(1)
C21	23(1)	26(1)	15(1)	0(1)	4(1)	0(1)
C22	37(1)	29(1)	23(1)	-7(1)	6(1)	6(1)
C23	24(1)	45(1)	21(1)	4(1)	7(1)	0(1)
C24	17(1)	18(1)	16(1)	0(1)	2(1)	2(1)
O5	24(2)	31(2)	31(2)	-8(2)	-7(2)	6(2)

Table 5. Hydrogen coordinates [$\times 10^4$] and isotropic displacement parameters [$\text{\AA}^2 \times 10^3$].

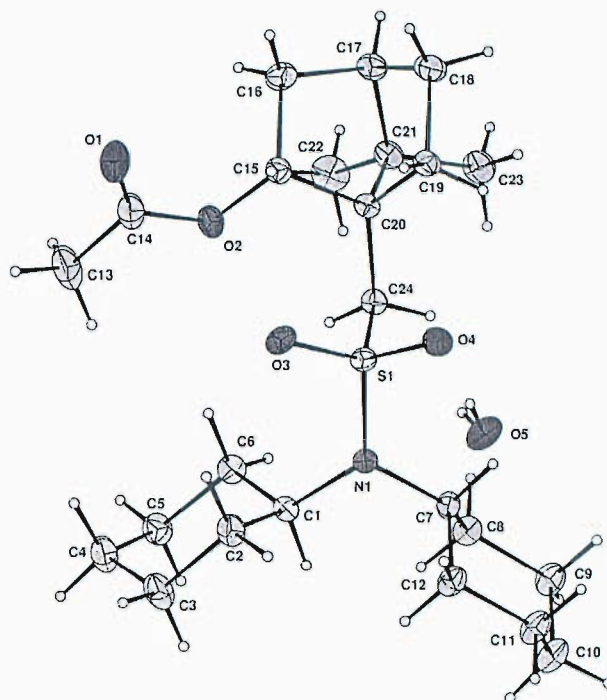
Atom	<i>x</i>	<i>y</i>	<i>z</i>	U_{eq}	<i>S.o.f.</i>
H1	4393	7477	3595	22	1
H2A	1504	8285	3602	28	1
H2B	2706	8580	4134	28	1
H3A	2853	6763	4454	35	1
H3B	1198	7156	4506	35	1
H4A	1368	5447	3989	35	1
H4B	621	6323	3529	35	1
H5A	2310	5369	2921	30	1
H5B	3559	5600	3440	30	1
H6A	2266	7178	2614	25	1
H6B	3911	6761	2571	25	1
H7	5835	9808	2979	21	1
H8A	6735	8229	2530	25	1
H8B	6542	7599	3199	25	1
H9A	8989	8079	3101	31	1
H9B	8569	9309	2965	31	1
H10A	9354	9157	4035	36	1
H10B	8198	8220	4171	36	1
H11A	7477	10419	3902	33	1
H11B	7296	9846	4590	33	1
H12A	5030	9951	4041	28	1
H12B	5463	8725	4184	28	1
H13A	-1421	6536	1959	63	1
H13B	300	6467	2058	63	1
H13C	-410	6095	1390	63	1
H15	756	9570	1387	21	1
H16A	710	8467	212	29	1
H16B	203	9693	335	29	1
H17	2497	9492	-356	27	1
H18A	1747	11152	316	32	1
H18B	3452	11076	143	32	1
H19A	2262	10891	1369	24	1
H19B	3967	10831	1197	24	1
H22A	3633	7557	-67	44	1
H22B	2482	7460	509	44	1
H22C	4182	7344	655	44	1
H23A	5774	8884	662	45	1
H23B	5212	10039	428	45	1
H23C	5368	9077	-80	45	1
H24A	4817	8983	1682	20	1
H24B	3602	8076	1767	20	1
H99	3750(50)	11400(30)	3349(18)	20(14)	0.33
H98	3130(40)	12310(40)	3630(30)	50(20)	0.33

Table 6. Hydrogen bonds [\AA and $^\circ$].

<i>D</i> -H \cdots <i>A</i>	<i>d</i> (<i>D</i> -H)	<i>d</i> (H \cdots <i>A</i>)	<i>d</i> (<i>D</i> \cdots <i>A</i>)	\angle (<i>DHA</i>)
O5-H99 \cdots O4	0.846(10)	2.060(18)	2.883(4)	164(5)
O5-H98 \cdots O1 ⁱ	0.844(10)	2.108(11)	2.952(4)	178(5)

Symmetry transformations used to generate equivalent atoms:

(i) $-x, y+1/2, -z+1/2$

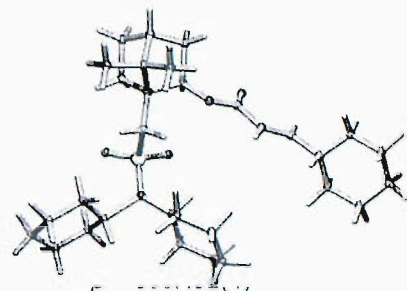


Thermal ellipsoids drawn at the 50% probability level



Table 1. Crystal data and structure refinement details.

Identification code	03sot088
Empirical formula	C ₆₂ H ₁₀₂ N ₂ O ₈ S ₂
Formula weight	1067.58
Temperature	120(2) K
Wavelength	0.71069 Å
Crystal system	Monoclinic
Space group	C2
Unit cell dimensions	$a = 23.5470(16)$ Å $b = 11.5630(8)$ Å $c = 11.2080(6)$ Å
Volume	3001.0(3) Å ³
Z	2
Density (calculated)	1.181 Mg / m ³
Absorption coefficient	0.143 mm ⁻¹
$F(000)$	1168
Crystal	Block; Colourless
Crystal size	0.2 × 0.2 × 0.2 mm ³
θ range for data collection	3.17 – 27.74°
Index ranges	-30 ≤ h ≤ 26, -15 ≤ k ≤ 15, -13 ≤ l ≤ 14
Reflections collected	20112
Independent reflections	6870 [$R_{int} = 0.0362$]
Completeness to $\theta = 27.50^\circ$	99.7 %
Absorption correction	Semi-empirical from equivalents
Max. and min. transmission	0.9986 and 0.9859
Refinement method	Full-matrix least-squares on F^2
Data / restraints / parameters	6870 / 113 / 341
Goodness-of-fit on F^2	1.503
Final R indices [$F^2 > 2\sigma(F^2)$]	$R1 = 0.1038$, $wR2 = 0.2594$
R indices (all data)	$R1 = 0.1247$, $wR2 = 0.2740$
Absolute structure parameter	0.0(2)
Extinction coefficient	0.023(4)
Largest diff. peak and hole	1.072 and -1.303 e Å ⁻³



Diffractometer: Nonius KappaCCD area detector (ϕ scans and ω scans to fill asymmetric unit). **Cell determination:** DirAx (Duisenberg, A.J.M.(1992). *J. Appl. Cryst.* 25, 92-96.) **Data collection:** Collect (Collect: Data collection software, R. Hoof, Nonius B.V., 1998). **Data reduction and cell refinement:** Denzo (Z. Otwinowski & W. Minor, *Methods in Enzymology* (1997) Vol. 276: *Macromolecular Crystallography*, part A, pp. 307-326; C. W. Carter, Jr. & R. M. Sweet, Eds., Academic Press). **Absorption correction:** Sheldrick, G. M. SADABS - Bruker Nonius area detector scaling and absorption correction - V2.10 **Structure solution:** SHELXS97 (G. M. Sheldrick, *Acta Cryst.* (1990) A46 467-473). **Structure refinement:** SHELXL97 (G. M. Sheldrick (1997), University of Göttingen, Germany). **Graphics:** Cameron - A Molecular Graphics Package. (D. M. Watkin, L. Pearce and C. K. Prout, Chemical Crystallography Laboratory, University of Oxford, 1993).

Special details: All hydrogen atoms were placed in idealised positions and refined using a riding model. The SO₂ group occupies 2 positions with occupancies of 70 and 30%

Table 2. Atomic coordinates [$\times 10^4$], equivalent isotropic displacement parameters [$\text{\AA}^2 \times 10^3$] and site occupancy factors. U_{eq} is defined as one third of the trace of the orthogonalized U^{ij} tensor.

Atom	x	y	z	U_{eq}	<i>S.o.f.</i>
N1	2837(2)	7104(5)	9528(5)	39(1)	1
O1	2780(2)	10259(4)	5513(4)	43(1)	1
O2	3223(2)	8585(4)	6037(4)	33(1)	1
C1	2312(2)	6686(6)	8715(6)	59(2)	1
C2	2377(2)	5621(5)	8096(6)	51(2)	1
C3	1854(2)	5330(6)	7196(6)	54(2)	1
C4	1303(2)	5543(6)	7555(7)	65(2)	1
C5	1257(2)	6615(6)	8272(7)	62(2)	1
C6	1787(2)	6901(5)	9193(5)	46(2)	1
C7	3014(3)	6272(6)	10797(5)	68(2)	1
C8	2960(3)	6891(5)	11880(5)	55(2)	1
C9	3140(3)	6177(7)	12982(5)	75(3)	1
C10	3651(3)	5473(7)	13018(5)	74(3)	1
C11	3725(3)	4911(5)	11858(5)	59(2)	1
C12	3544(3)	5640(6)	10742(5)	63(2)	1
C13	1283(2)	8508(6)	2214(5)	47(2)	1
C14	801(2)	8012(8)	1405(5)	56(2)	1
C15	249(2)	8216(7)	1834(5)	52(2)	1
C16	263(2)	8061(7)	3124(5)	48(2)	1
C17	786(2)	8515(6)	3948(5)	43(2)	1
C18	1346(2)	8297(5)	3514(4)	34(1)	1
C19	1833(2)	8929(6)	4251(5)	32(1)	1
C20	2316(2)	8474(6)	4868(5)	32(1)	1
C21	2777(3)	9230(6)	5483(5)	32(1)	1
C22	3685(2)	9190(5)	6775(5)	29(1)	1
C23	4149(3)	9603(7)	6054(6)	42(2)	1
C24	4698(3)	8996(7)	6699(6)	39(2)	1
C25	4875(3)	9587(6)	7947(6)	36(1)	1
C26	4404(3)	9173(6)	8621(5)	31(1)	1
C27	4022(2)	8380(5)	7704(5)	26(1)	1
C28	4472(3)	7822(6)	7034(6)	35(1)	1
C29	4922(3)	7091(7)	7847(8)	49(2)	1
C30	4224(3)	7093(7)	5948(7)	44(2)	1
C31A	3655(2)	7504(5)	8248(5)	26(1)	0.70
S1A	3254(1)	8093(4)	9286(3)	29(1)	0.70
O3A	2890(3)	8967(6)	8643(6)	41(1)	0.70
O4A	3653(3)	8393(6)	10352(6)	41(1)	0.70
C31B	3655(2)	7504(5)	8248(5)	26(1)	0.30
S1B	3092(3)	8103(11)	8969(8)	29(1)	0.30
O3B	2659(7)	8557(15)	8092(16)	41(1)	0.30
O4B	3411(7)	8837(15)	9964(15)	41(1)	0.30

Table 3. Bond lengths [\AA] and angles [$^\circ$].

N1–C1	1.477(7)	C1–C2	1.434(6)
N1–S1B	1.491(13)	C1–C6	1.456(6)
N1–S1A	1.563(6)	C2–C3	1.481(6)
N1–C7	1.705(7)	C3–C4	1.448(7)
O1–C21	1.190(8)	C4–C5	1.492(7)
O2–C21	1.344(7)	C5–C6	1.505(6)
O2–C22	1.424(7)	C7–C8	1.435(6)

C7-C12	1.456(6)	C22-C23	1.548(9)
C8-C9	1.482(6)	C23-C24	1.533(9)
C9-C10	1.448(7)	C24-C28	1.530(9)
C10-C11	1.491(6)	C24-C25	1.544(9)
C11-C12	1.506(6)	C25-C26	1.528(8)
C13-C14	1.437(6)	C26-C27	1.540(7)
C13-C18	1.459(6)	C27-C31A	1.528(7)
C14-C15	1.484(6)	C27-C28	1.546(8)
C15-C16	1.451(7)	C28-C30	1.508(9)
C16-C17	1.495(6)	C28-C29	1.523(9)
C17-C18	1.508(6)	C31A-S1A	1.763(7)
C18-C19	1.479(7)	S1A-O4A	1.422(8)
C19-C20	1.326(9)	S1A-O3A	1.433(8)
C20-C21	1.466(8)	S1B-O3B	1.38(2)
C22-C27	1.513(7)	S1B-O4B	1.491(18)

C1-N1-S1B	110.5(5)
C1-N1-S1A	127.9(5)
S1B-N1-S1A	17.6(3)
C1-N1-C7	112.4(5)
S1B-N1-C7	137.0(5)
S1A-N1-C7	119.4(4)
C21-O2-C22	116.5(5)
C2-C1-C6	119.8(4)
C2-C1-N1	115.4(5)
C6-C1-N1	112.9(4)
C1-C2-C3	112.1(4)
C4-C3-C2	116.6(4)
C3-C4-C5	116.6(4)
C4-C5-C6	114.8(4)
C1-C6-C5	111.3(4)
C8-C7-C12	119.7(4)
C8-C7-N1	112.2(5)
C12-C7-N1	109.3(4)
C7-C8-C9	111.8(4)
C10-C9-C8	116.5(4)
C9-C10-C11	116.7(4)
C10-C11-C12	114.8(4)
C7-C12-C11	111.2(4)
C14-C13-C18	119.3(4)
C13-C14-C15	111.8(4)
C16-C15-C14	116.1(4)
C15-C16-C17	116.1(4)
C16-C17-C18	114.4(4)
C13-C18-C19	113.8(5)
C13-C18-C17	111.0(4)
C19-C18-C17	111.9(4)
C20-C19-C18	126.8(6)
C19-C20-C21	120.1(6)
O1-C21-O2	122.8(5)
O1-C21-C20	127.5(6)
O2-C21-C20	109.7(5)
O2-C22-C27	110.2(4)
O2-C22-C23	112.6(5)
C27-C22-C23	102.6(5)
C24-C23-C22	103.2(5)
C28-C24-C23	102.7(5)
C28-C24-C25	102.7(5)
C23-C24-C25	106.9(6)
C26-C25-C24	102.0(5)
C25-C26-C27	104.2(4)
C22-C27-C31A	114.8(4)
C22-C27-C26	105.1(4)
C31A-C27-C26	115.6(4)
C22-C27-C28	104.2(4)
C31A-C27-C28	113.8(5)
C26-C27-C28	101.7(4)
C30-C28-C29	107.3(6)
C30-C28-C24	113.5(5)
C29-C28-C24	113.8(5)
C30-C28-C27	115.2(5)

C29–C28–C27	113.9(5)
C24–C28–C27	92.8(5)
C27–C31A–S1A	114.6(4)
O4A–S1A–O3A	119.6(5)
O4A–S1A–N1	111.9(4)
O3A–S1A–N1	105.4(4)
O4A–S1A–C31A	107.3(4)
O3A–S1A–C31A	106.5(4)
N1–S1A–C31A	105.1(3)
O3B–S1B–N1	106.9(9)
O3B–S1B–O4B	121.3(13)
N1–S1B–O4B	108.3(9)

Table 4. Anisotropic displacement parameters [$\text{\AA}^2 \times 10^3$]. The anisotropic displacement factor exponent takes the form: $-2\pi^2[h^2 a^{*2} U^{11} + \dots + 2 h k a^* b^* U^{12}]$.

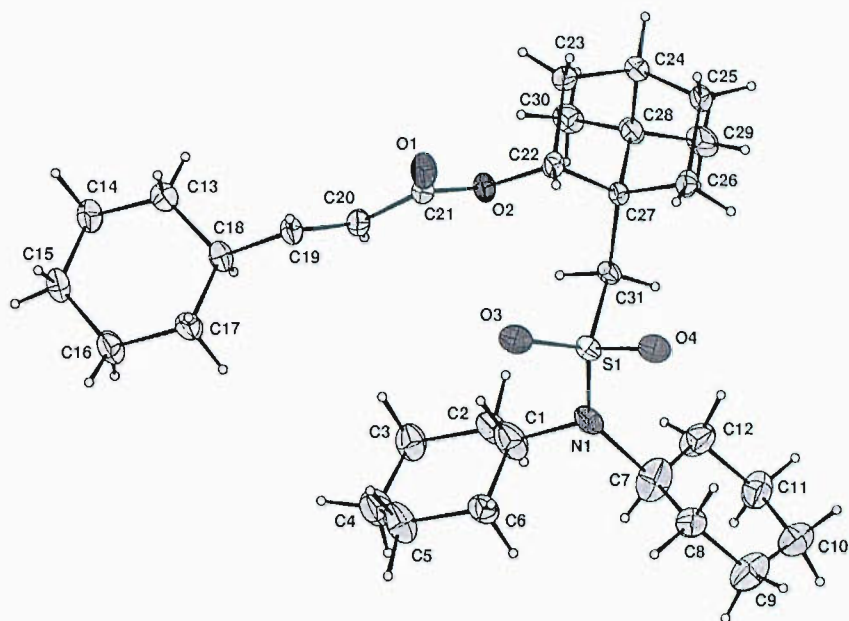
Atom	U^{11}	U^{22}	U^{33}	U^{23}	U^{13}	U^{12}
N1	30(3)	38(3)	51(3)	-9(2)	9(2)	-6(2)
O1	43(3)	30(2)	50(3)	2(2)	-7(2)	0(2)
O2	29(2)	30(2)	36(2)	0(2)	-4(2)	-2(2)
C1	38(3)	68(4)	71(4)	-25(4)	11(3)	3(3)
C2	35(3)	58(4)	62(4)	-23(3)	13(3)	-9(3)
C3	48(4)	54(4)	55(4)	-12(3)	0(3)	-3(3)
C4	50(4)	83(5)	62(4)	-19(4)	9(3)	-8(4)
C5	39(3)	64(4)	81(5)	-14(4)	2(3)	7(3)
C6	34(3)	57(4)	48(3)	-8(3)	13(3)	2(3)
C7	85(5)	64(4)	55(4)	-12(4)	7(4)	26(4)
C8	45(3)	78(5)	44(3)	1(3)	13(3)	4(3)
C9	101(5)	79(5)	45(4)	-3(4)	13(4)	-1(4)
C10	71(5)	102(6)	50(4)	20(4)	14(4)	5(4)
C11	65(4)	56(4)	51(4)	6(3)	-4(3)	-2(3)
C12	67(4)	75(5)	49(4)	20(4)	19(3)	26(4)
C13	35(3)	64(5)	42(3)	-3(3)	6(3)	-4(3)
C14	41(4)	83(6)	40(4)	-8(4)	-3(3)	-14(4)
C15	31(3)	69(5)	50(4)	6(4)	-8(3)	-6(4)
C16	34(3)	54(4)	52(4)	-9(4)	0(3)	-8(3)
C17	35(3)	53(4)	40(3)	-8(3)	7(3)	-11(3)
C18	28(3)	29(3)	43(3)	-4(3)	-1(2)	2(2)
C19	28(3)	33(3)	34(3)	-2(2)	0(2)	-4(2)
C20	30(3)	35(3)	30(3)	1(2)	1(2)	-2(2)
C21	30(3)	37(3)	26(3)	1(2)	1(2)	-2(2)
C22	33(3)	25(3)	26(3)	2(2)	-2(2)	-7(2)
C23	39(4)	51(4)	34(3)	12(3)	1(3)	-14(3)
C24	29(3)	54(4)	33(3)	-1(3)	6(2)	-10(3)
C25	31(3)	41(3)	33(3)	4(3)	-2(2)	-12(3)
C26	33(3)	29(3)	27(3)	1(2)	-2(2)	-4(2)
C27	24(3)	29(3)	25(2)	1(2)	0(2)	-5(2)
C28	26(3)	42(4)	38(3)	-3(3)	6(2)	-3(2)
C29	31(3)	52(4)	64(5)	4(4)	14(3)	13(3)
C30	39(4)	48(4)	48(4)	-12(3)	14(3)	-3(3)
C31A	23(3)	22(3)	33(3)	2(2)	6(2)	-2(2)
S1A	26(2)	26(1)	37(2)	-2(1)	8(1)	-1(1)
O3A	42(3)	36(3)	49(3)	-4(2)	17(2)	2(2)
O4A	42(3)	36(3)	49(3)	-4(2)	17(2)	2(2)

C31B	23(3)	22(3)	33(3)	2(2)	6(2)	-2(2)
S1B	26(2)	26(1)	37(2)	-2(1)	8(1)	-1(1)
O3B	42(3)	36(3)	49(3)	-4(2)	17(2)	2(2)
O4B	42(3)	36(3)	49(3)	-4(2)	17(2)	2(2)

Table 5. Hydrogen coordinates [$\times 10^4$] and isotropic displacement parameters [$\text{\AA}^2 \times 10^3$].

Atom	<i>x</i>	<i>y</i>	<i>z</i>	U_{eq}	<i>S.o.f.</i>
H1	2274	7258	8036	71	1
H2A	2457	4988	8698	62	1
H2B	2711	5684	7678	62	1
H3A	1866	5777	6447	64	1
H3B	1874	4500	6990	64	1
H4A	1213	4873	8038	78	1
H4B	1003	5575	6812	78	1
H5A	926	6531	8698	75	1
H5B	1172	7274	7703	75	1
H6A	1774	7725	9427	55	1
H6B	1791	6427	9930	55	1
H7	2707	5665	10713	82	1
H8A	2553	7133	11832	66	1
H8B	3201	7597	11939	66	1
H9A	3206	6699	13694	90	1
H9B	2815	5660	13072	90	1
H10A	3648	4860	13633	89	1
H10B	3993	5965	13300	89	1
H11A	3499	4185	11762	71	1
H11B	4137	4701	11916	71	1
H12A	3855	6196	10666	76	1
H12B	3483	5137	10015	76	1
H13A	1267	9356	2089	56	1
H13B	1640	8230	1955	56	1
H14A	863	7169	1339	67	1
H14B	777	8354	588	67	1
H15A	121	9016	1615	62	1
H15B	-46	7687	1388	62	1
H16A	231	7224	3284	57	1
H16B	-81	8443	3337	57	1
H17A	809	8155	4757	51	1
H17B	740	9359	4045	51	1
H18	1433	7454	3640	41	1
H19	1797	9746	4286	39	1
H20	2362	7658	4911	39	1
H22	3532	9859	7187	35	1
H23A	4051	9364	5193	50	1
H23B	4193	10454	6096	50	1
H24	5014	8950	6212	46	1
H25A	5262	9329	8360	43	1
H25B	4874	10439	7869	43	1
H26A	4179	9834	8849	37	1
H26B	4573	8740	9363	37	1
H29A	4739	6392	8096	73	1
H29B	5091	7538	8567	73	1
H29C	5227	6871	7400	73	1
H30A	4529	6908	5489	67	1

H30B	3915	7522	5428	67	1
H30C	4067	6376	6222	67	1
H31A	3912	6893	8664	31	0.70
H31B	3384	7133	7579	31	0.70
H31C	3915	7035	8854	31	0.30
H31D	3473	6975	7594	31	0.30

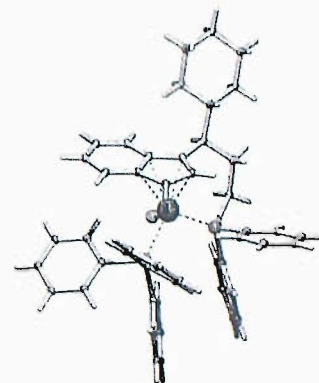


Thermal ellipsoids drawn at the 35% probability level, only one position of the disordered SO_2 group is shown.



Table 1. Crystal data and structure refinement details.

Identification code	04sot0853
Empirical formula	$C_{51}H_{50}ClP_2Ru$ $C_{48}H_{47}P_2RuCl \cdot 0.5 C_6H_6$
Formula weight	861.37
Temperature	120(2) K
Wavelength	0.71069 Å
Crystal system	Orthorhombic
Space group	$P2_12_12_1$
Unit cell dimensions	$a = 10.3279(3)$ Å $b = 22.1649(7)$ Å $c = 36.0432(13)$ Å
Volume	$8250.9(5)$ Å ³
Z	8 (2 molecules)
Density (calculated)	1.387 Mg / m ³
Absorption coefficient	0.558 mm ⁻¹
$F(000)$	3576
Crystal	Slab; Orange
Crystal size	$0.2 \times 0.09 \times 0.03$ mm ³
θ range for data collection	2.91 – 27.73°
Index ranges	$-13 \leq h \leq 8, -28 \leq k \leq 28, -47 \leq l \leq 43$
Reflections collected	60647
Independent reflections	18821 [$R_{int} = 0.1023$]
Completeness to $\theta = 25.00^\circ$	99.3 %
Absorption correction	Semi-empirical from equivalents
Max. and min. transmission	0.9835 and 0.8966
Refinement method	Full-matrix least-squares on F^2
Data / restraints / parameters	18821 / 36 / 956
Goodness-of-fit on F^2	1.041
Final R indices [$F^2 > 2\sigma(F^2)$]	$R1 = 0.0635, wR2 = 0.1255$
R indices (all data)	$R1 = 0.1012, wR2 = 0.1430$
Absolute structure parameter	0.00(3)
Largest diff. peak and hole	0.754 and $-1.135 e \text{ \AA}^{-3}$



Diffractometer: *Nonius KappaCCD* area detector (ϕ scans and ω scans to fill *asymmetric unit*). **Cell determination:** DirAx (Duisenberg, A.J.M.(1992). *J. Appl. Cryst.* 25, 92-96.) **Data collection:** Collect (Collect: Data collection software, R. Hooft, Nonius B.V., 1998). **Data reduction and cell refinement:** *Denzo* (Z. Otwinowski & W. Minor, *Methods in Enzymology* (1997) Vol. 276: *Macromolecular Crystallography*, part A, pp. 307-326; C. W. Carter, Jr. & R. M. Sweet, Eds., Academic Press). **Absorption correction:** Sheldrick, G. M. SADABS - Bruker Nonius area detector scaling and absorption correction - V2.10 **Structure solution:** *SHELXS97* (G. M. Sheldrick, *Acta Cryst.* (1990) A46 467-473). **Structure refinement:** *SHELXL97* (G. M. Sheldrick (1997), University of Göttingen, Germany). **Graphics:** Cameron - A Molecular Graphics Package. (D. M. Watkin, L. Pearee and C. K. Prout, Chemical Crystallography Laboratory, University of Oxford, 1993).

Special details: All hydrogen atoms were placed in idealised positions and refined using a riding model. The geometry and thermal parameters of the benzene were restrained. C10=R, C58=R

Table 2. Atomic coordinates [$\times 10^4$], equivalent isotropic displacement parameters [$\text{\AA}^2 \times 10^3$] and site occupancy factors. U_{eq} is defined as one third of the trace of the orthogonalized U^{ij} tensor.

Atom	x	y	z	U_{eq}	$S.o.f.$
Ru1	5937(1)	7834(1)	6378(1)	18(1)	1
C11	3942(1)	7735(1)	6021(1)	24(1)	1
P1	6692(1)	8390(1)	5897(1)	21(1)	1
P2	6665(1)	6862(1)	6234(1)	19(1)	1
C1	4768(4)	8174(2)	6886(1)	20(1)	1
C2	3433(4)	8084(2)	6953(1)	23(1)	1
C3	3035(4)	7604(2)	7162(1)	28(1)	1
C4	3939(4)	7181(2)	7302(1)	29(1)	1
C5	5236(4)	7232(2)	7230(1)	29(1)	1
C6	5677(4)	7728(2)	7020(1)	22(1)	1
C7	6956(4)	7922(2)	6907(1)	22(1)	1
C8	6826(4)	8495(2)	6740(1)	20(1)	1
C9	5481(4)	8648(2)	6707(1)	19(1)	1
C10	4975(4)	9245(2)	6565(1)	23(1)	1
C11	4960(4)	9714(2)	6889(1)	22(1)	1
C12	3989(5)	9532(2)	7189(1)	31(1)	1
C13	4022(5)	9954(2)	7523(2)	39(1)	1
C14	3766(4)	10608(2)	7402(1)	36(1)	1
C15	4691(5)	10789(2)	7110(2)	33(1)	1
C16	4677(4)	10365(2)	6780(1)	30(1)	1
C17	5748(4)	9478(2)	6232(1)	24(1)	1
C18	5709(4)	9080(2)	5879(1)	26(1)	1
C19	8381(4)	8672(2)	5922(1)	28(1)	1
C20	8775(4)	9154(2)	5700(1)	28(1)	1
C21	10068(5)	9333(2)	5706(2)	42(2)	1
C22	10960(5)	9023(2)	5929(2)	45(2)	1
C23	10576(4)	8550(2)	6145(2)	35(1)	1
C24	9271(4)	8380(2)	6145(1)	29(1)	1
C25	6652(4)	8157(2)	5413(1)	23(1)	1
C26	7746(4)	7906(2)	5242(1)	28(1)	1
C27	7728(4)	7740(2)	4877(1)	29(1)	1
C28	6640(4)	7804(2)	4663(1)	33(1)	1
C29	5530(5)	8046(2)	4830(2)	33(1)	1
C30	5530(4)	8222(2)	5195(1)	28(1)	1
C31	6938(4)	6574(2)	5767(1)	21(1)	1
C32	6022(4)	6709(2)	5495(1)	26(1)	1
C33	6096(4)	6447(2)	5144(1)	28(1)	1
C34	7093(4)	6054(2)	5059(1)	31(1)	1
C35	8016(4)	5909(2)	5323(2)	35(1)	1
C36	7930(4)	6164(2)	5677(1)	27(1)	1
C37	8169(4)	6702(2)	6477(1)	20(1)	1
C38	9394(4)	6871(2)	6336(2)	27(1)	1
C39	10503(4)	6821(2)	6557(2)	35(1)	1
C40	10424(4)	6611(2)	6907(2)	34(1)	1
C41	9226(4)	6446(2)	7055(1)	31(1)	1
C42	8127(4)	6486(2)	6844(1)	24(1)	1
C43	5627(4)	6243(2)	6394(1)	23(1)	1
C44	6028(4)	5645(2)	6372(1)	26(1)	1
C45	5229(4)	5177(2)	6487(1)	29(1)	1
C46	4007(4)	5307(2)	6621(1)	29(1)	1
C47	3600(4)	5891(2)	6649(1)	26(1)	1
C48	4392(4)	6364(2)	6530(1)	28(1)	1
Ru2	1137(1)	7253(1)	8621(1)	17(1)	1

C12	-824(1)	7307(1)	8992(1)	22(1)	1
P3	1977(1)	6662(1)	9077(1)	19(1)	1
P4	1910(1)	8220(1)	8758(1)	20(1)	1
C49	-79(4)	6885(2)	8113(1)	21(1)	1
C50	-1434(4)	6893(2)	8077(1)	23(1)	1
C51	-1983(5)	7377(2)	7896(1)	29(1)	1
C52	-1257(4)	7863(2)	7766(1)	32(1)	1
C53	71(4)	7878(2)	7815(1)	27(1)	1
C54	689(4)	7382(2)	7993(1)	22(1)	1
C55	2033(4)	7254(2)	8075(1)	22(1)	1
C56	2067(4)	6663(2)	8228(1)	21(1)	1
C57	782(4)	6440(2)	8273(1)	19(1)	1
C58	394(4)	5816(2)	8393(1)	20(1)	1
C59	321(4)	5414(2)	8038(1)	25(1)	1
C60	1584(4)	5390(2)	7819(2)	38(1)	1
C61	1424(4)	5029(2)	7465(2)	36(1)	1
C62	904(4)	4399(2)	7535(2)	38(1)	1
C63	-319(5)	4419(2)	7747(2)	44(2)	1
C64	-171(5)	4774(2)	8114(1)	32(1)	1
C65	1255(4)	5570(2)	8695(1)	24(1)	1
C68	1164(4)	5925(2)	9064(1)	23(1)	1
C69	3688(4)	6454(2)	9043(1)	23(1)	1
C70	4189(4)	5968(2)	9244(1)	28(1)	1
C71	5506(4)	5846(2)	9237(2)	33(1)	1
C72	6332(4)	6213(2)	9035(2)	33(1)	1
C73	5866(4)	6689(2)	8836(1)	30(1)	1
C74	4539(4)	6804(2)	8835(1)	25(1)	1
C75	1860(4)	6835(2)	9566(1)	22(1)	1
C76	701(4)	6744(2)	9764(1)	25(1)	1
C77	617(4)	6889(2)	10136(1)	28(1)	1
C78	1669(4)	7123(2)	10324(1)	33(1)	1
C79	2819(4)	7215(2)	10137(1)	32(1)	1
C80	2918(4)	7079(2)	9764(1)	25(1)	1
C81	2097(4)	8533(2)	9230(1)	24(1)	1
C82	1342(4)	8305(2)	9517(1)	27(1)	1
C83	1419(4)	8566(2)	9867(1)	33(1)	1
C84	2230(4)	9044(2)	9935(2)	37(1)	1
C85	2957(4)	9283(2)	9646(2)	35(1)	1
C86	2888(4)	9037(2)	9296(2)	32(1)	1
C87	929(4)	8856(2)	8585(1)	24(1)	1
C88	-404(4)	8820(2)	8642(2)	32(1)	1
C89	-1171(4)	9335(2)	8610(2)	38(1)	1
C90	-645(4)	9870(2)	8494(2)	38(2)	1
C91	667(4)	9906(2)	8419(2)	37(1)	1
C92	1440(4)	9398(2)	8464(1)	29(1)	1
C93	3528(4)	8370(2)	8557(1)	26(1)	1
C94	4632(4)	8285(2)	8776(2)	26(1)	1
C95	5862(4)	8359(2)	8621(2)	32(1)	1
C96	5999(5)	8505(2)	8257(2)	36(1)	1
C97	4906(4)	8581(2)	8035(2)	31(1)	1
C98	3683(4)	8510(2)	8188(1)	28(1)	1
C99	6531(4)	9532(2)	4462(2)	106(1)	1
C100	6184(3)	10104(2)	4585(2)	101(3)	1
C101	7132(5)	10504(2)	4705(2)	106(1)	1
C102	8426(4)	10332(2)	4702(2)	106(1)	1
C103	8773(3)	9760(2)	4579(2)	106(1)	1
C104	7825(4)	9360(2)	4459(2)	106(1)	1

Table 3. Bond lengths [Å] and angles [°].

Ru1–C8	2.166(4)	C33–C34	1.383(6)
Ru1–C7	2.188(4)	C34–C35	1.387(7)
Ru1–C9	2.210(4)	C35–C36	1.398(7)
Ru1–P1	2.2652(12)	C37–C42	1.407(6)
Ru1–C1	2.319(4)	C37–C38	1.414(5)
Ru1–P2	2.3392(10)	C38–C39	1.400(6)
Ru1–C6	2.341(5)	C39–C40	1.348(7)
Ru1–Cl1	2.4389(10)	C40–C41	1.396(6)
P1–C25	1.821(5)	C41–C42	1.370(6)
P1–C18	1.837(4)	C43–C44	1.390(5)
P1–C19	1.855(4)	C43–C48	1.392(6)
P2–C37	1.818(4)	C44–C45	1.389(5)
P2–C31	1.823(5)	C45–C46	1.382(6)
P2–C43	1.836(4)	C46–C47	1.365(5)
C1–C2	1.414(5)	C47–C48	1.395(6)
C1–C9	1.434(6)	Ru2–C56	2.152(4)
C1–C6	1.448(5)	Ru2–C55	2.174(4)
C2–C3	1.368(6)	Ru2–C57	2.227(4)
C3–C4	1.415(6)	Ru2–P3	2.2756(12)
C4–C5	1.369(6)	Ru2–C54	2.327(4)
C5–C6	1.410(6)	Ru2–P4	2.3385(11)
C6–C7	1.448(6)	Ru2–C49	2.362(4)
C7–C8	1.414(5)	Ru2–Cl2	2.4301(11)
C8–C9	1.434(5)	P3–C75	1.808(5)
C9–C10	1.514(5)	P3–C69	1.831(4)
C10–C17	1.533(6)	P3–C68	1.836(4)
C10–C11	1.563(6)	P4–C87	1.845(4)
C11–C16	1.525(5)	P4–C81	1.847(5)
C11–C12	1.527(6)	P4–C93	1.851(4)
C12–C13	1.525(6)	C49–C50	1.406(5)
C13–C14	1.537(6)	C49–C54	1.424(6)
C14–C15	1.477(7)	C49–C57	1.448(5)
C15–C16	1.513(6)	C50–C51	1.378(6)
C17–C18	1.548(6)	C51–C52	1.394(6)
C19–C24	1.381(6)	C52–C53	1.383(6)
C19–C20	1.396(6)	C53–C54	1.424(6)
C20–C21	1.394(6)	C54–C55	1.448(6)
C21–C22	1.405(7)	C55–C56	1.424(5)
C22–C23	1.363(7)	C56–C57	1.425(5)
C23–C24	1.400(6)	C57–C58	1.503(5)
C25–C26	1.402(6)	C58–C65	1.509(6)
C25–C30	1.407(6)	C58–C59	1.560(6)
C26–C27	1.367(7)	C59–C60	1.526(6)
C27–C28	1.369(6)	C59–C64	1.532(5)
C28–C29	1.401(6)	C60–C61	1.514(7)
C29–C30	1.371(7)	C61–C62	1.519(6)
C31–C32	1.393(6)	C62–C63	1.477(7)
C31–C36	1.407(6)	C63–C64	1.545(7)
C32–C33	1.397(6)	C65–C68	1.546(6)

C69-C74	1.391(6)	C87-C92	1.382(5)
C69-C70	1.398(6)	C87-C88	1.394(6)
C70-C71	1.388(6)	C88-C89	1.394(6)
C71-C72	1.386(7)	C89-C90	1.369(6)
C72-C73	1.363(6)	C90-C91	1.384(6)
C73-C74	1.394(6)	C91-C92	1.390(6)
C75-C76	1.409(6)	C93-C98	1.376(7)
C75-C80	1.412(6)	C93-C94	1.400(6)
C76-C77	1.381(7)	C94-C95	1.398(6)
C77-C78	1.382(6)	C95-C96	1.357(7)
C78-C79	1.381(7)	C96-C97	1.395(7)
C79-C80	1.382(7)	C97-C98	1.386(6)
C81-C82	1.392(6)	C99-C100	1.3900
C81-C86	1.404(6)	C99-C104	1.3900
C82-C83	1.391(7)	C100-C101	1.3900
C83-C84	1.374(6)	C101-C102	1.3900
C84-C85	1.391(7)	C102-C103	1.3900
C85-C86	1.376(7)	C103-C104	1.3900
C8-Ru1-C7	37.89(15)	C31-P2-C43	96.8(2)
C8-Ru1-C9	38.24(14)	C37-P2-Ru1	110.34(13)
C7-Ru1-C9	63.97(15)	C31-P2-Ru1	125.28(14)
C8-Ru1-P1	86.92(12)	C43-P2-Ru1	115.52(13)
C7-Ru1-P1	116.94(11)	C2-C1-C9	132.9(4)
C9-Ru1-P1	92.31(11)	C2-C1-C6	118.6(4)
C8-Ru1-C1	61.66(15)	C9-C1-C6	108.5(3)
C7-Ru1-C1	62.16(15)	C2-C1-Ru1	126.6(3)
C9-Ru1-C1	36.83(14)	C9-C1-Ru1	67.4(2)
P1-Ru1-C1	127.31(10)	C6-C1-Ru1	72.7(2)
C8-Ru1-P2	128.36(11)	C3-C2-C1	119.8(4)
C7-Ru1-P2	96.97(11)	C2-C3-C4	120.8(4)
C9-Ru1-P2	159.90(12)	C5-C4-C3	121.7(4)
P1-Ru1-P2	102.72(4)	C4-C5-C6	118.8(4)
C1-Ru1-P2	129.96(10)	C5-C6-C7	132.6(4)
C8-Ru1-C6	61.44(15)	C5-C6-C1	120.2(4)
C7-Ru1-C6	37.09(14)	C7-C6-C1	107.1(3)
C9-Ru1-C6	61.77(15)	C5-C6-Ru1	130.2(3)
P1-Ru1-C6	148.26(10)	C7-C6-Ru1	65.7(2)
C1-Ru1-C6	36.19(14)	C1-C6-Ru1	71.1(3)
P2-Ru1-C6	99.43(10)	C8-C7-C6	107.5(3)
C8-Ru1-C11	137.39(11)	C8-C7-Ru1	70.2(2)
C7-Ru1-C11	150.97(11)	C6-C7-Ru1	77.2(2)
C9-Ru1-C11	100.15(11)	C7-C8-C9	109.8(3)
P1-Ru1-C11	86.35(4)	C7-C8-Ru1	71.9(2)
C1-Ru1-C11	90.31(10)	C9-C8-Ru1	72.5(2)
P2-Ru1-C11	94.12(4)	C8-C9-C1	106.8(3)
C6-Ru1-C11	114.53(10)	C8-C9-C10	124.6(3)
C25-P1-C18	101.0(2)	C1-C9-C10	127.9(4)
C25-P1-C19	99.5(2)	C8-C9-Ru1	69.2(2)
C18-P1-C19	103.96(19)	C1-C9-Ru1	75.7(2)
C25-P1-Ru1	124.81(13)	C10-C9-Ru1	127.3(3)
C18-P1-Ru1	106.81(16)	C9-C10-C17	112.4(3)
C19-P1-Ru1	118.01(16)	C9-C10-C11	109.4(4)
C37-P2-C31	104.13(19)	C17-C10-C11	111.6(3)
C37-P2-C43	101.59(19)	C16-C11-C12	107.8(3)

C16-C11-C10	116.0(4)	C56-Ru2-C54	61.62(15)
C12-C11-C10	111.1(3)	C55-Ru2-C54	37.32(15)
C13-C12-C11	112.4(4)	C57-Ru2-C54	61.23(14)
C12-C13-C14	110.5(4)	P3-Ru2-C54	148.13(10)
C15-C14-C13	110.4(4)	C56-Ru2-P4	122.89(11)
C14-C15-C16	112.6(4)	C55-Ru2-P4	92.57(11)
C15-C16-C11	112.5(4)	C57-Ru2-P4	156.47(11)
C10-C17-C18	115.9(3)	P3-Ru2-P4	104.15(4)
C17-C18-P1	115.6(3)	C54-Ru2-P4	99.30(10)
C24-C19-C20	119.9(4)	C56-Ru2-C49	61.28(15)
C24-C19-P1	119.8(3)	C55-Ru2-C49	61.76(15)
C20-C19-P1	120.2(4)	C57-Ru2-C49	36.63(14)
C21-C20-C19	119.3(4)	P3-Ru2-C49	124.26(10)
C20-C21-C22	119.8(5)	C54-Ru2-C49	35.34(14)
C23-C22-C21	120.9(4)	P4-Ru2-C49	131.39(11)
C22-C23-C24	119.2(5)	C56-Ru2-C12	139.75(11)
C19-C24-C23	121.0(4)	C55-Ru2-C12	148.54(12)
C26-C25-C30	117.4(4)	C57-Ru2-C12	102.28(10)
C26-C25-P1	121.0(3)	P3-Ru2-C12	87.01(4)
C30-C25-P1	121.7(3)	C54-Ru2-C12	111.32(11)
C27-C26-C25	121.2(4)	P4-Ru2-C12	97.10(4)
C26-C27-C28	121.6(4)	C49-Ru2-C12	89.99(10)
C27-C28-C29	118.1(5)	C75-P3-C69	100.5(2)
C30-C29-C28	121.3(4)	C75-P3-C68	100.6(2)
C29-C30-C25	120.4(4)	C69-P3-C68	102.46(18)
C32-C31-C36	118.2(4)	C75-P3-Ru2	123.83(13)
C32-C31-P2	117.9(3)	C69-P3-Ru2	117.73(15)
C36-C31-P2	123.4(4)	C68-P3-Ru2	108.62(15)
C31-C32-C33	120.7(4)	C87-P4-C81	94.6(2)
C34-C33-C32	120.2(4)	C87-P4-C93	103.05(19)
C33-C34-C35	120.3(5)	C81-P4-C93	101.4(2)
C34-C35-C36	119.4(4)	C87-P4-Ru2	116.19(13)
C35-C36-C31	121.1(4)	C81-P4-Ru2	125.11(14)
C42-C37-C38	117.1(4)	C93-P4-Ru2	112.99(13)
C42-C37-P2	119.5(3)	C50-C49-C54	121.1(4)
C38-C37-P2	122.7(3)	C50-C49-C57	131.0(4)
C39-C38-C37	120.4(5)	C54-C49-C57	107.9(3)
C40-C39-C38	120.7(5)	C50-C49-Ru2	126.6(3)
C39-C40-C41	120.1(5)	C54-C49-Ru2	71.0(2)
C42-C41-C40	120.3(5)	C57-C49-Ru2	66.6(2)
C41-C42-C37	121.3(4)	C51-C50-C49	117.6(4)
C44-C43-C48	118.5(4)	C50-C51-C52	122.6(4)
C44-C43-P2	121.4(3)	C53-C52-C51	120.7(4)
C48-C43-P2	120.1(3)	C52-C53-C54	118.9(4)
C45-C44-C43	121.2(4)	C53-C54-C49	119.0(4)
C46-C45-C44	119.4(4)	C53-C54-C55	132.2(4)
C47-C46-C45	120.3(4)	C49-C54-C55	108.7(4)
C46-C47-C48	120.6(4)	C53-C54-Ru2	128.4(3)
C43-C48-C47	120.0(4)	C49-C54-Ru2	73.7(3)
C56-Ru2-C55	38.42(15)	C55-C54-Ru2	65.6(2)
C56-Ru2-C57	37.93(15)	C56-C55-C54	106.4(3)
C55-Ru2-C57	63.98(15)	C56-C55-Ru2	70.0(2)
C56-Ru2-P3	87.37(12)	C54-C55-Ru2	77.1(3)
C55-Ru2-P3	119.50(11)	C55-C56-C57	109.9(4)
C57-Ru2-P3	90.18(11)	C55-C56-Ru2	71.6(2)

C57-C56-Ru2	73.9(2)	C95-C94-C93	119.9(5)
C56-C57-C49	106.9(3)	C96-C95-C94	120.6(5)
C56-C57-C58	126.9(3)	C95-C96-C97	119.9(4)
C49-C57-C58	125.3(3)	C98-C97-C96	119.7(5)
C56-C57-Ru2	68.2(2)	C93-C98-C97	121.1(4)
C49-C57-Ru2	76.8(2)	C100-C99-C104	120.0
C58-C57-Ru2	128.7(3)	C101-C100-C99	120.0
C57-C58-C65	112.5(3)	C100-C101-C102	120.0
C57-C58-C59	107.5(4)	C103-C102-C101	120.0
C65-C58-C59	114.5(3)	C102-C103-C104	120.0
C60-C59-C64	110.1(4)	C103-C104-C99	120.0
C60-C59-C58	113.8(4)		
C64-C59-C58	113.5(4)		
C61-C60-C59	111.2(4)		
C60-C61-C62	112.5(4)		
C63-C62-C61	111.2(4)		
C62-C63-C64	111.9(4)		
C59-C64-C63	110.6(4)		
C58-C65-C68	113.7(3)		
C65-C68-P3	116.5(3)		
C74-C69-C70	118.4(4)		
C74-C69-P3	120.4(3)		
C70-C69-P3	121.1(3)		
C71-C70-C69	120.2(4)		
C72-C71-C70	119.9(4)		
C73-C72-C71	120.9(4)		
C72-C73-C74	119.3(4)		
C69-C74-C73	121.3(4)		
C76-C75-C80	117.2(4)		
C76-C75-P3	121.3(3)		
C80-C75-P3	121.5(3)		
C77-C76-C75	120.8(4)		
C76-C77-C78	120.9(4)		
C79-C78-C77	119.5(5)		
C78-C79-C80	120.4(4)		
C79-C80-C75	121.2(4)		
C82-C81-C86	119.3(5)		
C82-C81-P4	119.3(3)		
C86-C81-P4	121.1(4)		
C83-C82-C81	119.4(4)		
C84-C83-C82	121.3(5)		
C83-C84-C85	119.3(5)		
C86-C85-C84	120.6(4)		
C85-C86-C81	120.1(5)		
C92-C87-C88	118.2(4)		
C92-C87-P4	124.1(3)		
C88-C87-P4	116.7(3)		
C89-C88-C87	120.2(4)		
C90-C89-C88	120.5(4)		
C89-C90-C91	119.9(4)		
C90-C91-C92	119.5(4)		
C87-C92-C91	121.4(4)		
C98-C93-C94	118.8(4)		
C98-C93-P4	121.6(3)		
C94-C93-P4	119.3(4)		

Table 4. Anisotropic displacement parameters [$\text{\AA}^2 \times 10^3$]. The anisotropic displacement factor exponent takes the form: $-2\pi^2[h^2 a^{*2} U^{11} + \dots + 2 h k a^* b^* U^{12}]$.

Atom	U^{11}	U^{22}	U^{33}	U^{23}	U^{13}	U^{12}
Ru1	19(1)	18(1)	16(1)	-1(1)	-1(1)	0(1)
Cl1	22(1)	32(1)	19(1)	-4(1)	-4(1)	0(1)
P1	24(1)	20(1)	18(1)	1(1)	3(1)	1(1)
P2	20(1)	19(1)	19(1)	1(1)	1(1)	0(1)
C1	23(2)	22(2)	15(2)	-1(2)	-2(2)	0(2)
C2	26(2)	22(2)	19(3)	-7(2)	2(2)	-3(2)
C3	34(2)	27(2)	23(3)	-10(2)	13(2)	-7(2)
C4	45(3)	23(2)	20(3)	1(2)	7(2)	-9(2)
C5	44(3)	20(2)	23(3)	-2(2)	0(2)	0(2)
C6	32(2)	21(2)	14(2)	-4(2)	0(2)	3(2)
C7	24(2)	24(2)	17(3)	-2(2)	-6(2)	3(2)
C8	19(2)	19(2)	23(3)	-5(2)	2(2)	-4(2)
C9	22(2)	19(2)	15(2)	-2(2)	0(2)	2(2)
C10	27(2)	18(2)	23(3)	5(2)	-5(2)	0(2)
C11	25(2)	26(2)	15(2)	-4(2)	0(2)	2(2)
C12	52(3)	22(2)	19(3)	-1(2)	6(2)	-2(2)
C13	61(3)	28(2)	29(3)	-9(2)	12(3)	-2(2)
C14	48(3)	27(2)	32(3)	-9(2)	20(3)	1(2)
C15	45(3)	18(2)	36(3)	-6(2)	8(3)	8(2)
C16	35(2)	23(2)	33(3)	2(2)	9(2)	4(2)
C17	34(2)	17(2)	20(2)	2(2)	9(2)	-1(2)
C18	32(2)	25(2)	22(3)	0(2)	2(2)	6(2)
C19	29(2)	28(2)	26(3)	-3(2)	4(2)	0(2)
C20	38(3)	27(2)	20(3)	-7(2)	13(2)	-3(2)
C21	49(3)	34(3)	41(4)	-13(2)	20(3)	-14(2)
C22	29(3)	58(3)	46(4)	-20(3)	8(3)	-14(2)
C23	23(2)	48(3)	35(3)	-14(3)	0(2)	-7(2)
C24	28(2)	32(2)	26(3)	-4(2)	1(2)	-3(2)
C25	28(2)	23(2)	18(3)	0(2)	7(2)	-3(2)
C26	33(2)	28(2)	23(3)	-2(2)	0(2)	-4(2)
C27	36(2)	32(2)	20(3)	-2(2)	7(2)	-5(2)
C28	43(3)	34(2)	20(3)	-4(2)	-2(2)	-2(2)
C29	38(3)	39(2)	23(3)	0(2)	-9(2)	5(2)
C30	31(2)	29(2)	24(3)	-4(2)	0(2)	5(2)
C31	21(2)	18(2)	25(3)	-3(2)	-2(2)	-4(2)
C32	26(2)	25(2)	27(3)	-4(2)	3(2)	1(2)
C33	34(2)	28(2)	23(3)	2(2)	-9(2)	-7(2)
C34	38(3)	37(2)	20(3)	-12(2)	2(2)	-10(2)
C35	32(3)	40(3)	32(3)	-14(2)	4(2)	-6(2)
C36	27(2)	27(2)	27(3)	-7(2)	-6(2)	1(2)
C37	22(2)	16(2)	22(3)	-2(2)	-1(2)	0(2)
C38	26(2)	27(2)	29(3)	-1(2)	2(2)	1(2)
C39	22(2)	34(2)	48(4)	-7(3)	-4(2)	0(2)
C40	32(2)	26(2)	42(4)	-3(2)	-5(2)	6(2)
C41	40(3)	28(2)	24(3)	-5(2)	-6(2)	11(2)
C42	29(2)	23(2)	20(3)	1(2)	-3(2)	5(2)
C43	21(2)	29(2)	20(2)	-1(2)	2(2)	0(2)

C44	21(2)	26(2)	30(3)	-2(2)	4(2)	1(2)
C45	29(2)	22(2)	37(3)	2(2)	0(2)	-2(2)
C46	27(2)	27(2)	31(3)	3(2)	-2(2)	-6(2)
C47	24(2)	25(2)	29(3)	-2(2)	7(2)	-4(2)
C48	28(2)	22(2)	34(3)	0(2)	-1(2)	8(2)
Ru2	20(1)	17(1)	14(1)	0(1)	1(1)	-1(1)
Cl2	21(1)	27(1)	18(1)	-1(1)	2(1)	-2(1)
P3	22(1)	19(1)	16(1)	0(1)	-2(1)	0(1)
P4	20(1)	19(1)	20(1)	0(1)	1(1)	0(1)
C49	21(2)	26(2)	14(2)	-6(2)	-1(2)	-3(2)
C50	23(2)	23(2)	22(3)	-1(2)	-4(2)	0(2)
C51	39(3)	27(2)	21(3)	-7(2)	-10(2)	0(2)
C52	47(3)	23(2)	25(3)	-5(2)	-12(2)	9(2)
C53	43(3)	21(2)	16(3)	-2(2)	6(2)	1(2)
C54	32(2)	25(2)	9(2)	-1(2)	0(2)	0(2)
C55	32(2)	18(2)	15(2)	-2(2)	5(2)	-3(2)
C56	29(2)	22(2)	11(2)	-4(2)	0(2)	2(2)
C57	24(2)	19(2)	13(2)	-5(2)	4(2)	-4(2)
C58	25(2)	17(2)	20(3)	1(2)	5(2)	2(2)
C59	29(2)	25(2)	21(3)	-4(2)	2(2)	-6(2)
C60	41(3)	38(2)	35(3)	-17(2)	3(3)	2(2)
C61	39(3)	42(3)	26(3)	-14(2)	4(2)	-7(2)
C62	55(3)	26(2)	33(3)	-10(2)	-2(3)	9(2)
C63	61(3)	29(2)	41(4)	-12(2)	11(3)	-13(2)
C64	48(3)	21(2)	27(3)	-4(2)	6(2)	-5(2)
C65	27(2)	15(2)	31(3)	-2(2)	-2(2)	-5(2)
C68	24(2)	24(2)	21(3)	-1(2)	-2(2)	-1(2)
C69	26(2)	23(2)	19(3)	-3(2)	-4(2)	-6(2)
C70	32(2)	23(2)	29(3)	-6(2)	-13(2)	2(2)
C71	37(3)	28(2)	35(3)	-11(2)	-12(2)	6(2)
C72	19(2)	37(2)	43(3)	-15(2)	-4(2)	4(2)
C73	19(2)	36(2)	35(3)	-11(2)	-1(2)	1(2)
C74	27(2)	21(2)	27(3)	-1(2)	-4(2)	0(2)
C75	25(2)	19(2)	22(3)	3(2)	-3(2)	1(2)
C76	31(2)	24(2)	20(3)	0(2)	0(2)	-3(2)
C77	31(2)	37(2)	16(3)	3(2)	5(2)	-1(2)
C78	47(3)	36(2)	14(3)	-1(2)	-5(2)	1(2)
C79	41(3)	34(2)	21(3)	-2(2)	-8(2)	-2(2)
C80	25(2)	30(2)	19(3)	-4(2)	1(2)	-4(2)
C81	22(2)	22(2)	27(3)	1(2)	4(2)	3(2)
C82	32(2)	23(2)	26(3)	-6(2)	9(2)	-2(2)
C83	40(3)	36(2)	22(3)	-8(2)	5(2)	-1(2)
C84	40(3)	41(3)	29(3)	-17(2)	4(2)	3(2)
C85	37(3)	35(2)	32(3)	-11(2)	-1(2)	-10(2)
C86	30(2)	29(2)	35(3)	-10(2)	6(2)	-11(2)
C87	19(2)	23(2)	31(3)	-3(2)	3(2)	-2(2)
C88	31(2)	26(2)	40(3)	6(2)	-8(3)	-3(2)
C89	27(2)	30(2)	58(4)	6(3)	-4(3)	1(2)
C90	29(2)	30(2)	53(4)	6(2)	-9(2)	2(2)
C91	32(2)	26(2)	54(4)	9(2)	-12(3)	-3(2)
C92	24(2)	31(2)	32(3)	4(2)	-3(2)	-5(2)
C93	35(2)	16(2)	28(3)	0(2)	3(2)	-2(2)
C94	29(2)	16(2)	35(3)	3(2)	0(2)	-2(2)
C95	20(2)	35(2)	41(3)	2(3)	8(2)	0(2)
C96	32(3)	33(2)	42(3)	1(2)	11(3)	-2(2)

C97	43(3)	27(2)	23(3)	-3(2)	6(2)	-7(2)
C98	29(2)	20(2)	35(3)	-1(2)	6(2)	-4(2)
C99	98(2)	75(2)	146(3)	-21(2)	-10(2)	0(2)
C100	77(4)	83(4)	145(7)	6(5)	41(5)	3(4)
C101	98(2)	75(2)	146(3)	-21(2)	-10(2)	0(2)
C102	98(2)	75(2)	146(3)	-21(2)	-10(2)	0(2)
C103	98(2)	75(2)	146(3)	-21(2)	-10(2)	0(2)
C104	98(2)	75(2)	146(3)	-21(2)	-10(2)	0(2)

Table 5. Hydrogen coordinates [$\times 10^4$] and isotropic displacement parameters [$\text{\AA}^2 \times 10^3$].

Atom	<i>x</i>	<i>y</i>	<i>z</i>	U_{eq}	<i>S.o.f.</i>
H2	2814	8356	6852	27	1
H3	2140	7553	7214	34	1
H4	3638	6854	7449	35	1
H5	5827	6938	7319	35	1
H7	7740	7704	6940	26	1
H8	7524	8743	6660	24	1
H10	4061	9183	6483	27	1
H11	5838	9707	7006	26	1
H12A	3107	9533	7082	37	1
H12B	4182	9116	7272	37	1
H13A	4879	9928	7645	47	1
H13B	3357	9828	7705	47	1
H14A	2871	10643	7306	43	1
H14B	3855	10880	7618	43	1
H15A	5575	10799	7216	40	1
H15B	4476	11201	7024	40	1
H16A	5331	10501	6598	36	1
H16B	3817	10385	6659	36	1
H17A	6663	9526	6308	28	1
H17B	5418	9884	6166	28	1
H18A	6003	9325	5666	32	1
H18B	4798	8964	5832	32	1
H20	8168	9357	5546	34	1
H21	10346	9665	5559	50	1
H22	11843	9143	5930	53	1
H23	11187	8339	6293	43	1
H24	8994	8058	6300	34	1
H26	8514	7849	5383	34	1
H27	8489	7577	4768	35	1
H28	6637	7689	4410	39	1
H29	4761	8088	4688	40	1
H30	4769	8389	5301	33	1
H32	5340	6982	5550	31	1
H33	5459	6539	4962	34	1
H34	7145	5882	4818	38	1
H35	8700	5639	5265	42	1
H36	8553	6059	5860	32	1
H38	9466	7019	6089	33	1
H39	11321	6936	6459	42	1
H40	11185	6575	7054	40	1
H41	9173	6304	7303	37	1
H42	7321	6366	6947	29	1
H44	6862	5555	6276	31	1

H45	5519	4771	6473	35	1
H46	3449	4989	6695	34	1
H47	2770	5977	6749	31	1
H48	4088	6768	6542	34	1
H50	-1953	6577	8175	27	1
H51	-2893	7379	7857	35	1
H52	-1677	8186	7642	38	1
H53	563	8213	7731	32	1
H55	2751	7514	8034	26	1
H56	2832	6449	8292	25	1
H58	-502	5844	8497	24	1
H59	-332	5608	7871	30	1
H60A	1863	5805	7757	45	1
H60B	2267	5203	7974	45	1
H61A	2272	4999	7338	43	1
H61B	824	5246	7297	43	1
H62A	754	4193	7295	45	1
H62B	1554	4162	7675	45	1
H63A	-601	4002	7803	52	1
H63B	-998	4611	7593	52	1
H64A	-1018	4794	8242	38	1
H64B	445	4561	8279	38	1
H65A	2164	5578	8608	29	1
H65B	1019	5144	8743	29	1
H68A	1531	5671	9264	28	1
H68B	236	5988	9122	28	1
H70	3626	5720	9387	34	1
H71	5842	5511	9370	40	1
H72	7235	6132	9034	40	1
H73	6440	6940	8700	36	1
H74	4210	7127	8690	30	1
H76	-32	6580	9641	30	1
H77	-176	6827	10264	34	1
H78	1602	7220	10580	39	1
H79	3548	7372	10266	38	1
H80	3712	7151	9638	30	1
H82	778	7973	9474	33	1
H83	900	8411	10062	39	1
H84	2295	9209	10178	44	1
H85	3506	9620	9690	42	1
H86	3376	9208	9099	38	1
H88	-790	8444	8702	39	1
H89	-2066	9314	8669	46	1
H90	-1180	10215	8464	45	1
H91	1037	10275	8338	45	1
H92	2339	9423	8411	35	1
H94	4545	8177	9030	32	1
H95	6609	8308	8771	38	1
H96	6839	8554	8154	43	1
H97	4998	8681	7780	37	1
H98	2941	8559	8035	33	1
H99	5883	9258	4379	128	1
H100	5300	10221	4587	122	1
H101	6896	10895	4789	128	1
H102	9074	10605	4784	128	1
H103	9657	9642	4577	128	1
H104	8061	8969	4375	128	1



Table 1. Crystal data and structure refinement details.

Identification code	04sot0639	
Empirical formula	C ₅₄ H ₅₃ ClP ₂ Ru	
Formula weight	900.42	
Temperature	120(2) K	
Wavelength	0.71073 Å	
Crystal system	Orthorhombic	
Space group	<i>Pbca</i>	
Unit cell dimensions	<i>a</i> = 11.287(5) Å <i>b</i> = 22.456(7) Å <i>c</i> = 33.133(11) Å	
Volume	8398(5) Å ³	
<i>Z</i>	8	
Density (calculated)	1.424 Mg / m ³	
Absorption coefficient	0.552 mm ⁻¹	
<i>F</i> (000)	3744	
Crystal	Shard; Light red	
Crystal size	0.08 × 0.08 × 0.02 mm ³	
θ range for data collection	3.05 – 27.50°	
Index ranges	–14 ≤ <i>h</i> ≤ 10, –29 ≤ <i>k</i> ≤ 19, –42 ≤ <i>l</i> ≤ 40	
Reflections collected	37035	
Independent reflections	9513 [<i>R</i> _{int} = 0.1480]	
Completeness to $\theta = 27.50^\circ$	98.6 %	
Absorption correction	Semi-empirical from equivalents	
Max. and min. transmission	0.9890 and 0.9572	
Refinement method	Full-matrix least-squares on <i>F</i> ²	
Data / restraints / parameters	9513 / 0 / 523	
Goodness-of-fit on <i>F</i> ²	1.031	
Final <i>R</i> indices [<i>F</i> ² > 2σ(<i>F</i> ²)]	<i>R</i> 1 = 0.0894, <i>wR</i> 2 = 0.1549	
<i>R</i> indices (all data)	<i>R</i> 1 = 0.2010, <i>wR</i> 2 = 0.1940	
Largest diff. peak and hole	0.898 and –0.606 e Å ⁻³	

Diffractometer: Nonius KappaCCD area detector (ϕ scans and ω scans to fill asymmetric unit). **Cell determination:** DirAx (Duisenberg, A.J.M.(1992). *J. Appl. Cryst.* 25, 92-96.) **Data collection:** Collect (Collect: Data collection software, R. Hooft, Nonius B.V., 1998). **Data reduction and cell refinement:** Denzo (Z. Otwinowski & W. Minor, *Methods in Enzymology* (1997) Vol. 276: *Macromolecular Crystallography*, part A, pp. 307–326; C. W. Carter, Jr. & R. M. Sweet, Eds., Academic Press). **Absorption correction:** Sheldrick, G. M. SADABS - Bruker Nonius area detector scaling and absorption correction - V2.10 **Structure solution:** SHELXS97 (G. M. Sheldrick, *Acta Cryst.* (1990) A46 467–473). **Structure refinement:** SHELXL97 (G. M. Sheldrick (1997), University of Göttingen, Germany). **Graphics:** Cameron - A Molecular Graphics Package. (D. M. Watkin, L. Pearce and C. K. Prout, *Chemical Crystallography Laboratory*, University of Oxford, 1993).

Special details: All hydrogen atoms were placed in idealised positions and refined using a riding model.

Table 2. Atomic coordinates [$\times 10^4$], equivalent isotropic displacement parameters [$\text{\AA}^2 \times 10^3$] and site occupancy factors. U_{eq} is defined as one third of the trace of the orthogonalized U^{ij} tensor.

Atom	x	y	z	U_{eq}	$S.o.f.$
C1	2741(6)	1464(3)	1565(2)	30(2)	1
C2	3827(6)	1149(3)	1612(2)	36(2)	1
C3	4066(6)	861(3)	1234(2)	31(2)	1
C4	4985(6)	483(3)	1107(2)	40(2)	1
C5	4935(6)	226(3)	732(3)	45(2)	1
C6	3993(6)	340(3)	471(2)	41(2)	1
C7	3128(6)	733(3)	575(2)	36(2)	1
C8	3152(6)	1016(3)	959(2)	30(2)	1
C9	2351(6)	1433(3)	1158(2)	29(2)	1
C10	1163(5)	1632(3)	994(2)	29(2)	1
C11	331(6)	1088(3)	944(2)	32(2)	1
C12	281(6)	702(3)	1328(2)	41(2)	1
C13	-537(6)	167(3)	1294(2)	45(2)	1
C14	-1771(7)	356(3)	1165(2)	48(2)	1
C15	-1751(7)	726(3)	779(2)	47(2)	1
C16	-930(6)	1262(3)	818(2)	37(2)	1
C17	1259(6)	1992(3)	605(2)	31(2)	1
C18	1960(6)	2572(3)	615(2)	34(2)	1
C19	3895(6)	2120(3)	148(2)	31(2)	1
C20	4721(6)	1660(3)	129(2)	38(2)	1
C21	4940(6)	1388(3)	-234(2)	43(2)	1
C22	4356(7)	1571(3)	-583(2)	45(2)	1
C23	3543(6)	2032(3)	-559(2)	42(2)	1
C24	3320(6)	2301(3)	-203(2)	34(2)	1
C25	4129(6)	3217(3)	523(2)	35(2)	1
C26	5328(7)	3261(3)	427(2)	37(2)	1
C27	5834(7)	3804(3)	335(2)	42(2)	1
C28	5146(8)	4306(3)	326(2)	49(2)	1
C29	3961(8)	4270(3)	410(2)	57(2)	1
C30	3456(7)	3720(3)	516(2)	47(2)	1
C31	2762(6)	3191(3)	1617(2)	38(2)	1
C32	2940(7)	3777(3)	1489(2)	51(2)	1
C33	1985(8)	4158(3)	1443(3)	64(3)	1
C34	852(8)	3973(3)	1525(2)	55(2)	1
C35	664(7)	3392(3)	1651(2)	39(2)	1
C36	1613(6)	3012(3)	1685(2)	37(2)	1
C37	5286(6)	3179(3)	1721(2)	38(2)	1
C38	6009(6)	3313(3)	1399(2)	39(2)	1
C39	6961(7)	3708(3)	1440(3)	53(2)	1
C40	7182(8)	3957(3)	1816(3)	54(2)	1
C41	6484(7)	3819(3)	2144(3)	57(2)	1
C42	5520(6)	3433(3)	2093(2)	41(2)	1
C43	3915(6)	2404(3)	2185(2)	33(2)	1
C44	4805(6)	2023(3)	2314(2)	38(2)	1
C45	4846(6)	1815(3)	2708(2)	40(2)	1
C46	3986(7)	1984(3)	2978(2)	44(2)	1
C47	3092(7)	2368(3)	2859(2)	44(2)	1
C48	3043(6)	2570(3)	2465(2)	37(2)	1
P1	3561(2)	2472(1)	642(1)	30(1)	1
P2	4011(2)	2668(1)	1657(1)	33(1)	1
Cl1	6168(2)	1936(1)	1110(1)	40(1)	1
Ru1	4031(1)	1912(1)	1200(1)	30(1)	1
C1S	2279(11)	185(5)	2246(4)	91(3)	1

C2S	1378(11)	-217(5)	2263(3)	82(3)	1
C3S	635(9)	-171(5)	2548(3)	81(3)	1
C4S	723(11)	207(5)	2842(4)	101(4)	1
C5S	1686(12)	652(5)	2830(3)	88(3)	1
C6S	2422(10)	632(6)	2541(3)	93(4)	1

Table 3. Bond lengths [Å] and angles [°].

C1–C9	1.420(8)	C26–C27	1.380(9)
C1–C2	1.424(9)	C27–C28	1.369(10)
C1–Ru1	2.142(6)	C28–C29	1.369(10)
C2–C3	1.435(9)	C29–C30	1.406(10)
C2–Ru1	2.202(6)	C31–C36	1.376(9)
C3–C4	1.405(9)	C31–C32	1.396(9)
C3–C8	1.420(9)	C31–P2	1.841(7)
C3–Ru1	2.364(6)	C32–C33	1.385(10)
C4–C5	1.372(9)	C33–C34	1.371(11)
C5–C6	1.394(10)	C34–C35	1.385(10)
C6–C7	1.361(9)	C35–C36	1.375(9)
C7–C8	1.421(9)	C37–C38	1.376(9)
C8–C9	1.460(8)	C37–C42	1.386(9)
C8–Ru1	2.383(6)	C37–P2	1.852(7)
C9–C10	1.514(8)	C38–C39	1.400(10)
C9–Ru1	2.185(6)	C39–C40	1.387(10)
C10–C17	1.525(8)	C39–H39	0.9500
C10–C11	1.550(8)	C40–C41	1.380(11)
C11–C16	1.534(9)	C41–C42	1.401(10)
C11–C12	1.540(9)	C43–C44	1.387(9)
C12–C13	1.521(9)	C43–C48	1.403(9)
C13–C14	1.517(10)	C43–P2	1.850(7)
C14–C15	1.526(10)	C44–C45	1.386(9)
C15–C16	1.524(9)	C45–C46	1.375(9)
C17–C18	1.525(8)	C46–C47	1.385(9)
C18–P1	1.823(7)	C47–C48	1.382(9)
C19–C24	1.392(8)	P1–Ru1	2.2989(19)
C19–C20	1.394(9)	P2–Ru1	2.2733(19)
C19–P1	1.855(6)	C11–Ru1	2.431(2)
C20–C21	1.372(9)	C1S–C2S	1.362(13)
C21–C22	1.393(10)	C1S–C6S	1.411(14)
C22–C23	1.386(10)	C2S–C3S	1.266(12)
C23–C24	1.349(9)	C3S–C4S	1.296(13)
C25–C30	1.361(9)	C4S–C5S	1.476(15)
C25–C26	1.393(9)	C5S–C6S	1.269(13)
C25–P1	1.835(7)		

C9-C1-C2	110.3(6)
C9-C1-Ru1	72.5(3)
C2-C1-Ru1	73.2(4)
C1-C2-C3	106.9(6)
C1-C2-Ru1	68.6(3)
C3-C2-Ru1	77.9(4)
C4-C3-C8	119.5(6)
C4-C3-C2	132.3(6)
C8-C3-C2	108.2(6)
C4-C3-Ru1	127.0(4)
C8-C3-Ru1	73.3(3)
C2-C3-Ru1	65.6(3)
C5-C4-C3	119.6(7)
C4-C5-C6	121.1(7)
C7-C6-C5	120.5(7)
C6-C7-C8	120.2(7)
C3-C8-C7	118.6(6)
C3-C8-C9	108.5(6)
C7-C8-C9	132.7(6)
C3-C8-Ru1	71.9(4)
C7-C8-Ru1	133.3(4)
C9-C8-Ru1	64.1(3)
C1-C9-C8	105.5(5)
C1-C9-C10	126.9(6)
C8-C9-C10	125.2(6)
C1-C9-Ru1	69.2(3)
C8-C9-Ru1	78.9(4)
C10-C9-Ru1	130.3(4)
C9-C10-C17	113.4(5)
C9-C10-C11	110.1(5)
C17-C10-C11	111.7(5)
C16-C11-C12	109.5(5)
C16-C11-C10	113.0(5)
C12-C11-C10	112.1(5)
C13-C12-C11	113.9(6)
C14-C13-C12	110.9(6)
C13-C14-C15	111.9(6)
C16-C15-C14	111.7(6)
C15-C16-C11	112.6(6)
C10-C17-C18	118.1(5)
C17-C18-P1	114.2(4)
C24-C19-C20	119.3(6)
C24-C19-P1	121.2(5)
C20-C19-P1	119.5(5)
C21-C20-C19	119.4(7)
C20-C21-C22	120.8(7)
C23-C22-C21	119.0(7)
C24-C23-C22	120.6(7)
C23-C24-C19	120.9(7)
C30-C25-C26	118.7(6)
C30-C25-P1	124.4(6)
C26-C25-P1	116.9(5)
C27-C26-C25	121.0(7)
C28-C27-C26	119.8(7)
C29-C28-C27	120.1(7)

C28-C29-C30	119.9(7)
C25-C30-C29	120.4(7)
C36-C31-C32	117.4(7)
C36-C31-P2	121.6(5)
C32-C31-P2	120.9(6)
C33-C32-C31	120.3(7)
C34-C33-C32	121.1(7)
C33-C34-C35	119.2(7)
C36-C35-C34	119.3(7)
C35-C36-C31	122.6(7)
C38-C37-C42	119.1(7)
C38-C37-P2	120.6(5)
C42-C37-P2	120.3(6)
C37-C38-C39	121.2(7)
C40-C39-C38	118.8(8)
C41-C40-C39	120.9(8)
C40-C41-C42	119.2(8)
C37-C42-C41	120.7(7)
C44-C43-C48	117.9(6)
C44-C43-P2	116.5(5)
C48-C43-P2	125.6(5)
C43-C44-C45	121.5(7)
C46-C45-C44	119.8(7)
C45-C46-C47	119.9(6)
C48-C47-C46	120.3(7)
C47-C48-C43	120.6(6)
C18-P1-C25	102.9(3)
C18-P1-C19	102.1(3)
C25-P1-C19	97.4(3)
C18-P1-Ru1	109.6(2)
C25-P1-Ru1	126.2(2)
C19-P1-Ru1	115.4(2)
C31-P2-C43	103.1(3)
C31-P2-C37	102.0(3)
C43-P2-C37	97.8(3)
C31-P2-Ru1	115.9(2)
C43-P2-Ru1	113.0(2)
C37-P2-Ru1	122.0(2)
C1-Ru1-C9	38.3(2)
C1-Ru1-C2	38.2(2)
C9-Ru1-C2	64.3(2)
C1-Ru1-P2	88.20(18)
C9-Ru1-P2	113.68(18)
C2-Ru1-P2	99.65(19)
C1-Ru1-P1	123.59(18)
C9-Ru1-P1	90.97(17)
C2-Ru1-P1	154.12(19)
P2-Ru1-P1	97.20(7)
C1-Ru1-C3	61.0(2)
C9-Ru1-C3	61.7(2)
C2-Ru1-C3	36.4(2)
P2-Ru1-C3	135.56(17)
P1-Ru1-C3	126.02(17)
C1-Ru1-C8	60.6(2)
C9-Ru1-C8	37.0(2)

C2–Ru1–C8	60.4(2)
P2–Ru1–C8	148.19(16)
P1–Ru1–C8	95.50(16)
C3–Ru1–C8	34.8(2)
C1–Ru1–C11	138.95(18)
C9–Ru1–C11	149.78(17)
C2–Ru1–C11	101.37(18)
P2–Ru1–C11	94.32(6)
P1–Ru1–C11	96.78(6)
C3–Ru1–C11	90.64(16)
C8–Ru1–C11	112.98(16)
C2S–C1S–C6S	121.9(11)
C3S–C2S–C1S	118.1(11)
C2S–C3S–C4S	124.3(11)
C3S–C4S–C5S	118.7(11)
C6S–C5S–C4S	118.5(11)
C5S–C6S–C1S	118.2(12)

Table 4. Anisotropic displacement parameters [$\text{\AA}^2 \times 10^3$]. The anisotropic displacement factor exponent takes the form: $-2\pi^2[h^2 a^{*2} U^{11} + \dots + 2 h k a^* b^* U^{12}]$.

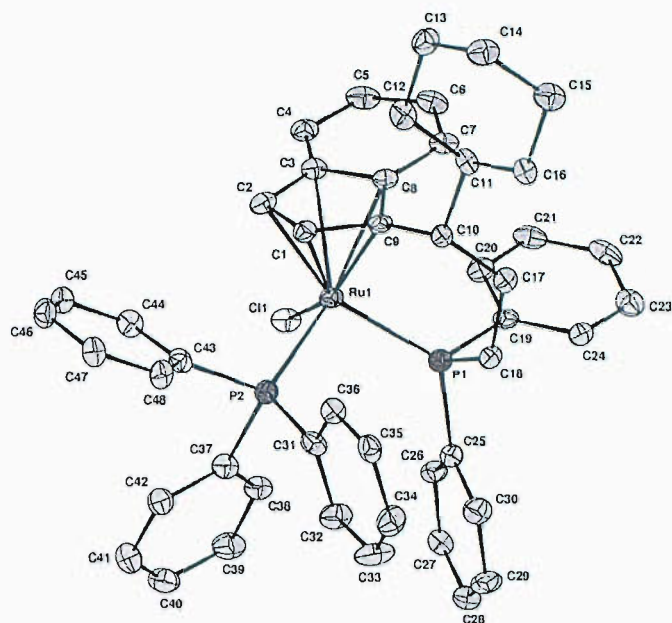
Atom	U^{11}	U^{22}	U^{33}	U^{23}	U^{13}	U^{12}
C1	35(4)	28(4)	29(4)	5(3)	4(3)	-5(3)
C2	29(4)	28(4)	50(4)	9(3)	-3(4)	0(3)
C3	14(4)	27(3)	53(4)	2(3)	-4(4)	-1(3)
C4	33(5)	30(4)	56(5)	7(4)	-4(4)	-8(4)
C5	26(4)	31(4)	76(6)	-4(4)	9(4)	-2(4)
C6	29(4)	37(4)	55(5)	-9(4)	12(4)	-9(4)
C7	32(4)	24(3)	52(5)	-1(3)	6(4)	-1(3)
C8	27(4)	23(3)	40(4)	1(3)	5(3)	-2(3)
C9	26(4)	23(3)	38(4)	4(3)	-1(3)	-6(3)
C10	25(4)	30(3)	31(4)	-2(3)	-1(3)	4(3)
C11	28(4)	40(4)	29(4)	-7(3)	0(3)	-3(3)
C12	26(4)	48(4)	50(5)	-3(4)	-1(3)	3(4)
C13	36(5)	42(4)	58(5)	11(4)	-8(4)	-1(4)
C14	33(5)	40(4)	70(5)	2(4)	2(4)	-2(4)
C15	28(4)	44(4)	70(5)	-5(4)	-3(4)	-2(4)
C16	34(4)	42(4)	34(4)	-4(3)	-3(4)	-1(4)
C17	22(4)	33(4)	38(4)	-2(3)	-1(3)	9(3)
C18	40(5)	30(4)	32(4)	4(3)	-2(3)	2(3)
C19	34(4)	26(3)	33(4)	3(3)	7(3)	-7(3)
C20	38(5)	35(4)	41(4)	5(3)	5(4)	-1(4)
C21	36(5)	33(4)	60(5)	-7(4)	15(4)	-10(4)
C22	41(5)	47(5)	46(5)	-18(4)	19(4)	-21(4)
C23	41(5)	44(4)	41(4)	-1(4)	5(4)	-12(4)
C24	35(4)	30(4)	37(4)	4(3)	0(3)	0(3)
C25	36(5)	30(4)	39(4)	1(3)	-8(4)	1(3)
C26	43(5)	28(4)	39(4)	0(3)	3(4)	3(3)
C27	48(5)	38(4)	39(4)	-5(3)	-5(4)	-4(4)
C28	57(6)	38(5)	51(5)	3(4)	-9(4)	-15(4)
C29	63(6)	26(4)	82(6)	5(4)	-21(5)	9(4)
C30	40(5)	37(4)	65(5)	-2(4)	-10(4)	11(4)

C31	42(5)	36(4)	37(4)	-13(3)	0(4)	1(4)
C32	32(5)	36(4)	85(6)	4(4)	-10(4)	5(4)
C33	49(6)	30(4)	115(8)	13(5)	-1(5)	-2(4)
C34	58(6)	48(5)	61(5)	0(4)	-12(5)	20(5)
C35	40(5)	44(4)	35(4)	-11(4)	-5(3)	10(4)
C36	30(4)	39(4)	41(4)	-6(3)	-1(3)	7(4)
C37	30(4)	36(4)	46(5)	-1(4)	-1(4)	0(3)
C38	36(5)	32(4)	48(4)	-2(3)	1(4)	0(4)
C39	45(5)	43(5)	70(6)	3(4)	5(5)	-6(4)
C40	58(6)	37(4)	69(6)	-3(4)	-11(5)	-7(4)
C41	57(6)	56(5)	59(6)	-1(4)	-23(5)	-8(5)
C42	35(4)	43(4)	46(5)	0(4)	-5(4)	-2(4)
C43	27(4)	37(4)	36(4)	-1(3)	-4(3)	-7(3)
C44	27(4)	43(4)	46(5)	-4(4)	-1(3)	5(4)
C45	41(5)	41(4)	39(4)	3(4)	-10(4)	-1(4)
C46	52(5)	51(5)	28(4)	0(3)	-4(4)	4(4)
C47	44(5)	54(5)	32(4)	-2(4)	-3(4)	1(4)
C48	25(4)	46(4)	39(4)	-2(3)	-4(3)	12(3)
P1	27(1)	27(1)	38(1)	0(1)	1(1)	2(1)
P2	32(1)	31(1)	37(1)	1(1)	-4(1)	1(1)
Cl1	27(1)	32(1)	60(1)	-1(1)	2(1)	0(1)
Ru1	26(1)	25(1)	38(1)	1(1)	-2(1)	1(1)
C1S	99(9)	79(7)	96(9)	18(7)	-1(7)	-15(7)
C2S	116(10)	71(7)	59(7)	3(5)	-8(7)	-5(7)
C3S	58(7)	105(8)	78(7)	-50(7)	1(6)	-10(6)
C4S	102(10)	89(9)	113(10)	9(8)	21(8)	22(8)
C5S	113(10)	72(7)	78(8)	-13(6)	-17(7)	16(7)
C6S	79(8)	134(11)	66(7)	28(8)	2(7)	-28(8)

Table 5. Hydrogen coordinates [$\times 10^4$] and isotropic displacement parameters [$\text{\AA}^2 \times 10^3$].

Atom	x	y	z	U_{eq}	$S.o.f.$
H1	2336	1667	1775	36	1
H2	4302	1133	1848	43	1
H4	5639	406	1280	47	1
H5	5552	-34	649	53	1
H6	3954	140	218	49	1
H7	2507	819	391	43	1
H10	798	1898	1201	35	1
H11	666	834	723	39	1
H12A	1091	561	1391	50	1
H12B	14	953	1556	50	1
H13A	-212	-117	1093	54	1
H13B	-580	-39	1557	54	1
H14A	-2139	591	1385	57	1
H14B	-2264	-3	1122	57	1
H15A	-1484	474	552	57	1
H15B	-2564	866	718	57	1
H16A	-1261	1541	1020	44	1
H16B	-898	1473	556	44	1
H17A	445	2086	514	37	1
H17B	1619	1732	397	37	1
H18A	1700	2808	851	41	1

H18B	1770	2805	370	41	1
H20	5129	1536	365	46	1
H21	5497	1071	-248	52	1
H22	4512	1382	-834	53	1
H23	3139	2160	-795	50	1
H24	2764	2618	-191	41	1
H26	5804	2912	426	44	1
H27	6657	3829	278	50	1
H28	5492	4679	261	59	1
H29	3480	4617	396	68	1
H30	2639	3699	584	57	1
H32	3719	3914	1433	61	1
H33	2116	4554	1353	77	1
H34	204	4239	1495	66	1
H35	-113	3258	1712	47	1
H36	1470	2610	1760	44	1
H38	5860	3134	1144	47	1
H39	7446	3803	1215	63	1
H40	7823	4227	1847	65	1
H41	6655	3983	2402	69	1
H42	5021	3345	2317	49	1
H44	5399	1902	2128	46	1
H45	5467	1557	2790	48	1
H46	4005	1837	3247	52	1
H47	2511	2493	3048	52	1
H48	2414	2824	2384	44	1
H1S	2827	165	2029	109	1
H2S	1309	-524	2067	99	1
H3S	-30	-429	2545	97	1
H4S	179	198	3060	122	1
H5S	1753	946	3035	105	1
H6S	3054	911	2524	112	1



Thermal ellipsoids drawn at the 30% probability level, hydrogens and benzene solvent omitted for clarity



Table 1. Crystal data and structure refinement.

Identification code	04sot0541	
Empirical formula	C ₅₀ H ₅₀ F ₆ NP ₃ Ru	
Formula weight	972.89	
Temperature	120(2) K	
Wavelength	0.71073 Å	
Crystal system	Monoclinic	
Space group	P2 ₁ /c	
Unit cell dimensions	<i>a</i> = 18.381(3) Å	$\alpha = 90^\circ$
	<i>b</i> = 11.8778(10) Å	$\beta = 101.822(11)^\circ$
	<i>c</i> = 25.151(3) Å	$\gamma = 90^\circ$
Volume	5374.6(11) Å ³	
<i>Z</i>	4	
Density (calculated)	1.202 Mg / m ³	
Absorption coefficient	0.432 mm ⁻¹	
<i>F</i> (000)	2000	
Crystal	Block; yellow	
Crystal size	0.10 × 0.10 × 0.10 mm ³	
θ range for data collection	3.02 – 27.50°	
Index ranges	–23 ≤ <i>h</i> ≤ 23, –14 ≤ <i>k</i> ≤ 15, –28 ≤ <i>l</i> ≤ 32	
Reflections collected	49236	
Independent reflections	12314 [<i>R</i> _{int} = 0.0578]	
Completeness to $\theta = 27.50^\circ$	99.7 %	
Absorption correction	Semi-empirical from equivalents	
Max. and min. transmission	0.9581 and 0.9581	
Refinement method	Full-matrix least-squares on <i>F</i> ²	
Data / restraints / parameters	12314 / 0 / 552	
Goodness-of-fit on <i>F</i> ²	1.090	
Final <i>R</i> indices [<i>F</i> ² > 2σ(<i>F</i> ²)]	<i>R</i> 1 = 0.0743, <i>wR</i> 2 = 0.2037	
<i>R</i> indices (all data)	<i>R</i> 1 = 0.1158, <i>wR</i> 2 = 0.2227	
Extinction coefficient	0.0013(5)	
Largest diff. peak and hole	1.003 and –0.915 e Å ⁻³	

Diffraction: Nonius KappaCCD area detector (ϕ scans and ω scans to fill *asymmetric unit* sphere). **Cell determination:** DirAx (Duisenberg, A.J.M.(1992). *J. Appl. Cryst.* 25, 92-96.) **Data collection:** Collect (Collect: Data collection software, R. Hooft, Nonius B.V., 1998). **Data reduction and cell refinement:** Denzo (Z. Otwinowski & W. Minor, *Methods in Enzymology* (1997) Vol. 276: *Macromolecular Crystallography*, part A, pp. 307–326; C. W. Carter, Jr. & R. M. Sweet, Eds., Academic Press). **Absorption correction:** SORTAV (R. H. Blessing, *Acta Cryst.* A51 (1995) 33–37; R. H. Blessing, *J. Appl. Cryst.* 30 (1997) 421–426). **Structure solution:** SHELXS97 (G. M. Sheldrick, *Acta Cryst.* (1990) A46 467–473). **Structure refinement:** SHELXL97 (G. M. Sheldrick (1997), University of Göttingen, Germany). **Graphics:** Cameron - A Molecular Graphics Package. (D. M. Watkin, L. Pearce and C. K. Prout, Chemical Crystallography Laboratory, University of Oxford, 1993).

Special details: Solvent molecules have been removed using the Squeeze module of Platon.

Table 2. Atomic coordinates [$\times 10^4$], equivalent isotropic displacement parameters [$\text{Å}^2 \times 10^3$] and site

occupancy factors. U_{eq} is defined as one third of the trace of the orthogonalized U^{ij} tensor.

Atom	x	y	z	U_{eq}	$S.o.f.$
C1	2870(4)	4654(4)	2661(2)	61(2)	1
C2	2503(4)	3604(4)	2507(2)	68(2)	1
C3	2972(4)	2881(4)	2306(2)	66(2)	1
C4	3697(4)	3389(4)	2383(2)	60(2)	1
C5	4402(4)	3024(5)	2313(2)	68(2)	1
C6	5000(4)	3725(6)	2438(2)	78(2)	1
C7	4919(4)	4830(6)	2632(2)	78(2)	1
C8	4260(4)	5227(5)	2711(2)	66(2)	1
C9	3609(4)	4506(4)	2601(2)	58(1)	1
C10	2614(4)	5619(4)	2951(3)	70(2)	1
C11	2876(4)	5463(5)	3609(3)	83(2)	1
C12	2382(6)	4525(6)	3788(3)	117(3)	1
C13	2709(5)	4411(8)	4441(3)	114(3)	1
C14	2676(5)	5424(7)	4721(3)	102(3)	1
C15	3123(5)	6267(7)	4489(3)	107(3)	1
C16	2869(5)	6514(7)	3897(3)	101(2)	1
C17	1788(5)	5801(5)	2731(3)	97(3)	1
C18	1563(4)	6224(5)	2130(3)	89(2)	1
C19	1332(3)	5999(5)	987(3)	70(2)	1
C20	942(3)	5505(5)	519(4)	91(2)	1
C21	772(4)	6059(7)	31(4)	113(3)	1
C22	990(4)	7213(6)	30(4)	108(3)	1
C23	1380(4)	7681(5)	491(4)	91(2)	1
C24	1560(3)	7124(4)	964(3)	74(2)	1
C25	800(4)	4272(5)	1586(4)	95(3)	1
C26	839(4)	3139(5)	1576(4)	102(3)	1
C27	211(6)	2490(8)	1552(5)	142(4)	1
C28	-444(6)	2980(11)	1529(6)	182(6)	1
C29	-514(6)	4098(11)	1520(7)	189(6)	1
C30	107(4)	4776(8)	1551(5)	139(4)	1
C31	3642(3)	2573(4)	1013(2)	48(1)	1
C32	3670(3)	1435(4)	927(2)	59(1)	1
C33	4334(4)	888(5)	940(2)	72(2)	1
C34	4972(4)	1496(6)	1028(2)	73(2)	1
C35	4981(3)	2670(5)	1118(2)	67(2)	1
C36	4298(3)	3203(4)	1105(2)	58(1)	1
C37	2824(3)	4157(4)	333(2)	57(1)	1
C38	3060(4)	3589(7)	-86(2)	99(3)	1
C39	3047(5)	4107(8)	-568(3)	123(4)	1
C40	2835(4)	5188(8)	-650(3)	104(3)	1
C41	2617(4)	5798(6)	-245(3)	86(2)	1
C42	2615(3)	5275(5)	251(2)	62(1)	1
C43	2044(3)	2387(4)	756(2)	62(1)	1
C44	2001(4)	1447(5)	1076(3)	74(2)	1
C45	1409(5)	673(6)	951(4)	102(3)	1
C46	885(6)	850(9)	516(6)	149(5)	1
C47	899(6)	1780(11)	190(5)	153(5)	1
C48	1497(4)	2547(6)	314(3)	100(3)	1
C49	3385(2)	6712(4)	1430(2)	41(1)	1
C50	3648(4)	7656(5)	1307(3)	87(2)	1
P1	2795(1)	3422(1)	973(1)	44(1)	1
P2	1618(1)	5173(1)	1598(1)	64(1)	1
N1	3153(2)	5859(3)	1524(2)	45(1)	1
Ru1	2767(1)	4385(1)	1779(1)	43(1)	1

P3	2684(1)	9367(1)	2526(1)	66(1)	1
F1	2170(3)	8691(3)	2844(2)	110(2)	1
F2	3135(3)	8255(3)	2483(2)	127(2)	1
F3	2187(4)	8949(5)	1966(2)	155(2)	1
F4	2192(3)	10436(3)	2486(4)	171(3)	1
F5	3210(4)	9723(6)	3045(2)	199(4)	1
F6	3213(2)	10023(3)	2193(2)	84(1)	1

Table 3. Bond lengths [Å] and angles [°].

C1–C9	1.407(8)	C17–C18	1.567(10)
C1–C2	1.434(6)	C17–H17A	0.9900
C1–C10	1.486(7)	C17–H17B	0.9900
C1–Ru1	2.209(5)	C18–P2	1.847(6)
C2–C3	1.382(8)	C18–H18A	0.9900
C2–Ru1	2.192(5)	C18–H18B	0.9900
C2–H2	0.9500	C19–C20	1.378(10)
C3–C4	1.439(8)	C19–C24	1.405(7)
C3–Ru1	2.210(5)	C19–P2	1.807(7)
C3–H3	0.9500	C20–C21	1.371(11)
C4–C5	1.410(8)	C20–H20	0.9500
C4–C9	1.457(7)	C21–C22	1.429(10)
C4–Ru1	2.359(5)	C21–H21	0.9500
C5–C6	1.363(9)	C22–C23	1.352(11)
C5–H5	0.9500	C22–H22	0.9500
C6–C7	1.419(9)	C23–C24	1.342(10)
C6–H6	0.9500	C23–H23	0.9500
C7–C8	1.352(9)	C24–H24	0.9500
C7–H7	0.9500	C25–C26	1.348(9)
C8–C9	1.452(8)	C25–C30	1.394(10)
C8–H8	0.9500	C25–P2	1.840(6)
C9–Ru1	2.319(5)	C26–C27	1.379(9)
C10–C17	1.521(11)	C26–H26	0.9500
C10–C11	1.637(9)	C27–C28	1.328(15)
C10–H10	1.0000	C27–H27	0.9500
C11–C16	1.445(9)	C28–C29	1.334(14)
C11–C12	1.561(9)	C28–H28	0.9500
C11–H11	1.0000	C29–C30	1.385(12)
C12–C13	1.634(12)	C29–H29	0.9500
C12–H12A	0.9900	C30–H30	0.9500
C12–H12B	0.9900	C31–C32	1.371(7)
C13–C14	1.401(11)	C31–C36	1.396(7)
C13–H13A	0.9900	C31–P1	1.841(4)
C13–H13B	0.9900	C32–C33	1.378(8)
C14–C15	1.489(11)	C32–H32	0.9500
C14–H14A	0.9900	C33–C34	1.357(9)
C14–H14B	0.9900	C33–H33	0.9500
C15–C16	1.495(10)	C34–C35	1.412(8)
C15–H15A	0.9900	C34–H34	0.9500
C15–H15B	0.9900	C35–C36	1.400(7)
C16–H16A	0.9900	C35–H35	0.9500
C16–H16B	0.9900	C36–H36	0.9500

C37-C42	1.385(7)	Ru1-C3-H3	117.8
C37-C38	1.393(7)	C5-C4-C3	134.7(5)
C37-P1	1.841(5)	C5-C4-C9	120.2(5)
C38-C39	1.354(10)	C3-C4-C9	105.0(5)
C38-H38	0.9500	C5-C4-Ru1	129.5(4)
C39-C40	1.345(11)	C3-C4-Ru1	66.1(3)
C39-H39	0.9500	C9-C4-Ru1	70.3(3)
C40-C41	1.376(11)	C6-C5-C4	120.2(5)
C40-H40	0.9500	C6-C5-H5	119.9
C41-C42	1.396(8)	C4-C5-H5	119.9
C41-H41	0.9500	C5-C6-C7	120.4(6)
C42-H42	0.9500	C5-C6-H6	119.8
C43-C48	1.350(8)	C7-C6-H6	119.8
C43-C44	1.389(8)	C8-C7-C6	122.3(6)
C43-P1	1.846(5)	C8-C7-H7	118.9
C44-C45	1.410(9)	C6-C7-H7	118.9
C44-H44	0.9500	C7-C8-C9	119.7(5)
C45-C46	1.317(14)	C7-C8-H8	120.2
C45-H45	0.9500	C9-C8-H8	120.2
C46-C47	1.380(15)	C1-C9-C8	133.0(5)
C46-H46	0.9500	C1-C9-C4	109.8(5)
C47-C48	1.412(13)	C8-C9-C4	117.2(6)
C47-H47	0.9500	C1-C9-Ru1	67.7(3)
C48-H48	0.9500	C8-C9-Ru1	125.4(3)
C49-N1	1.142(5)	C4-C9-Ru1	73.4(3)
C49-C50	1.284(7)	C1-C10-C17	109.0(5)
C50-H50A	0.9800	C1-C10-C11	110.6(5)
C50-H50B	0.9800	C17-C10-C11	116.7(5)
C50-H50C	0.9800	C1-C10-H10	106.7
P1-Ru1	2.3390(12)	C17-C10-H10	106.7
P2-Ru1	2.2699(15)	C11-C10-H10	106.7
N1-Ru1	2.042(4)	C16-C11-C12	114.0(6)
P3-F5	1.517(5)	C16-C11-C10	112.2(6)
P3-F4	1.549(5)	C12-C11-C10	107.7(6)
P3-F2	1.575(4)	C16-C11-H11	107.6
P3-F1	1.575(4)	C12-C11-H11	107.6
P3-F3	1.593(5)	C10-C11-H11	107.6
P3-F6	1.609(3)	C11-C12-C13	103.4(7)
C9-C1-C2	105.8(5)	C11-C12-H12A	111.1
C9-C1-C10	124.0(5)	C13-C12-H12A	111.1
C2-C1-C10	128.7(5)	C11-C12-H12B	111.1
C9-C1-Ru1	76.2(3)	C13-C12-H12B	111.1
C2-C1-Ru1	70.3(3)	H12A-C12-H12B	109.0
C10-C1-Ru1	129.3(4)	C14-C13-C12	112.9(7)
C3-C2-C1	110.2(5)	C14-C13-H13A	109.0
C3-C2-Ru1	72.4(3)	C12-C13-H13A	109.0
C1-C2-Ru1	71.6(3)	C14-C13-H13B	109.0
C3-C2-H2	124.9	C12-C13-H13B	109.0
C1-C2-H2	124.9	H13A-C13-H13B	107.8
Ru1-C2-H2	122.6	C13-C14-C15	107.2(7)
C2-C3-C4	108.7(4)	C13-C14-H14A	110.3
C2-C3-Ru1	71.0(3)	C15-C14-H14A	110.3
C4-C3-Ru1	77.4(3)	C13-C14-H14B	110.3
C2-C3-H3	125.6	C15-C14-H14B	110.3
C4-C3-H3	125.6	H14A-C14-H14B	108.5

C14-C15-C16	115.9(8)	C28-C29-H29	119.9
C14-C15-H15A	108.3	C30-C29-H29	119.9
C16-C15-H15A	108.3	C29-C30-C25	119.0(9)
C14-C15-H15B	108.3	C29-C30-H30	120.5
C16-C15-H15B	108.3	C25-C30-H30	120.5
H15A-C15-H15B	107.4	C32-C31-C36	119.7(5)
C11-C16-C15	107.3(7)	C32-C31-P1	126.1(4)
C11-C16-H16A	110.2	C36-C31-P1	114.0(3)
C15-C16-H16A	110.2	C31-C32-C33	121.5(6)
C11-C16-H16B	110.3	C31-C32-H32	119.3
C15-C16-H16B	110.3	C33-C32-H32	119.3
H16A-C16-H16B	108.5	C34-C33-C32	119.0(5)
C10-C17-C18	116.2(5)	C34-C33-H33	120.5
C10-C17-H17A	108.2	C32-C33-H33	120.5
C18-C17-H17A	108.2	C33-C34-C35	122.2(5)
C10-C17-H17B	108.2	C33-C34-H34	118.9
C18-C17-H17B	108.2	C35-C34-H34	118.9
H17A-C17-H17B	107.4	C36-C35-C34	117.5(6)
C17-C18-P2	116.1(4)	C36-C35-H35	121.2
C17-C18-H18A	108.3	C34-C35-H35	121.2
P2-C18-H18A	108.3	C31-C36-C35	120.0(5)
C17-C18-H18B	108.3	C31-C36-H36	120.0
P2-C18-H18B	108.3	C35-C36-H36	120.0
H18A-C18-H18B	107.4	C42-C37-C38	118.2(5)
C20-C19-C24	118.5(7)	C42-C37-P1	121.8(4)
C20-C19-P2	120.3(4)	C38-C37-P1	120.0(4)
C24-C19-P2	121.0(5)	C39-C38-C37	120.3(6)
C21-C20-C19	122.9(6)	C39-C38-H38	119.8
C21-C20-H20	118.5	C37-C38-H38	119.8
C19-C20-H20	118.5	C40-C39-C38	121.6(7)
C20-C21-C22	116.8(8)	C40-C39-H39	119.2
C20-C21-H21	121.6	C38-C39-H39	119.2
C22-C21-H21	121.6	C39-C40-C41	120.5(7)
C23-C22-C21	119.4(8)	C39-C40-H40	119.7
C23-C22-H22	120.3	C41-C40-H40	119.7
C21-C22-H22	120.3	C40-C41-C42	118.8(7)
C24-C23-C22	123.4(7)	C40-C41-H41	120.6
C24-C23-H23	118.3	C42-C41-H41	120.6
C22-C23-H23	118.3	C37-C42-C41	120.5(6)
C23-C24-C19	118.9(7)	C37-C42-H42	119.7
C23-C24-H24	120.5	C41-C42-H42	119.7
C19-C24-H24	120.5	C48-C43-C44	118.0(6)
C26-C25-C30	118.6(6)	C48-C43-P1	122.4(5)
C26-C25-P2	122.3(5)	C44-C43-P1	119.4(4)
C30-C25-P2	119.0(5)	C43-C44-C45	121.8(7)
C25-C26-C27	120.8(8)	C43-C44-H44	119.1
C25-C26-H26	119.6	C45-C44-H44	119.1
C27-C26-H26	119.6	C46-C45-C44	118.8(9)
C28-C27-C26	120.0(9)	C46-C45-H45	120.6
C28-C27-H27	120.0	C44-C45-H45	120.6
C26-C27-H27	120.0	C45-C46-C47	121.5(9)
C27-C28-C29	121.3(8)	C45-C46-H46	119.3
C27-C28-H28	119.3	C47-C46-H46	119.3
C29-C28-H28	119.3	C46-C47-C48	119.5(9)
C28-C29-C30	120.2(11)	C46-C47-H47	120.3

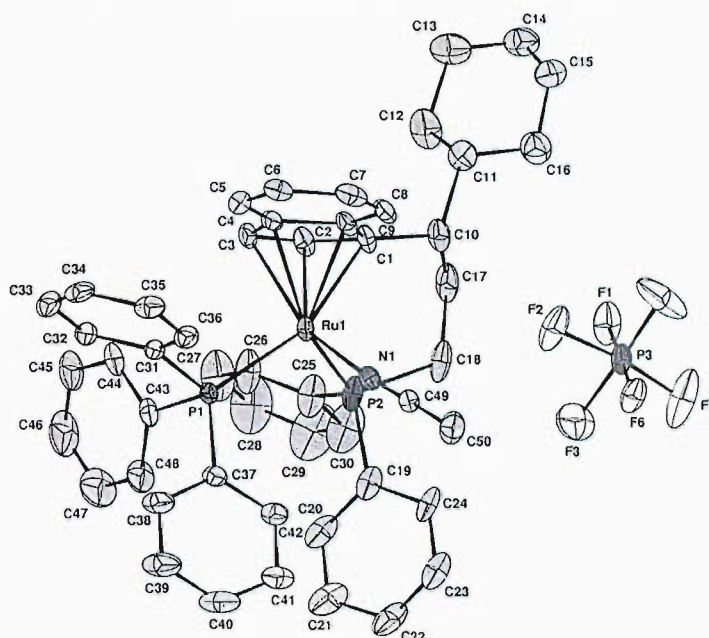
C48-C47-H47	120.3	F5-P3-F1	92.8(3)
C43-C48-C47	120.4(9)	F4-P3-F1	92.8(3)
C43-C48-H48	119.8	F2-P3-F1	89.2(2)
C47-C48-H48	119.8	F5-P3-F3	175.4(5)
N1-C49-C50	177.8(5)	F4-P3-F3	88.7(4)
C49-C50-H50A	109.5	F2-P3-F3	83.9(3)
C49-C50-H50B	109.5	F1-P3-F3	89.7(3)
H50A-C50-H50B	109.5	F5-P3-F6	88.1(3)
C49-C50-H50C	109.5	F4-P3-F6	88.7(2)
H50A-C50-H50C	109.5	F2-P3-F6	89.2(2)
H50B-C50-H50C	109.5	F1-P3-F6	178.3(2)
C31-P1-C37	97.6(2)	F3-P3-F6	89.4(3)
C31-P1-C43	103.0(2)		
C37-P1-C43	102.2(3)		
C31-P1-Ru1	112.91(15)		
C37-P1-Ru1	122.43(17)		
C43-P1-Ru1	115.72(18)		
C19-P2-C25	102.0(3)		
C19-P2-C18	101.5(3)		
C25-P2-C18	103.9(3)		
C19-P2-Ru1	119.43(17)		
C25-P2-Ru1	119.2(2)		
C18-P2-Ru1	108.6(2)		
C49-N1-Ru1	173.7(4)		
N1-Ru1-C2	140.91(16)		
N1-Ru1-C1	103.15(16)		
C2-Ru1-C1	38.03(17)		
N1-Ru1-C3	148.7(2)		
C2-Ru1-C3	36.6(2)		
C1-Ru1-C3	63.01(18)		
N1-Ru1-P2	87.27(11)		
C2-Ru1-P2	89.22(19)		
C1-Ru1-P2	91.56(18)		
C3-Ru1-P2	119.41(18)		
N1-Ru1-C9	90.91(16)		
C2-Ru1-C9	60.2(2)		
C1-Ru1-C9	36.1(2)		
C3-Ru1-C9	60.97(18)		
P2-Ru1-C9	125.26(15)		
N1-Ru1-P1	94.31(10)		
C2-Ru1-P1	124.40(13)		
C1-Ru1-P1	158.25(14)		
C3-Ru1-P1	95.39(13)		
P2-Ru1-P1	102.25(5)		
C9-Ru1-P1	132.40(14)		
N1-Ru1-C4	112.32(17)		
C2-Ru1-C4	60.4(2)		
C1-Ru1-C4	61.6(2)		
C3-Ru1-C4	36.5(2)		
P2-Ru1-C4	149.12(15)		
C9-Ru1-C4	36.29(17)		
P1-Ru1-C4	99.86(13)		
F5-P3-F4	95.1(5)		
F5-P3-F2	92.3(4)		
F4-P3-F2	172.3(4)		

Symmetry transformations used to generate equivalent atoms:

Table 4. Anisotropic displacement parameters [$\text{\AA}^2 \times 10^3$]. The anisotropic displacement factor exponent takes the form: $-2\pi^2[h^2 a^{*2} U^{11} + \dots + 2 h k a^* b^* U^{12}]$.

Atom	U^{11}	U^{22}	U^{33}	U^{23}	U^{13}	U^{12}
C1	105(5)	40(2)	48(3)	-15(2)	38(3)	-24(3)
C2	116(5)	48(3)	53(3)	-11(2)	44(3)	-37(3)
C3	119(5)	32(2)	47(3)	-7(2)	19(3)	-18(3)
C4	99(5)	42(3)	34(3)	2(2)	1(3)	-12(3)
C5	92(5)	50(3)	57(3)	0(2)	4(3)	17(3)
C6	88(5)	87(4)	48(3)	0(3)	-8(3)	8(4)
C7	87(5)	100(5)	43(3)	6(3)	1(3)	-18(4)
C8	112(5)	51(3)	35(3)	-9(2)	17(3)	-25(3)
C9	99(4)	48(3)	33(2)	-8(2)	26(3)	-23(3)
C10	94(5)	58(3)	73(4)	-16(3)	54(4)	-15(3)
C11	106(5)	90(4)	70(4)	2(3)	59(4)	20(4)
C12	176(9)	103(5)	103(6)	-11(4)	98(6)	-41(5)
C13	115(7)	161(9)	82(5)	30(5)	53(5)	2(5)
C14	100(6)	135(7)	77(5)	14(5)	33(4)	30(5)
C15	123(7)	105(6)	87(5)	11(4)	8(5)	28(5)
C16	106(6)	106(6)	94(6)	-8(4)	26(5)	4(5)
C17	154(8)	62(4)	105(6)	-20(3)	96(6)	-4(4)
C18	78(4)	49(3)	159(7)	-26(4)	69(5)	3(3)
C19	27(3)	55(3)	128(6)	-5(3)	18(3)	0(2)
C20	43(3)	63(4)	157(8)	26(4)	-4(4)	-6(3)
C21	52(4)	97(5)	170(9)	38(6)	-25(5)	-12(4)
C22	67(5)	73(4)	168(9)	32(5)	-11(5)	8(4)
C23	62(4)	54(4)	158(8)	9(4)	27(5)	4(3)
C24	53(3)	33(3)	141(6)	3(3)	33(4)	9(2)
C25	66(4)	70(4)	166(8)	-17(4)	65(5)	-21(3)
C26	96(5)	65(4)	167(8)	-30(4)	78(5)	-36(4)
C27	121(8)	119(7)	210(11)	-40(7)	93(8)	-68(6)
C28	118(9)	154(10)	304(17)	-29(10)	113(10)	-85(8)
C29	88(7)	167(10)	340(20)	20(11)	116(10)	-38(7)
C30	59(4)	117(6)	262(13)	-5(7)	81(6)	-13(4)
C31	54(3)	49(3)	39(2)	-3(2)	6(2)	19(2)
C32	70(4)	56(3)	48(3)	-4(2)	10(3)	23(3)
C33	83(5)	63(3)	70(4)	4(3)	21(3)	32(3)
C34	81(4)	91(4)	52(3)	22(3)	23(3)	55(4)
C35	59(3)	93(4)	53(3)	15(3)	18(3)	23(3)
C36	62(3)	61(3)	51(3)	5(2)	14(3)	18(3)
C37	57(3)	71(3)	41(3)	-3(2)	5(2)	29(3)
C38	125(6)	129(6)	44(3)	9(3)	24(4)	82(5)
C39	137(7)	185(8)	53(4)	21(5)	33(4)	99(7)
C40	85(5)	168(8)	58(4)	39(5)	14(4)	43(5)
C41	98(5)	101(5)	54(4)	17(3)	4(4)	3(4)
C42	54(3)	76(3)	53(3)	4(3)	5(3)	6(3)
C43	53(3)	54(3)	75(4)	-30(3)	4(3)	7(2)

C44	83(4)	57(3)	83(4)	-37(3)	18(3)	-15(3)
C45	84(5)	75(5)	141(7)	-48(4)	10(5)	-24(4)
C46	101(7)	106(7)	215(14)	-71(8)	-25(8)	-22(6)
C47	102(7)	156(9)	164(11)	-50(8)	-58(7)	10(7)
C48	68(4)	90(5)	118(6)	-37(4)	-37(4)	9(4)
C49	44(3)	40(2)	42(2)	-3(2)	17(2)	-7(2)
C50	115(6)	61(4)	93(5)	-6(3)	39(4)	8(4)
P1	47(1)	42(1)	44(1)	-10(1)	8(1)	10(1)
P2	51(1)	41(1)	112(1)	-14(1)	47(1)	-7(1)
N1	44(2)	54(2)	44(2)	-8(2)	21(2)	2(2)
Ru1	55(1)	31(1)	48(1)	-9(1)	25(1)	-7(1)
P3	84(1)	42(1)	80(1)	-12(1)	34(1)	-18(1)
F1	130(4)	75(2)	149(4)	-17(2)	88(3)	-37(2)
F2	150(4)	55(2)	204(5)	22(3)	99(4)	4(2)
F3	189(6)	122(4)	134(4)	-1(3)	-14(4)	-75(4)
F4	138(4)	66(3)	353(10)	-2(4)	155(6)	-1(2)
F5	258(8)	264(7)	69(3)	-30(4)	22(4)	-181(7)
F6	95(3)	51(2)	119(3)	11(2)	50(2)	-8(2)

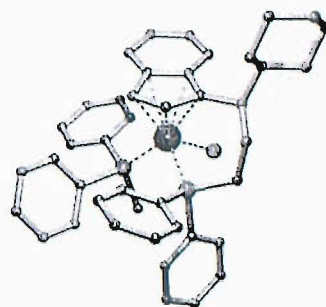


Thermal ellipsoids drawn at the 50% probability level



Table 1. Crystal data and structure refinement details.

Identification code	04sot0962
Empirical formula	C ₄₃ H ₄₅ ClP ₂ Ru
Formula weight	760.25
Temperature	120(2) K
Wavelength	0.71073 Å
Crystal system	Monoclinic
Space group	<i>P</i> 2 ₁ / <i>n</i>
Unit cell dimensions	<i>a</i> = 11.705(3) Å <i>b</i> = 18.729(4) Å <i>c</i> = 16.9282(17) Å
Volume	3597.3(12) Å ³
<i>Z</i>	4
Density (calculated)	1.404 Mg / m ³
Absorption coefficient	0.629 mm ⁻¹
<i>F</i> (000)	1576
Crystal	Needle; Pale Orange
Crystal size	0.14 × 0.04 × 0.03 mm ³
θ range for data collection	3.30 – 27.56°
Index ranges	-15 ≤ <i>h</i> ≤ 15, -24 ≤ <i>k</i> ≤ 24, -21 ≤ <i>l</i> ≤ 21
Reflections collected	66387
Independent reflections	8266 [<i>R</i> _{int} = 0.0747]
Completeness to $\theta = 27.50^\circ$	99.8 %
Absorption correction	Semi-empirical from equivalents
Max. and min. transmission	0.9814 and 0.9170
Refinement method	Full-matrix least-squares on <i>F</i> ²
Data / restraints / parameters	8266 / 0 / 425
Goodness-of-fit on <i>F</i> ²	1.022
Final <i>R</i> indices [<i>F</i> ² > 2σ(<i>F</i> ²)]	<i>R</i> 1 = 0.0354, <i>wR</i> 2 = 0.0702
<i>R</i> indices (all data)	<i>R</i> 1 = 0.0499, <i>wR</i> 2 = 0.0749
Largest diff. peak and hole	0.530 and -0.441 e Å ⁻³



Diffractometer: Nonius KappaCCD area detector (ϕ scans and ω scans to fill *asymmetric unit*). **Cell determination:** DirAx (Duisenberg, A.J.M.(1992). *J. Appl. Cryst.* 25, 92-96.) **Data collection:** Collect (Collect: Data collection software, R. Hooft, Nonius B.V., 1998). **Data reduction and cell refinement:** Denzo (Z. Otwinowski & W. Minor, *Methods in Enzymology* (1997) Vol. 276: *Macromolecular Crystallography*, part A, pp. 307–326; C. W. Carter, Jr. & R. M. Sweet, Eds., Academic Press). **Absorption correction:** Sheldrick, G. M. SADABS - Bruker Nonius area detector scaling and absorption correction - V2.10 **Structure solution:** SHELXS97 (G. M. Sheldrick, *Acta Cryst.* (1990) A46 467–473). **Structure refinement:** SHELXL97 (G. M. Sheldrick (1997), University of Göttingen, Germany). **Graphics:** Cameron - A Molecular Graphics Package. (D. M. Watkin, L. Pearce and C. K. Prout, *Chemical Crystallography Laboratory*, University of Oxford, 1993).

Special details: All hydrogen atoms were placed in idealised positions and refined using a riding model.

Table 2. Atomic coordinates [$\times 10^4$], equivalent isotropic displacement parameters [$\text{\AA}^2 \times 10^3$] and site occupancy factors. U_{eq} is defined as one third of the trace of the orthogonalized U^{ij} tensor.

Atom	x	y	z	U_{eq}	$S.o.f.$
Ru1	3683(1)	2413(1)	1409(1)	13(1)	1
Cl1	5442(1)	1689(1)	1921(1)	22(1)	1
P1	3697(1)	2702(1)	2694(1)	15(1)	1
P2	2525(1)	1405(1)	1312(1)	16(1)	1
C1	3311(2)	3530(1)	1139(1)	16(1)	1
C2	2616(2)	3119(1)	489(1)	17(1)	1
C3	3421(2)	2802(1)	58(1)	17(1)	1
C4	3234(2)	2398(1)	-665(2)	23(1)	1
C5	4187(2)	2178(1)	-932(2)	27(1)	1
C6	5349(2)	2332(1)	-481(2)	24(1)	1
C7	5559(2)	2718(1)	221(2)	20(1)	1
C8	4595(2)	2980(1)	501(1)	16(1)	1
C9	4537(2)	3415(1)	1196(1)	16(1)	1
C10	5564(2)	3713(1)	1818(1)	17(1)	1
C11	6114(2)	4356(1)	1469(2)	17(1)	1
C12	5405(2)	5044(1)	1414(2)	21(1)	1
C13	5951(2)	5638(1)	1008(2)	24(1)	1
C14	7240(2)	5763(1)	1442(2)	24(1)	1
C15	7952(2)	5076(1)	1523(2)	24(1)	1
C16	7394(2)	4490(1)	1931(2)	23(1)	1
C17	5258(2)	3883(1)	2633(1)	19(1)	1
C18	5040(2)	3222(1)	3118(1)	20(1)	1
C19	2486(2)	3266(1)	2846(1)	17(1)	1
C20	1429(2)	3272(1)	2250(2)	20(1)	1
C21	487(2)	3681(1)	2349(2)	24(1)	1
C22	591(2)	4086(1)	3046(2)	25(1)	1
C23	1633(2)	4078(1)	3647(2)	24(1)	1
C24	2578(2)	3673(1)	3549(2)	22(1)	1
C25	3770(2)	2025(1)	3487(1)	17(1)	1
C26	4797(2)	1636(1)	3787(2)	21(1)	1
C27	4828(2)	1088(1)	4342(2)	26(1)	1
C28	3827(2)	918(1)	4599(2)	29(1)	1
C29	2795(2)	1298(1)	4306(2)	27(1)	1
C30	2765(2)	1849(1)	3758(2)	21(1)	1
C31	976(2)	1560(1)	1298(1)	18(1)	1
C32	233(2)	1909(1)	637(2)	21(1)	1
C33	-904(2)	2099(1)	654(2)	25(1)	1
C34	-1317(2)	1952(1)	1339(2)	26(1)	1
C35	-596(2)	1611(1)	1995(2)	24(1)	1
C36	538(2)	1408(1)	1974(2)	21(1)	1
C37	2465(2)	846(1)	410(1)	18(1)	1
C38	3494(2)	781(1)	141(2)	20(1)	1
C39	3554(2)	299(1)	-470(2)	23(1)	1
C40	2596(2)	-125(1)	-820(2)	25(1)	1
C41	1560(2)	-51(1)	-570(2)	26(1)	1
C42	1497(2)	430(1)	42(2)	23(1)	1
C43	2965(2)	719(1)	2091(2)	20(1)	1

Table 3. Bond lengths [\AA] and angles [$^\circ$].

Ru1–C1	2.163(2)	C12–C13	1.528(3)
Ru1–C2	2.186(2)	C13–C14	1.525(3)
Ru1–C9	2.198(2)	C14–C15	1.520(3)
Ru1–P1	2.2379(6)	C15–C16	1.528(3)
Ru1–P2	2.3058(7)	C17–C18	1.542(3)
Ru1–C8	2.332(2)	C19–C20	1.391(3)
Ru1–C3	2.349(2)	C19–C24	1.395(3)
Ru1–Cl1	2.4397(7)	C20–C21	1.386(3)
P1–C25	1.833(2)	C21–C22	1.383(4)
P1–C19	1.835(2)	C22–C23	1.383(4)
P1–C18	1.838(2)	C23–C24	1.385(3)
P2–C43	1.823(2)	C25–C26	1.392(3)
P2–C31	1.830(2)	C25–C30	1.403(3)
P2–C37	1.840(2)	C26–C27	1.387(3)
C1–C2	1.423(3)	C27–C28	1.383(4)
C1–C9	1.431(3)	C28–C29	1.384(4)
C2–C3	1.453(3)	C29–C30	1.383(3)
C3–C4	1.409(3)	C31–C36	1.394(3)
C3–C8	1.434(3)	C31–C32	1.399(3)
C4–C5	1.367(3)	C32–C33	1.384(3)
C5–C6	1.415(4)	C33–C34	1.390(4)
C6–C7	1.361(4)	C34–C35	1.376(4)
C7–C8	1.414(3)	C35–C36	1.389(3)
C8–C9	1.445(3)	C37–C42	1.389(3)
C9–C10	1.498(3)	C37–C38	1.393(3)
C10–C17	1.541(3)	C38–C39	1.388(3)
C10–C11	1.551(3)	C39–C40	1.382(4)
C11–C12	1.523(3)	C40–C41	1.386(3)
C11–C16	1.531(3)	C41–C42	1.388(3)
C1–Ru1–C2	38.19(9)	C1–Ru1–Cl1	136.17(6)
C1–Ru1–C9	38.30(8)	C2–Ru1–Cl1	150.91(6)
C2–Ru1–C9	64.49(8)	C9–Ru1–Cl1	98.92(6)
C1–Ru1–P1	85.65(6)	P1–Ru1–Cl1	89.17(2)
C2–Ru1–P1	114.36(6)	P2–Ru1–Cl1	90.02(3)
C9–Ru1–P1	93.33(6)	C8–Ru1–Cl1	90.24(6)
C1–Ru1–P2	133.81(6)	C3–Ru1–Cl1	114.56(6)
C2–Ru1–P2	102.79(6)	C25–P1–C19	101.19(10)
C9–Ru1–P2	166.02(6)	C25–P1–C18	101.44(11)
P1–Ru1–P2	97.55(2)	C19–P1–C18	104.89(11)
C1–Ru1–C8	61.39(8)	C25–P1–Ru1	122.14(7)
C2–Ru1–C8	61.88(8)	C19–P1–Ru1	116.98(8)
C9–Ru1–C8	37.07(8)	C18–P1–Ru1	108.01(8)
P1–Ru1–C8	129.43(6)	C43–P2–C31	102.97(11)
P2–Ru1–C8	133.02(6)	C43–P2–C37	98.35(11)
C1–Ru1–C3	61.46(8)	C31–P2–C37	104.12(11)
C2–Ru1–C3	37.15(8)	C43–P2–Ru1	117.96(8)
C9–Ru1–C3	61.99(8)	C31–P2–Ru1	115.74(8)
P1–Ru1–C3	147.10(6)	C37–P2–Ru1	115.28(7)
P2–Ru1–C3	104.53(6)	C2–C1–C9	110.1(2)
C8–Ru1–C3	35.69(8)	C2–C1–Ru1	71.78(13)

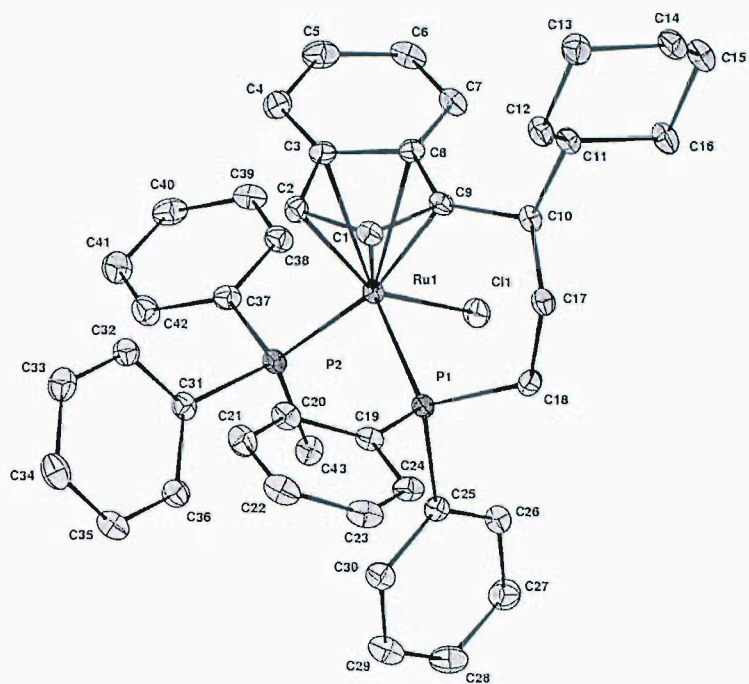
C9-C1-Ru1	72.16(12)	C36-C31-C32	118.0(2)
C1-C2-C3	106.97(19)	C36-C31-P2	121.32(19)
C1-C2-Ru1	70.03(13)	C32-C31-P2	120.26(17)
C3-C2-Ru1	77.53(13)	C33-C32-C31	121.0(2)
C4-C3-C8	120.3(2)	C32-C33-C34	120.0(2)
C4-C3-C2	132.4(2)	C35-C34-C33	119.6(2)
C8-C3-C2	107.4(2)	C34-C35-C36	120.5(2)
C4-C3-Ru1	129.33(16)	C35-C36-C31	120.8(2)
C8-C3-Ru1	71.50(13)	C42-C37-C38	118.7(2)
C2-C3-Ru1	65.33(12)	C42-C37-P2	123.48(18)
C5-C4-C3	118.9(2)	C38-C37-P2	117.47(18)
C4-C5-C6	121.0(2)	C39-C38-C37	120.4(2)
C7-C6-C5	121.5(2)	C40-C39-C38	120.6(2)
C6-C7-C8	119.3(2)	C39-C40-C41	119.3(2)
C7-C8-C3	119.0(2)	C40-C41-C42	120.3(2)
C7-C8-C9	132.0(2)	C41-C42-C37	120.7(2)
C3-C8-C9	109.02(19)		
C7-C8-Ru1	126.56(16)		
C3-C8-Ru1	72.81(12)		
C9-C8-Ru1	66.42(12)		
C1-C9-C8	106.1(2)		
C1-C9-C10	127.5(2)		
C8-C9-C10	126.29(19)		
C1-C9-Ru1	69.54(12)		
C8-C9-Ru1	76.51(13)		
C10-C9-Ru1	121.37(15)		
C9-C10-C17	112.59(18)		
C9-C10-C11	110.96(19)		
C17-C10-C11	112.91(18)		
C12-C11-C16	110.14(19)		
C12-C11-C10	114.18(18)		
C16-C11-C10	112.21(19)		
C11-C12-C13	111.15(19)		
C14-C13-C12	111.6(2)		
C15-C14-C13	111.7(2)		
C14-C15-C16	111.30(19)		
C15-C16-C11	111.0(2)		
C10-C17-C18	114.56(19)		
C17-C18-P1	117.03(17)		
C20-C19-C24	118.8(2)		
C20-C19-P1	118.91(17)		
C24-C19-P1	122.24(19)		
C21-C20-C19	120.6(2)		
C22-C21-C20	120.0(2)		
C23-C22-C21	119.9(2)		
C22-C23-C24	120.2(2)		
C23-C24-C19	120.4(2)		
C26-C25-C30	118.4(2)		
C26-C25-P1	120.68(17)		
C30-C25-P1	120.68(18)		
C27-C26-C25	120.8(2)		
C28-C27-C26	120.0(2)		
C27-C28-C29	120.1(2)		
C30-C29-C28	120.0(2)		
C29-C30-C25	120.6(2)		

Table 4. Anisotropic displacement parameters [$\text{\AA}^2 \times 10^3$]. The anisotropic displacement factor exponent takes the form: $-2\pi^2[h^2 a^{*2} U^{11} + \dots + 2 h k a^* b^* U^{12}]$.

Atom	U^{11}	U^{22}	U^{33}	U^{23}	U^{13}	U^{12}
Ru1	12(1)	14(1)	15(1)	0(1)	4(1)	0(1)
Cl1	17(1)	24(1)	25(1)	4(1)	5(1)	5(1)
P1	14(1)	16(1)	16(1)	0(1)	4(1)	-1(1)
P2	15(1)	15(1)	18(1)	-1(1)	5(1)	-2(1)
C1	17(1)	13(1)	19(1)	2(1)	7(1)	1(1)
C2	14(1)	18(1)	19(1)	4(1)	2(1)	2(1)
C3	20(1)	15(1)	17(1)	4(1)	6(1)	1(1)
C4	26(1)	22(1)	20(1)	1(1)	4(1)	-5(1)
C5	40(2)	21(1)	23(1)	-2(1)	13(1)	-3(1)
C6	30(1)	18(1)	31(1)	3(1)	18(1)	2(1)
C7	18(1)	18(1)	26(1)	2(1)	9(1)	0(1)
C8	20(1)	14(1)	16(1)	3(1)	5(1)	0(1)
C9	16(1)	14(1)	19(1)	2(1)	6(1)	-1(1)
C10	14(1)	16(1)	19(1)	-1(1)	4(1)	-2(1)
C11	16(1)	17(1)	20(1)	-2(1)	6(1)	-3(1)
C12	17(1)	19(1)	26(1)	2(1)	5(1)	-3(1)
C13	24(1)	19(1)	28(1)	4(1)	4(1)	-2(1)
C14	22(1)	21(1)	29(1)	0(1)	8(1)	-7(1)
C15	18(1)	24(1)	32(2)	-2(1)	9(1)	-5(1)
C16	15(1)	21(1)	33(2)	4(1)	6(1)	0(1)
C17	18(1)	18(1)	20(1)	-2(1)	4(1)	-6(1)
C18	20(1)	22(1)	16(1)	1(1)	0(1)	-4(1)
C19	21(1)	14(1)	19(1)	1(1)	9(1)	0(1)
C20	21(1)	18(1)	23(1)	-3(1)	9(1)	1(1)
C21	19(1)	26(1)	30(1)	1(1)	8(1)	1(1)
C22	28(1)	17(1)	35(2)	2(1)	18(1)	5(1)
C23	37(2)	14(1)	27(1)	-2(1)	17(1)	-2(1)
C24	28(1)	19(1)	20(1)	1(1)	10(1)	-2(1)
C25	19(1)	16(1)	15(1)	-3(1)	5(1)	-2(1)
C26	20(1)	24(1)	21(1)	0(1)	5(1)	-3(1)
C27	29(1)	24(1)	26(1)	4(1)	6(1)	1(1)
C28	41(2)	22(1)	28(2)	7(1)	14(1)	0(1)
C29	32(1)	22(1)	31(2)	-3(1)	18(1)	-4(1)
C30	23(1)	19(1)	22(1)	-2(1)	9(1)	-1(1)
C31	18(1)	15(1)	20(1)	-5(1)	5(1)	-4(1)
C32	21(1)	21(1)	20(1)	-2(1)	5(1)	-4(1)
C33	22(1)	23(1)	27(1)	0(1)	1(1)	2(1)
C34	20(1)	24(1)	37(2)	-4(1)	9(1)	1(1)
C35	23(1)	24(1)	30(1)	1(1)	13(1)	-1(1)
C36	22(1)	19(1)	22(1)	0(1)	6(1)	-2(1)
C37	22(1)	14(1)	18(1)	0(1)	7(1)	-1(1)
C38	22(1)	17(1)	22(1)	0(1)	8(1)	-3(1)
C39	27(1)	23(1)	23(1)	4(1)	12(1)	2(1)
C40	36(2)	21(1)	19(1)	-2(1)	10(1)	0(1)
C41	29(1)	25(1)	25(1)	-7(1)	6(1)	-8(1)
C42	22(1)	23(1)	25(1)	-5(1)	8(1)	-5(1)
C43	22(1)	16(1)	22(1)	-2(1)	5(1)	0(1)

Table 5. Hydrogen coordinates [$\times 10^4$] and isotropic displacement parameters [$\text{\AA}^2 \times 10^3$].

Atom	<i>x</i>	<i>y</i>	<i>z</i>	U_{eq}	<i>S.o.f.</i>
H1	3005	3836	1485	20	1
H2	1784	3062	362	21	1
H4	2457	2280	-961	28	1
H5	4069	1918	-1427	32	1
H6	5997	2162	-673	29	1
H7	6344	2812	519	24	1
H10	6179	3330	1935	20	1
H11	6129	4226	899	21	1
H12A	5375	5197	1969	25	1
H12B	4587	4956	1096	25	1
H13A	5895	5508	433	29	1
H13B	5502	6085	1013	29	1
H14A	7583	6118	1134	29	1
H14B	7286	5961	1992	29	1
H15A	8763	5169	1849	29	1
H15B	7999	4914	975	29	1
H16A	7421	4631	2499	28	1
H16B	7853	4043	1949	28	1
H17A	4544	4186	2522	23	1
H17B	5911	4164	2976	23	1
H18A	5018	3380	3672	24	1
H18B	5725	2898	3177	24	1
H20	1352	2993	1772	24	1
H21	-230	3684	1937	29	1
H22	-53	4368	3113	30	1
H23	1700	4352	4129	29	1
H24	3292	3672	3963	26	1
H26	5486	1747	3609	26	1
H27	5537	829	4547	32	1
H28	3847	540	4977	35	1
H29	2108	1179	4481	32	1
H30	2057	2112	3564	25	1
H32	513	2018	170	25	1
H33	-1402	2328	197	30	1
H34	-2094	2087	1355	32	1
H35	-876	1514	2465	29	1
H36	1020	1163	2426	25	1
H38	4158	1070	377	24	1
H39	4260	258	-649	28	1
H40	2646	-463	-1229	30	1
H41	891	-330	-818	32	1
H42	785	476	211	28	1
H43A	2936	914	2623	30	1
H43B	3770	562	2109	30	1
H43C	2426	312	1960	30	1

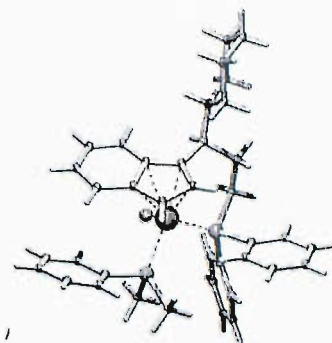


Thermal ellipsoids drawn at the 50% probability level, hydrogen atoms omitted for clarity.



Table 1. Crystal data and structure refinement details.

Identification code	04sot0854
Empirical formula	$C_{39.50}H_{44.50}ClP_2Ru$ $C_{38}H_{43}RuP_2Cl_2 \cdot 0.25C_6H_6$
Formula weight	717.71
Temperature	120(2) K
Wavelength	0.71073 Å
Crystal system	Monoclinic
Space group	C2
Unit cell dimensions	$a = 31.43(3)$ Å $b = 14.804(5)$ Å $c = 22.104(15)$ Å
Volume	7383(8) Å ³
Z	8 (2 Molecules)
Density (calculated)	1.291 Mg / m ³
Absorption coefficient	0.609 mm ⁻¹
$F(000)$	2980
Crystal	Rod; Pale Red
Crystal size	0.18 × 0.03 × 0.02 mm ³
θ range for data collection	3.04 – 25.03°
Index ranges	-37 ≤ h ≤ 37, -17 ≤ k ≤ 17, -26 ≤ l ≤ 26
Reflections collected	45138
Independent reflections	12976 [$R_{int} = 0.1294$]
Completeness to $\theta = 25.03^\circ$	99.6 %
Absorption correction	Semi-empirical from equivalents
Max. and min. transmission	0.9879 and 0.8983
Refinement method	Full-matrix least-squares on F^2
Data / restraints / parameters	12976 / 29 / 782
Goodness-of-fit on F^2	1.039
Final R indices [$F^2 > 2\sigma(F^2)$]	$RI = 0.0755$, $wR2 = 0.1764$
R indices (all data)	$RI = 0.1113$, $wR2 = 0.1954$
Absolute structure parameter	0.05(5)
Largest diff. peak and hole	1.591 and -1.028 e Å ⁻³



Diffractometer: Nonius KappaCCD area detector (ϕ scans and ω scans to fill *asymmetric unit*). **Cell determination:** DirAx (Duisenberg, A.J.M.(1992). *J. Appl. Cryst.* 25, 92-96.) **Data collection:** Collect (Collect: Data collection software, R. Hooft, Nonius B.V., 1998). **Data reduction and cell refinement:** Denzo (Z. Otwinowski & W. Minor, *Methods in Enzymology* (1997) Vol. 276: *Macromolecular Crystallography*, part A, pp. 307-326; C. W. Carter, Jr. & R. M. Sweet, Eds., Academic Press). **Absorption correction:** Sheldrick, G. M. SADABS - Bruker Nonius area detector scaling and absorption correction - V2.10 **Structure solution:** SHELXS97 (G. M. Sheldrick, *Acta Cryst.* (1990) A46 467-473). **Structure refinement:** SHELXL97 (G. M. Sheldrick (1997), University of Göttingen, Germany). **Graphics:** Cameron - A Molecular Graphics Package. (D. M. Watkin, L. Pearce and C. K. Prout, *Chemical Crystallography Laboratory, University of Oxford*, 1993).

Special details: All hydrogen atoms were placed in idealised positions and refined using a riding model. The benzene solvent is half occupied. C10=R, C48=S

Table 2. Atomic coordinates [$\times 10^4$], equivalent isotropic displacement parameters [$\text{\AA}^2 \times 10^3$] and site occupancy factors. U_{eq} is defined as one third of the trace of the orthogonalized U^{ij} tensor.

Atom	x	y	z	U_{eq}	<i>S.o.f.</i>
Ru1	7303(1)	950(1)	5051(1)	23(1)	1
Cl1	7452(1)	-641(2)	4972(2)	32(1)	1
P1	6385(1)	861(2)	3748(2)	25(1)	1
P2	7808(1)	1349(2)	4702(2)	26(1)	1
C1	6937(4)	1831(6)	5374(7)	27(2)	1
C2	7534(5)	2118(6)	5834(6)	25(2)	1
C3	7926(5)	1424(7)	6433(8)	33(3)	1
C4	8565(5)	1342(8)	7121(7)	33(3)	1
C5	8804(5)	588(8)	7597(7)	40(3)	1
C6	8455(5)	-119(8)	7449(7)	37(3)	1
C7	7856(5)	-82(7)	6822(7)	36(3)	1
C8	7561(4)	677(6)	6300(6)	22(2)	1
C9	6963(4)	929(7)	5626(6)	28(2)	1
C10	6443(4)	392(6)	5328(6)	23(2)	1
C11	6339(5)	571(7)	5906(7)	33(3)	1
C12	5874(4)	-73(6)	5726(7)	27(2)	1
C13	5828(6)	25(8)	6355(8)	43(3)	1
C14	5727(5)	1012(9)	6419(7)	47(3)	1
C15	6195(5)	1625(8)	6617(7)	38(3)	1
C16	6216(5)	1543(7)	5954(7)	34(3)	1
C17	5878(4)	512(7)	4382(6)	28(2)	1
C18	5930(5)	150(7)	3795(7)	31(3)	1
C19	5943(4)	1896(6)	3226(6)	26(2)	1
C20	5315(4)	1879(7)	2588(6)	28(2)	1
C21	4979(6)	2631(9)	2159(7)	43(3)	1
C22	5282(5)	3493(8)	2398(8)	41(3)	1
C23	5888(5)	3518(6)	3039(7)	33(3)	1
C24	6219(5)	2723(7)	3459(7)	33(3)	1
C25	6273(4)	354(7)	2907(7)	32(3)	1
C26	6191(5)	873(8)	2315(7)	36(2)	1
C27	6141(5)	509(9)	1722(8)	48(3)	1
C28	6160(5)	-432(10)	1655(8)	54(4)	1
C29	6222(5)	-960(9)	2212(7)	44(3)	1
C30	6290(4)	-585(6)	2853(7)	29(2)	1
C31	7602(5)	2347(7)	4062(7)	31(3)	1
C32	7888(4)	529(7)	4188(7)	30(2)	1
C33	8583(5)	1596(7)	5652(7)	32(3)	1
C34	8810(5)	2477(7)	5922(7)	38(3)	1
C35	9378(6)	2625(8)	6691(9)	58(4)	1
C36	9758(5)	1919(8)	7205(8)	47(3)	1
C37	9538(4)	1043(7)	6941(7)	33(2)	1
C38	8963(4)	883(7)	6190(6)	27(2)	1
Ru2	2749(1)	4031(1)	445(1)	23(1)	1
Cl2	2520(1)	5623(2)	68(2)	32(1)	1
P3	2365(1)	4124(2)	981(2)	26(1)	1
P4	1896(1)	3631(2)	-911(2)	28(1)	1
C39	3429(4)	3153(6)	1489(6)	23(2)	1
C40	3294(4)	2870(6)	759(7)	29(2)	1
C41	3517(4)	3556(7)	579(6)	26(2)	1
C42	3545(5)	3627(8)	-6(7)	38(3)	1
C43	3792(5)	4407(9)	-5(7)	43(3)	1
C44	3988(4)	5115(7)	546(7)	36(3)	1
C45	3965(4)	5072(6)	1118(7)	29(2)	1
C46	3734(4)	4292(6)	1164(7)	30(3)	1

C47	3662(4)	4046(7)	1699(6)	27(2)	1
C48	3886(4)	4588(7)	2458(6)	28(2)	1
C49	4565(4)	4424(7)	3228(7)	31(2)	1
C50	4733(5)	3444(7)	3526(7)	37(3)	1
C51	5426(4)	3342(8)	4239(7)	41(3)	1
C52	5698(5)	3981(9)	4974(7)	46(3)	1
C53	5526(4)	4943(8)	4712(7)	39(3)	1
C54	4845(4)	5054(7)	3973(7)	34(3)	1
C55	3508(4)	4463(7)	2627(6)	26(2)	1
C56	2864(4)	4833(7)	1932(6)	30(2)	1
C57	2292(4)	3088(6)	1349(6)	23(2)	1
C58	2273(5)	3113(7)	1949(7)	34(3)	1
C59	2180(5)	2370(8)	2213(8)	44(3)	1
C60	2108(5)	1485(8)	1815(7)	40(3)	1
C61	2137(4)	1458(6)	1240(7)	33(3)	1
C62	2239(4)	2258(6)	1018(7)	31(3)	1
C63	1625(4)	4635(7)	364(7)	28(2)	1
C64	1128(4)	4111(8)	-69(7)	36(3)	1
C65	578(5)	4479(8)	-581(8)	44(3)	1
C66	499(6)	5418(8)	-668(8)	50(3)	1
C67	985(5)	5944(9)	-242(7)	43(3)	1
C68	1555(5)	5560(6)	269(7)	33(3)	1
C69	1465(5)	2637(7)	-1124(7)	34(3)	1
C70	1290(4)	4464(8)	-1581(7)	38(3)	1
C71	2063(4)	3390(7)	-1535(7)	32(3)	1
C72	2225(4)	4105(7)	-1732(6)	24(2)	1
C73	2395(4)	3943(7)	-2148(7)	35(3)	1
C74	2433(5)	3065(8)	-2319(8)	44(3)	1
C75	2312(6)	2336(8)	-2075(9)	52(4)	1
C76	2113(6)	2495(8)	-1702(8)	45(3)	1
C77	0	2638(9)	0	42(2)	0.50
C78	512(3)	2179(8)	366(10)	42(2)	0.50
C79	512(3)	1237(8)	366(10)	42(2)	0.50
C80	0	781(9)	0	42(2)	0.50
C81	5000	4201(9)	0	42(2)	0.50
C82	5156(6)	3746(8)	672(5)	42(2)	0.50
C83	5156(7)	2802(8)	673(5)	42(2)	0.50
C84	5000	2347(9)	0	42(2)	0.50

Table 3. Bond lengths [\AA] and angles [$^\circ$].

Ru1-C9	2.157(10)	P2-C33	1.832(11)
Ru1-C1	2.162(10)	C1-C9	1.429(15)
Ru1-C2	2.182(10)	C1-C2	1.441(14)
Ru1-P1	2.252(5)	C2-C3	1.434(15)
Ru1-P2	2.272(3)	C3-C4	1.451(16)
Ru1-C8	2.308(10)	C3-C8	1.468(14)
Ru1-C3	2.309(12)	C4-C5	1.347(15)
Ru1-C11	2.432(2)	C5-C6	1.380(16)
P1-C25	1.798(11)	C6-C7	1.355(16)
P1-C18	1.836(10)	C7-C8	1.402(14)
P1-C19	1.837(10)	C8-C9	1.412(14)
P2-C32	1.796(10)	C9-C10	1.496(14)
P2-C31	1.824(10)	C10-C11	1.547(14)

C10-C17	1.545(14)	C41-C46	1.449(14)
C11-C16	1.512(14)	C42-C43	1.389(15)
C11-C12	1.547(13)	C43-C44	1.384(16)
C12-C13	1.501(14)	C44-C45	1.318(16)
C13-C14	1.523(17)	C45-C46	1.405(14)
C14-C15	1.511(15)	C46-C47	1.398(15)
C15-C16	1.515(15)	C47-C48	1.520(15)
C17-C18	1.514(15)	C48-C55	1.483(14)
C19-C24	1.376(14)	C48-C49	1.568(14)
C19-C20	1.416(14)	C49-C54	1.529(15)
C20-C21	1.365(14)	C49-C50	1.527(14)
C21-C22	1.453(17)	C50-C51	1.572(15)
C22-C23	1.372(16)	C51-C52	1.526(16)
C23-C24	1.409(14)	C52-C53	1.490(17)
C25-C26	1.378(15)	C53-C54	1.552(14)
C25-C30	1.399(14)	C55-C56	1.559(14)
C26-C27	1.322(16)	C57-C58	1.371(14)
C27-C28	1.406(17)	C57-C62	1.379(14)
C28-C29	1.354(18)	C58-C59	1.368(15)
C29-C30	1.393(15)	C59-C60	1.504(18)
C33-C34	1.406(15)	C60-C61	1.337(16)
C33-C38	1.406(14)	C61-C62	1.402(14)
C34-C35	1.379(17)	C63-C64	1.370(14)
C35-C36	1.386(16)	C63-C68	1.379(14)
C36-C37	1.393(16)	C64-C65	1.359(15)
C37-C38	1.378(14)	C65-C66	1.401(16)
Ru2-C39	2.171(9)	C66-C67	1.350(17)
Ru2-C40	2.172(10)	C67-C68	1.411(15)
Ru2-C47	2.201(10)	C71-C72	1.370(14)
Ru2-P3	2.205(3)	C71-C76	1.414(15)
Ru2-P4	2.310(5)	C72-C73	1.368(14)
Ru2-C41	2.325(10)	C73-C74	1.381(15)
Ru2-C46	2.325(10)	C74-C75	1.371(16)
Ru2-C12	2.436(2)	C75-C76	1.361(17)
P3-C57	1.824(10)	C77-C78 ⁱ	1.376(5)
P3-C56	1.842(11)	C77-C78	1.376(5)
P3-C63	1.850(10)	C78-C79	1.395(8)
P4-C71	1.819(11)	C79-C80	1.374(5)
P4-C69	1.826(10)	C80-C79 ⁱ	1.374(5)
P4-C70	1.848(11)	C81-C82 ⁱⁱ	1.373(5)
C39-C40	1.418(15)	C81-C82	1.373(5)
C39-C47	1.423(14)	C82-C83	1.398(8)
C40-C41	1.436(14)	C83-C84	1.375(5)
C41-C42	1.361(16)	C84-C83 ⁱⁱ	1.375(5)
C9-Ru1-C1	38.6(4)	C9-Ru1-C8	36.7(4)
C9-Ru1-C2	64.7(4)	C1-Ru1-C8	62.3(3)
C1-Ru1-C2	38.8(4)	C2-Ru1-C8	62.9(3)
C9-Ru1-P1	91.9(3)	P1-Ru1-C8	126.1(3)
C1-Ru1-P1	87.4(3)	P2-Ru1-C8	134.8(3)
C2-Ru1-P1	118.9(3)	C9-Ru1-C3	62.4(4)
C9-Ru1-P2	162.5(3)	C1-Ru1-C3	62.3(4)
C1-Ru1-P2	127.8(3)	C2-Ru1-C3	37.1(4)
C2-Ru1-P2	97.9(3)	P1-Ru1-C3	149.5(3)
P1-Ru1-P2	99.05(13)	P2-Ru1-C3	102.8(3)

C8-Ru1-C3	37.1(3)	C12-C13-C14	109.9(9)
C9-Ru1-C11	103.1(3)	C15-C14-C13	112.2(9)
C1-Ru1-C11	141.4(3)	C14-C15-C16	111.2(9)
C2-Ru1-C11	148.2(3)	C11-C16-C15	109.2(9)
P1-Ru1-C11	89.48(10)	C18-C17-C10	114.3(8)
P2-Ru1-C11	90.75(10)	C17-C18-P1	113.4(7)
C8-Ru1-C11	89.5(2)	C24-C19-C20	117.7(9)
C3-Ru1-C11	111.2(3)	C24-C19-P1	120.2(8)
C25-P1-C18	102.6(5)	C20-C19-P1	122.1(7)
C25-P1-C19	100.4(5)	C21-C20-C19	123.1(10)
C18-P1-C19	103.6(5)	C20-C21-C22	117.9(11)
C25-P1-Ru1	120.1(4)	C23-C22-C21	119.2(10)
C18-P1-Ru1	108.5(4)	C22-C23-C24	120.9(10)
C19-P1-Ru1	119.4(3)	C19-C24-C23	120.9(10)
C32-P2-C31	100.8(5)	C26-C25-C30	117.7(10)
C32-P2-C33	101.5(5)	C26-C25-P1	121.4(8)
C31-P2-C33	101.4(5)	C30-C25-P1	120.8(9)
C32-P2-Ru1	118.5(3)	C27-C26-C25	122.0(11)
C31-P2-Ru1	121.3(4)	C26-C27-C28	121.6(12)
C33-P2-Ru1	110.4(4)	C29-C28-C27	117.8(12)
C9-C1-C2	108.0(8)	C28-C29-C30	121.2(12)
C9-C1-Ru1	70.5(5)	C29-C30-C25	119.7(11)
C2-C1-Ru1	71.4(5)	C34-C33-C38	117.2(10)
C3-C2-C1	107.4(8)	C34-C33-P2	123.3(8)
C3-C2-Ru1	76.3(6)	C38-C33-P2	119.3(8)
C1-C2-Ru1	69.9(5)	C35-C34-C33	120.6(10)
C2-C3-C4	134.4(10)	C34-C35-C36	121.9(11)
C2-C3-C8	107.8(9)	C35-C36-C37	117.7(10)
C4-C3-C8	117.7(10)	C38-C37-C36	121.2(10)
C2-C3-Ru1	66.6(6)	C37-C38-C33	121.3(10)
C4-C3-Ru1	129.9(7)	C39-Ru2-C40	38.1(4)
C8-C3-Ru1	71.4(6)	C39-Ru2-C47	38.0(4)
C5-C4-C3	120.0(10)	C40-Ru2-C47	63.8(4)
C4-C5-C6	121.5(10)	C39-Ru2-P3	88.2(3)
C7-C6-C5	121.4(10)	C40-Ru2-P3	118.9(3)
C6-C7-C8	121.7(10)	C47-Ru2-P3	92.5(3)
C7-C8-C9	135.4(10)	C39-Ru2-P4	128.3(3)
C7-C8-C3	117.6(9)	C40-Ru2-P4	99.0(3)
C9-C8-C3	107.1(9)	C47-Ru2-P4	162.7(3)
C7-C8-Ru1	127.3(7)	P3-Ru2-P4	97.98(13)
C9-C8-Ru1	65.9(5)	C39-Ru2-C41	61.2(4)
C3-C8-Ru1	71.5(6)	C40-Ru2-C41	37.1(4)
C8-C9-C1	109.3(9)	C47-Ru2-C41	61.0(4)
C8-C9-C10	124.7(10)	P3-Ru2-C41	149.0(3)
C1-C9-C10	125.3(9)	P4-Ru2-C41	104.5(3)
C8-C9-Ru1	77.5(5)	C39-Ru2-C46	61.1(4)
C1-C9-Ru1	70.9(6)	C40-Ru2-C46	62.3(3)
C10-C9-Ru1	125.9(6)	C47-Ru2-C46	35.8(4)
C9-C10-C11	109.9(8)	P3-Ru2-C46	126.0(3)
C9-C10-C17	114.2(8)	P4-Ru2-C46	136.0(3)
C11-C10-C17	113.2(8)	C41-Ru2-C46	36.3(3)
C16-C11-C12	111.3(8)	C39-Ru2-C12	141.3(2)
C16-C11-C10	115.6(8)	C40-Ru2-C12	148.7(3)
C12-C11-C10	112.7(8)	C47-Ru2-C12	103.7(3)
C13-C12-C11	112.6(9)	P3-Ru2-C12	88.93(10)

P4–Ru2–C12	90.26(10)	C55–C56–P3	114.4(7)
C41–Ru2–C12	111.7(3)	C58–C57–C62	117.8(9)
C46–Ru2–C12	90.5(3)	C58–C57–P3	120.9(7)
C57–P3–C56	103.9(5)	C62–C57–P3	121.3(8)
C57–P3–C63	100.9(4)	C59–C58–C57	123.8(10)
C56–P3–C63	104.0(5)	C58–C59–C60	116.2(11)
C57–P3–Ru2	118.2(3)	C61–C60–C59	120.0(10)
C56–P3–Ru2	107.5(4)	C60–C61–C62	119.4(11)
C63–P3–Ru2	120.4(4)	C57–C62–C61	122.7(11)
C71–P4–C69	101.6(5)	C64–C63–C68	118.2(9)
C71–P4–C70	101.7(5)	C64–C63–P3	121.3(8)
C69–P4–C70	99.5(5)	C68–C63–P3	120.3(8)
C71–P4–Ru2	110.4(4)	C65–C64–C63	121.8(11)
C69–P4–Ru2	121.6(4)	C64–C65–C66	120.8(12)
C70–P4–Ru2	119.1(4)	C67–C66–C65	118.1(11)
C40–C39–C47	108.9(9)	C66–C67–C68	121.0(11)
C40–C39–Ru2	71.0(6)	C63–C68–C67	120.1(10)
C47–C39–Ru2	72.2(5)	C72–C71–C76	120.5(10)
C39–C40–C41	106.8(8)	C72–C71–P4	117.2(8)
C39–C40–Ru2	70.9(5)	C76–C71–P4	121.6(9)
C41–C40–Ru2	77.3(6)	C73–C72–C71	119.0(10)
C42–C41–C40	133.2(10)	C72–C73–C74	119.8(10)
C42–C41–C46	119.2(10)	C75–C74–C73	122.3(11)
C40–C41–C46	107.6(9)	C76–C75–C74	118.1(11)
C42–C41–Ru2	127.1(7)	C75–C76–C71	120.1(11)
C40–C41–Ru2	65.7(5)	C78 ⁱ –C77–C78	120.8(8)
C46–C41–Ru2	71.8(6)	C77–C78–C79	119.6(5)
C41–C42–C43	117.9(11)	C80–C79–C78	119.4(5)
C44–C43–C42	122.5(11)	C79–C80–C79 ⁱ	121.1(8)
C45–C44–C43	121.2(11)	C82 ⁱⁱ –C81–C82	121.3(8)
C44–C45–C46	119.1(10)	C81–C82–C83	119.4(5)
C47–C46–C45	132.2(10)	C84–C83–C82	119.3(5)
C47–C46–C41	107.8(9)	C83–C84–C83 ⁱⁱ	121.3(8)
C45–C46–C41	120.0(10)		
C47–C46–Ru2	67.2(5)		
C45–C46–Ru2	126.6(7)		
C41–C46–Ru2	71.8(5)		
C46–C47–C39	108.4(9)		
C46–C47–C48	125.0(10)		
C39–C47–C48	126.0(9)		
C46–C47–Ru2	76.9(6)		
C39–C47–Ru2	69.9(5)		
C48–C47–Ru2	126.2(6)		
C55–C48–C47	112.1(8)		
C55–C48–C49	115.6(9)		
C47–C48–C49	110.5(8)		
C54–C49–C50	110.4(9)		
C54–C49–C48	113.7(8)		
C50–C49–C48	114.5(8)		
C49–C50–C51	110.2(9)		
C52–C51–C50	111.5(9)		
C53–C52–C51	113.3(9)		
C52–C53–C54	111.8(9)		
C49–C54–C53	114.0(9)		
C48–C55–C56	115.2(9)		

Symmetry transformations used to generate equivalent atoms:

(i) $-x, y, -z$ (ii) $-x+1, y, -z$

Table 4. Anisotropic displacement parameters [$\text{\AA}^2 \times 10^3$]. The anisotropic displacement factor exponent takes the form: $-2\pi^2[h^2 a^{*2} U^{11} + \dots + 2 h k a^* b^* U^{12}]$.

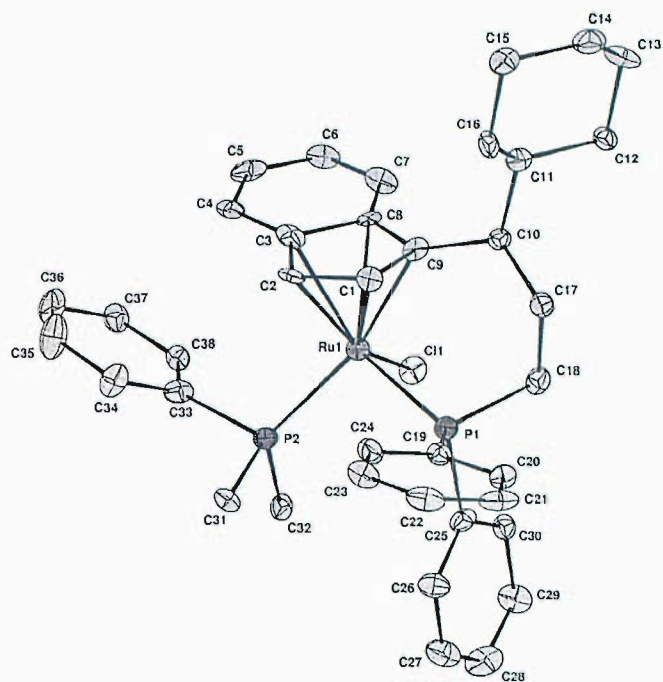
Atom	U^{11}	U^{22}	U^{33}	U^{23}	U^{13}	U^{12}
Ru1	25(1)	20(1)	24(1)	1(1)	17(1)	3(1)
Cl1	37(1)	21(1)	35(2)	1(1)	24(1)	4(1)
P1	29(1)	21(1)	26(1)	0(1)	19(1)	1(1)
P2	26(2)	29(1)	23(2)	0(1)	17(1)	0(1)
C1	31(6)	22(5)	31(6)	3(4)	22(5)	7(4)
C2	50(7)	16(5)	28(6)	1(4)	34(6)	-1(4)
C3	48(7)	33(6)	46(7)	-6(5)	43(7)	0(5)
C4	39(7)	46(6)	27(7)	-2(5)	27(6)	-1(5)
C5	24(6)	66(8)	15(6)	8(6)	9(5)	20(6)
C6	45(7)	42(6)	34(7)	8(5)	31(6)	11(5)
C7	49(7)	30(6)	43(7)	14(5)	37(7)	16(5)
C8	26(5)	32(6)	16(5)	-11(4)	17(5)	0(4)
C9	40(6)	23(5)	35(6)	-18(5)	31(5)	-3(5)
C10	23(5)	24(5)	20(5)	1(4)	14(5)	1(4)
C11	39(6)	34(5)	29(6)	-4(5)	25(6)	-6(5)
C12	32(6)	28(5)	32(6)	-3(4)	26(5)	-2(4)
C13	55(8)	56(7)	40(7)	14(6)	42(7)	11(6)
C14	42(6)	74(8)	33(7)	-7(7)	29(6)	-1(7)
C15	29(6)	55(7)	37(7)	-12(6)	26(6)	3(5)
C16	36(6)	38(6)	45(7)	-16(5)	35(6)	-15(5)
C17	29(6)	28(5)	30(6)	-1(5)	21(5)	-1(4)
C18	30(6)	26(5)	29(6)	-2(5)	17(5)	-3(5)
C19	32(6)	24(5)	29(6)	-1(4)	24(5)	1(4)
C20	24(6)	29(5)	23(6)	7(4)	13(5)	8(4)
C21	39(7)	70(9)	23(6)	12(6)	23(6)	28(6)
C22	56(8)	42(7)	43(7)	13(6)	41(7)	24(6)
C23	50(7)	16(5)	45(7)	13(5)	38(7)	14(5)
C24	32(6)	38(6)	31(6)	6(5)	23(5)	0(5)
C25	26(6)	44(7)	26(6)	-12(5)	19(5)	-1(5)
C26	44(6)	34(6)	33(6)	9(6)	28(6)	10(5)
C27	48(7)	63(8)	45(8)	11(6)	37(7)	10(6)
C28	37(7)	85(10)	46(8)	-16(7)	31(7)	13(7)
C29	49(7)	44(6)	45(7)	9(6)	35(6)	12(6)
C30	29(6)	28(5)	34(6)	-5(5)	24(5)	-4(4)
C31	37(6)	32(6)	33(7)	6(5)	28(6)	0(5)
C32	21(5)	39(6)	34(7)	-7(5)	20(5)	-4(4)
C33	30(6)	42(6)	29(6)	2(5)	23(5)	11(5)
C34	30(6)	24(6)	32(7)	8(5)	11(6)	6(5)
C35	46(8)	32(6)	78(10)	-11(7)	36(8)	-10(6)
C36	14(6)	61(8)	39(7)	1(6)	9(6)	0(5)
C37	30(6)	35(6)	41(7)	-2(5)	27(6)	1(5)
C38	34(6)	18(5)	34(6)	-3(5)	26(5)	-2(4)
Ru2	24(1)	19(1)	25(1)	2(1)	16(1)	1(1)
Cl2	36(1)	24(1)	37(2)	6(1)	26(1)	4(1)

P3	26(1)	22(1)	28(2)	1(1)	18(1)	1(1)
P4	29(2)	25(1)	30(2)	0(1)	21(1)	-1(1)
C39	17(5)	17(5)	28(6)	6(4)	13(5)	0(4)
C40	29(6)	17(5)	33(6)	-3(4)	19(5)	-2(4)
C41	16(5)	32(5)	17(6)	15(5)	7(5)	11(4)
C42	30(6)	51(7)	17(6)	1(5)	10(5)	-4(5)
C43	26(6)	81(9)	30(7)	26(6)	22(6)	15(6)
C44	26(6)	33(6)	31(7)	6(5)	13(5)	3(5)
C45	28(6)	22(5)	27(6)	10(5)	16(5)	5(4)
C46	19(5)	35(6)	39(7)	0(5)	20(5)	6(4)
C47	23(5)	27(5)	28(6)	13(5)	17(5)	18(5)
C48	26(6)	26(5)	29(6)	2(5)	18(5)	-5(4)
C49	26(6)	43(6)	27(6)	2(5)	19(5)	3(5)
C50	36(6)	41(6)	25(6)	3(5)	17(6)	11(5)
C51	21(6)	62(8)	34(7)	4(6)	17(6)	7(5)
C52	32(6)	72(8)	22(6)	9(6)	15(5)	10(6)
C53	21(6)	53(7)	27(7)	5(5)	10(5)	-2(5)
C54	34(6)	36(6)	28(6)	1(5)	20(5)	-1(5)
C55	30(6)	29(5)	23(6)	-8(4)	20(5)	-4(4)
C56	24(6)	39(6)	27(6)	-2(5)	18(5)	0(4)
C57	23(5)	28(5)	18(5)	5(4)	15(5)	4(4)
C58	43(7)	23(5)	48(7)	0(5)	36(6)	0(5)
C59	31(7)	63(8)	44(8)	26(6)	28(6)	12(6)
C60	28(6)	47(7)	28(7)	22(5)	14(6)	11(5)
C61	29(6)	16(5)	45(7)	11(5)	23(6)	-4(4)
C62	32(6)	25(5)	39(7)	-2(5)	25(6)	-2(4)
C63	16(5)	35(6)	30(6)	11(5)	14(5)	4(4)
C64	34(6)	29(5)	41(7)	3(6)	24(5)	0(5)
C65	45(7)	52(7)	34(7)	6(6)	26(6)	-2(6)
C66	41(8)	50(7)	49(8)	22(6)	28(7)	30(6)
C67	42(7)	43(6)	46(7)	12(6)	31(6)	9(6)
C68	31(6)	26(5)	27(6)	-1(5)	14(5)	6(4)
C69	36(7)	40(6)	20(6)	-7(5)	18(6)	-10(5)
C70	24(6)	50(6)	24(6)	2(5)	11(5)	5(5)
C71	27(6)	41(6)	23(6)	2(5)	15(5)	8(5)
C72	13(4)	27(5)	23(5)	0(5)	9(4)	1(4)
C73	32(6)	22(5)	35(6)	11(5)	17(5)	4(5)
C74	61(8)	50(7)	38(7)	-7(6)	40(7)	-3(6)
C75	87(10)	30(6)	62(10)	-10(6)	60(9)	-4(6)
C76	71(9)	33(6)	59(9)	-3(6)	56(8)	-8(6)
C77	51(5)	22(4)	50(6)	0	35(5)	0
C78	51(5)	22(4)	50(6)	0	35(5)	0
C79	51(5)	22(4)	50(6)	0	35(5)	0
C80	51(5)	22(4)	50(6)	0	35(5)	0
C81	51(5)	22(4)	50(6)	0	35(5)	0
C82	51(5)	22(4)	50(6)	0	35(5)	0
C83	51(5)	22(4)	50(6)	0	35(5)	0
C84	51(5)	22(4)	50(6)	0	35(5)	0

Table 5. Hydrogen coordinates [$\times 10^4$] and isotropic displacement parameters [$\text{\AA}^2 \times 10^3$].

Atom	<i>x</i>	<i>y</i>	<i>z</i>	U_{eq}	<i>S.o.f.</i>
H1	6588	2181	4974	33	1
H2	7647	2666	5754	30	1
H4	8814	1820	7236	40	1
H5	9223	543	8046	48	1
H6	8639	-642	7794	45	1
H7	7630	-584	6734	43	1
H10	6558	-258	5406	28	1
H11	6722	416	6488	39	1
H12A	5482	51	5154	33	1
H12B	5982	-705	5734	33	1
H13A	6197	-193	6913	52	1
H13B	5495	-346	6178	52	1
H14A	5332	1202	5879	56	1
H14B	5728	1076	6866	56	1
H15A	6587	1464	7175	45	1
H15B	6108	2258	6643	45	1
H16A	5833	1737	5400	40	1
H16B	6531	1938	6103	40	1
H17A	5545	203	4257	34	1
H17B	5781	1164	4266	34	1
H18A	5528	96	3221	37	1
H18B	6104	-463	3983	37	1
H20	5120	1318	2453	34	1
H21	4559	2593	1717	52	1
H22	5063	4032	2114	49	1
H23	6089	4080	3201	39	1
H24	6638	2758	3909	40	1
H26	6170	1511	2334	43	1
H27	6090	892	1331	57	1
H28	6130	-688	1233	65	1
H29	6220	-1598	2165	52	1
H30	6349	-965	3252	34	1
H31A	7906	2467	4058	46	1
H31B	7568	2867	4300	46	1
H31C	7221	2241	3485	46	1
H32A	8166	758	4159	45	1
H32B	7502	420	3617	45	1
H32C	8040	-36	4509	45	1
H34	8570	2976	5570	46	1
H35	9513	3229	6873	70	1
H36	10156	2029	7721	56	1
H37	9788	547	7285	40	1
H38	8822	279	6032	32	1
H39	3372	2804	1789	27	1
H40	3095	2331	448	35	1
H42	3401	3159	-403	46	1
H43	3827	4456	-397	52	1
H44	4143	5642	512	43	1
H45	4102	5562	1494	34	1
H48	3844	5237	2301	34	1
H49	4759	4577	3025	37	1
H50A	4572	3048	3046	45	1

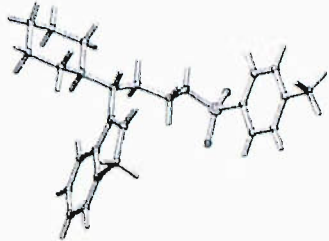
H50B	4558	3255	3743	45	1
H51A	5527	2711	4447	49	1
H51B	5596	3472	4004	49	1
H52A	5573	3789	5260	55	1
H52B	6135	3931	5386	55	1
H53A	5722	5177	4537	47	1
H53B	5666	5305	5198	47	1
H54A	4658	4940	4186	41	1
H54B	4757	5687	3772	41	1
H55A	3702	4765	3167	32	1
H55B	3487	3810	2700	32	1
H56A	2880	5444	1766	36	1
H56B	2693	4896	2174	36	1
H58	2326	3680	2196	41	1
H59	2162	2410	2624	52	1
H60	2042	946	1972	47	1
H61	2090	901	985	39	1
H62	2273	2227	624	38	1
H64	1170	3473	-11	43	1
H65	241	4095	-883	53	1
H66	115	5677	-1017	60	1
H67	942	6582	-288	52	1
H68	1891	5939	548	40	1
H69A	1213	2455	-1713	51	1
H69B	1217	2781	-1019	51	1
H69C	1735	2141	-754	51	1
H70A	1457	5056	-1519	57	1
H70B	1076	4505	-1409	57	1
H70C	1017	4273	-2172	57	1
H72	2220	4703	-1583	29	1
H73	2487	4432	-2319	43	1
H74	2546	2962	-2615	53	1
H75	2367	1736	-2165	62	1
H76	2006	2003	-1553	54	1
H77	0	3280	0	50	0.50
H78	863	2502	617	50	0.50
H79	863	914	617	50	0.50
H80	0	139	0	50	0.50
H81	5000	4842	0	50	0.50
H82	5262	4071	1132	50	0.50
H83	5263	2478	1133	50	0.50
H84	5000	1705	0	50	0.50



One of the two identical molecules in the asymmetric unit, solvent omitted for clarity and thermal ellipsoids drawn at the 35% probability level.



Table 1. Crystal data and structure refinement details.

Identification code	04sot0921	
Empirical formula	C ₂₅ H ₃₁ NO ₂ S	
Formula weight	409.57	
Temperature	120(2) K	
Wavelength	0.71073 Å	
Crystal system	Monoclinic	
Space group	<i>P</i> 2 ₁ / <i>c</i>	
Unit cell dimensions	<i>a</i> = 18.840(9) Å <i>b</i> = 5.801(2) Å <i>c</i> = 21.553(18) Å	
Volume	2174(2) Å ³	
<i>Z</i>	4	
Density (calculated)	1.251 Mg / m ³	
Absorption coefficient	0.170 mm ⁻¹	
<i>F</i> (000)	880	
Crystal	Needle; Colourless	
Crystal size	0.31 × 0.03 × 0.02 mm ³	
θ range for data collection	3.32 – 27.32°	
Index ranges	–24 ≤ <i>h</i> ≤ 24, –7 ≤ <i>k</i> ≤ 7, –27 ≤ <i>l</i> ≤ 27	
Reflections collected	25097	
Independent reflections	4822 [<i>R</i> _{int} = 0.1445]	
Completeness to $\theta = 25.00^\circ$	99.8 %	
Absorption correction	Semi-empirical from equivalents	
Max. and min. transmission	0.9966 and 0.9492	
Refinement method	Full-matrix least-squares on <i>F</i> ²	
Data / restraints / parameters	4822 / 150 / 268	
Goodness-of-fit on <i>F</i> ²	1.023	
Final <i>R</i> indices [<i>F</i> ² > 2 σ (<i>F</i> ²)]	<i>R</i> 1 = 0.1090, <i>wR</i> 2 = 0.2411	
<i>R</i> indices (all data)	<i>R</i> 1 = 0.2129, <i>wR</i> 2 = 0.2912	
Extinction coefficient	0.0014(14)	
Largest diff. peak and hole	0.763 and –0.812 e Å ⁻³	

Diffractometer: *Nonius KappaCCD* area detector (ϕ scans and ω scans to fill *asymmetric unit*). **Cell determination:** Df:Ax (Duisenberg, A.J.M.(1992). *J. Appl. Cryst.* 25, 92-96.) **Data collection:** Collect (Collect: Data collection software, R. Hooft, Nonius B.V., 1998). **Data reduction and cell refinement:** *Denzo* (Z. Otwinowski & W. Minor, *Methods in Enzymology* (1997) Vol. 276: *Macromolecular Crystallography*, part A, pp. 307–326; C. W. Carter, Jr. & R. M. Sweet, Eds., Academic Press). **Absorption correction:** Sheldrick, G. M. SADABS - Bruker Nonius area detector scaling and absorption correction - V2.10 **Structure solution:** *SHELXS97* (G. M. Sheldrick, *Acta Cryst.* (1990) A46 467–473). **Structure refinement:** *SHELXL97* (G. M. Sheldrick (1997), University of Göttingen, Germany). **Graphics:** Cameron - A Molecular Graphics Package. (D. M. Watkin, L. Pearce and C. K. Prout, Chemical Crystallography Laboratory, University of Oxford, 1993).

Special details: All hydrogen atoms were placed in idealised positions and refined using a riding model. There is a considerable amount of thermal motion within the crystal, resulting in an elevated *R* factor

Table 2. Atomic coordinates [$\times 10^4$], equivalent isotropic displacement parameters [$\text{\AA}^2 \times 10^3$] and site occupancy factors. U_{eq} is defined as one third of the trace of the orthogonalized U^{ij} tensor.

Atom	x	y	z	U_{eq}	<i>S.o.f.</i>
S1	168(1)	5342(2)	1560(1)	48(1)	1
N1	779(3)	6762(8)	2180(2)	51(1)	1
O1	576(2)	4226(6)	1207(2)	58(1)	1
O2	-259(3)	3992(6)	1849(2)	70(1)	1
C1	3349(4)	9255(10)	2118(2)	59(2)	1
C2	3785(4)	7345(12)	2449(3)	68(2)	1
C3	4284(5)	6293(13)	2207(3)	79(2)	1
C4	4366(5)	7115(14)	1637(3)	83(2)	1
C5	3947(5)	9029(13)	1309(3)	77(2)	1
C6	3452(4)	10073(12)	1544(2)	65(2)	1
C7	2930(4)	12094(10)	1286(3)	69(2)	1
C8	2533(4)	12267(11)	1760(2)	65(2)	1
C9	2777(4)	10656(11)	2245(3)	59(2)	1
C10	2513(4)	10275(15)	2811(3)	83(2)	1
C11	3157(3)	10551(11)	3503(3)	61(2)	1
C12	3593(6)	12639(14)	3599(3)	105(3)	1
C13	4253(5)	12893(14)	4274(3)	102(3)	1
C14	4022(5)	12453(13)	4849(3)	86(2)	1
C15	3583(5)	10400(20)	4762(3)	142(5)	1
C16	2909(5)	10160(20)	4083(3)	135(4)	1
C17	1936(6)	8840(30)	2716(4)	174(6)	1
C18	1256(4)	8507(13)	2057(3)	73(2)	1
C19	-460(3)	7356(8)	1011(2)	41(1)	1
C20	-927(4)	8694(11)	1227(3)	59(2)	1
C21	-1378(4)	10347(11)	813(3)	67(2)	1
C22	-1388(3)	10752(9)	175(3)	57(2)	1
C23	-940(3)	9339(9)	-43(3)	51(1)	1
C24	-469(3)	7658(9)	370(2)	49(1)	1
C25	-1850(4)	12687(11)	-257(3)	80(2)	1

Table 3. Bond lengths [Å] and angles [°].

S1–O2	1.426(4)	C10–C17	1.321(11)
S1–O1	1.429(4)	C10–C11	1.526(8)
S1–N1	1.614(5)	C11–C12	1.433(9)
S1–C19	1.756(5)	C11–C16	1.508(8)
N1–C18	1.444(8)	C12–C13	1.514(10)
C1–C2	1.400(9)	C13–C14	1.484(10)
C1–C6	1.406(7)	C14–C15	1.420(11)
C1–C9	1.457(9)	C15–C16	1.530(9)
C2–C3	1.381(10)	C17–C18	1.514(10)
C3–C4	1.381(9)	C19–C20	1.381(7)
C4–C5	1.388(10)	C19–C24	1.386(7)
C5–C6	1.363(10)	C20–C21	1.361(8)
C6–C7	1.494(9)	C21–C22	1.389(8)
C7–C8	1.484(9)	C22–C23	1.382(8)
C8–C9	1.344(7)	C22–C25	1.504(8)
C9–C10	1.500(8)	C23–C24	1.386(7)
O2–S1–O1	119.6(2)	N1–C18–C17	106.2(6)
O2–S1–N1	105.2(3)	C20–C19–C24	120.0(5)
O1–S1–N1	108.2(3)	C20–C19–S1	119.9(4)
O2–S1–C19	108.2(3)	C24–C19–S1	120.1(4)
O1–S1–C19	107.7(2)	C21–C20–C19	119.5(5)
N1–S1–C19	107.4(2)	C20–C21–C22	122.4(6)
C18–N1–S1	120.2(4)	C23–C22–C21	117.4(5)
C2–C1–C6	117.6(7)	C23–C22–C25	121.1(6)
C2–C1–C9	132.6(6)	C21–C22–C25	121.5(6)
C6–C1–C9	109.8(6)	C22–C23–C24	121.4(5)
C3–C2–C1	120.5(6)	C19–C24–C23	119.3(5)
C2–C3–C4	120.7(7)		
C3–C4–C5	119.5(8)		
C6–C5–C4	120.2(6)		
C5–C6–C1	121.5(7)		
C5–C6–C7	131.0(6)		
C1–C6–C7	107.4(6)		
C8–C7–C6	103.3(5)		
C9–C8–C7	112.1(6)		
C8–C9–C1	107.3(6)		
C8–C9–C10	127.9(7)		
C1–C9–C10	124.8(5)		
C17–C10–C9	118.5(6)		
C17–C10–C11	121.0(6)		
C9–C10–C11	113.1(5)		
C12–C11–C16	110.5(6)		
C12–C11–C10	115.2(5)		
C16–C11–C10	114.3(5)		
C11–C12–C13	115.7(6)		
C14–C13–C12	112.9(7)		
C15–C14–C13	112.1(6)		
C14–C15–C16	115.4(8)		
C11–C16–C15	111.8(6)		
C10–C17–C18	125.1(9)		

Table 4. Anisotropic displacement parameters [$\text{\AA}^2 \times 10^3$]. The anisotropic displacement factor exponent takes the form: $-2\pi^2[h^2 a^{*2} U^{11} + \dots + 2 h k a^* b^* U^{12}]$.

Atom	U^{11}	U^{22}	U^{33}	U^{23}	U^{13}	U^{12}
S1	69(1)	40(1)	41(1)	2(1)	27(1)	2(1)
N1	62(3)	64(3)	29(2)	4(2)	19(2)	10(3)
O1	83(3)	51(2)	46(2)	2(2)	32(2)	18(2)
O2	115(4)	46(2)	70(3)	-1(2)	60(3)	-13(2)
C1	62(4)	70(4)	28(2)	13(2)	0(3)	-28(3)
C2	72(5)	80(4)	44(3)	7(3)	14(3)	-24(4)
C3	85(6)	89(5)	47(4)	1(3)	8(4)	-12(4)
C4	82(6)	109(6)	54(4)	-20(4)	22(4)	-23(5)
C5	97(6)	95(5)	32(3)	-3(3)	16(3)	-41(4)
C6	78(5)	85(4)	26(2)	-11(3)	13(3)	-42(4)
C7	92(5)	64(4)	34(3)	11(3)	6(3)	-33(4)
C8	66(4)	79(4)	34(3)	19(3)	3(3)	-18(3)
C9	44(4)	79(4)	42(3)	12(3)	3(3)	-19(3)
C10	48(4)	142(6)	48(3)	33(4)	4(3)	-25(4)
C11	51(4)	86(4)	41(3)	6(3)	12(3)	-18(3)
C12	166(9)	95(5)	52(4)	0(4)	41(5)	-44(6)
C13	144(8)	106(6)	47(4)	-16(4)	26(4)	-69(6)
C14	112(7)	92(5)	50(4)	-6(3)	26(4)	19(5)
C15	105(7)	265(13)	40(4)	13(6)	11(4)	-92(8)
C16	73(6)	280(13)	40(3)	30(6)	8(3)	-59(7)
C17	108(8)	359(17)	63(5)	-97(7)	44(5)	-132(10)
C18	60(4)	114(5)	49(3)	-24(3)	25(3)	-29(4)
C19	43(3)	38(3)	38(3)	-7(2)	11(2)	-6(2)
C20	63(4)	80(4)	37(3)	-15(3)	21(3)	5(3)
C21	52(4)	78(4)	58(4)	-27(3)	8(3)	16(3)
C22	55(4)	51(3)	50(3)	-16(3)	3(3)	-2(3)
C23	55(4)	46(3)	45(3)	3(2)	13(3)	2(3)
C24	55(4)	53(3)	46(3)	2(2)	27(3)	2(3)
C25	69(5)	66(4)	69(4)	-7(3)	-13(3)	21(4)

Table 5. Hydrogen coordinates [$\times 10^4$] and isotropic displacement parameters [$\text{\AA}^2 \times 10^3$].

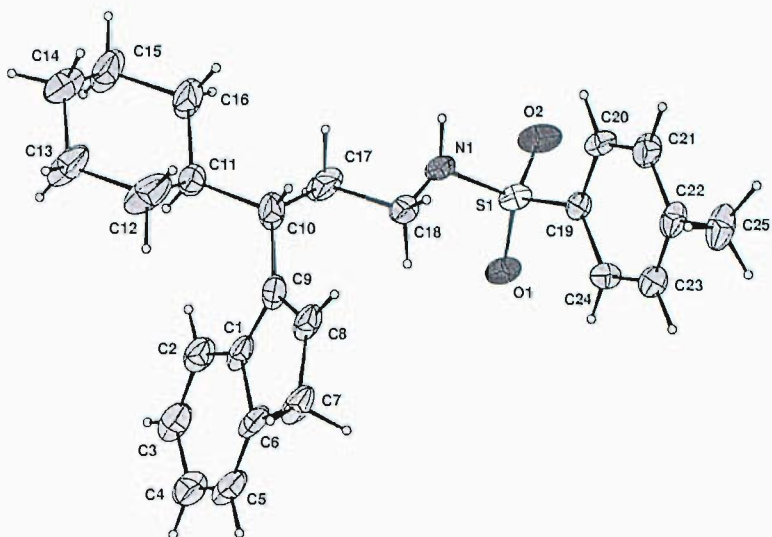
Atom	<i>x</i>	<i>y</i>	<i>z</i>	U_{eq}	<i>S.o.f.</i>
H1	570(40)	7110(100)	2470(30)	70(20)	1
H2	3736	6766	2844	81	1
H3	4574	4992	2435	95	1
H4	4708	6376	1471	100	1
H5	4005	9612	919	93	1
H7A	3226	13513	1294	82	1
H7B	2557	11820	821	82	1
H8	2152	13387	1726	78	1
H10	2239	11768	2788	100	1
H11	3529	9284	3536	74	1
H12A	3239	13959	3538	126	1
H12B	3802	12740	3243	126	1
H13A	4667	11803	4297	122	1
H13B	4464	14474	4313	122	1
H14A	4489	12330	5267	104	1
H14B	3716	13774	4899	104	1
H15A	3379	10327	5121	171	1
H15B	3930	9066	4821	171	1
H16A	2685	8599	4046	162	1
H16B	2505	11293	4057	162	1
H17A	1717	9272	3050	208	1
H17B	2169	7298	2848	208	1
H18A	967	9966	1913	87	1
H18B	1432	7999	1702	87	1
H20	-933	8464	1662	71	1
H21	-1697	11257	967	80	1
H23	-954	9524	-486	61	1
H24	-157	6723	216	59	1
H25A	-1569	14141	-114	120	1
H25B	-2346	12797	-210	120	1
H25C	-1936	12386	-728	120	1

Table 6. Hydrogen bonds [\AA and $^\circ$].

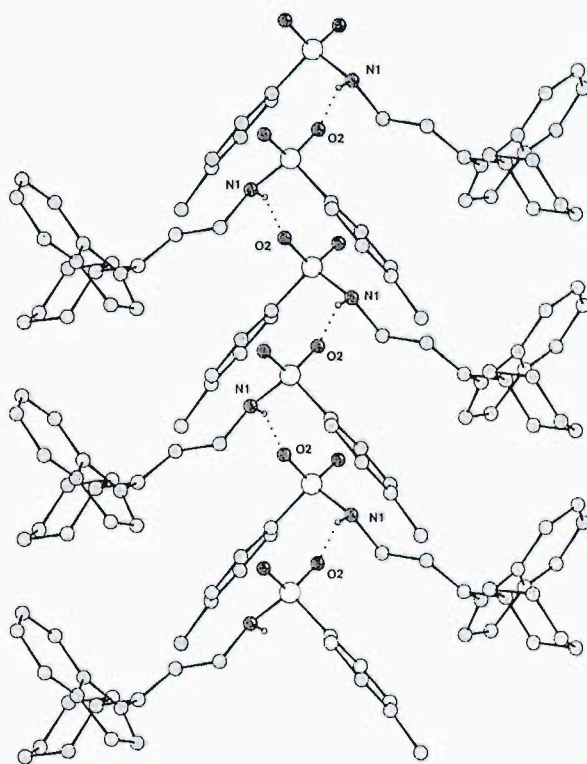
$D-H\cdots A$	$d(D-H)$	$d(H\cdots A)$	$d(D\cdots A)$	$\angle(DHA)$
$N1-H1\cdots O2^i$	0.89(6)	2.08(6)	2.932(6)	160(6)

Symmetry transformations used to generate equivalent atoms:

(i) $-x, y+1/2, -z+1/2$



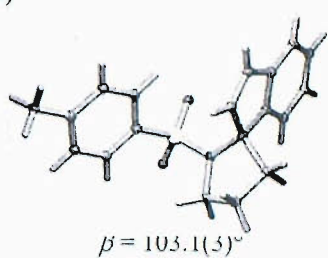
Thermal ellipsoids drawn at the 30% probability level



Part of one of the hydrogen bonded chains that extends down the *b* axis



Table 1. Crystal data and structure refinement details.

Identification code	04sot0963 (PWRI6.82)	
Empirical formula	C ₁₉ H ₁₉ NO ₂ S	
Formula weight	325.41	
Temperature	120(2) K	
Wavelength	0.71073 Å	
Crystal system	Monoclinic	
Space group	<i>P</i> 2 ₁ / <i>c</i>	
Unit cell dimensions	<i>a</i> = 17.81(7) Å <i>b</i> = 7.282(5) Å <i>c</i> = 12.94(6) Å	
Volume	1635(10) Å ³	
<i>Z</i>	4	
Density (calculated)	1.322 Mg / m ³	
Absorption coefficient	0.207 mm ⁻¹	
<i>F</i> (000)	688	
Crystal	Plate; Colourless	
Crystal size	0.15 × 0.1 × 0.01 mm ³	
θ range for data collection	3.18 – 27.65°	
Index ranges	-20 ≤ <i>h</i> ≤ 23, -9 ≤ <i>k</i> ≤ 9, -16 ≤ <i>l</i> ≤ 12	
Reflections collected	12852	
Independent reflections	3723 [<i>R</i> _{int} = 0.0915]	
Completeness to $\theta = 27.50^\circ$	98.9 %	
Absorption correction	Semi-empirical from equivalents	
Max. and min. transmission	0.9979 and 0.9696	
Refinement method	Full-matrix least-squares on <i>F</i> ²	
Data / restraints / parameters	3723 / 0 / 209	
Goodness-of-fit on <i>F</i> ²	1.017	
Final <i>R</i> indices [<i>F</i> ² > 2σ(<i>F</i> ²)]	<i>R</i> 1 = 0.0866, <i>wR</i> 2 = 0.1950	
<i>R</i> indices (all data)	<i>R</i> 1 = 0.1684, <i>wR</i> 2 = 0.2331	
Largest diff. peak and hole	0.429 and -0.349 e Å ⁻³	

Diffractometer: *Nonius KappaCCD* area detector (ϕ scans and ω scans to fill *asymmetric unit*). **Cell determination:** DirAx (Duisenberg, A.J.M.(1992). *J. Appl. Cryst.* 25, 92-96.) **Data collection:** Collect (Collect: Data collection software, R. Hooft, Nonius B.V., 1998). **Data reduction and cell refinement:** *Denzo* (Z. Otwinowski & W. Minor, *Methods in Enzymology* (1997) Vol. 276: *Macromolecular Crystallography*, part A, pp. 307–326; C. W. Carter, Jr. & R. M. Sweet, Eds., Academic Press). **Absorption correction:** Sheldrick, G. M. SADABS - Bruker Nonius area detector scaling and absorption correction - V2.10 **Structure solution:** *SHELXS97* (G. M. Sheldrick, *Acta Cryst.* (1990) A46 467–473). **Structure refinement:** *SHELXL97* (G. M. Sheldrick (1997), University of Göttingen, Germany). **Graphics:** Cameron - A Molecular Graphics Package. (D. M. Watkin, L. Pearce and C. K. Prout, Chemical Crystallography Laboratory, University of Oxford, 1993).

Special details: All hydrogen atoms were placed in idealised positions and refined using a riding model.

Table 2. Atomic coordinates [$\times 10^4$], equivalent isotropic displacement parameters [$\text{\AA}^2 \times 10^3$] and site occupancy factors. U_{eq} is defined as one third of the trace of the orthogonalized U^{ij} tensor.

Atom	x	y	z	U_{eq}	$S.o.f.$
C1	2844(3)	4117(6)	1431(4)	41(1)	1
C2	3286(2)	2728(6)	1312(4)	41(1)	1
C3	3868(3)	2383(6)	2289(4)	43(1)	1
C4	4455(3)	1104(6)	2559(5)	47(1)	1
C5	4916(3)	1075(7)	3579(5)	57(2)	1
C6	4792(3)	2332(7)	4340(4)	54(1)	1
C7	4215(3)	3645(6)	4087(4)	43(1)	1
C8	3747(3)	3648(5)	3047(4)	40(1)	1
C9	3105(2)	4937(6)	2553(4)	40(1)	1
C10	3384(3)	6947(5)	2508(4)	42(1)	1
C11	2665(3)	8071(6)	2359(5)	52(1)	1
C12	2231(3)	7167(5)	3114(4)	45(1)	1
C13	1121(2)	3424(5)	2401(3)	32(1)	1
C14	449(2)	4363(5)	2441(4)	36(1)	1
C15	-194(2)	4208(5)	1608(4)	38(1)	1
C16	-191(2)	3136(5)	716(4)	35(1)	1
C17	485(2)	2228(5)	694(4)	34(1)	1
C18	1134(2)	2340(5)	1517(3)	31(1)	1
C19	-895(3)	2980(6)	-182(4)	46(1)	1
N1	2496(2)	5214(4)	3151(3)	37(1)	1
O1	1704(2)	4297(4)	4363(2)	43(1)	1
O2	2370(2)	1945(4)	3530(2)	38(1)	1
S1	1954(1)	3633(1)	3454(1)	35(1)	1

Table 3. Bond lengths [Å] and angles [°].

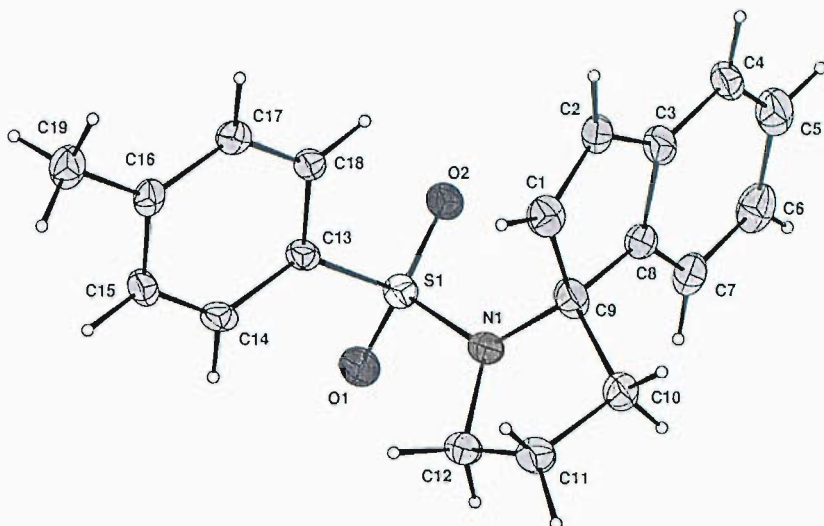
C1–C2	1.312(6)	C11–C12	1.526(8)
C1–C9	1.541(9)	C12–N1	1.496(5)
C2–C3	1.464(9)	C13–C14	1.389(7)
C3–C4	1.385(7)	C13–C18	1.394(7)
C3–C8	1.397(7)	C13–S1	1.780(9)
C4–C5	1.389(10)	C14–C15	1.388(9)
C5–C6	1.399(8)	C15–C16	1.395(7)
C6–C7	1.388(7)	C16–C17	1.380(7)
C7–C8	1.413(9)	C16–C19	1.508(9)
C8–C9	1.506(8)	C17–C18	1.386(9)
C9–N1	1.482(8)	N1–S1	1.608(5)
C9–C10	1.551(6)	O1–S1	1.433(6)
C10–C11	1.495(8)	O2–S1	1.427(3)
C2–C1–C9	110.4(5)	O2–S1–C13	108.0(2)
C1–C2–C3	110.9(5)	O1–S1–C13	107.3(4)
C4–C3–C8	119.5(6)	N1–S1–C13	108.5(3)
C4–C3–C2	132.9(5)		
C8–C3–C2	107.6(5)		
C3–C4–C5	120.1(5)		
C4–C5–C6	120.3(5)		
C7–C6–C5	120.7(6)		
C6–C7–C8	118.2(5)		
C3–C8–C7	121.1(5)		
C3–C8–C9	109.6(5)		
C7–C8–C9	129.3(4)		
N1–C9–C8	116.0(4)		
N1–C9–C1	116.3(5)		
C8–C9–C1	101.4(4)		
N1–C9–C10	99.8(3)		
C8–C9–C10	112.6(4)		
C1–C9–C10	111.2(4)		
C11–C10–C9	104.4(4)		
C10–C11–C12	103.0(4)		
N1–C12–C11	103.2(4)		
C14–C13–C18	118.9(5)		
C14–C13–S1	120.4(4)		
C18–C13–S1	120.7(4)		
C15–C14–C13	119.8(5)		
C14–C15–C16	122.1(4)		
C17–C16–C15	116.8(5)		
C17–C16–C19	121.7(5)		
C15–C16–C19	121.5(5)		
C16–C17–C18	122.4(5)		
C17–C18–C13	119.9(4)		
C9–N1–C12	112.1(3)		
C9–N1–S1	125.5(3)		
C12–N1–S1	119.1(3)		
O2–S1–O1	119.2(2)		
O2–S1–N1	107.6(3)		
O1–S1–N1	105.9(3)		

Table 4. Anisotropic displacement parameters [$\text{\AA}^2 \times 10^3$]. The anisotropic displacement factor exponent takes the form: $-2\pi^2[h^2 a^{*2} U^{11} + \dots + 2 h k a^* b^* U^{12}]$.

Atom	U^{11}	U^{22}	U^{33}	U^{23}	U^{13}	U^{12}
C1	38(3)	46(3)	41(3)	1(2)	12(2)	-2(2)
C2	31(3)	48(3)	44(3)	-8(2)	10(2)	-7(2)
C3	34(3)	37(2)	63(3)	0(2)	22(3)	-3(2)
C4	35(3)	33(2)	79(4)	7(2)	28(3)	3(2)
C5	41(3)	43(3)	89(4)	15(3)	21(3)	3(2)
C6	41(3)	58(3)	57(3)	12(3)	1(3)	-5(2)
C7	36(3)	40(3)	52(3)	1(2)	8(2)	-7(2)
C8	37(3)	32(2)	57(3)	-3(2)	24(2)	-8(2)
C9	32(3)	35(2)	54(3)	6(2)	13(2)	3(2)
C10	38(3)	33(2)	55(3)	2(2)	13(2)	-2(2)
C11	49(3)	31(2)	82(4)	-1(2)	23(3)	2(2)
C12	43(3)	30(2)	69(3)	-9(2)	26(3)	-1(2)
C13	33(2)	25(2)	40(2)	0(2)	13(2)	1(2)
C14	40(3)	22(2)	51(3)	3(2)	25(2)	1(2)
C15	27(2)	28(2)	62(3)	8(2)	19(2)	1(2)
C16	31(2)	27(2)	48(3)	13(2)	12(2)	-4(2)
C17	39(3)	27(2)	40(3)	2(2)	17(2)	-5(2)
C18	31(2)	21(2)	42(3)	2(2)	13(2)	0(2)
C19	37(3)	40(2)	61(3)	14(2)	10(3)	-6(2)
N1	36(2)	28(2)	52(2)	-7(2)	19(2)	1(2)
O1	44(2)	50(2)	39(2)	-6(1)	18(2)	0(1)
O2	38(2)	31(2)	47(2)	5(1)	11(2)	4(1)
S1	35(1)	32(1)	39(1)	-1(1)	14(1)	-1(1)

Table 5. Hydrogen coordinates [$\times 10^4$] and isotropic displacement parameters [$\text{\AA}^2 \times 10^3$].

Atom	x	y	z	U_{eq}	$S.o.f.$
H1	2422	4555	901	49	1
H2	3235	2038	677	49	1
H4	4542	246	2046	56	1
H5	5319	196	3761	68	1
H6	5106	2287	5039	65	1
H7	4136	4517	4598	52	1
H10A	3752	7284	3176	50	1
H10B	3637	7121	1908	50	1
H11A	2364	8010	1616	63	1
H11B	2785	9371	2553	63	1
H12A	2369	7739	3826	54	1
H12B	1667	7255	2838	54	1
H14	430	5108	3037	43	1
H15	-650	4854	1647	45	1
H17	507	1499	92	41	1
H18	1587	1680	1479	37	1
H19A	-1254	2092	8	69	1
H19B	-741	2566	-824	69	1
H19C	-1146	4181	-312	69	1



Thermal ellipsoids drawn at the 35% probability level